

Models of dephasing at low temperatures

INAUGURALDISSERTATION

zur

Erlangung der Würde eines Doktors der Philosophie

vorgelegt der

Philosophisch-Naturwissenschaftlichen Fakultät

der Universität Basel

von

Florian Marquardt

aus Berlin (Deutschland)

Basel, 2002

Genehmigt von der Philosophisch-Naturwissenschaftlichen Fakultät auf Antrag von

Prof. Dr. Christoph Bruder

Prof. Dr. Daniel Loss

Prof. Dr. Hermann Grabert

Basel, den 22. Oktober 2002

Prof. Dr. Marcel Tanner
Dekan

Meinen Eltern gewidmet

Contents

1	Dephasing: An introduction	5
1.1	Some examples	5
1.2	Dephasing involves measurement	9
1.3	Entanglement does not imply dephasing	10
1.4	Fluctuating environments	12
1.5	Interference effects and measures of dephasing	13
1.6	Some important questions	15
1.7	The role of simple model systems	16
2	Dephasing in tunneling through localized levels	19
2.1	Introduction	19
2.2	Preliminaries	21
2.2.1	Spin-boson model with diagonal coupling	21
2.2.2	Independent boson model	23
2.2.3	Single-particle Green's function	25
2.2.4	Dephasing and two-particle Green's function	29
2.2.5	Time-evolution of Green's functions	31
2.3	Dephasing in sequential tunneling through a double-dot	33
2.3.1	The model	34
2.3.2	Qualitative discussion	35
2.3.3	Decay rate and connection to $P(E)$ theory	38
2.3.4	Evaluation for different bath spectra	42
2.3.5	Discussion of the results	45
2.3.6	Sequential tunneling through the double-dot	49
2.4	Cotunneling and connection to the Feynman-Vernon influence functional	60
2.4.1	Two-particle Green's function and influence functional	60
2.4.2	Cotunneling expressions for the independent boson model	63
2.4.3	Generalized influence functional for cotunneling	67
2.4.4	Dephasing in cotunneling: General discussion	69
2.4.5	Perturbative evaluation of the cotunneling rate	72
2.4.6	Interference in cotunneling through a double-dot	74
2.5	Dephasing by correlated two-particle tunneling	76

2.6	Conclusions	79
3	Aharonov-Bohm ring with fluctuating magnetic flux	81
3.1	Introduction	81
3.2	Caldeira-Leggett model in vector potential gauge	82
3.3	The model	86
3.4	Qualitative semiclassical discussion of dephasing in this model	88
3.5	Effective mass, interaction and persistent current	89
3.6	Two-particle Green's function and dephasing	91
3.7	Variable particle number	95
3.8	Single-particle Green's function	96
3.9	Cotunneling through the Aharonov-Bohm ring	97
3.10	Comparison with other models	103
3.11	Conclusions	104
4	Fermi sea in a damped harmonic oscillator	105
4.1	Introduction	105
4.2	The model	105
4.3	Solution by bosonization and diagonalisation	107
4.4	Evaluation of the Green's function for $T = 0$	112
4.5	Discussion of the Green's function	115
4.6	Finite particle number: Center-of-mass motion in excited Fock states . . .	121
4.7	Two-particle Green's function: decay of populations and dephasing	124
4.8	Conclusions	128
5	The role of friction in the description of low-temperature dephasing	129
5.1	Introduction	129
5.2	The influence functional and dephasing in simple situations	131
5.3	Decay rates from S_I and Golden Rule: Dependence on the spectra of bath and system motion	135
5.4	Cancellation of S_R and S_I in lowest-order perturbation theory	137
5.5	Exactly solvable linear systems: "Cancellation to all orders" for the damped oscillator	138
5.6	Power-law behaviour in quantum Brownian motion	143
5.7	Qualitative discussion of other models: Nonlinear coupling and Pauli principle	146
5.8	Conclusions	151
6	Summary and open questions	153
A	Appendices	157
A.1	Proof of $\langle \exp \hat{A} \rangle = \exp \left(\langle \hat{A}^2 \rangle / 2 \right)$	157
A.2	Current expression for sequential tunneling through the double-dot	158

A.3	Cotunneling rate contributions	158
A.4	Exact integral expressions for the cotunneling rate for the Ohmic bath at $T = 0$	159
A.5	Derivation of the transformed spectrum for the Caldeira-Leggett model in vector gauge	160
A.6	Coupled oscillator problem for the damped Fermi sea	161
A.7	Two-particle Green's function of damped Fermi sea	163
A.8	Some quantities for the damped oscillator	165
A.9	Density matrix propagator from the Wigner density evolution	166
Bibliography		169

Chapter 1

Dephasing: An introduction

In brief, “dephasing” denotes the destruction of quantum-mechanical interference effects due to the influence of a fluctuating environment. It is a subject important not only because of its connection to fundamental issues (the quantum measurement process and the quantum-classical transition [Giulini96]) but also because of its role in the suppression of phenomena resulting from quantum interference effects, such as those studied in mesoscopic physics (including Aharonov-Bohm interference, weak localization and universal conductance fluctuations) or in the field of quantum information processing. In this chapter we will give a qualitative introduction to dephasing, which is also denoted as “decoherence”. The major emphasis is on the physical picture, not on the mathematical formalism. A more extended overview along these lines (with even less formulas) can be found in [Marquardt01].

1.1 Some examples

In the following, a few simple examples will introduce the most important concepts connected to dephasing.

Let us consider a version of the standard double-slit interference setup: Two wave packets, representing one and the same particle, have been separated and travel along two different paths, in order to be recombined later on. In the region where the wave packets overlap, an interference pattern will develop in the probability density $|\Psi(x)|^2$. If a screen is placed at this point, the pattern becomes visible in the distribution of particles hitting the screen, when the experiment is repeated many times. Now assume a fluctuating force acts on the particle on its way towards the screen. An example is the fluctuating electric field inside a metal. As a consequence, the pattern will become blurred (see Fig. 1.1). Qualitatively, the pattern has become a classical superposition of many different “ideal” patterns, each of them shifted by a random amount. This “washes out” the pattern and decreases the difference between maxima and minima of the intensity. In particular, if the situation is symmetric, then the intensity at the minima can have been strictly zero in the ideal case, without fluctuations. This perfect destructive interference

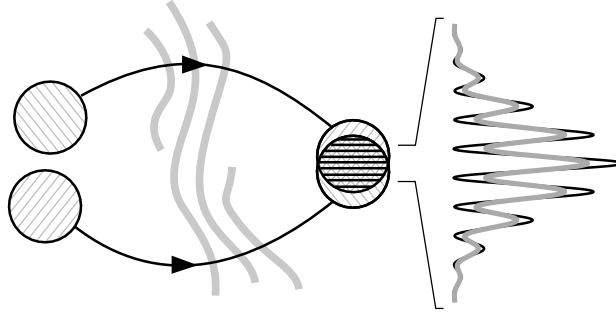


Figure 1.1: The interference pattern (black curve), that forms in the region where two wave packets overlap, is blurred (gray curve) due to dephasing brought about by the fluctuating environment.

is lifted.

Putting it in a more formal way, the major effect of the fluctuating force will be to introduce an additional relative phase ϕ between the two paths, i.e. between the two wave packets Ψ_1 and Ψ_2 . Therefore, at the time when the wave packets overlap, the interference term in the probability density will depend on an extra phase factor $e^{i\phi}$:

$$\begin{aligned} |\Psi_1(x) + e^{i\phi}\Psi_2(x)|^2 &= |\Psi_1(x)|^2 + |\Psi_2(x)|^2 + \\ &2 \operatorname{Re} [\Psi_1^*(x)\Psi_2(x)e^{i\phi}] . \end{aligned} \quad (1.1)$$

As the phase ϕ depends on the random force, it will fluctuate from run to run. The interference pattern which is actually observed in many repeated runs of the experiment will be determined by the average probability density. In general, the average over the fluctuating phase factor $\exp(i\phi)$ will be a number of magnitude less than one. Therefore, the interference term in (1.1) is suppressed and the pattern is blurred. It is this randomization of the phase, brought about by the fluctuating environment, which is called “dephasing”. A more detailed account of the present example will be given in Section (5.2).

Often, the phase ϕ can be taken to be a Gaussian random variable, at least approximately [Stern90]. In that case, one can evaluate explicitly the average over the fluctuating phase factor (assuming $\langle\phi\rangle = 0$):

$$\langle e^{i\phi} \rangle = e^{-\frac{1}{2}\langle\phi^2\rangle} . \quad (1.2)$$

The time interval during which the wave packets have been separated will influence the variance of the phase. If the time interval grows, the effects of the random force accumulate, the variance $\langle\phi^2\rangle$ grows, and the interference term is suppressed even further. In the simplest possible case, this decay proceeds exponentially in time, with

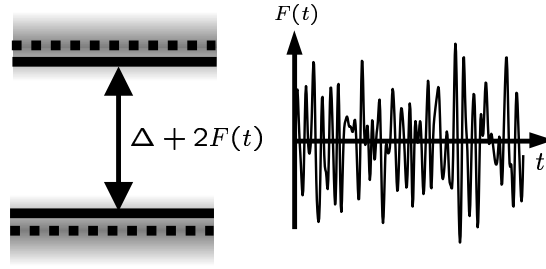


Figure 1.2: The fluctuations of the energy levels around their average value (dashed line) are determined by a classical random process $F(\cdot)$ in Eq. (1.4).

$$\langle e^{i\phi} \rangle \propto e^{-t/\tau_\phi}. \quad (1.3)$$

That defines a “dephasing time” τ_ϕ . In other cases, one often simply chooses to define τ_ϕ by the condition $\langle \phi^2(\tau_\phi) \rangle = 1$, although the usefulness of such a definition depends on whether the function describing the temporal decay has a single time scale associated to it. A counter-example would be a power-law decay in time, $\propto t^{-\gamma}$.

As another simple example of dephasing, we will now discuss a spin in a fluctuating magnetic field, i.e. a two-level system subject to noise. In general, the spin will be acted upon by a fixed magnetic field as well, for example in an NMR experiment. Then, it is obviously important whether the fluctuating component of the field points along the static field or perpendicular to it. In the first case, the Hamiltonian of the two-level system is given by:

$$\hat{H} = \frac{\Delta}{2} \hat{\sigma}_z + F(t) \hat{\sigma}_z. \quad (1.4)$$

Here we have assumed the fluctuating field F to be represented by a *classical* random process, such that the Hamiltonian is actually time-dependent. This description is good at higher temperatures or for nonequilibrium noise, but it fails at low temperatures, where F has to be treated quantum-mechanically (see Section 2.2.1). Nevertheless, it allows us to point out the most important features: The energy difference between the two levels fluctuates, as it is given by $\Delta + 2F(t)$ at each instant of time (see Fig. 1.2). Therefore, if one starts out from a coherent superposition

$$\frac{1}{\sqrt{2}}(|+\rangle + |-\rangle) \quad (1.5)$$

of the two levels at $t = 0$, the state at time t will be given by

$$\frac{1}{\sqrt{2}} \left(e^{-i(\Delta t + \phi(t))/2} |+\rangle + e^{i(\Delta t + \phi(t))/2} |-\rangle \right), \quad (1.6)$$

where the random phase ϕ is the time-integral over the fluctuating component of the energy difference:

$$\phi(t) = 2 \int_0^t dt' F(t'). \quad (1.7)$$

The situation considered here may be called “pure dephasing”, since the only effect of the fluctuations is to randomize the relative phase between the two states, not to induce any transitions. It will form the basis for a substantial part of the work described in this thesis (Chapters 2 and 3).

Any observable that depends on the coherence between $|+\rangle$ and $|-\rangle$ (such as the components of the spin perpendicular to z) will be affected. For example, the expectation value of the x component is

$$\langle \hat{\sigma}_x \rangle(t) = \cos(\Delta t + \phi(t)), \quad (1.8)$$

for a given particular realization of the random process $F(\cdot)$. After averaging over $F(\cdot)$, i.e. over the fluctuating phase difference $\phi(t)$, one observes decaying oscillations, since the different spins in the ensemble get out of phase in the course of time:

$$\langle \langle \hat{\sigma}_x \rangle(t) \rangle = \cos(\Delta t) e^{-\frac{1}{2} \langle \phi^2(t) \rangle}. \quad (1.9)$$

The outer bracket stands for averaging over $F(\cdot)$, and we have assumed $F(\cdot)$ to be a Gaussian random process, in order to be able to apply Eq. (1.2).

The strength of dephasing will be reduced whenever it is likely that positive fluctuations of F will be followed by negative fluctuations, because then their effects on the phase cancel. Formally, this may be observed most easily by noting that the variance of the phase is directly connected to the correlation function of the field F :

$$\langle \phi(t)^2 \rangle = 4 \int_0^t dt_1 \int_0^t dt_2 \langle F(t_1) F(t_2) \rangle. \quad (1.10)$$

If the correlation function decays sufficiently rapidly, we may approximate this in the long-time limit as

$$\langle \phi(t)^2 \rangle \approx 4t \int_{-\infty}^{+\infty} ds \langle F(s) F(0) \rangle, \quad (1.11)$$

such that the decay rate will be given by the time-integral over the correlation function. This will be reduced if the positive contribution at $s = 0$ is compensated by negative tails. These things can be seen most clearly with the help of the power spectrum of the fluctuations, which is defined as the Fourier transform of the correlator:

$$\langle FF \rangle_\omega \equiv \frac{1}{2\pi} \int_{-\infty}^{+\infty} dt e^{i\omega t} \langle F(t) F(0) \rangle. \quad (1.12)$$

In terms of this spectrum, the decay rate is determined by the zero frequency component:

$$\langle \phi(t)^2 \rangle \approx 8\pi \langle FF \rangle_{\omega=0} t. \quad (1.13)$$

The other important possibility consists in the fluctuating magnetic field being perpendicular to the static field. Then, we have a Hamiltonian of the form

$$\hat{H} = \frac{\Delta}{2} \hat{\sigma}_z + F(t) \hat{\sigma}_x, \quad (1.14)$$

and there will be transitions between $|+\rangle$ and $|-\rangle$ induced by F . In the case of a classical noise field F , this corresponds to induced absorption and emission, both proceeding at an equal rate which may be determined using Fermi's Golden Rule in the case of weak coupling. This rate is determined by the power spectrum of F , evaluated at the transition frequency $\omega = \Delta$. Therefore, in contrast to the previous case of “pure dephasing”, the physical picture does not depend qualitatively on the low-frequency properties of the bath spectrum (as long as the coupling is weak enough).

In a quantum-mechanical treatment, \hat{F} is actually to be taken as an operator that describes some variable of the environment. For example, in the case of crystal lattice vibrations, \hat{F} may denote the deviation of an atom from its equilibrium position. In the context of quantum dissipative systems, the environment is often called a “bath”, since it takes the role of a heat bath which forces the system to relax to equilibrium and to “lose its phase”. The Hamiltonian of the bath is to be included in the full Hamiltonian \hat{H} , such that the combined time-evolution of “system” and “bath” is unitary. If the bath consists of a collection of harmonic oscillators (e.g. the normal modes of a crystal lattice or of the vacuum electromagnetic field), then the quantum-mechanical version of a Hamiltonian like (1.4) or (1.14) is an example of the so-called “spin-boson model” [Leggett87, Weiss00].

In the quantum version of Eq. (1.14), the system relaxes into its ground state by spontaneous emission of energy into the bath, at $T = 0$.

1.2 Dephasing involves measurement

In the previous section a classical picture of the noise has been used, and dephasing is introduced by the random fluctuations of the phase which are a consequence of the fluctuating external field acting on the system. However, at low temperatures the bath is to be treated quantum-mechanically, such that the field cannot be described as a classical random process any longer. Then, it is often useful to change the perspective and to ask what happens to the quantum-mechanical state of the bath when it is acted upon by the force which is due to the system [Stern90]. In the example of the two wave packets traveling along different paths, the bath will end up in either of two states $|\chi_1\rangle$ or $|\chi_2\rangle$, depending on which way the electron has traveled. After taking the trace over the bath

degrees of freedom, which corresponds to averaging over the classical fluctuating field, the interference term of Eq. (1.1) will be changed into (compare Chapter 5):

$$2 \operatorname{Re} [\Psi_1^*(x) \Psi_2(x) \langle \chi_1 | \chi_2 \rangle] . \quad (1.15)$$

Therefore, the suppression factor $\langle \exp(i\phi) \rangle$ is now replaced by the overlap of the two bath states (which is also a number of magnitude not larger than one). If the bath is able to distinguish easily between the two paths that the electron takes, the bath states will differ strongly, such that the overlap is very small and the interference is suppressed. In such a case, the bath acts like a measuring device (or “which-way detector”), which determines the path of the electron and therefore destroys the interference pattern. The state of the electron (system) and that of the bath have become entangled.

Although this result is intuitively appealing, there are several important caveats: First of all, this simple picture assumes the two paths are sufficiently separated (compared to the extent of each wave packet), such that the quantum fluctuations around these paths do not play a role and we only have to calculate two different bath states. Therefore, this is essentially a semiclassical picture, as far as the treatment of the system-bath interaction is concerned. Furthermore, it neglects the backaction of the bath onto the system. This backaction will lead to effects like a renormalization of the particle’s effective mass or the external potential, which will change the time-evolution of the wave packets themselves. More importantly, the final bath states will be excited states in general, such that the energy for this excitation will have to be provided by the system, leading to energy relaxation (friction) within the system. In particular, if the system itself is a Fermi system at low temperatures, this relaxation may be prohibited by the Pauli principle, resulting in a suppression of dephasing. Finally, the formation of an entangled state of system and bath does not necessarily imply dephasing. In some situations, the bath states may be nearly orthogonal as long as the wave packets are separate, but they will evolve back towards the same state once the wave packets approach each other and form an interference pattern. This will be the case if the bath is sufficiently fast, such that it can adapt instantaneously to the presence of the particle. This fact is illustrated in the next section. The most well-known example is provided by the coupling of an electron to optical phonons, where the resulting lattice distortion (i.e. the polaron) follows the motion of the electron adiabatically.

All of these points will be made more explicit in concrete examples throughout this thesis.

1.3 Entanglement does not imply dephasing

When the system is coupled to a bath, it is no longer in a “pure” quantum-mechanical state. Instead, it has become entangled with the bath, which acts as a sort of measurement device, as has been emphasized in the previous section. Therefore, the state of the system itself has become a “mixed” state, which is described by the reduced density matrix of

the system. However, this fact may be completely unrelated to dephasing, which can be seen in a very simple example.

Consider a molecule made up out of two atoms. As long as the molecule remains in the ground state of its relative motion, it will act as a single quantum-mechanical particle that is able to show perfectly coherent interference effects. The total wave function of the two atoms at x_1 and x_2 splits into center-of-mass and relative motion:

$$\Psi(x_1, x_2) = \Psi_{CM}\left(\frac{x_1 + x_2}{2}\right)\Psi_{rel}(x_1 - x_2). \quad (1.16)$$

However, we might take the point of view that atom 1 is our “system” in question, which is coupled to a “bath” that consists of the other atom. The fact that this “bath” does not contain infinitely many degrees of freedom, and therefore does not usually lead to irreversible processes, is unimportant for the purposes of this example. The reduced density matrix of atom 1,

$$\rho(x'_1, x_1) = \int dx_2 \Psi(x'_1, x_2)\Psi^*(x_1, x_2), \quad (1.17)$$

decays as a function of the distance $|x_1 - x'_1|$, due to the decay of the relative wave function with respect to $|x_1 - x_2|$ (see Fig. 1.3). Therefore, the situation is qualitatively altered from that of an isolated atom in some extended pure state, where there is no such decay of the off-diagonal elements.

Nevertheless, whenever an interference experiment is done, the resulting interference pattern will not show any sign of dephasing. Of course, it will be different from what would have been obtained with a single atom in the same setup, because the total mass of the molecule is larger and its interaction with external potentials may be different. From the point of view taken here, this only amounts to a renormalization of the effective mass and the effective potential for atom 1. If the detector only accepts atom 1 (as this is considered to be the “system” in our model), the interference pattern will appear smeared to a small extent, since it is perfect only with respect to the center-of-mass coordinate, around which atom 1 fluctuates. However, this effect does not become stronger with increasing length of the interference paths traveled by the molecule, in contrast to what would be expected if it were a genuine dephasing effect. Moreover, it becomes *less* important for increased interaction strength (tighter binding), although then the decay of the off-diagonal elements of the density matrix (with respect to the relative coordinate) is even stronger. Therefore, this simple example shows why the appearance of a strongly mixed state (described by the reduced density matrix of the system), as well as the resulting fluctuations in the momentum or energy of the system alone, are not to be taken, by themselves, as signs of dephasing.

It should also be mentioned that the decrease in visibility of the interference pattern described here depends on the method of detection. The conclusions presented above hold only for a “fast” detector, such as an idealized von Neumann projection measurement (realized approximately by a fast particle hitting a screen). If the detection is carried

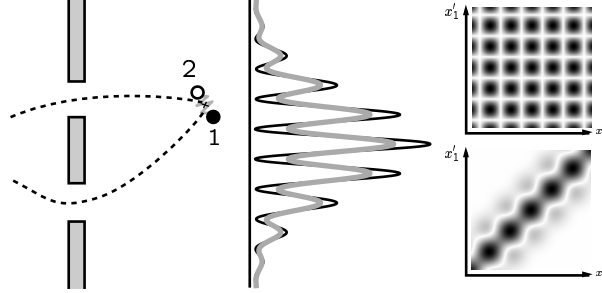


Figure 1.3: The center-of-mass coordinate of a molecule will show perfectly coherent interference (black line). If only the “system”, atom 1, is detected, the pattern is blurred on the scale of the binding length (gray line). To the right, the reduced density matrix $\rho(x'_1, x_1)$ of atom 1 is shown without (top) and with (bottom) coupling to the other atom, for a superposition of plane waves: $\Psi(x_1) \propto \cos(kx_1)$ for the atom alone, and $\Psi(x_1, x_2) \propto \cos(k(x_1 + x_2)/2) \exp(-((x_1 - x_2)/\sigma)^2)$ for the molecule ($k\sigma = 3$; darker gray values indicate larger $|\rho|$).

out such that there is only a weak coupling to atom 1 and only a small amount of energy is transferred to the system, then the detector effectively acts on the complete molecule as a whole. Thus, the results may be qualitatively different, possibly leading to an enhancement of the visibility of the interference pattern. Such an effect is actually observed in models of transport interference experiments at low temperatures and bias voltages, such as those discussed in Chapters 2 and 3 of this thesis.

1.4 Fluctuating environments

Any system with infinitely many degrees of freedom may take the role of an environment which leads to irreversible relaxation and dephasing when coupled to a quantum-mechanical system.

In particular, for an electron, the fluctuating force may be due to electric or magnetic fields. An electron moving through free space or around the nucleus of an atom is acted upon by the fluctuations of the electromagnetic field in vacuum. For the atom, this leads to spontaneous emission, giving a finite natural linewidth of the atomic levels. In free space, energy and momentum conservation preclude emission of radiation, unless the electron is accelerated or decelerated by some external force.

Inside a metal or a semiconductor, the electron feels the fluctuating electric field generated by all the other electrons and ions. This includes the coupling to the vibrating crystal lattice, i.e. electron-phonon scattering, as well as electron-electron scattering. In a dirty sample, the equilibrium electric field fluctuations due to the motion of the other electrons represent the Nyquist noise, which at low frequencies is qualitatively stronger

than the noise in a clean sample, since the charge redistribution proceeds only slowly, in a diffusive manner. In the context of mesoscopic physics [Imry97], where one studies interference effects in micrometer-sized electronic circuits, the electric field fluctuations may also originate from the Nyquist noise in a nearby gate that is used to control the static potential felt by the electrons. If a current runs through the system, the shot noise will be an additional source of dephasing. In most investigations of dephasing in mesoscopic systems, one tries to go to the linear response regime, where the applied bias voltage is sufficiently low, such that effects of shot noise or electron heating do not play a role. However, there have also been experiments in which such nonequilibrium dephasing has been introduced deliberately, by capacitively coupling a quantum dot to a current-carrying wire that acts both as a detector of charge on the dot and as a source of shot noise [Buks98, Aleiner97]. Equilibrium and nonequilibrium current noise will also lead to fluctuations of the magnetic field, which can influence interference effects mainly via the Aharonov-Bohm phase.

Scattering off magnetic impurities, leading to spin flips, is another very important source of dephasing. If there is no static magnetic field, the spin levels are degenerate, such that this corresponds essentially to an environment with a power spectrum that has all its strength concentrated at zero frequency. This is a particularly powerful dephasing mechanism, as no energy transfer between system and bath is needed. Only at sufficiently low temperatures these spins will be screened by the Kondo effect, such that they become inert. Likewise, the electron may scatter off nonmagnetic two-level systems, which can form when an electron or an ion at a defect site can tunnel between two adjacent positions.

1.5 Interference effects and measures of dephasing

There is no general definition of dephasing and no single measure of its strength. However, in all cases dephasing is ultimately recognized by looking at some measurable quantity and concluding that it deviates from its “ideal” behaviour, which would be observed without coupling to a fluctuating environment and which should depend on some quantum-mechanical interference effect.

Regarding simple systems with discrete levels, the linewidth observed in spectroscopy can be taken as a measure of the dephasing rate, as it is not only affected by energy-relaxation processes but also by the “pure dephasing” mentioned previously. Turning to nonlinear response, one may prepare a two-level system in a coherent superposition of ground state and excited state by applying a suitable pulse of resonant radiation (Rabi pulse). After a time span of free evolution, another such pulse may be used to bring back the system to its ground state, provided its intermediate time-evolution has been fully coherent. The dependence of the ground state population after the second pulse on the intermediate time interval will show an interference pattern (Ramsey fringes) whose decay is due to dephasing. The decay time for this case is not necessarily simply related to that determined by spectroscopy (a simple relation only holds if a master equation description

applies).

The interference pattern in any kind of double-slit experiment will be blurred due to dephasing, as has been explained above in a simple example. However, it must be kept in mind that the interaction with the environment may also renormalize properties of the particle or the effective potential that acts on the particle. This will alter the pattern as well, and it is an important task to disentangle the effects of dephasing from “mere renormalization” (see the discussion in Sections 1.2 and 1.3).

For electrons in mesoscopic systems, there are interference setups like an Aharonov-Bohm ring, where the current through the device depends periodically on the applied magnetic flux (see Chapter 3). In such devices, deviations of the interference pattern from its “ideal” shape will often occur because of inaccuracies in the geometry or the presence of impurities. More importantly, at finite temperatures the Fermi surface becomes smeared and the resulting average over a range of electronic wavelengths decreases the visibility of the interference pattern. It requires some effort to distinguish this effect from temperature-dependent dephasing (see [Hansen01] for an experiment in which this analysis was performed).

Although the elastic scattering from impurities changes the interference pattern, it does not really destroy the interference itself and is unrelated to dephasing [Imry97]. It is completely analogous to the scattering of monochromatic light in a disordered medium. This will lead to a complicated “speckle pattern”. Since the conductance of a phase-coherent sample depends on the probability of transmission through the sample, it is determined by the details of the interference pattern brought about by the particular arrangement of impurities. Changes in the Fermi wavelength or an applied magnetic field alter the phases of the different interfering paths and lead to reproducible, sample-specific fluctuations of the conductance. As these fluctuations turn out to be of the same size generically, given by the conductance quantum $2e^2/h$, they are termed “universal conductance fluctuations”. If the size of contributing interference paths is very large, then a very small change in magnetic field δB is sufficient to appreciably alter the conductance, since it will completely change the Aharonov-Bohm phase for these paths. Therefore, δB may be taken as a measure of dephasing, since it can be used to determine the typical length L_ϕ of paths that are still able to interfere.

Another important mesoscopic interference effect is the phenomenon of “weak localization” [Kramer93], where the resistance of the sample is (usually) enhanced beyond its classical value due to constructive interference of electron waves that have been scattered off the impurities in the disordered sample. This is analogous to the “coherent backscattering” of radiation from any kind of disordered medium. The effect depends crucially on the constructive interference between pairs of time-reversed scattering paths. Therefore, the application of a magnetic field will suppress weak localization, as the resulting Aharonov-Bohm phase will fluctuate randomly for long paths that enclose more than a flux quantum $\Phi_0 = hc/e$. However, if the magnetic field is so weak that the respective path lengths would have to be longer than the dephasing length L_ϕ , these paths do not contribute to the effect anyway. Therefore, the magnetic field dependence of the conduc-

tance may be used to extract the dephasing length L_ϕ or an associated dephasing time τ_ϕ . In contrast to the interference effects mentioned previously, the weak-localization effect is not affected by thermal averaging.

As the temperature gets lower, thermal fluctuations of the environment get weaker, ultimately vanishing at $T = 0$. This means that the strength of dephasing decreases with decreasing temperature. For this reason, it has come as a surprise when a saturation of the dephasing time at low temperatures was observed some years ago [Mohanty97a, 97b,01] in a set of careful weak localization experiments. Such a saturation had been measured in previous experiments as well. However, in the new experiments considerable effort was made to rule out extrinsic effects such as heating of the sample by the current, external microwave noise or the presence of magnetic impurities.

As the “orthodox” theory of dephasing in weak localization [Altshuler82, Chakravarty86] predicts a vanishing dephasing rate at $T = 0$, these results have stirred a considerable controversy. It was suggested [Mohanty97a, 97b] that zero-point fluctuations of the environment may be responsible for the findings, as they are present even at zero temperature. A theory has been developed that maintains the finite dephasing rate at $T = 0$ to be a nonperturbative consequence of electron-electron interaction [Golubev98, 99,02a]. Qualitatively, it is consistent with the suggestion about the role of zero-point fluctuations. It deviates strongly from the established theory at low temperatures and has been the subject of severe criticism [Aleiner99, Vavilov99, Imry02]. A number of suggestions for “extrinsic effects” have been put forward to explain the experimental observations [Aleiner99, Zawadowski99, Imry99], such as $1/f$ noise due to two-level fluctuators or weak nonequilibrium noise that does not heat the sample appreciably but leads to a saturation of the dephasing rate. Subsequent experiments [Gougam00, Natelson01] seem to be partly in contradiction with a generic saturation of the dephasing rate at low temperatures, although that also seems to depend on the interpretation of the measurement results [Golubev01]. In summary, the experimental results of [Mohanty97a, 97b] have not yet been explained convincingly. In addition, a possible saturation of the dephasing rate has also been reported for transport through quantum dots (see, e. g. [Pivin99]).

1.6 Some important questions

This controversy has led to renewed interest in dephasing of mesoscopic systems, particularly at low temperatures. Some questions of importance are the following ones:

How reliable is the simple classical picture of a phase being randomized by fluctuating external noise? In particular, what is the meaning of the zero-point fluctuations of the bath in this picture, as opposed to the thermal fluctuations dominating at frequencies lower than the temperature? When do the former lead to “mere renormalization effects” and how is it possible to distinguish these from “true” dephasing? Under which circumstances is the suppression of off-diagonal terms in the reduced system density matrix itself already a good indicator of dephasing? How reliable are simple arguments based

on Golden Rule and energy conservation, related to the connection between dephasing and the trace left in the bath by the particle (“which-way” detection)? When does perturbation theory fail qualitatively? How does the dephasing rate depend on the energy supplied by an external perturbation (frequencies excited in linear response, bias voltage applied in a transport measurement)? What is the influence of the Pauli principle in a system of degenerate fermions on these effects? How strong are the qualitative differences in behaviour resulting from different bath spectra?

1.7 The role of simple model systems

Apart from investigations dealing directly with the problem of weak localization in a disordered system of interacting electrons, several “toy models” have been analyzed [Cedraschi00, Zaikin00, Nagaev02, Guinea02, Golubev02d] to address the question whether decoherence at zero temperature is possible at all, contrary to the expectations based on perturbation theory.

One of the difficulties faced by models involving discrete levels consists in the fact that destruction of phase coherence for a superposition of excited states of finite excitation energy is perfectly possible even at zero temperature, due to spontaneous emission of energy into the bath. An example is provided by an atom that has been prepared in a coherent superposition of ground state and excited state. After some time, this superposition will have been destroyed, because the atom in the excited state has relaxed by spontaneous emission of a photon. This may be viewed as a consequence of the zero-point fluctuations of the vacuum electromagnetic field acting on the atom (in addition to the radiation reaction [Milonni94]). Therefore, “zero-temperature dephasing” is rather the rule than the exception in such systems, whose coherence is studied in quantum computing, for example. It is apparent in the finite decay rate of the correlator of the atom’s dipole moment or similar quantities. However, if one were to reduce the level separation, the Golden Rule decay rate would decrease as well, due to the decrease of the bath spectrum at low frequencies, finally vanishing in the limit of zero level distance.

It is only in the zero-frequency limit of the linear response in a system with a continuous spectrum (relevant for weak-localization and other linear transport interference experiments) that perturbation theory suggests in general a vanishing dephasing rate, because then the external perturbation does not supply energy to the system. Therefore, at $T = 0$ the system is not able to leave a trace in the bath (at least according to this simple picture), which is a prerequisite for decoherence. Consequently, in several of the models analyzed in this thesis, we have taken care to emphasize such features.

In Chapter 2, we will analyze dephasing in tunneling transport through localized levels coupled to a bath, both for sequential tunneling and cotunneling. Although we are still dealing with discrete levels, the tunnel coupling of these levels to the electron states in the reservoirs introduces aspects of continuous spectra and enables us to discuss in particular the behaviour in the limit of a vanishing energy supply (vanishing bias voltage

and temperature). The Pauli principle comes into play indirectly, due to the blocking of final states in the tunneling process. In Chapter 3, we discuss a model system of a clean Aharonov-Bohm ring subject to a fluctuating magnetic flux. This is a kind of generalization of Quantum Brownian motion to the many-particle case. For the model of fermions in a damped harmonic oscillator (Chapter 4), the Pauli principle is also essential in the dynamics of the isolated system itself, since the bath can induce transitions between different levels, which may be blocked by the presence of other fermions.

Although the models analyzed in this thesis do not address the problem of dephasing in weak localization itself, they do confirm that there is no hint of a “generic” mechanism leading to dephasing at zero temperature, in contrast to what had been suggested in the wake of the experimental findings on a possible saturation of the dephasing rate (see above). In Chapter 5, we analyze in more detail the difficulties encountered in an application of the Feynman-Vernon influence functional to dephasing at low temperatures, which may be at the origin of the theoretical findings supporting the notion of generic zero-temperature dephasing in weak localization.

Chapter 2

Dephasing in tunneling through localized levels

2.1 Introduction

The most obvious situation to consider when analyzing interference effects and their destruction via dephasing is a double-slit experiment or some variation on this theme, like the Mach-Zehnder interferometer. The analysis is relatively straightforward if we deal with single photons, electrons, neutrons or atoms that pass through such a setup. In these examples, the dephasing mechanisms include fluctuations in the refractive index, absorption of photons, and fluctuations of the electric or magnetic field. In all of these cases, we need to consider only a single particle at a time. Furthermore, this particle is far above its ground state. Therefore, zero-point fluctuations of the environment will definitely be able to spoil the coherence: spontaneous emission may take place, when the particle transfers part of its energy to the bath, revealing its trajectory. In the example of a single electron flying through an interference setup, this might be the “bremsstrahlung” associated with the scattering from some potential (although the resulting dephasing effect can be estimated to be extremely weak in realistic situations).

On the other hand, in a mesoscopic electronic transport interference experiment, we usually have to care about the presence of the other electrons in the sample. In particular, the Pauli principle may become important at lower temperatures, blocking transitions that would otherwise have been induced by the coupling to the bath. Therefore, we are led to a many-body problem, beyond that associated with the infinite number of bath degrees of freedom. A full analysis of interacting electrons in a nontrivial interference geometry (like the Mach-Zehnder setup) represents a very difficult problem, even within the Luttinger model of interacting electrons in one dimension, which is exactly solvable only for the case of pure forward-scattering.

In the present work, we have chosen to consider the simpler case of tunneling through localized levels coupled to a bath. Then, the analysis simplifies at least in the regime of small tunnel coupling, when tunneling may be treated as a perturbation while the

interaction with the bath is taken into account completely. In the case of tunneling through a double-dot configuration, the closest optical analogy would be a Mach-Zehnder interference setup with Fabry-Perot cavities placed inside each interferometer arm. In this analogy, dephasing would be brought about by fluctuations of the refractive index inside the cavities, or simply fluctuations of the geometrical distance between the mirrors. Apart from the double-dot geometry, we will also discuss tunneling through the discrete levels on an Aharonov-Bohm ring coupled to a fluctuating magnetic flux (Chapter 3), which is amenable to the same kind of analysis. In both cases, the coupling of the bath to the electrons on the localized levels is diagonal, i.e. it does not induce transitions between the different levels. This is called the “independent boson” model, which will be introduced in the next section.

In all of the following discussion, we will be interested in dephasing of the electronic motion alone. This has been the subject of attention in the debate on low-temperature dephasing in weak-localization. We do not consider the electron’s spin degree of freedom. This would be important both as a system to be dephased (with applications in quantum information theory), as well as a kind of bath that may lead to dephasing itself (in the form of localized spins).

2.2 Preliminaries

In this section, we will introduce the “independent boson” model, which forms the basis both for the analysis of dephasing in the double-dot setup, as well as in the Aharonov-Bohm ring. The discussion will be rather detailed, because it provides much of the background for later sections.

2.2.1 Spin-boson model with diagonal coupling

We start the discussion with the simplest version of the spin-boson model, which is obtained if one assumes the coupling between spin and bath to be diagonal in the energy eigenbasis of the spin [Weiss00]. This is the generalization of (1.4) to a quantum field \hat{F} :

$$\hat{H} = \frac{\Delta}{2} \hat{\sigma}_z + \hat{\sigma}_z \hat{F} + \hat{H}_B. \quad (2.1)$$

The fluctuating field \hat{F} is assumed to be linear in the coordinates (and momenta) of the set of harmonic oscillators described by \hat{H}_B . As explained previously, it will lead to fluctuations in the energy difference of the two levels, which give rise to dephasing of an initially coherent superposition of these states. However, it does not transfer population from one level to the other, i.e. there is no energy relaxation associated with this kind of coupling to the environment. In this sense, it represents an example of “*pure dephasing*”. The diagonally coupled spin-boson model is still exactly solvable, although it already leads to nontrivial results for the time-evolution of the density matrix. These results usually cannot be understood any more in terms of the simple Golden Rule calculation of decay rates. It turns out that the power spectrum of the fluctuations in \hat{F} is decisive for the qualitative long-time behaviour of the density matrix. In fact, this model represents an example where the deviation from exponential decay is most pronounced. This is in contrast to the case of non-diagonal coupling, where exponential decay takes place generically and its rate may be calculated from the Golden Rule in the appropriate regime of weak coupling and short bath correlation time. The diagonally coupled model corresponds in many respects to a free particle coupled to a linear bath (“Quantum Brownian motion” in the case of the “Ohmic” bath), while the non-diagonal model is rather similar to a damped harmonic oscillator. Moreover, the mathematics of the diagonally coupled spin-boson model is directly connected to the independent boson model, to the “ $P(E)$ theory” of tunneling in a dissipative environment, and to the Luttinger model of interacting electrons in one dimension.

The fluctuations of \hat{F} may be characterized completely by prescribing the spectrum $\langle \hat{F} \hat{F} \rangle_\omega^{T=0}$ at zero temperature:

$$\langle \hat{F}(t) \hat{F}(0) \rangle^{T=0} = \int_0^\infty d\omega \langle \hat{F} \hat{F} \rangle_\omega^{T=0} e^{-i\omega t}. \quad (2.2)$$

As usual, it is understood that the expectation value is to be taken with respect to the bath Hamiltonian \hat{H}_B alone, prior to coupling to the system. In the following, we will refer to $\langle \hat{F}\hat{F} \rangle_\omega^{T=0} \geq 0$ as the “bath spectrum”. Since we are dealing with a *linear* bath (i.e. a bath of harmonic oscillators), the bath spectrum contains enough information to deduce the behaviour of the system under the action of the bath at any temperature, for arbitrarily strong coupling. At finite temperatures, the correlator of \hat{F} is given by

$$\langle \hat{F}(t)\hat{F}(0) \rangle = \int_0^\infty d\omega \langle \hat{F}\hat{F} \rangle_\omega^{T=0} ((2n(\omega) + 1) \cos(\omega t) - i \sin(\omega t)). \quad (2.3)$$

The strength of the fluctuations $\langle \{ \hat{F}(t), \hat{F}(0) \} \rangle / 2$ is given by the real-valued time-symmetric (cosine) part of the correlator. It grows as $2n(\omega) + 1 = \coth(\omega/2T)$, with the Bose-distribution function $n(\omega) = 1/(\exp(\beta\omega) - 1)$, where $\beta = 1/T$ and $\hbar \equiv k_B \equiv 1$. In contrast, the response of the linear bath is determined, via Kubo’s formula, by the commutator $\langle [\hat{F}(t), \hat{F}(0)] \rangle / 2$, which is equal to the imaginary antisymmetric (sine) part. It is temperature-independent, since it is only determined by the masses and spring constants of the oscillators.

Given the bath spectrum, we may calculate the time-evolution of the spin’s reduced density matrix for an initial state that consists in a coherent superposition of the two energy eigenstates, $|-\rangle$ and $|+\rangle$. In the simplest situation, bath and system have been independent prior to $t = 0$, such that the total initial density matrix factorizes into that of the system, $\hat{\rho}_0^S$, and the thermal equilibrium density matrix of the bath, $\hat{\rho}_{eq}^B$. Since the populations remain unchanged, we have to consider only the off-diagonal term,

$$\rho_{+-}^S(t) \equiv \text{tr}_B \langle + | \hat{U}(t) \hat{\rho}_0^S \otimes \hat{\rho}_{eq}^B \hat{U}^\dagger(t) | - \rangle, \quad (2.4)$$

where tr_B denotes the trace over the bath degrees of freedom and \hat{U} is the time-evolution operator for the full Hamiltonian \hat{H} . Now the important simplification brought about by the diagonal coupling is that it does not lead to transitions between energy eigenstates of the system. Therefore, we have

$$\langle + | \hat{U}(t) | + \rangle = e^{-i\frac{\Delta}{2}t} \hat{U}_+(t), \quad (2.5)$$

where $\hat{U}_+(t) = \exp(-i\hat{H}_+t)$ describes the time-evolution of the bath under the influence of the system being in the state $|+\rangle$, with an analogous formula for the state $|-\rangle$:

$$\hat{H}_\pm = \pm \hat{F} + \hat{H}_B. \quad (2.6)$$

The problem has been reduced to one concerning only the bath degrees of freedom:

$$\rho_{+-}^S(t) = \rho_{+-}^S(0) e^{-i\Delta t} \text{tr}_B [\hat{\rho}_{eq}^B \hat{U}_-^\dagger(t) \hat{U}_+(t)]. \quad (2.7)$$

The trace in this formula represents the thermally averaged overlap between the two different bath states which evolve out of the initial bath state under the influence of the system being either in state $|-\rangle$ or $|+\rangle$ (compare the discussion in Section 1.2). It is the simplest example of the Feynman-Vernon influence functional, where, in the general case, the time-evolution of the bath under the influence of an arbitrary system trajectory has to be evaluated (see Chapter 5). Going over to the interaction representation with respect to \hat{H}_B , the trace is equal to

$$\text{tr}_B[\hat{\rho}_{eq}^B \hat{T} \exp(-i \int_0^t ds \hat{F}(s)) \hat{T} \exp(-i \int_0^t ds \hat{F}(s))] . \quad (2.8)$$

Here \hat{T} ($\hat{\bar{T}}$) is the (anti-)time-ordering symbol. In general, such an expression may be evaluated, for example, by introducing Keldysh time-ordering and using the linked-cluster expansion to obtain an exponential containing the correlator of \hat{F} (generalizing Eq. (1.2) to the quantum case). However, since we will solve the same kind of problem below using a canonical transformation, we only quote the result:

$$\exp \left[- \int_0^t dt_1 \int_0^t dt_2 \left\langle \left\{ \hat{F}(t_1), \hat{F}(t_2) \right\} \right\rangle \right] . \quad (2.9)$$

The exponent is given by a double time integral over the purely real symmetrized bath correlator, describing the fluctuations (including the zero-point fluctuations). This is a direct generalization of Eq. (1.10). In general, the magnitude of the exponent grows in time, such that the off-diagonal element $\rho_{+-}^S(t)$ of the density matrix is suppressed. However, whether it is suppressed completely down to zero in the course of time, and whether this decay is exponential or not, completely depends on the low-frequency behaviour of the bath spectrum. This point will be discussed further below. If there had been an additional imaginary part of the exponent, it would have signalled a shift of the transition frequency Δ brought about by the coupling to the bath. For the Hamiltonian given above, the transition frequency is unaltered, since both states couple to the bath with equal strength, such that their energies are shifted by the same amount.

2.2.2 Independent boson model

The simplest kind of extension of the diagonal spin-boson model obviously consists in considering more than just two levels, where each of them may couple to the bath fluctuations with a different coupling constant. This remains exactly solvable as long as the coupling remains diagonal in the energy eigenbasis of the system. More generally, we may take the different levels to couple to different fluctuating variables $\hat{F}_{1,2,\dots}$, which may refer to independent baths, but which may also be correlated. In the case discussed above, we had two fully anticorrelated variables, $\pm \hat{F}$. Finally, since we are interested in tunneling transport, the different levels may actually be single-particle states which can be occupied by a variable total number of particles. The most general Hamiltonian describing this kind of situation is

$$\hat{H} = \sum_j (\varepsilon_j + \hat{F}_j) \hat{n}_j + \hat{H}_B. \quad (2.10)$$

Here j is the level index, ε_j the unperturbed level energy, and $\hat{n}_j = \hat{d}_j^\dagger \hat{d}_j$ is the number of particles on level j . In all of the following, we will consider fermions (i.e. electrons). Again, the fluctuating variables \hat{F}_j are assumed to depend linearly on the coordinates (and momenta) of the bath oscillators described by \hat{H}_B . They have to be characterized by the spectra $\left\langle \hat{F}_l \hat{F}_j \right\rangle_\omega^{T=0}$, which are defined like in Eq. (2.2). In the following discussion of the general properties of this model, we will restrict ourselves to the case where the different variables commute, $[\hat{F}_l, \hat{F}_j] = 0$. As a consequence, the spectrum $\left\langle \hat{F}_l \hat{F}_j \right\rangle_\omega^{T=0}$ is real-valued. This represents only a slight restriction, since the different \hat{F}_l can still be correlated. If we think of a set of localized states coupling to the distortion field of a crystal lattice, this condition is fulfilled, since the charges only couple to the coordinates (not the momenta) of the lattice atoms.

The Hamiltonian (2.10) is known as the “independent boson model” [Mahan81]. One of its major (and earliest) applications is the ionization of an electron in a core-level of an atom by an impinging X-ray. Since the electron charge couples via the Coulomb force to the sea of other electrons, these will rearrange after a hole has been created inside the atom. The density fluctuations of the electrons are described approximately by a harmonic oscillator bath of the Ohmic fluctuation spectrum (see 2.2.5), such that one ends up with (2.10), for the special case of a single level, and with \hat{F} representing the potential energy of the given electron in the field of the other electrons. The coupling to the bath of other electrons modifies the spectral density of the single level, which is visible in the X-ray absorption spectrum. The Hamiltonian given above also arises in the discussion of dephasing for a set of localized states, if the coupling to the bath (e.g. a fluctuating gate voltage) cannot induce tunneling between these levels.

Most parts of the following discussion of the independent boson model can be found in the book of [Mahan81], for the case of a *single* particle occupying any of the given states.

The most straightforward solution proceeds via a unitary transformation. One introduces the fluctuating phases $\hat{\phi}_j$, whose time-derivatives are given by the \hat{F}_j :

$$\dot{\hat{\phi}}_j \equiv i[\hat{H}_B, \hat{\phi}_j] = -\hat{F}_j. \quad (2.11)$$

The exponent generating the unitary transformation is defined as:

$$\hat{\chi} = \sum_j \hat{\phi}_j \hat{n}_j. \quad (2.12)$$

Applying the transformation to the Hamiltonian in Eq. (2.10) yields:

$$\hat{H}' = e^{-i\hat{\chi}} \hat{H} e^{+i\hat{\chi}} = \sum_j \varepsilon_j \hat{n}_j - \sum_{lj} J_{lj} \hat{n}_l \hat{n}_j + \hat{H}_B. \quad (2.13)$$

The coupling between system and bath has been eliminated, resulting in an effective interaction between particles on the different levels. Physically, this interaction may be understood most easily in the case of coupling to a crystal lattice: The presence of a particle on any level distorts the lattice, in such a way that the overall energy is reduced. Although the distortions produced by different particles superpose linearly, the associated energies do not. However, this Ising-type interaction is still comparatively simple, insofar as it does not lead to transitions between the different levels. It is similar to the mean-field interaction between quasiparticles in Landau's Fermi liquid theory. The coupling constants are given by:

$$J_{lj} = \int_0^\infty d\omega \frac{\langle \hat{F}_l \hat{F}_j \rangle_\omega^{T=0}}{\omega}. \quad (2.14)$$

They are real-valued and independent of temperature. The effective interaction reduces to a simple energy shift for each level separately only in two cases: Either there is at most one particle in the system, or the \hat{F}_j are uncorrelated, i.e. each level couples to a different bath. Then, only the contributions $l = j$ remain, and we can use $\hat{n}_j^2 = \hat{n}_j$, since we are dealing with fermions.

If this kind of effective interaction were the only change brought about by coupling to the bath, there would be no dephasing. The problem would have become quite simple, apart from calculating the partition function, which would still amount to an Ising problem with arbitrary couplings. However, the canonical transformation also changes the particle annihilation and creation operators,

$$\hat{d}'_j = e^{-i\hat{\chi}} \hat{d}_j e^{i\hat{\chi}} = e^{i\hat{\phi}_j} \hat{d}_j, \quad (2.15)$$

and $\hat{d}'_j^\dagger = \hat{d}_j^\dagger e^{-i\hat{\phi}_j}$. This will affect all Green's functions and, therefore, also the time-evolution of the single-particle density matrix. In addition, it becomes important if a tunneling part is added to the Hamiltonian, where the operators $\hat{d}_j^{(\dagger)}$ appear, such that they have to be transformed according to (2.15). However, since the phases $\hat{\phi}_j$ and the particle operators $\hat{d}_j^{(\dagger)}$ commute (even at different times, when evolved according to \hat{H}'), the evaluation of Green's functions always splits into a part referring to the particles and a separate average over the bath operators. This is the major simplification brought about by the diagonal coupling, and we have discussed it already in connection with the diagonal spin-boson model.

2.2.3 Single-particle Green's function

As an important example, consider a single-particle Green's function like:

$$\langle \hat{d}_j(t) \hat{d}_j^\dagger(0) \rangle = \text{tr}[\hat{\rho} e^{i\hat{H}t} \hat{d}_j e^{-i\hat{H}t} \hat{d}_j^\dagger]. \quad (2.16)$$

Here $\hat{\rho} = \exp(-\beta\hat{H})/Z$ is a canonical density matrix. If a grand-canonical average is desired, the trace also refers to a sum over different particle numbers, \hat{H} in the exponent has to be replaced by $\hat{H} - \mu\hat{N}$, and $\hat{\rho}$ is the grand-canonical density matrix $\hat{\rho}_{gc} = \exp(-\beta(\hat{H} - \mu\hat{N}))/Z_{gc}$, normalized by the grand-canonical partition function Z_{gc} . Apart from that, nothing changes in the following derivation.

Introducing the unitary transformation from above, we find

$$\begin{aligned} \langle \hat{d}_j(t)\hat{d}_j^\dagger(0) \rangle &= \text{tr} \left[\frac{e^{-\beta\hat{H}'}}{Z} e^{i\hat{H}'t} \hat{d}_j' e^{-i\hat{H}'t} \hat{d}_j'^\dagger(0) \right] \\ &= \left\langle \hat{d}_j(t)\hat{d}_j^\dagger(0) \right\rangle_{el} \left\langle e^{i\hat{\phi}_j(t)} e^{-i\hat{\phi}_j(0)} \right\rangle. \end{aligned} \quad (2.17)$$

In the second line, the splitting into electronic and bath contributions has been performed. The bath average and the time-evolution of $\hat{\phi}_j$ are determined by \hat{H}_B alone. Furthermore, we have defined the electronic part as:

$$\left\langle \hat{d}_j(t)\hat{d}_j^\dagger(0) \right\rangle_{el} \equiv \text{tr} \left[\frac{e^{-\beta\hat{H}'_{el}}}{Z'_{el}} e^{i\hat{H}'_{el}t} \hat{d}_j e^{-i\hat{H}'_{el}t} \hat{d}_j^\dagger \right]. \quad (2.18)$$

Here $\hat{H}'_{el} \equiv \hat{H}' - \hat{H}_B$ contains the original energies of the single-particle levels as well as the effective interaction, and $Z'_{el} \equiv \text{tr} \exp(-\beta\hat{H}'_{el})$. Although there is no scattering between different levels, the electronic part is not simply related to the original Green's function (without interaction to the bath). Only in the case of a single particle, we have the relatively simple result

$$\left\langle \hat{d}_j(t)\hat{d}_j^\dagger(0) \right\rangle_{el} = \left\langle \hat{d}_j\hat{d}_j^\dagger \right\rangle_{el} e^{-i(\epsilon_j - J_{jj})t}. \quad (2.19)$$

This formula incorporates the shift of the level energy, $-J_{jj}$, as well as a possible change in the equilibrium occupation of the level due to this shift (in the grand-canonical case). In general, the energy of the extra particle in the field of the other particles will depend on the configuration of these particles, over which a thermal average has to be performed, according to Eq. (2.18). If the temperature is so low that only the ground-state configuration (assumed to be non-degenerate) contributes, we have

$$\left\langle \hat{d}_j(t)\hat{d}_j^\dagger(0) \right\rangle_{el} = \left\langle \hat{d}_j\hat{d}_j^\dagger \right\rangle_{el} e^{-i(\epsilon_j + \delta E_j)t}, \quad (2.20)$$

with a level shift determined by the occupation numbers $n_l = \langle \hat{n}_l \rangle$ in the ground state:

$$\delta E_j = -J_{jj} - 2 \sum_{l \neq j} J_{lj} n_l. \quad (2.21)$$

Turning now to the bath correlator in Eq. (2.17), we may evaluate it using the relation

$$\left\langle e^{\hat{A}} e^{\hat{B}} \right\rangle = e^{(\langle \hat{A}^2 \rangle + \langle \hat{B}^2 \rangle + 2\langle \hat{A}\hat{B} \rangle)/2}, \quad (2.22)$$

which is valid for operators \hat{A} and \hat{B} that are linear in the bosonic variables of the harmonic oscillator bath and have a vanishing expectation value. It is derived by employing the Baker-Hausdorff identity $e^{\hat{A}}e^{\hat{B}} = e^{\hat{A}+\hat{B}}e^{[\hat{A},\hat{B}]/2}$ and the relation $\langle e^{\hat{A}+\hat{B}} \rangle = e^{\langle (\hat{A}+\hat{B})^2 \rangle / 2}$ (see Appendix A.1). This yields the important formula:

$$\langle e^{i\hat{\phi}_l(t)} e^{-i\hat{\phi}_j(0)} \rangle = \exp(\langle \hat{\phi}_l(t) \hat{\phi}_j(0) \rangle - \langle \hat{\phi}_l \hat{\phi}_j \rangle) \equiv e^{K_{lj}(t)}. \quad (2.23)$$

In the evaluation of the Green's function (2.17), we have $l = j$:

$$\langle \hat{d}_j(t) \hat{d}_j^\dagger(0) \rangle = \langle \hat{d}_j(t) \hat{d}_j^\dagger(0) \rangle_{el} e^{K_{jj}(t)}. \quad (2.24)$$

The real part of the correlator $K_{jj}(t)$ in the exponent determines the decay of the single-particle Green's function. This decay is solely due to the fluctuations of the phase brought about by coupling to the bath, as the population of a level cannot change. The magnitude of $\exp(K_{jj}(t))$ is never larger than one, since it can be represented as a thermally averaged overlap of two different bath states (compare the discussion for the diagonal spin-boson model).

In order to evaluate $K_{lj}(t)$ in terms of the bath spectrum, we employ the relation (2.11) between the phase $\hat{\phi}_j$ and the fluctuating field \hat{F}_j :

$$\begin{aligned} K_{lj}(t) &= \int_{-\infty}^{\infty} d\omega \langle \hat{\phi}_l \hat{\phi}_j \rangle_{\omega} (e^{-i\omega t} - 1) \\ &= \int_{-\infty}^{\infty} d\omega \frac{\langle \hat{F}_l \hat{F}_j \rangle_{\omega}}{\omega^2} (e^{-i\omega t} - 1). \end{aligned} \quad (2.25)$$

The imaginary part of the exponent $K_{lj}(t)$ is determined by the linear response of the bath and describes the resulting shift of the system's energy. At short times we have $K_{lj}(t) = -itJ_{lj}$, since the antisymmetric part of the correlator is temperature-independent (compare (2.3)):

$$\langle \hat{F}_l \hat{F}_j \rangle_{\omega} = \langle \hat{F}_l \hat{F}_j \rangle_{|\omega|}^{T=0} (\theta(\omega) + n(|\omega|)). \quad (2.26)$$

Therefore, the term $K_{jj}(t)$ in the exponent compensates the contribution from the energy shift $+itJ_{jj}$ at short times, compare Eq. (2.19). It means that the particle's energy is not reduced instantaneously after it has entered the level: the bath first has to adapt to the presence of the extra particle. One might wonder why the same cannot be said about the contributions to the energy shift due to the interaction J_{lj} ($l \neq j$) with other particles, see Eq. (2.21). However, these derive from the energy of the additional particle in the field \hat{F}_j whose average has already been shifted to a nonzero value by the presence of the other particles.

The density of states (DOS) for level j , which may be probed in a tunneling experiment, is given by the imaginary part of the retarded Green's function, $-Im G_{jj}^R(\omega)/\pi$,

with $G_{jj}^R(\omega) \equiv \int_0^\infty dt e^{i\omega t} G_{jj}^R(t)$. Since we are dealing only with one level, we will omit the level index j in the following formulas, i.e. $K(t) \equiv K_{jj}(t)$, $\hat{d} \equiv \hat{d}_j$ etc. We have:

$$\begin{aligned} iG^R(t) &= \theta(t) \left\langle \left\{ \hat{d}(t), \hat{d}^\dagger(0) \right\} \right\rangle \\ &= \theta(t) \left(\left\langle \hat{d}(t) \hat{d}^\dagger(0) \right\rangle_{el} e^{K(t)} + \left\langle \hat{d}^\dagger(0) \hat{d}(t) \right\rangle_{el} e^{K(-t)} \right) \end{aligned} \quad (2.27)$$

Note $K(-t) = K^*(t)$, according to Eq. (2.25).

The DOS is related to the integral

$$\frac{1}{\pi} \text{Re} \int_0^\infty dt e^{K(t)} e^{i\omega t} = \frac{1}{2\pi} \int_{-\infty}^{+\infty} dt e^{K(t)} e^{i\omega t} \equiv P(\omega). \quad (2.28)$$

Here we have introduced the quantity $P(\omega)$, which can be interpreted as a probability density of emitting an energy ω into the bath while tunneling onto the level (see below). Formally, this interpretation is possible since $P(\omega)$ is real-valued and fulfills the properties [Ingold92, Schön98]:

$$\int d\omega P(\omega) = e^{K(0)} = 1 \quad (2.29)$$

$$P(\omega) \geq 0 \quad (2.30)$$

In terms of $P(\omega)$, the DOS may be written as

$$-\frac{1}{\pi} \text{Im} G^R(\omega) = \int d\tilde{\omega} A^+(\tilde{\omega}) P(\omega - \tilde{\omega}) + A^-(\tilde{\omega}) P(-(\omega - \tilde{\omega})), \quad (2.31)$$

where $A^\pm(\omega)$ denote the Fourier transforms of the electronic parts of the Green's function in (2.27) (without $\theta(t)$).

In the simplest case of at most one particle in the system, we have $A^+(\omega) = \langle \hat{d} \hat{d}^\dagger \rangle \delta(\omega - \epsilon_j + J_{jj})$ and $A^-(\omega) = \langle \hat{d}^\dagger \hat{d} \rangle \delta(\omega - \epsilon_j + J_{jj})$, compare Eq. (2.19). Then, the lineshape of the level is determined completely by the shape of $P(\omega)$.

In particular, at zero temperature, $P(\omega)$ vanishes for $\omega \leq 0$, which can be deduced from the fact that the same holds for $\langle \hat{\phi} \hat{\phi} \rangle_\omega$ entering $K(t)$ (see Eq. 2.25). In the case of an initially empty level ($\langle \hat{d}^\dagger \hat{d} \rangle_{el} = 0$), one therefore obtains a DOS which vanishes below the renormalized energy. This has a simple physical interpretation - at zero temperature, it is only possible to feed extra energy into the bath while tunneling onto the level, whereas no energy can be received from the bath. Formally, this is expressed by the fact that the quantum correlator of the fluctuating field, Eq. (2.2), is asymmetric in frequency space. Although qualitatively it is correct to think of the zero-point fluctuations of the environment as being responsible for a certain “smearing” of the level energy (expressed

by $P(\omega)$), it would be wrong to keep only the symmetrized, real-valued “fluctuation” part of the bath correlator in Eq. (2.3). This would amount to replacing the quantum bath with a classical fluctuating field of the same fluctuation spectrum (but with vanishing linear response). Then, energy can both be fed into or taken out of the system in equal measure by the bath, resulting in a symmetric DOS.

In the general case, the average over electronic configurations with varying effective level energy will yield several delta peaks in the spectral functions $A^\pm(\omega)$, which means the DOS consists of a weighted superposition of several copies of the lineshape $P(\omega)$, each shifted by a different amount.

2.2.4 Dephasing and two-particle Green’s function

However, the single-particle Green’s function is not the quantity to look at in discussions of dephasing. In fact, there are situations when the single-particle Green’s function shows some decay due to coupling to the environment, while the dephasing rate is actually zero. Instead, one usually analyzes the time-evolution of the single-particle reduced density matrix in some nonequilibrium situation. For example, one might imagine preparing the system initially in an arbitrary coherent superposition of its unperturbed energy eigenstates and observe the decay of the off-diagonal terms in the density matrix which describe the interference between these states (see the example of the diagonal spin-boson model above). A less arbitrary (and usually more physical) way of preparing the system in a nonequilibrium state consists in applying some small perturbation and observing the subsequent relaxation of the density matrix. According to Kubo’s formula, this involves calculating the commutator of the observable with the perturbation. The single-particle density matrix at time t is given as $\langle \hat{d}_j^\dagger(t) \hat{d}_l(t) \rangle$, such that the observable in our case may be taken as $\hat{d}_j^\dagger(t) \hat{d}_l(t)$. In most cases, the external perturbation can be expressed by single-particle operators, i.e. a linear combination of $\hat{d}_i^\dagger \hat{d}_k$. Therefore, we are led to calculating the two-particle Green’s function

$$\langle \hat{d}_j^\dagger(t) \hat{d}_l(t) \hat{d}_l^\dagger(0) \hat{d}_j(0) \rangle. \quad (2.32)$$

Since the bath does not change the state of the particles, only two different level indices may occur in this expression, otherwise it vanishes. The only other possibility of pairing indices would be $\langle \hat{d}_j^\dagger(t) \hat{d}_j(t) \hat{d}_l^\dagger(0) \hat{d}_l(0) \rangle = \langle \hat{n}_j \hat{n}_l \rangle_{el}$.

The evaluation of (2.32) proceeds as before, with splitting into the electronic part and an average over exponentials of the form $\exp(i\hat{\phi}_l(t))$. Since we have assumed that the phases commute when taken at the same time, $[\hat{\phi}_l(t), \hat{\phi}_j(t)] = 0$, the exponentials acting at the same time may be combined:

$$\exp[-i\hat{\phi}_j(t)] \exp[i\hat{\phi}_l(t)] = \exp[i(\hat{\phi}_l(t) - \hat{\phi}_j(t))]. \quad (2.33)$$

This yields for Eq. (2.32):

$$\left\langle \hat{d}_j^\dagger(t) \hat{d}_l(t) \hat{d}_l^\dagger(0) \hat{d}_j(0) \right\rangle_{el} \left\langle e^{i(\hat{\phi}_l(t) - \hat{\phi}_j(t))} e^{-i(\hat{\phi}_l - \hat{\phi}_j)} \right\rangle. \quad (2.34)$$

Again, the electronic expectation value is calculated with respect to $\hat{H}'_{el} = \hat{H}' - \hat{H}_B$, which contains the effective interaction between electrons. In particular, this means that Wick's theorem cannot be applied to rewrite it in terms of pairwise combinations of the electron operators. The average over the fluctuating phases is evaluated just as for the single-particle Green's function, with the phase difference $\hat{\phi}_l - \hat{\phi}_j$ taking the place of the phase itself. It yields:

$$\exp \left[\left\langle (\hat{\phi}_l(t) - \hat{\phi}_j(t))(\hat{\phi}_l - \hat{\phi}_j) \right\rangle - \left\langle (\hat{\phi}_l - \hat{\phi}_j)^2 \right\rangle \right] = \exp[K_{ll}(t) + K_{jj}(t) - K_{lj}(t) - K_{jl}(t)] \quad (2.35)$$

The decay of the two-particle Green's function in time leads to a decay of the single-particle density matrix, which is due to “pure” dephasing in this model. By comparing (2.35) with the corresponding result (2.24) for the single-particle Green's function, it may be noted that dephasing of the superposition between levels l and j may be strongly suppressed compared with the decay of each single level itself. This will be the case if the phase difference $\hat{\phi}_l - \hat{\phi}_j$ is small, although the fluctuations of $\hat{\phi}_l$ and $\hat{\phi}_j$ individually are large. Physically, it means that the bath cannot distinguish easily between levels l and j . In the extreme case, they might even couple to the same bath operator, $\hat{\phi}_l = \hat{\phi}_j$, which means there will be no dephasing at all. This may also happen in more complicated models of dephasing, involving transitions between different states induced by the bath. If the coupling is such that transitions from l to l' and j to j' are accompanied by the emission of one and the same quantum into the bath (with equal transition amplitude), then a coherent superposition of l and j , such as $(|l\rangle + |j\rangle)|\chi\rangle$, will be transferred into a coherent superposition of l' and j' , $(|l'\rangle + |j'\rangle)|\chi'\rangle$, where $\chi^{(\prime)}$ denotes the initial (final) state of the bath. For example, long-wavelength phonons may scatter an electron and yet be ineffective in dephasing if the distance between the paths that contribute to electronic interference is sufficiently smaller than the wavelength. A similar situation occurs in the case of “bremsstrahlung” of a single electron going through an interference setup, mentioned before. There will always be a large (and, in the long-time limit, even infinite) number of infrared photons emitted by the electron. However, those photons whose wavelength is much larger than the distance between the two slits in a double-slit experiment will not deteriorate the interference pattern on the screen.

Note that the opposite situation cannot occur: If dephasing takes place, one always necessarily has a decay of the single-particle Green's function as well. More quantitatively, we have derived the following inequality between the real part of the exponent governing the decay of the two-particle Green's function and that of the single-particle Green's function:

$$\text{Re} \left[\left\langle (\hat{\phi}_l(t) - \hat{\phi}_j(t))(\hat{\phi}_l - \hat{\phi}_j) \right\rangle - \left\langle (\hat{\phi}_l - \hat{\phi}_j)^2 \right\rangle \right] \geq$$

$$2\text{Re}[\langle \hat{\phi}_l(t)\hat{\phi}_l \rangle - \langle \hat{\phi}_l\hat{\phi}_l \rangle + \langle \hat{\phi}_j(t)\hat{\phi}_j \rangle - \langle \hat{\phi}_j\hat{\phi}_j \rangle] \quad . \quad (2.36)$$

In this sense, the decay of the single-particle Green's functions of levels l and j provides an upper bound on the strength of dephasing (note that both sides are nonpositive, so the inequality for the magnitudes would be reversed). The inequality (2.36) can be proven by bringing everything to the left hand side and using

$$\langle \hat{\phi}^2 \rangle - \frac{1}{2} \langle \{ \hat{\phi}(t), \hat{\phi} \} \rangle \geq 0, \quad (2.37)$$

which holds for any hermitean operator $\hat{\phi}$, with $\hat{\phi} \equiv \hat{\phi}_l + \hat{\phi}_j$ in our case. (Eq. (2.37) itself may be derived directly by writing down the thermal equilibrium correlator in terms of the matrix elements of $\hat{\phi}$, and using $\cos(\omega t) \leq 1$). Dephasing becomes of maximum strength if the two levels couple to the bath with equal strength but opposite sign: $\hat{F}_l = -\hat{F}_j$. In that case, the inequality becomes an equality. On the other hand, for independent bath fluctuations \hat{F}_l and \hat{F}_j , another equality holds, with the factor of 2 dropped on the right hand side. Then, the bath part of the two-particle Green's function factorizes into the corresponding single-particle expressions, as expected.

Formally, the decay of the two-particle Green's function is usually overestimated by looking at that of the single-particle Green's function because of vertex corrections that are able to reduce the decay of the former. Put more simply, averaging a wave function over a fluctuating field leads to a larger reduction in magnitude than averaging a density matrix. Although qualitatively the same can be said in general, not just for the independent boson model, I am not aware of any similar relation between dephasing rate and single-particle decay rate for the general case.

Summarizing, the temporal evolution of any Green's function in the independent boson model is governed by exponentials of phase-correlators $K_{lj}(t)$, which are directly connected to the power spectrum $\langle \hat{F}_l \hat{F}_j \rangle_\omega$ of the fluctuating fields \hat{F}_l , see Eq. (2.25). The DOS of a single level j is determined by $P_{jj}(\omega)$, which is the Fourier transform of $\exp(K_{jj}(t))$, see Eq. (2.28).

2.2.5 Time-evolution of Green's functions

We will conclude this section by discussing briefly the time-evolution of $\exp(K_{jj}(t))$ for different bath spectra. A more detailed analysis of the resulting Fourier transform $P_{jj}(\omega)$ is contained in the next section, dealing with dephasing in sequential tunneling through a double-dot system. Again, we omit the level index j in the following, for brevity.

In general, $K(t)$ starts from 0 at $t = 0$ and decays towards $-\langle \hat{\phi}^2 \rangle$ in the long-time limit. Whenever this value is finite, the decay of the Green's function is incomplete, i.e. it does not decay towards zero. Correspondingly, $P(\omega)$ contains a “quasiparticle” delta peak of strength $\exp(-\langle \hat{\phi}^2 \rangle)$ over an incoherent background. From

$$\langle \hat{\phi}^2 \rangle = \int_{-\infty}^{+\infty} d\omega \frac{\langle \hat{F} \hat{F} \rangle_{\omega}}{\omega^2}, \quad (2.38)$$

we observe that this is the case whenever the bath spectrum $\langle \hat{F} \hat{F} \rangle_{\omega}^{T=0}$ rises like ω^s at low frequencies, with $s > 1$ ($s > 2$) at $T = 0$ ($T > 0$), or if it vanishes at low ω (gapped bath, Einstein oscillator). In contrast, for $s \leq 1$ ($s \leq 2$) at $T = 0$ ($T > 0$), the decay is complete and the DOS shows no delta peak any more. For $s < 1$ ($s < 2$), one has $K(t) \propto -t^{1-s} (-t^{2-s})$ in the long-time limit. In the special cases $s = 1$ ($s = 2$), the increase of $K(t)$ with time turns out to be logarithmic: $K(t) \propto -\ln(\omega_c t) (-\ln(Tt))$, where ω_c denotes a cutoff-frequency beyond which the bath spectrum falls off towards zero. In that case, the Green's function decays with a power-law in time, the exponent being given by the strength of the bath fluctuations. Exponents $s \leq 0$ lead to an infrared divergence of the energy shift J_{jj} and the coupling constants J_{lj} (see Eq. (2.14)). An example is provided by $1/f$ -fluctuations ($s = -1$), which may occur due to defect tunneling of charges in a solid, if the tunnel barriers are randomly distributed. However, for such a spectrum it is questionable whether the bath itself is really in equilibrium at the lowest frequencies, as we are assuming it here.

The case of $s = 1$ is known as the ‘‘Ohmic bath’’. It is of particular importance, since it describes the equilibrium electric field fluctuations in a disordered conductor (Nyquist noise) and the fluctuations of the electron density in a clean Fermi liquid (at a given point of space, in any dimension). Moreover, it is the force spectrum that, in the treatment of Quantum Brownian motion of a free particle [Caldeira83], leads to velocity-proportional friction and to normal diffusion at finite temperatures.

We may write the Ohmic spectrum as

$$\langle \hat{F} \hat{F} \rangle_{\omega}^{T=0} = 2\alpha\omega \quad (2.39)$$

at low frequencies, with α a dimensionless parameter characterizing the strength of the fluctuations (known as the Kondo parameter in some applications; see [Weiss00], where it is denoted by K). From the general discussion given above, it follows that, at finite temperature $T > 0$, the temporal decay of the Green's function in the long-time limit proceeds exponentially, with the rate given by $2\pi\alpha T$. At $T = 0$, it turns into a power-law decay $(\omega_c t)^{-2\alpha}$.

From these examples, it is observed that an exponential decay with a finite decay rate is rather the exception than the rule in the case of a diagonal coupling between system and bath. In all the other cases, with an incomplete decay, a power-law decay or a decay of the form $\exp(-ct^{\nu})$ ($\nu \neq 1$), a calculation of the rate according to the Golden Rule (i.e. like in Eq. (1.11)) yields either zero or infinity. In contrast, a non-diagonal coupling leads to transitions between different levels, which, at $T = 0$, simply correspond to spontaneous emission of energy into the bath. Then, the Golden Rule picture usually describes most of the qualitative physics correctly over a wide range of coupling strengths.

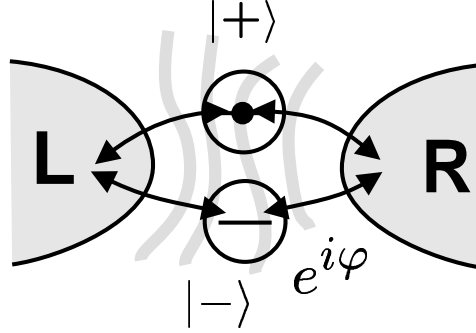


Figure 2.1: The double-dot “double-slit” setup under the influence of a fluctuating environment, with a fixed phase difference φ between the two paths.

2.3 Dephasing in sequential tunneling through a double-dot

In this section, we will present a model that is able to give insights into most of the questions raised in the introduction (Chapter 1), concerning the role of zero-point fluctuations and the Pauli principle in low-temperature dephasing.

The model is a kind of very simple mesoscopic double-slit setup. It consists of two single-level quantum dots which are tunnel-coupled to two leads, with a possible phase difference between the two interfering paths (see Fig. 2.1). Due to destructive interference, the tunneling current may be completely suppressed. Coupling the dots to a bath may partly destroy the phase coherence and enable the electron to go through the setup. If the coupling strength to the bath is the same for the two dots, and the levels have been degenerate, mere renormalization effects will not be able to lift the destructive interference. Thus, a finite tunneling current may be taken as a genuine sign of dephasing. This criterion for dephasing has been employed before in a model of dephasing due to spin-flip transitions in first-order tunneling transport through one or two dots [König02]. It will also be used in our analysis of cotunneling transport through localized levels in general (Section 2.4), and an Aharonov-Bohm ring coupled to a fluctuating magnetic flux (Chapter 3).

The presence of the Fermi sea in the leads introduces some aspects related to the Pauli principle and to the behaviour of systems with a continuous spectrum that cannot be analyzed in simpler models of discrete systems coupled to a bath. In [Aleiner97], a somewhat related discussion has been given of dephasing in a which-way interferometer, consisting of an Aharonov-Bohm ring with a quantum dot embedded in one of its arms and coupled to an external quantum point contact acting as a measuring device, although there the emphasis was placed on dephasing by nonequilibrium current fluctuations in the point contact.

The influence of phonons on sequential tunneling through two quantum dots *in series*

has been studied experimentally in [Fujisawa98]. There, inelastic transitions induced by piezoelectric coupling to acoustic phonons in GaAs have been essential for obtaining a finite current for off-resonant levels. This kind of setup has been analyzed theoretically in [Stoof96, Brandes99, Keil02]. Recent experimental work on double-dots in parallel [Holleitner02] puts emphasis on the states of the “artificial molecule” generated by introducing a tunnel-coupling between the dots, including the resulting spin physics. This has been motivated in part by suggestions to use such a setup for quantum computation [Loss98]. Recent theoretical works considering a double-dot geometry have investigated spin and Kondo physics [Loss00, Boese02, König02]. For a recent work, where the destruction of interference in resonant tunneling through an Aharonov-Bohm ring was studied numerically in a tight-binding model with coupling to optical phonons, see [Haule99].

Our analysis of dephasing in sequential tunneling through a double-dot will take into account exactly the system-bath coupling (employing the independent boson model introduced before), while we treat the tunnel-coupling only in leading order.

In the following sections, we will first consider only the coupling to one lead. By calculating the tunneling decay rate for an electron that has been placed on the two dots in a symmetric superposition of states, we can emphasize the most important physical effects that are relevant for dephasing in the sequential tunneling situation. We will derive the general formula for this rate, building on the concepts of the $P(E)$ theory of tunneling in a dissipative environment [Ingold92, Schön98]. Following this, we will evaluate the dependence of the tunneling rate on the bias voltage and the bath spectra, concentrating mostly on the case $T = 0$. We will interpret the results in terms of “renormalization effects” and “true dephasing”. In the final section, we will derive a master equation for the case of weak tunnel coupling, which allows us to calculate the sequential tunneling current as a function of bias voltage, temperature, and phase difference.

2.3.1 The model

We consider a Hamiltonian describing two degenerate single-level quantum dots, with respective single-particle states $|+\rangle$ and $|-\rangle$ (spin is excluded for simplicity, since we are interested in dephasing of the electronic motion). Each of them is tunnel-coupled to the same lead with the same strength, but involving a possible phase difference between the tunnel amplitudes (see Fig. 2.1). The phase difference φ is assumed not to depend on the final electronic state k in the lead. This means we assume the dots to couple to the same point, to within less than a Fermi wavelength. In addition, the particle number on each dot couples to a fluctuating potential \hat{F} , whose dynamics is derived from a linear bath. This represents an example of the independent boson model introduced above. The coupling strength is taken to be the same for both dots, while the sign is assumed to be opposite, such that the bath can distinguish between an electron being on dot $|+\rangle$ or $|-\rangle$:

$$\hat{H} = \epsilon(\hat{n}_+ + \hat{n}_-) + \hat{F}(\hat{n}_+ - \hat{n}_-) + U\hat{n}_+\hat{n}_- +$$

$$\hat{H}_L + \hat{H}_R + \hat{H}_B + \hat{V} \quad (2.40)$$

Here \hat{n}_\pm are the particle numbers on the two dots (equal to 0 or 1), and \hat{H}_B is the bath Hamiltonian, governing the dynamics of the fluctuating potential \hat{F} . U is the Coulomb repulsion energy, which we will take to be infinite, such that double-occupancy is forbidden. \hat{H}_L, \hat{H}_R contain the energies of the electrons in the left and right reservoirs:

$$\hat{H}_{L(R)} = \sum_k \epsilon_k \hat{a}_{L(R)k}^\dagger \hat{a}_{L(R)k} . \quad (2.41)$$

The tunneling between the dots and the leads is described by $\hat{V} = \hat{V}_L + \hat{V}_R$, with

$$\hat{V}_R = \sum_k t_k^R \hat{a}_{Rk}^\dagger (\hat{d}_+ + e^{i\varphi} \hat{d}_-) + h.c. \quad (2.42)$$

for the right junction, and

$$\hat{V}_L = \sum_k t_k^L \hat{a}_{Lk}^\dagger (\hat{d}_+ + \hat{d}_-) + h.c. \quad (2.43)$$

for the left junction.

Here \hat{d}_\pm are the annihilation operators for the two dots ($\hat{n}_\pm = \hat{d}_\pm^\dagger \hat{d}_\pm$) and the phase-factor of $e^{i\varphi}$ controls the interference between tunneling events along either the upper or lower path. The tunneling phase difference might be thought of as arising due to the Aharonov-Bohm phase from a magnetic flux penetrating the region between the quantum dots.

2.3.2 Qualitative discussion

In this and the following three sections, we first analyze the escape of a single electron into the right lead, where the electron is assumed to start out in a symmetric superposition of the two dot levels, which is formed by an electron tunneling onto the dots from the left lead. In the situation without any bath, this is the state $|e\rangle \equiv (|+\rangle + |-\rangle)/\sqrt{2}$. Without dephasing, the tunneling decay is made impossible in the case of perfect destructive interference, which will be obtained for $\varphi = \pi$, while maximal constructive interference is present for $\varphi = 0$. Therefore, we will only consider the coupling \hat{V}_R to the right lead and drop the index R for now. It should be noted that the attribution of the phase factor to one of the tunnel couplings represents a certain choice of gauge, which affects the wave functions but no physically observable quantities.

For simplicity, we will assume a zero-temperature situation throughout the following qualitative discussion, with a bias $eV > 0$ applied between the two dots and the lead in such a way that the electron is allowed to tunnel into the lead (see Fig. 2.2).

Without the bath and for perfect constructive interference ($\varphi = 0$), the tunneling decay rate Γ will take on its maximum value of $2\Gamma_0$, with

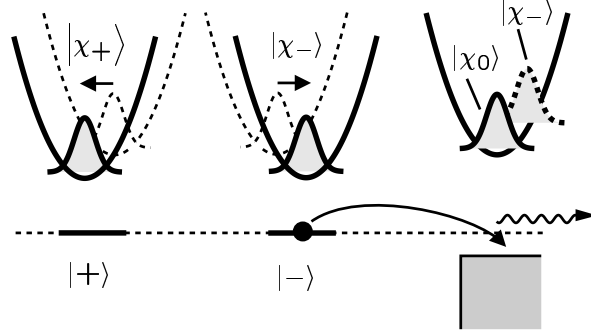


Figure 2.2: The ground state $|\chi_+\rangle$ ($|\chi_-\rangle$) which the bath assumes in the presence of an electron on dot $|+\rangle$ ($|-\rangle$), shown schematically for a single bath oscillator (see main text). After the electron has tunneled into the lead, $|\chi_-\rangle$ becomes a superposition of excited states (dashed), while the state $|\chi_0\rangle$ represents the ground state of the bath in the new potential.

$$\Gamma_0 \equiv 2\pi D \langle |t_k|^2 \rangle, \quad (2.44)$$

where D is the lead density of states at the Fermi energy, $\langle |t_k|^2 \rangle$ is the average of $|t_k|^2$ at this energy, and the bias voltage V does not enter in this case, as long as it is positive (permitting decay). For $\varphi = \pi$, Γ vanishes due to perfect destructive interference. In general, we have

$$\Gamma = \Gamma_0(1 + \cos \varphi). \quad (2.45)$$

If the bath is included in the description, the following happens:

First of all, the energy of a single extra electron on any of the two dots will be renormalized from its initial value of ϵ , since the bath relaxes to a ground state of lower energy in presence of the electron. We will assume that the value of ϵ has been chosen exactly to compensate for this energy change, which is given by $-\int_0^\infty d\omega \langle \hat{F} \hat{F} \rangle / \omega$, see Eqs. (2.13) and (2.14). Then, the energy of an electron on the dot (and the bath in its new ground state) is the same as that of the electron being in the lead, at the Fermi energy of $\epsilon_F \equiv 0$ (for $V = 0$). Since we consider only a single electron, we may also disregard the effective interaction between electrons on the different dot levels, which is induced by the bath (see Eq. (2.13)).

Tunneling of an electron from the dots to the lead will not change the bath state, but it will displace the origin of the harmonic oscillators comprising the bath, since the coupling to \hat{F} is switched off ($\hat{n}_+ - \hat{n}_-$ changes to zero). Therefore, the original ground state of the bath will become a superposition of excited states in the new bath potential (see Fig. 2.2). On the other hand, since energy conservation has to be fulfilled with respect to the total energy of the electrons and the bath before and after the tunneling event, only those

excited bath states can be reached whose energies are not greater than eV , the energy supplied to the electron by the bias voltage. This leads to the Coulomb-blockade type *suppression* of the tunneling rate at low bias voltages, for $\varphi = 0$. Physically, this effect is just the same as that described by Franck-Condon overlap integrals evaluated between vibronic states for electronic transitions in molecules.

In contrast, for the case of destructive interference ($\varphi = \pi$), the bath may actually *enhance* the tunneling rate from its initial value of 0, since it partly destroys the phase coherence that is a presupposition for perfect interference. An electron coming from the left lead will form the following entangled state with the bath, instead of the symmetric superposition $|e\rangle = (|+\rangle + |-\rangle)/\sqrt{2}$:

$$(|+\rangle |\chi_+\rangle + |-\rangle |\chi_-\rangle)/\sqrt{2}. \quad (2.46)$$

Here the states $|\chi_\pm\rangle$ denote the respective ground states of the bath for a bath Hamiltonian given by $\hat{H}_B \pm \hat{F}$, which are related to each other by a parity transformation (This also means we assume there to be no phase factor between these states). Actually, the entangled state considered here will be formed only if the electron is given barely enough energy to enter the double-dot at all. Otherwise, excited bath states may be created at this step. These complications will be taken care of in the complete discussion of the sequential tunneling current (Section 2.3.6).

The bath measures (to some extent) which dot the electron resides on, such that the reduced system density matrix (for the electron on the two dots) becomes mixed and its off-diagonal elements get suppressed by the overlap factor $\langle\chi_+|\chi_-\rangle$. Put differently, the phase factor between the two dot states in the wave function of the electron (initially equal to +1) becomes uncertain. Therefore, there is a finite probability of

$$P_o = (1 - \text{Re} \langle\chi_+|\chi_-\rangle)/2 \quad (2.47)$$

to find the electron in the odd state $|o\rangle \equiv (|+\rangle - |-\rangle)/\sqrt{2}$. This state is allowed to decay into the lead at $\varphi = \pi$, at the rate $2\Gamma_0$. In this way, the interference-induced blockade of electron tunneling is lifted by dephasing.

However, this simple picture is true only for large bias voltages, when energy conservation permits any final state of the bath after the tunneling event. If the maximum energy supplied to the electron is limited, the suppression discussed above (for the case of $\varphi = 0$) will apply again. In particular, if the bias voltage is turned to zero, energy conservation only allows the state $|\chi_0\rangle$ to be reached, which is the ground state of the bath in the absence of any electrons on the dots. Then, the tunneling rate is exactly zero again, despite the fact that the reduced density matrix of the electron may be mixed to a strong extent. The reason is the following: When the overlap of the entangled state (2.46) with the state $|\chi_0\rangle$ is taken, the two overlap factors $\langle\chi_0|\chi_+\rangle$ and $\langle\chi_0|\chi_-\rangle$ turn out to be the same, *if* the coupling of the bath to the two dots is symmetric (i.e. of equal strength, only of opposite sign), which we have assumed in writing down the Hamiltonian, Eq. (2.40). Therefore, the electronic state resulting from the projection onto $|\chi_0\rangle$

is equal to the symmetric combination, whose decay is forbidden. Thus, energy conservation and Pauli blocking prevent a finite tunneling rate at zero bias voltage, in spite of the mixed state of the electron coupled to the bath. If the coupling were asymmetric, then destructive interference would be lost even without dephasing, just as it would be the case for initially asymmetric bare tunnel couplings, rendering this case uninteresting for our purposes of distinguishing renormalization effects from real dephasing.

However, whether we are indeed able to claim that dephasing actually vanishes in the limit of low bias voltages will depend on the behaviour of the tunneling rate as a function of V and on the comparison of the cases $\varphi = 0$ and $\varphi = \pi$. Here, the bath spectrum, and, above all, its low-frequency properties, enter. In order to be able to discuss $\Gamma(V, \varphi)$ quantitatively, we will make use of the concepts of the $P(E)$ theory of tunneling in a dissipative environment.

2.3.3 Decay rate and connection to $P(E)$ theory

The tunneling rate Γ will be calculated using the standard Fermi Golden Rule, i.e. lowest order perturbation theory in the bare tunneling rate Γ_0 , but taking into account exactly the bath coupling. In deriving the formula for Γ , it turns out to be useful to assume that the bath oscillators do *not* get shifted in the tunneling event (unlike the qualitative considerations from above), but it is rather the bath states which get displaced (in the opposite direction). Obviously, this amounts to the same, as long as we are interested only in overlap integrals of different bath states after the event. We define the displacement operator, which transforms the bath ground state of \hat{H}_B into that of $\hat{H}_B + \hat{F}$, as $\exp(i\hat{\phi})$, with a suitable hermitian operator $\hat{\phi}$ that is linear in the bosonic variables of the bath. In fact, this amounts to performing the canonical transformation (2.13) of the independent boson model, introduced in Section 2.2.2. In terms of the two dot states $+$ and $-$, we have $\hat{F}_+ = \hat{F}$ and $\hat{F}_- = -\hat{F}$, as well as $\hat{\phi}_+ = \hat{\phi}$ and $\hat{\phi}_- = -\hat{\phi}$. The transformation leads to $\hat{d}'_{\pm} = e^{\pm i\hat{\phi}} \hat{d}_{\pm}$ (compare Eq. (2.15)) in the transformed tunnel Hamiltonian \hat{V}'_R .

We will assume the tunnel-coupling to be sufficiently weak, such that we can use lowest-order perturbation theory to calculate the tunneling decay rate:

$$\Gamma = 2\pi \sum_f \left| \left\langle f | \hat{V}'_R | i \right\rangle \right|^2 \delta(E_f - E_i), \quad (2.48)$$

where the initial state $|i\rangle$ is given by the configuration involving the electron residing in the symmetric superposition on the dots, the unperturbed Fermi sea in the lead and the bath in its ground state $|i_B\rangle$ (which has become independent of the position of the electron, due to the above-mentioned transformation). At finite temperatures, an additional thermal average over the initial bath state and the initial state of the electrons in the lead has to be performed. The energies and eigenstates refer to the Hamiltonian without tunnel coupling. Applying the new tunneling Hamiltonian \hat{V}'_R to the initial state, we obtain the following expression:

$$\Gamma = \pi \sum_{kf_B} |t_k|^2 (1 - f(\epsilon_k + eV)) \times \left| \left\langle f_B | e^{+i\hat{\phi}} + e^{i\varphi} e^{-i\hat{\phi}} | i_B \right\rangle \right|^2 \delta(E_f^B - E_i^B + \epsilon_k), \quad (2.49)$$

Here $f(\cdot)$ is the Fermi function (for chemical potential equal to zero), and $E_{f,i}^B$ are the energies of the initial and final bath states. The energy supplied to the bath is equal to the energy lost by the electron (given by $-\epsilon_k$, since the renormalized dot energy is zero). Following the usual derivation of the $P(E)$ theory [Ingold92, Schön98], we express the energy-conserving δ function as an integral over time and also replace the sum over lead states k by an integral over the energy $E = -\epsilon_k$ supplied to the bath, finally yielding:

$$\Gamma = \Gamma_0 \int_{-\infty}^{+\infty} dE (1 - f(-E + eV)) \int_{-\infty}^{+\infty} \frac{dt}{2\pi} e^{iEt} \times \frac{1}{2} \left\langle (e^{-i\hat{\phi}(t)} + e^{-i\varphi} e^{i\hat{\phi}(t)}) (e^{i\hat{\phi}} + e^{i\varphi} e^{-i\hat{\phi}}) \right\rangle \quad (2.50)$$

For the case of arbitrary T , the brackets denote a thermal average over the initial bath state $|i_B\rangle$. We introduce the definitions (compare Eq. (2.28), where $P(E)$ has already been defined):

$$P_{(-)}(E) = \frac{1}{2\pi} \int_{-\infty}^{+\infty} dt e^{iEt} e^{\pm \langle \hat{\phi}(t)\hat{\phi} \rangle - \langle \hat{\phi}^2 \rangle}. \quad (2.51)$$

This permits us to write down our final result for the tunneling decay rate in terms of $P_{(-)}(E)$:

$$\Gamma = \Gamma_0 \int_{-\infty}^{+\infty} dE (1 - f(-E + eV)) (P(E) + \cos(\varphi) P_{(-)}(E)) \quad (2.52)$$

The formula given here constitutes the basic expression for the decay rate as a function of bias voltage and interference phase φ . We will evaluate it for different types of bath spectra in the next section.

By using the definitions

$$\gamma_{(-)} \equiv \Gamma_0 \int dE (1 - f(-E + eV)) P_{(-)}(E), \quad (2.53)$$

we can write

$$\Gamma = \gamma + \cos(\varphi) \gamma_{-}. \quad (2.54)$$

The strength of the dependence of Γ on the phase φ may be taken as a signature of phase coherence in our model. We define the “visibility” of the interference pattern by

$$v \equiv (\Gamma_{max} - \Gamma_{min})/(\Gamma_{max} + \Gamma_{min}), \quad (2.55)$$

which is equal to the ratio

$$v = \frac{\gamma_-}{\gamma}. \quad (2.56)$$

The visibility v will be 1 whenever the destructive interference is perfect, and it is zero if there is no dependence of Γ on φ .

The effects of the bath on the decay rate are encoded in the functions $P(E)$ and $P_-(E)$, whose general properties we will discuss now.

As usual, the function $P(E)$ describes the probability (density) that an electron will emit the energy E into the bath while tunneling into the lead. It is real, nonnegative and normalized to unity [Schön98, Ingold92], see Eqs. (2.29), (2.30).

At large times $|t| \rightarrow \infty$, the correlation function $\langle \hat{\phi}(t)\hat{\phi} \rangle$ in the exponent of the integral (2.51) will decay towards zero, for a continuous bath spectrum. This means that the integrand of $P(E)$ approaches the value of $z \equiv \exp(-\langle \hat{\phi}^2 \rangle)$, starting from 1 at $t = 0$. Therefore, $P(E)$ contains a “quasiparticle δ peak” of strength z at $E = 0$, if z does not vanish. It corresponds to the probability z of having no energy transfer at all from the electron to the bath (similar to the recoil-free emission of a γ ray by a nucleus inside a crystal, i.e. the Mössbauer effect).

The function $P_-(E)$ in front of the $\cos(\varphi)$ term in Eq. (2.52) is different: The integrand of $P_-(E)$ will increase at large times, towards the value of z , starting from z^2 at $t = 0$. This means that $P_-(E)$ can become negative (as demonstrated below), while it is still real-valued, because of $\langle \hat{\phi}(t)\hat{\phi} \rangle = \langle \hat{\phi}\hat{\phi}(t) \rangle^*$. Therefore, it cannot be interpreted as a probability density, in contrast to $P(E)$. Its normalization is given by:

$$\int dE P_-(E) = z^2. \quad (2.57)$$

If z is nonzero, $P_-(E)$ also has a δ peak at $E = 0$, of weight z , just as $P(E)$. As a consequence, in the case of destructive interference ($\varphi = \pi$), the tunneling rate Γ at $V \rightarrow 0$, $T = 0$ still vanishes even in the presence of the bath, since the δ peaks contained in $P(E)$ and $P_-(E)$ cancel exactly in the integral (2.52). The physical reason for this has been discussed above.

In the case of constructive interference ($\varphi = 0$), at $T = 0$ and for $V \rightarrow 0$, the integration over E will only capture the δ peaks contained in $P_{(-)}(E)$, yielding $\Gamma = 2z\Gamma_0$. Thus, the tunneling rate is suppressed by the constant factor z from its noninteracting value. However, this may be interpreted as a mere renormalization of the effective tunnel coupling, since the visibility v of the interference pattern is still equal to unity. In order to connect this result to the qualitative discussion from above, we note that the overlap of the two different bath ground states that are adapted to the absence or presence of an electron on dot \pm , is given by:

$$\langle \chi_0 | \chi_{\pm} \rangle = \langle \chi_0 | e^{\pm i \hat{\phi}} | \chi_0 \rangle = \exp(-\langle \hat{\phi}^2 \rangle / 2) = z^{1/2}, \quad (2.58)$$

Therefore, the magnitude squared of this overlap, that determines the probability of tunneling without exciting any bath mode, is equal to z .

On the other hand, for sufficiently large bias voltages (much larger than the cutoff frequency of the bath spectrum), the normalization conditions for $P_{(-)}(E)$ yield

$$\Gamma = \Gamma_0(1 + z^2 \cos(\varphi)). \quad (2.59)$$

The visibility is given by $v = z^2$. In this limiting case, where the restrictions due to energy conservation and the Pauli principle are no longer important, the tunneling rate Γ at the point $\varphi = \pi$ of destructive interference does not vanish. It takes the value $\Gamma_0(1 - z^2)$, which is small if the effects of the bath are weak (z near to 1) and is equal to one half the ideal maximum value $2\Gamma_0$ for a bath that is sufficiently strong to destroy phase coherence completely ($z = 0$), leading to an incoherent mixture of symmetric and antisymmetric states on the two dots. In the latter case, the visibility vanishes (even for arbitrary voltages), since then $P_{-}(E)$ is equal to zero, which makes Γ independent of φ . This will be true for the Ohmic bath, to be discussed in the next section.

As explained above, the reduced density matrix of the electron on the dots coupled to the bath predicts a finite probability of $(1 - \text{Re} \langle \chi_+ | \chi_- \rangle)/2$ to find the electron in the antisymmetric state if one starts out from the symmetric superposition before coupling it to the bath. The overlap factor of the bath states involved in this probability can be expressed as

$$\langle \chi_+ | \chi_- \rangle = \langle \chi_0 | (e^{-i \hat{\phi}})^2 | \chi_0 \rangle = z^2. \quad (2.60)$$

Comparing with the result $\Gamma(\varphi = \pi) = \Gamma_0(1 - z^2)$ given above, it may be observed that the decay rate at sufficiently large bias voltages is determined directly by the probability to find the electron in the state whose decay is not forbidden by destructive interference. It is only in this limiting case, where an arbitrary amount of energy is available for excitation of the bath, that the suppression of interference effects in the transport situation is correctly deduced from the electron's reduced density matrix in the presence of the bath. Formally, this holds because the sum over final bath states f_B in Eq. (2.49) is not restricted any more and corresponds to the insertion of a complete set of basis states. Thus, one obtains, directly from Eq. (2.49):

$$\Gamma = \frac{\Gamma_0}{2} \langle \chi_+ + e^{-i\varphi} \chi_- | \chi_+ + e^{i\varphi} \chi_- \rangle, \quad (2.61)$$

which reduces to Eq. (2.59) when the overlaps are evaluated, using Eq. (2.60). Physically, the case of high bias voltage corresponds to a kind of infinitely fast von Neumann projection measurement that determines the state of the electron, revealing the fluctuations due to the bath (compare the qualitative discussion in Section 1.3). In contrast, at

low bias voltages (low energy supply), a kind of “weak” measurement is carried out that takes a longer amount of time, such that only the low-frequency fluctuations of the bath are important for dephasing.

2.3.4 Evaluation for different bath spectra

We will restrict the discussion to $T = 0$ at first.

The simplest example for the bath is a single harmonic oscillator of frequency ω . This offers an approximate description of the interaction with optical phonon modes (“Einstein model”). In this case, $P(E)$ and $P_-(E)$ can be obtained easily by expanding the exponential in a Taylor series and using $\langle \hat{\phi}(t)\hat{\phi} \rangle = \langle \hat{\phi}^2 \rangle \exp(-i\omega t)$, before the integration over time is performed. For $P(E)$, the resulting series of δ peaks at harmonics of ω corresponds to all possible processes where the electron emits any number n of phonons into the bath while tunneling into the lead. The expression for $P_-(E)$ is the same, apart from alternating signs in front of the δ functions:

$$P_{(-)}(E) = z \sum_{n=0}^{\infty} \frac{\langle \pm \hat{\phi}^2 \rangle^n}{n!} \delta(E - n\omega). \quad (2.62)$$

Thus, every process involving the transfer of an even number of quanta to the bath will not ruin the destructive interference at $\varphi = \pi$, since the corresponding contributions from $P(E)$ and $P_-(E)$ cancel in Eq. (2.52). This is because the coupling between electron and bath is of the type $(\hat{n}_+ - \hat{n}_-)\hat{F}$, which gives a different sign of the interaction amplitude for a phonon emission process, depending on the dot. Therefore, the amplitude of emission of an *even* number of phonons will *not* depend on the dot, it is insensitive to the state of the electron, and the amplitudes of the electron tunneling from $|+\rangle$ and $|-\rangle$ will still interfere destructively.

In contrast, emission processes involving an odd number of quanta introduce a negative sign for an electron starting in state $|-\rangle$, “detecting” the path (or rather, the initial state) of the electron and interfering *constructively* with the processes from $|+\rangle$. This lifts the destructive interference and makes $\Gamma \neq 0$ at $\varphi = \pi$. However, below the frequency ω of the oscillator, destructive interference at $\varphi = \pi$ is still perfect since no quantum can be emitted, while the magnitude of Γ at $\varphi = 0$ is renormalized by the factor z , as has been discussed above in general for the limiting case $V \rightarrow 0$. The same holds true for any bath with a finite excitation gap, at $T = 0$. This is shown in Figs. 2.4 and 2.5, to be discussed in the next section.

We now pass on to arbitrary bath spectra. At first, we will cover the case $z \neq 0$ (“weak baths”), when we can apply perturbation theory to discuss the behaviour of $P_{(-)}(E)$ at low energy transfers E (and, consequently, that of Γ at low voltages). A Taylor-expansion of the exponent in Eq. (2.51) yields:

$$\begin{aligned}
P_{(-)}(E) &= \frac{z}{2\pi} \sum_{n=0}^{\infty} \frac{1}{n!} \int_{-\infty}^{+\infty} dt e^{iEt} \left[\pm \langle \hat{\phi}(t) \hat{\phi} \rangle \right]^n \\
&= z \sum_{n=0}^{\infty} \frac{(\pm 1)^n}{n!} (\langle \hat{\phi} \hat{\phi} \rangle_{\omega} * \dots * \langle \hat{\phi} \hat{\phi} \rangle_{\omega})(E)
\end{aligned} \tag{2.63}$$

The repeated convolution product contains n times the correlator $\langle \hat{\phi} \hat{\phi} \rangle_{\omega}$, for $n = 0$ it is to equal $\delta(E)$, and the negative sign holds for $P_{-}(E)$.

For the following discussion, we prescribe the spectrum of the fluctuating potential \hat{F} to be a power-law in frequency ω (at $T = 0$), with exponent s :

$$\langle \hat{F} \hat{F} \rangle_{\omega}^{T=0} = 2\alpha\omega_c \left(\frac{\omega}{\omega_c} \right)^s \theta(\omega_c - \omega) \theta(\omega), \tag{2.64}$$

The dimensionless parameter α characterizing the bath strength has been introduced before in the case of the Ohmic bath, $s = 1$ (see Eq. (2.39)). In order to be able to rely on perturbation theory, we have to ensure $z > 0$. Since $\langle \hat{\phi} \hat{\phi} \rangle_{\omega} = \langle \hat{F} \hat{F} \rangle_{\omega} / \omega^2$, the variance of the fluctuating phase, $\langle \hat{\phi}^2 \rangle$, will be finite only for $s > 1$ (at $T = 0$, otherwise $s > 2$). In that case, we have $z = \exp(-2\alpha/(s-1))$. This means the perturbative analysis presented above is restricted to a super-Ohmic bath, $s > 1$. The case of the Ohmic bath will be discussed separately further below.

After keeping only terms up to second order in the expansion of $P_{(-)}(E)$ given in Eq. (2.63), we get

$$P(E) + P_{-}(E) = z(2\delta(E) + (\langle \hat{\phi} \hat{\phi} \rangle_{\omega} * \langle \hat{\phi} \hat{\phi} \rangle_{\omega})(E) + \dots), \tag{2.65}$$

for the symmetric combination, that will determine the prefactor of $1 + \cos(\varphi)$ in the expression for Γ , Eq. (2.52), and

$$P(E) - P_{-}(E) = 2z \langle \hat{\phi} \hat{\phi} \rangle_E + \dots \tag{2.66}$$

for the antisymmetric combination (determining the prefactor of $1 - \cos(\varphi)$). Inserting these into (2.52), using the power law for $\langle \hat{\phi} \hat{\phi} \rangle_{\omega} = \langle \hat{F} \hat{F} \rangle_{\omega} / \omega^2$ given by (2.64), and performing the energy integrals, we find, for sufficiently low voltages ($2\alpha(eV/\omega_c)^{s-1} \ll s-1$):

$$\begin{aligned}
\Gamma \approx \frac{\Gamma_0}{2} z \{ & (1 + \cos(\varphi)) \left(1 + \frac{\alpha^2 C_s}{(s-1)} \left(\frac{eV}{\omega_c} \right)^{2(s-1)} \right) + \\
& (1 - \cos(\varphi)) \frac{2\alpha}{s-1} \left(\frac{eV}{\omega_c} \right)^{s-1} \} .
\end{aligned} \tag{2.67}$$

The numerical prefactor C_s is defined as $\int_0^1 (y(1-y))^{s-2} dy$.

From Eq. (2.67), we see that the destructive interference at $\varphi = \pi$ is perfect at $V = 0$, but gets lifted when increasing the bias voltage, with a power V^{s-1} . In contrast, the decay rate Γ at $\varphi = 0$ starts out from the constant value of $2z\Gamma_0$ and grows as $V^{2(s-1)}$. Therefore, the visibility v starts out at 1 for $V = 0$ but decreases as:

$$v \approx 1 - \frac{4\alpha}{s-1} \left(\frac{eV}{\omega_c} \right)^{s-1}. \quad (2.68)$$

For $s \downarrow 1$, the range in bias voltage V where these approximate expressions hold shrinks to zero (at constant α and ω_c). At $s = 1$, i.e. for the Ohmic bath, the probability z of not emitting energy into the bath vanishes completely. As discussed above, this means that there is no φ -dependence at all in Γ , and, consequently, the visibility is zero at all bias voltages. Furthermore, the tunneling rate vanishes for $eV \rightarrow 0$, even at $\varphi = 0$. This is the well-known Coulomb-blockade type of behaviour for tunneling in presence of Ohmic dissipation [Devoret90]. At higher bias voltages, the blockade is removed and Γ grows towards Γ_0 . The growth at low voltages is determined by the power-law behaviour of $P(E)$, which rises as $c\omega_c^{-2\alpha}E^{2\alpha-1}$, where the exponent is determined by the bath-strength rather than the exponent $s = 1$ of the bath spectrum. The dimensionless prefactor c must be found from the normalization condition for $P(E)$ and depends only on α (and the type of cutoff in the bath spectrum). Therefore, in the case of the Ohmic bath we have, at low V and $T = 0$:

$$\Gamma(V) = \Gamma_0 \frac{c}{2\alpha} \left(\frac{eV}{\omega_c} \right)^{2\alpha}. \quad (2.69)$$

Finally, we briefly discuss the case of finite temperatures, $T > 0$.

In that case, the variance of $\hat{\phi}$ is given by

$$\langle \hat{\phi}^2 \rangle = \int_0^\infty d\omega \langle \hat{\phi} \hat{\phi} \rangle_\omega^{(T=0)} \coth \left(\frac{\omega}{2T} \right), \quad (2.70)$$

which yields

$$\langle \hat{\phi}^2 \rangle \approx \langle \hat{\phi}^2 \rangle^{(T=0)} + 4\alpha \left(\frac{T}{\omega_c} \right)^{s-1} \int_0^\infty \frac{y^{s-2}}{e^y - 1} dy. \quad (2.71)$$

The approximation of extending the integral to infinity holds for temperatures much smaller than the bath cutoff ω_c . This formula gives the temperature-dependence of the renormalization factor $z = \exp \left(- \langle \hat{\phi}^2 \rangle \right)$. The second integral diverges for $s \leq 2$, because $z = 0$ for these cases, in contrast to $T = 0$ where $z = 0$ only for $s \leq 1$. Again, this results in complete absence of the interference effect in the tunneling rate $\Gamma(V, \varphi)$ (because $P_-(E)$ vanishes). It may seem surprising that an infinitesimally small temperature can yield such a drastic qualitative change compared to the zero-temperature case, since the difference should be observable only at very large times $t \gg 1/T$. However, it must be remembered

that our analysis is carried out for the limit $\Gamma_0 \rightarrow 0$, where the average decay time of the given state is infinitely large. At finite Γ_0 , the transition from one to the other case should turn out to be smooth.

Apart from the change in z with temperature, there are two other important differences to the case $T = 0$: First of all, even at $V \rightarrow 0$ the electron may emit energy into the bath, due to the thermal smearing of the Fermi surface in the lead. Secondly, it may now also absorb some energy during the tunneling process. Both facts will, in general, lead to a finite tunneling decay rate at $\varphi = \pi$, $V \rightarrow 0$ for any bath, where, at $T = 0$, the rate had vanished in any case.

We can approximate the visibility v at $V \rightarrow 0$ and finite T by using the expansion (2.63). Inserting the resulting expressions for $\gamma_{(-)}$ (2.53) into $v = \gamma_{-}/\gamma$, we obtain

$$v(T, V \rightarrow 0) \approx 1 - 4 \int d\epsilon \left\langle \hat{\phi} \hat{\phi} \right\rangle_{\epsilon} f(\epsilon). \quad (2.72)$$

We evaluate the integral for a power-law bath spectrum in the limit $T \ll \omega_c$:

$$\begin{aligned} \int d\epsilon \left\langle \hat{\phi} \hat{\phi} \right\rangle_{\epsilon} f(\epsilon) &= \\ &= \int_0^{\infty} d\epsilon \frac{\left\langle \hat{\phi} \hat{\phi} \right\rangle_{\epsilon}^{T=0}}{\sinh(\beta\epsilon)} \\ &\approx 2\alpha\omega_c^{1-s} \int_0^{\infty} d\epsilon \frac{\epsilon^{s-2}}{\sinh(\beta\epsilon)}. \end{aligned} \quad (2.73)$$

This yields:

$$1 - v(T, V \rightarrow 0) \approx 32\alpha \left(\frac{T}{\omega_c} \right)^{s-1} \left(\frac{1}{2} - 2^{-s} \right) \Gamma(s-1) \zeta(s-1), \quad (2.74)$$

where Γ is the Euler gamma function, and ζ the Riemann zeta function. Therefore, the decrease of the visibility with increasing temperature T (and $V \rightarrow 0$) is governed by the same power-law as that for increasing bias voltage V at $T = 0$, see Eq. (2.68).

2.3.5 Discussion of the results

The following discussion relates to the results obtained for $T = 0$, that are plotted in the figures.

In Fig. 2.3, several different types of bath spectra $\left\langle \hat{F} \hat{F} \right\rangle_E$ are shown. Cases (a),(b),(d) and (e) are power-laws of the form given in Eq. (2.64), for a cutoff frequency of $\omega_c = 1$. The last two (d,e) are of Ohmic type ($s = 1$, $z = 0$), which corresponds physically to gate voltage fluctuations due to Nyquist noise. Case (c) represents a bath with an excitation gap (for example optical phonons), with a spectrum given by an inverted parabola. In the

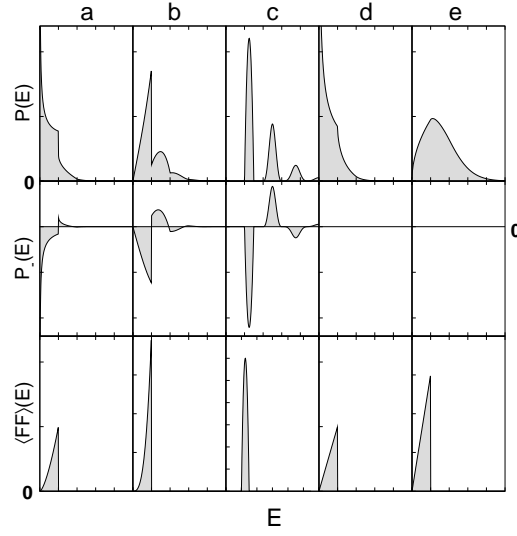


Figure 2.3: The bath spectrum $\langle \hat{F} \hat{F} \rangle_E$ (bottom) and the resulting functions $P(E)$ (top) and $P_-(E)$ (middle), plotted vs. energy E , for different baths. Energies are measured in units of the “bath cutoff” ω_c . Energy axis is the same in all panels (starting at $E = 0$, horizontal tick distance: 1); vertical tick distance in all panels is 0.5. *a*: $s = 1.5$, $\alpha = 0.25$; *b*: $s = 3$, $\alpha = 1$; *c*: Bath with gap; *d*: $s = 1$, $\alpha = 0.25$; *e*: $s = 1$, $\alpha = 0.75$ (*d,e* are Ohmic baths of different strength, $z = 0$)

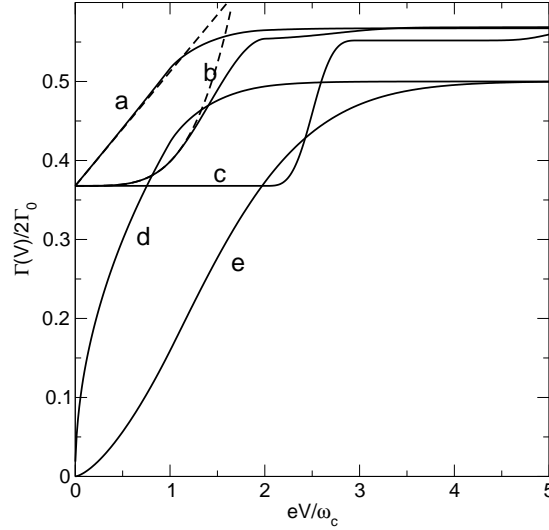


Figure 2.4: Decay rate Γ as a function of bias voltage V for the case of constructive interference ($\varphi = 0$), at $T = 0$. Curves correspond to different bath spectra shown in Fig. 2.3. Dashed lines correspond to approximation Eq. (2.67).

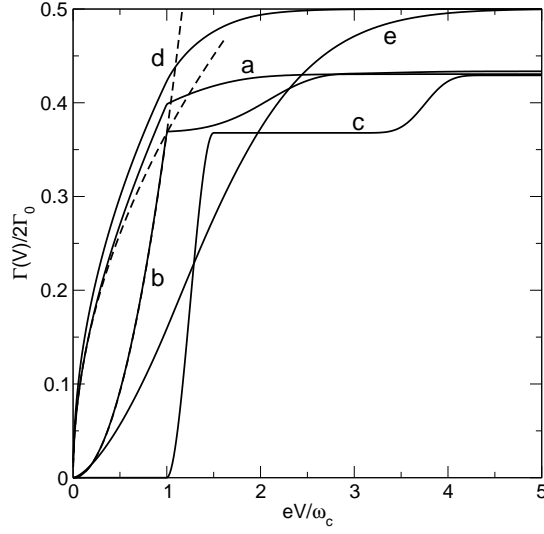


Figure 2.5: Decay rate $\Gamma(V)$ for the case of destructive interference ($\varphi = \pi$). Dashed lines refer to Eq. (2.67).

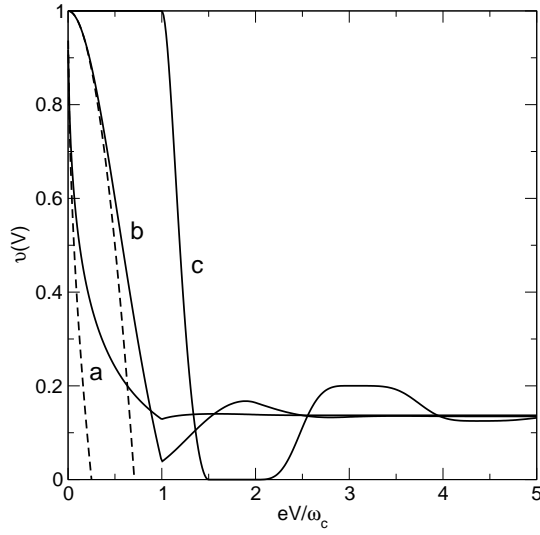


Figure 2.6: Visibility $v = (\Gamma_{\varphi=0} - \Gamma_{\varphi=\pi})/(\Gamma_{\varphi=0} + \Gamma_{\varphi=\pi})$ as a function of bias voltage V for different bath spectra (see Fig. 2.3). For the Ohmic bath (cases d,e) $v \equiv 0$. Dashed lines correspond to Eq. (2.68).

limit of infinitely small spectral bandwidth, it would correspond to the single harmonic oscillator (Einstein mode) discussed above. Case (b), with a bath spectrum rising as ω^3 , corresponds to the experimentally relevant case of piezoelectric coupling to acoustic phonons, which was determined to be the major inelastic mechanism in the experiments of [Fujisawa98] on double-dots in GaAs (see [Brandes99] for a theoretical analysis deriving this spectrum for wavelengths larger than the dot distance). The spectra for the first three cases (a,b,c) have been chosen to give the same renormalization factor, $z = 1/e$. The same figure shows the resulting functions $P(E)$ and $P_-(E)$. These have been obtained using the integral equation described in [Minnhagen76, Ingold92]. We recall that the low-energy behaviour of $P(E)$ is given by $\langle \hat{\phi} \hat{\phi} \rangle_E = \langle \hat{F} \hat{F} \rangle_E / E^2$ for the cases with $z \neq 0$, where perturbation theory may be applied. In case (c), the alternating signs of the different contributions to $P_-(E)$ may be observed, whose physical meaning has been explained above for the limiting case of the harmonic oscillator.

The resulting behaviour of $\Gamma(\varphi, V)$ at $T = 0$, calculated from Eq. (2.52), is shown in Figs. 2.4 and 2.5. In the case of constructive interference ($\varphi = 0$, Fig. 2.4), the decay rate for the “weak baths” (a,b,c) starts out from $\Gamma/2\Gamma_0 = z$ at $V = 0$ and goes to $\Gamma/2\Gamma_0 = (1+z^2)/2$ at $eV/\omega_c \gg 1$. The initial deviation from the constant value of z at low voltages is given by the power-law $V^{2(s-1)}$ contained in Eq. (2.67). In contrast, the decay rate for the Ohmic bath (d,e) starts at $\Gamma = 0$, rising with a power-law and saturating at a value of $\Gamma/2\Gamma_0 = 1/2$, corresponding to an equal admixture of odd and even states in the reduced density matrix of the electron coupled to the bath. For destructive interference ($\varphi = \pi$, Fig. 2.5), the behaviour of (a) and (b) at low voltages is given by V^{s-1} (see Eq. (2.67)), while the decay rate of the Ohmic bath (d,e) remains the same as that for $\varphi = 0$. In the special case (c) of the gapped bath, we observe perfect destructive interference up to the excitation threshold of the bath at $eV = \omega_c$, where $\Gamma(\varphi = \pi, V)$ increases in a stepwise manner for the first time, with the next increase at $eV = 3\omega_c$. Note that, on the other hand, $\Gamma(\varphi = 0, V)$ increases at even multiples of the excitation gap. The difference comes about because it is only the emission of an odd number of phonons into the bath that reveals the location of the electron, as discussed above. This feature would be absent, if the two dots were coupled to two independent baths, whereas the other qualitative properties would remain the same.

From the decay rates at $\varphi = 0$ and $\varphi = \pi$, we may calculate the visibility v of the “interference pattern” that is defined by the dependence of Γ on φ . The result is shown in Fig. 2.6. As we have noted before, the visibility is always zero for the Ohmic bath. On the other hand, for the “weak baths”, it is perfect (equal to 1) at $V \rightarrow 0$, due to the perfect destructive interference, regardless of the suppression factor z appearing in $\Gamma(\varphi = 0)$. In general, the visibility decreases towards higher bias voltages before saturating at the limiting value of z^2 . However, in contrast to intuitive expectation, the decrease may be nonmonotonous, i.e. the visibility of the interference effect may actually be enhanced by increasing the supply of energy available to the electron, although the decay rate Γ always increases monotonously at any V . This is particularly striking in case (c), where

the visibility drops down to zero in a certain range before rising again. The decrease down to the exact value of 0 is related to the special choice of $\langle \hat{\phi}^2 \rangle = 1$ ($z = 1/e$), which gives equal strengths of the peak at $E = 0$ and the first peak around $E = \omega_c$, which then are able to cancel in the integral γ_- over $P_-(E)$ that is proportional to the visibility. However, the physical reason for a dip in visibility is rather generic: In that energy range, the decay rate Γ for $\varphi = \pi$ has already increased due to dephasing, while the blockade-type suppression of the value of Γ for $\varphi = 0$ has not yet been lifted. This is a consequence of the even-odd effect discussed above.

2.3.6 Sequential tunneling through the double-dot

Up to now, we have discussed in detail the influence of the bath on the tunneling decay rate of an electron which has been placed onto the two dots in the symmetric superposition. In order to complete the picture, we have to calculate the sequential tunneling current through such a double-dot interference setup. This will be done by deriving and solving a master equation for the reduced density matrix of the double-dot system, taking into account the system-bath coupling exactly, while the tunnel-coupling is assumed to be infinitesimally small. However, in order to facilitate the understanding of the results, we first turn to a qualitative description of the situation without the bath.

At $\varphi = \pi$, tunneling is completely blocked, since the left reservoir only couples to the even state $|e\rangle$, while the right reservoir couples to the antisymmetric (odd) superposition, $|o\rangle$. At $\varphi = 0$, both reservoirs couple to $|e\rangle$, whereas $|o\rangle$ is completely decoupled from the leads (compare the discussion in [Boese02]). This means that a current may flow if $|o\rangle$ is empty. However, if $|o\rangle$ is filled, the current vanishes, because double-occupancy is forbidden in our model. Since there is no way to change the occupation of $|o\rangle$, the stationary density-matrix of the double-dot will be any convex combination of these two possibilities. At any value of φ in between these extremes, there is always the state $|\Psi\rangle = (|+\rangle - e^{-i\varphi} |-\rangle)/\sqrt{2}$, whose decay into the right lead is blocked by destructive interference. As there is a nonvanishing overlap between $|\Psi\rangle$ and the state $|e\rangle$ which is reached by tunneling from the left lead, one will observe an accumulation of population in $|\Psi\rangle$, until the current is blocked again. This holds at $T = 0$, while at finite temperatures the electron can decay towards the left lead and make a new attempt. Therefore, in this simple picture, the stationary current at $T = 0$ would be zero at any φ except for $\varphi = 0$, where it is undefined. However, one has to take into account that the coupling to the reservoirs does not only lead to decay but also to an effective tunnel coupling between $|+\rangle$ and $|-\rangle$. Although this cannot change the blockade of the current at $\varphi = \pi$ (leading only to an energy shift of $|e\rangle$ vs. $|o\rangle$), it does lift the blockade at other values of φ . This is because the blocked state $|\Psi\rangle$ is no longer stationary, such that an electron will not remain there forever. The degeneracy at $\varphi = 0$ still remains. Therefore, in the ideal case without coupling to a bath, we expect the current to vanish at $\varphi = \pi$ and to rise towards a maximal amplitude near $\varphi = 0$ which is determined by the effective tunnel-coupling. Introducing the bath will then lead to renormalization effects and spoil

the perfect destructive interference at higher values of the bias voltage (or temperature), qualitatively in the same way as it has been explained above. We will show that the actual visibility v_I of the interference pattern $I(\varphi)$ is given by a monotonous function of the visibility v introduced above (at symmetric bias).

We start with the Hamiltonian that is obtained after applying the unitary transformation of the independent boson model (2.13) onto our Hamiltonian (2.40):

$$\hat{H}' = \epsilon'(\hat{n}_+ + \hat{n}_-) + U'\hat{n}_+\hat{n}_- + \hat{H}_B + \hat{H}_L + \hat{H}_R + \hat{V}' \quad (2.75)$$

Here ϵ' is the (renormalized) energy of the two states, which we will take to be $\epsilon' = 0$ from now on. U' is the interaction constant that involves both the Coulomb repulsion as well as the effective attractive interaction induced by the bath. Because of $U = U' = \infty$, double-occupancy is forbidden.

The term which we will treat as a perturbation is given by \hat{V}' , describing the tunneling to the left and the right leads in the presence of the bath. It is the transformed version of \hat{V} , where the additional fluctuating phase factors $\exp(\pm i\hat{\phi})$ have been introduced:

$$\hat{V}' = \sum_{j=l,r} \sum_{\alpha=+,-} \hat{j}_\alpha \hat{d}_\alpha + h.c., \quad (2.76)$$

where

$$\hat{l}_\pm = e^{\pm i\hat{\phi}} \hat{l} \quad (2.77)$$

$$\hat{l} = \sum_k t_k^L \hat{a}_{Lk}^\dagger \quad (2.78)$$

$$\hat{r}_+ = e^{+i\hat{\phi}} \hat{r} \quad (2.79)$$

$$\hat{r}_- = e^{-i\hat{\phi}} e^{i\varphi} \hat{r} \quad (2.80)$$

$$\hat{r} = \sum_k t_k^R \hat{a}_{Rk}^\dagger. \quad (2.81)$$

As usual, the current through the device does not only depend on the rates for electrons to tunnel into and out of the dots, but also on the stationary state which the system assumes in the nonequilibrium situation, i.e. under an applied bias voltage.

We will now derive a master equation for the reduced density matrix $\hat{\rho}$ of the double-dot system, which contains the populations $\rho_{++}, \rho_{--}, \rho_{00}$ (“0” denoting “no electron”) and the coherences ρ_{+-} and ρ_{-+} (with $\rho_{00} = 1 - \rho_{++} - \rho_{--}$, $\rho_{\alpha 0} = \rho_{0\alpha} = 0$ for $\alpha \neq 0$, and $\rho_{-+} = \rho_{+-}^*$). We cannot simply use the standard kind of master equation, since we have to deal with two degenerate levels $|+\rangle$ and $|-\rangle$, and it is important that a tunneling event may create a coherent superposition of $|+\rangle$ and $|-\rangle$ (for example the even state $|e\rangle$).

Given the initial reduced density matrix $\hat{\rho}(0)$, and assuming the state of the environment (bath and reservoirs) to be independent of the electronic state on the dot at $t = 0$,

we obtain the time-evolution $\hat{\rho}(t)$ by tracing over the environmental degrees of freedom (“ E ”):

$$\begin{aligned}\hat{\rho}(t) &= \text{tr}_E[\hat{T}e^{-i\int_0^t ds \hat{V}'(s)}\hat{\rho}(0) \otimes \hat{\rho}_E \hat{\tilde{T}}e^{i\int_0^t ds \hat{V}'(s)}] \\ &= \hat{\rho}(0) - \int_0^t dt_1 \int_0^{t_1} dt_2 \text{tr}_E[\hat{V}'(t_1)\hat{V}'(t_2)\hat{\rho}(0) \otimes \hat{\rho}_E + h.c.] \\ &\quad + \int_0^t dt_1 \int_0^{t_1} dt_2 \text{tr}_E[\hat{V}'(t_1)\hat{\rho}(0) \otimes \hat{\rho}_E \hat{V}'(t_2)] + \dots\end{aligned}\quad (2.82)$$

Physically, by using factorized initial conditions, we neglect correlations between subsequent tunneling events which could be due to excitations in the electrodes or in the bath: Since the tunneling rate is very small, these excitations will have traveled away from the double-dot until the next event takes place. The entanglement between electron and bath (discussed in the previous sections) would preclude factorized initial conditions, if it were not treated indirectly in this approach (via the unitary transformation). Note that we do not have to make any secular approximation at this point, unlike the usual derivation of a master equation [Blum96]. It turns out that all contributions only depend on the time-difference $t_1 - t_2$ anyway, because the dot levels are degenerate. Therefore, in the long-time limit $t \rightarrow \infty$, the integration over $(t_1 + t_2)/2$ results in a factor t , and the endpoints of the integrals over $t_1 - t_2$ may be extended to ∞ . This yields the desired master equation that will determine the stationary $\hat{\rho}$, as well as the current, in the limit of weak tunnel coupling.

In the expectation values of products $\hat{V}'\hat{V}'$ only those contributions remain which combine $\hat{d}_\alpha\hat{j}_\alpha$ (tunneling out of the dots) with $\hat{j}_\beta^\dagger\hat{d}_\beta^\dagger$ (tunneling onto the dots):

$$\begin{aligned}\frac{d\hat{\rho}}{dt} &= - \sum_{\alpha,\beta,j} \int_0^\infty ds \left\{ \hat{d}_\alpha(s)\hat{d}_\beta^\dagger\hat{\rho} \left\langle \hat{j}_\alpha(s)\hat{j}_\beta^\dagger \right\rangle + h.c. \right. \\ &\quad \left. + \hat{d}_\alpha^\dagger(s)\hat{d}_\beta\hat{\rho} \left\langle \hat{j}_\alpha^\dagger(s)\hat{j}_\beta \right\rangle + h.c. \right\} \\ &\quad + \sum_{\alpha,\beta,j} \int_{-\infty}^{+\infty} ds \left\{ \hat{d}_\alpha(s)\hat{\rho}\hat{d}_\beta^\dagger \left\langle \hat{j}_\beta^\dagger\hat{j}_\alpha(s) \right\rangle + \right. \\ &\quad \left. \hat{d}_\alpha^\dagger(s)\hat{\rho}\hat{d}_\beta \left\langle \hat{j}_\beta\hat{j}_\alpha^\dagger(s) \right\rangle \right\} .\end{aligned}\quad (2.83)$$

(Note that there is no minus sign from fermion operator re-ordering in this factorization of dot and reservoir part, as the reservoir fermion operators are dragged past an even number of dot operators; compare e.g. [Schoeller99]; alternatively, it is also possible to define them as commuting operators, since there is no interaction between them). We get for the individual matrix elements (for brevity, the summation over $j = l, r$ is implied):

$$\dot{\rho}_{++} = -\rho_{++} \int_{-\infty}^{+\infty} ds \left\langle \hat{j}_+^\dagger(s)\hat{j}_+ \right\rangle$$

$$\begin{aligned}
& +\rho_{00} \int_{-\infty}^{+\infty} ds \left\langle \hat{j}_+ \hat{j}_+^\dagger(s) \right\rangle \\
& -\rho_{-+} \int_0^\infty ds \left\langle \hat{j}_+^\dagger(s) \hat{j}_- \right\rangle - h.c. ,
\end{aligned} \tag{2.84}$$

$$\begin{aligned}
\dot{\rho}_{+-} = & -\rho_{+-} \int_0^\infty ds \left\langle \hat{j}_+^\dagger(s) \hat{j}_+ \right\rangle \\
& -\rho_{+-} \int_0^\infty ds \left\langle \hat{j}_-^\dagger \hat{j}_-(s) \right\rangle \\
& +\rho_{00} \int_{-\infty}^{+\infty} ds \left\langle \hat{j}_- \hat{j}_+^\dagger(s) \right\rangle \\
& -\rho_{++} \int_0^\infty ds \left\langle \hat{j}_+^\dagger \hat{j}_-(s) \right\rangle \\
& -\rho_{--} \int_0^\infty ds \left\langle \hat{j}_+^\dagger(s) \hat{j}_- \right\rangle .
\end{aligned} \tag{2.85}$$

The equation for ρ_{--} follows from that for ρ_{++} by interchanging indices $+$ and $-$.

Now we have to evaluate environment correlators, such as the prefactor of ρ_{++} in the second equation (e.g. for $j = r$):

$$\left\langle \hat{r}_+^\dagger \hat{r}_-(s) \right\rangle = e^{i\varphi} \left\langle e^{-i\hat{\phi}} e^{-i\hat{\phi}(s)} \right\rangle \left\langle \hat{r}^\dagger \hat{r}(s) \right\rangle . \tag{2.86}$$

By introducing the bare tunneling rates $\Gamma_{R(L)0} = 2\pi D_{R(L)} \left\langle \left| t_k^{R(L)} \right|^2 \right\rangle$ (compare Eq. (2.44)), we get, using Eq. (2.81) (remember \hat{r} creates a reservoir electron):

$$\left\langle \hat{r}^\dagger \hat{r}(s) \right\rangle = \frac{\Gamma_{R0}}{2\pi} \int d\epsilon (1 - f_R(\epsilon)) e^{+i\epsilon s} . \tag{2.87}$$

Here we have neglected any energy-dependence of the tunnel-coupling and electrode DOS, assuming the relevant voltages and temperatures to be sufficiently small (but see below). The bath correlator evaluates to $\exp(-\langle \hat{\phi} \hat{\phi}(s) \rangle - \langle \hat{\phi}^2 \rangle)$, which can be expressed by using the definition (2.51) for $P_-(\omega)$. There, we have to set $s \mapsto -s$ because of the reversed order in the $\hat{\phi}$ -correlator:

$$e^{-\langle \hat{\phi} \hat{\phi}(s) \rangle - \langle \hat{\phi}^2 \rangle} = \int d\omega P_-(\omega) e^{i\omega s} . \tag{2.88}$$

Therefore, we obtain:

$$\begin{aligned}
& \int_0^\infty ds \left\langle \hat{r}_+^\dagger \hat{r}_-(s) \right\rangle = \\
& e^{i\varphi} \frac{\Gamma_{R0}}{2} \int d\epsilon (1 - f_R(\epsilon)) \tilde{P}_-^*(-\epsilon) ,
\end{aligned} \tag{2.89}$$

with

$$\begin{aligned}\tilde{P}_-(\epsilon) &= \frac{1}{\pi} \int d\omega P_-(\omega) \int_0^\infty ds e^{i(\epsilon-\omega)s} = \\ &P_-(\epsilon) + \frac{i}{\pi} \int d\omega \frac{P_-(\omega)}{\epsilon - \omega}.\end{aligned}\quad (2.90)$$

In order to abbreviate expressions like this, we introduce the following definitions for the effective in- and out-tunneling rates as well as the effective tunnel couplings generated by the electrodes:

$$\gamma_{L(-)} \equiv \Gamma_{L0} \int d\epsilon (1 - f_L(\epsilon)) P_{(-)}(-\epsilon) \quad (2.91)$$

$$\gamma_{L(-)}^{in} \equiv \Gamma_{L0} \int d\epsilon f_L(\epsilon) P_{(-)}(\epsilon) \quad (2.92)$$

$$\Delta_L \equiv -\frac{\Gamma_{L0}}{\pi} \int_{-\infty}^\Lambda d\epsilon (1 - f_L(\epsilon)) \int d\omega \frac{P_-(\omega)}{\epsilon + \omega} \quad (2.93)$$

$$\tilde{\gamma}_{L-} \equiv \gamma_{L-}[P \mapsto \tilde{P}] = \gamma_{L-} + i\Delta_L. \quad (2.94)$$

Analogous definitions hold for $L \mapsto R$. Eq. (2.91) is equivalent to the definition (2.53) used for $\gamma_{(-)}$ in previous sections. Note that the effective tunnel coupling $\Delta_{L(R)}$ depends on P_- , because it arises from transitions between the states $|+\rangle$ and $|-\rangle$, via an intermediate lead state. In the expression for $\Delta_{L(R)}$, the energy-dependence of the density of states and the tunnel coupling to the reservoir electrode should be kept in order to have a convergent integral. We will take this into account by introducing an effective upper energy cutoff Λ in the integral. Using these definitions, (2.89) is equal to $\exp(i\varphi)\tilde{\gamma}_{R-}^*/2$.

One might wonder why the effective tunnel couplings $\Delta_{L(R)}$ do depend on the occupation of electron states in the reservoirs. After all, in the non-interacting case, it is possible to calculate such a change of the single-particle Hamiltonian prior to filling in the electron states. Alternatively, in a calculation that already takes into account occupation factors, there would be two contributions which add up to an integral that does not depend on the Fermi function. However, we consider the interacting case $U = \infty$, such that (even without the bath) one of these contributions is missing (since it would involve intermediate states with double occupancy).

The general master equation for the reduced density matrix of the double-dot, derived in the limit of weak tunnel coupling but arbitrary electron-bath coupling, follows by inserting these definitions into Eqs. (2.84) and (2.85):

$$\begin{aligned}\dot{\rho}_{++} &= -\rho_{++}(\gamma_L + \gamma_R) \\ &\quad + \rho_{00}(\gamma_L^{in} + \gamma_R^{in}) \\ &\quad - \frac{\rho_{-+}}{2}(e^{i\varphi}\tilde{\gamma}_{R-} + \tilde{\gamma}_{L-}) - h.c.,\end{aligned}\quad (2.95)$$

$$\begin{aligned}
\dot{\rho}_{--} = & -\rho_{--}(\gamma_L + \gamma_R) \\
& + \rho_{00}(\gamma_L^{in} + \gamma_R^{in}) \\
& - \frac{\rho_{+-}}{2}(e^{-i\varphi}\tilde{\gamma}_{R-} + \tilde{\gamma}_{L-}) - h.c.,
\end{aligned} \tag{2.96}$$

$$\begin{aligned}
\dot{\rho}_{+-} = & -\rho_{+-}(\gamma_L + \gamma_R) \\
& + \rho_{00}(e^{i\varphi}\gamma_{R-}^{in} + \gamma_{L-}^{in}) \\
& - \frac{\rho_{++}}{2}(e^{i\varphi}\tilde{\gamma}_{R-}^* + \tilde{\gamma}_{L-}^*) \\
& - \frac{\rho_{--}}{2}(e^{i\varphi}\tilde{\gamma}_{R-} + \tilde{\gamma}_{L-}).
\end{aligned} \tag{2.97}$$

The ingredients of the master equation obtained here may be interpreted as follows: The imaginary part of the right hand side corresponds to the unitary time-evolution generated by the effective tunneling Hamiltonian

$$\hat{H}_{eff}^T = \frac{1}{2}(e^{i\varphi}\Delta_R + \Delta_L)|+\rangle\langle-| + h.c.. \tag{2.98}$$

The in-tunneling contributions in the equations for ρ_{++} and ρ_{--} depend on $P(E)$, while that for ρ_{+-} is determined by $P_-(E)$, since it describes the creation of a coherent superposition of $|+\rangle$ and $|-\rangle$ (which is hindered by the bath). This term would be absent in the usual master equation. In particular, if $\gamma_{L-}^{in} \rightarrow \gamma_L^{in}$, which will be the case at $T = 0$ for vanishing bias between the dots and the left electrode, an electron tunneling from the left lead will end up in the coherent superposition where $\rho_{+-} = \rho_{++} = \rho_{--}$. Taking into account that we are working in a transformed basis, this describes just the entangled state (2.46), confirming the starting point of our earlier discussion. Note that the out-tunneling contribution for ρ_{++} also depends on ρ_{+-} , for example. This reflects the fact that a superposition between the two states may be blocked from decaying into the lead, while each state separately can decay.

The stationary density matrix is obtained by demanding $d\hat{\rho}/dt = 0$ (and using the relations $\rho_{00} = 1 - \rho_{++} - \rho_{--}$ and $\rho_{-+} = \rho_{+-}^*$). We get the current from the contribution of the left electrode to the change $\dot{\rho}_{++} + \dot{\rho}_{--}$ in the double-dot occupation (which is equal to the right-going current in the stationary limit):

$$\begin{aligned}
\frac{I}{e} = & (\dot{\rho}_{++} + \dot{\rho}_{--})_L = \\
& 2\rho_{00}\gamma_L^{in} - \gamma_L(\rho_{++} + \rho_{--}) - 2\gamma_L Re[\rho_{+-}].
\end{aligned} \tag{2.99}$$

In order to evaluate the current as a function of temperature T , bias voltage V and phase difference φ , we will now specialize to the case of symmetric bias and left-right

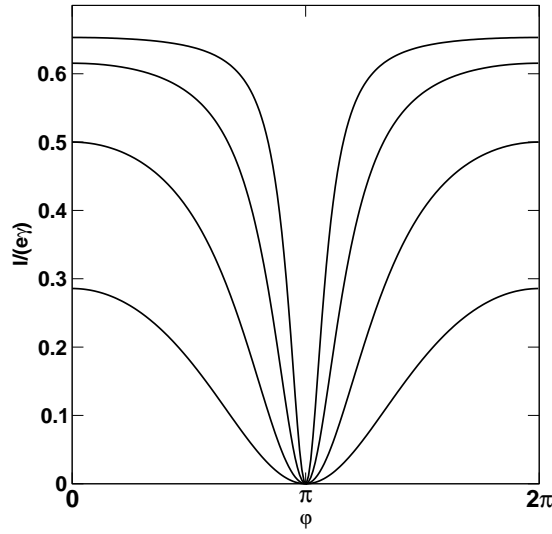


Figure 2.7: The shape of the “interference pattern” $I(\varphi)$ at $T = 0$, without coupling to a bath, for different values of the effective tunnel couplings $-\delta_L = -\delta_R = 0.5, 1, 2, 4$ (from bottom to top).

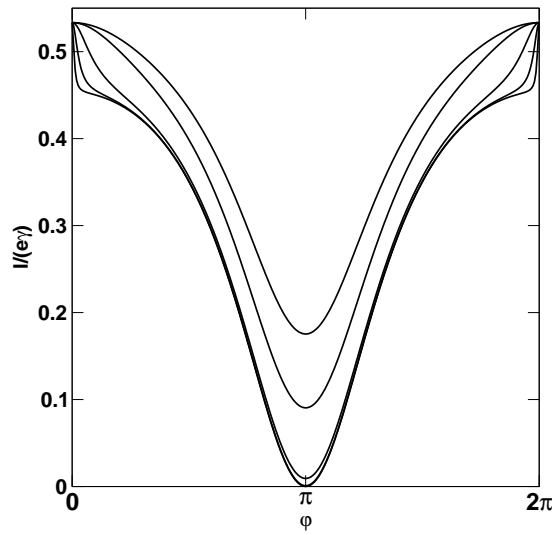


Figure 2.8: The current I for different values of the visibility $v = \gamma_- / \gamma = 0.8, 0.9, 0.99, 0.999, 0.9999$ (from top to bottom). The limits $\varphi \rightarrow 0$ and $v \rightarrow 1$ do not commute. Other parameters held fixed: $\lambda = e^{-\beta\mu} = 0.2$ and $\delta_L = \delta_R = -1$.

symmetric tunnel couplings ($\Gamma_{R0} = \Gamma_{L0} = \Gamma_0$). All essential features (in particular the perfect destructive interference in absence of the bath) are independent of this assumption.

We find from Eqs. (2.91)-(2.94), using $f(\epsilon) = 1 - f(-\epsilon)$:

$$\gamma_{R(-)} = \gamma_{L(-)}^{in} = \gamma_{(-)} \equiv \Gamma_0 \int d\epsilon f(\epsilon - \mu) P_{(-)}(\epsilon), \quad (2.100)$$

where $\mu = eV/2$ is the chemical potential of the left reservoir. This is definition (2.53), with eV replaced by μ (since we deal with the symmetric bias case). Furthermore, we use the condition of detailed balance, $P_{(-)}(-E) = \exp(-\beta E) P_{(-)}(E)$ (see, for example, [Ingold92]), which leads to

$$\gamma_{L(-)} = \gamma_{R(-)}^{in} = e^{-\beta\mu} \gamma_{(-)}. \quad (2.101)$$

The effective tunnel couplings are still different (because of the different Fermi distributions):

$$\Delta_{L(R)} = -\frac{\Gamma_0}{\pi} \int_{-\infty}^{\Lambda} d\epsilon f(-(\epsilon \mp \mu)) \int d\omega \frac{P_{-}(\omega)}{\epsilon + \omega}. \quad (2.102)$$

The lower sign belongs to the right electrode.

For the special case of $T = 0$, electrons always enter from the left and go to the right, such that we have $\gamma_L = \gamma_{L-} = \gamma_R^{in} = \gamma_{R-}^{in} = 0$ and $\gamma_{R(-)} = \gamma_{L(-)}^{in} = \gamma_{(-)}$, with

$$\gamma_{(-)} = \Gamma_0 \int_0^{\mu} d\epsilon P_{(-)}(\epsilon). \quad (2.103)$$

The effective tunnel couplings are, at $T = 0$:

$$\Delta_{L(R)} = -\frac{\Gamma_0}{\pi} \int d\omega P_{-}(\omega) \ln \left[\frac{\Lambda + \omega}{|\mu \pm \omega|} \right]. \quad (2.104)$$

Note that $\Delta_{L(R)}$ will have a logarithmic singularity at $\mu \rightarrow 0$, for $T = 0$. The cutoff Λ may be on the scale of the bandwidth of the reservoir's electronic energy band, for example. We assume $\Lambda \gg \mu, \omega$.

In the limit of high bias voltages ($\omega \ll \Lambda, \mu$), we obtain effective tunnel couplings whose magnitude goes as z^2 and decreases logarithmically with μ :

$$\Delta_L \approx \Delta_R \approx -\frac{\Gamma_0}{\pi} \ln \left[\frac{\Lambda}{\mu} \right] \int d\omega P_{-}(\omega) = -z^2 \frac{\Gamma_0}{\pi} \ln \left[\frac{\Lambda}{\mu} \right]. \quad (2.105)$$

By solving the master equation for the stationary density matrix and inserting into Eq. (2.99), we obtain the expression for the current through the double dot in terms of all of the quantities mentioned previously. In general (at arbitrary T), it is found that the current may be written as the product of γ with a dimensionless function of the phase difference φ and the ratios $v = \gamma_{-}/\gamma$, $\delta_{L(R)} = \Delta_{L(R)}/\gamma$ and $\beta\mu$:

$$I = e\gamma I_0[\varphi, \beta\mu, v, \delta_L, \delta_R]. \quad (2.106)$$

The complete expression for I_0 is very cumbersome (it is listed for $T = 0$ in Appendix A.2). Therefore, let us first discuss the situation without coupling to a bath. In that case, we obtain

$$\delta_L = \delta_R \equiv \delta = -\frac{\Gamma_0}{\pi} \int_{-\infty}^{\Lambda} \frac{d\epsilon}{\epsilon} f(\mu - \epsilon) \quad (2.107)$$

and $\gamma = \gamma_- = \Gamma_0 f(-\mu)$. The current turns out to be (with $\lambda \equiv e^{-\beta\mu}$):

$$\frac{I}{e\gamma} = \frac{4(1-\lambda)(\delta^2 + \lambda) \cos^2(\frac{\varphi}{2})}{3\delta^2 + 2(1+\lambda+\lambda^2) + 3\delta^2 \cos(\varphi)}. \quad (2.108)$$

Several points should be noticed about this expression: Firstly, the destructive interference at $\varphi = \pi$ remains perfect regardless of temperature, because there are no current-carrying states at all. At zero temperature ($\lambda = 0$), the maximal amplitude of the current is $I_{\max}/e\gamma = 2\delta^2/(3\delta^2 + 1)$, which vanishes when the effective tunnel coupling δ goes to zero. This has been explained above as a consequence of the possible transition into a current-blocking state, which can only be undone by the effective tunnel coupling. At finite temperatures ($\lambda > 0$), the maximal current is nonzero even for $\delta \rightarrow 0$, where it approaches the value of $I_{\max}/e\gamma = 2\lambda(1-\lambda)/(1+\lambda+\lambda^2)$. This has a maximum at around $T \sim \mu$. It vanishes for larger temperatures as μ/T , which is to be expected for tunneling through a localized level (decreasing derivative of the Fermi function). In addition, the shape of $I(\varphi)$ depends on δ and λ , with a sharper minimum at $\varphi = \pi$ in the case of larger $|\delta|$. In the limit of $\delta \rightarrow 0$, the current becomes a pure cosine. This is shown in Fig. 2.7 for the case of $T = 0$. At finite temperatures (as well as for $v \neq 1$) the behaviour is similar, except for the finite amplitude of the current at $\delta \rightarrow 0$.

Now we turn to the situation including the bath. The general expression for the current is very lengthy, and we will omit it here. However, it turns out that the maximal and minimal current are functions merely of v and $\lambda = e^{-\beta\mu}$, while they are independent of $\delta_{L,R}$.

The amplitude of the minimal current (at $\varphi = \pi$) is given by

$$\frac{I(\varphi = \pi)}{e\gamma} = \frac{2(1+\lambda)(1-\lambda^2)(1-v^2)}{3(1+\lambda)^2 + (1-\lambda)^2 v^2}, \quad (2.109)$$

while the maximal current (at $\varphi = 0$) is

$$\frac{I(\varphi = 0)}{e\gamma} = \frac{2}{3}(1-\lambda). \quad (2.110)$$

It should be noted that the expression (2.108) for the current in the ideal case seems to contradict this simple formula. However, that is because the limits $\varphi \rightarrow 0$ and $v \rightarrow 1$ do not commute. This is shown in Fig. 2.8. It means that for $T = 0$ and $\delta_{L,R} \rightarrow 0$ the

maximal current calculated according to (2.110), which is independent of $\delta_{L,R}$, and the “typical” amplitude of the current ($\propto \delta_L^2$) may deviate strongly. The peculiar behaviour near $\varphi = 0$ seems to be connected to the physical degeneracy of the case $\varphi = 0, v = 1$ which has been discussed above.

The dependence of the interference pattern $I(\varphi)$ on the bias voltage is shown in Fig. 2.9, for one specific example of a particular bath and at some finite temperature.

From these formulas, we obtain the visibility, defined in terms of the current:

$$v_I \equiv \frac{I(\varphi = 0) - I(\varphi = \pi)}{I(\varphi = 0) + I(\varphi = \pi)}. \quad (2.111)$$

It can be expressed entirely by the visibility v defined previously, as well as λ :

$$v_I = \frac{2(1 + \lambda + \lambda^2)v^2}{3(1 + \lambda)^2 - (1 + 4\lambda + \lambda^2)v^2}. \quad (2.112)$$

This is a monotonous mapping of v to the interval $[0, 1]$, with only a weak dependence on λ . The other parameters δ_L, δ_R only modify the amplitude and shape of the current pattern $I(\varphi)$. Therefore, all the statements about the visibility made in the previous discussion of the tunneling decay out of the symmetric superposition continue to hold qualitatively (with eV replaced by $\mu = eV/2$). In particular, at $T = 0$, we have

$$v_I = \frac{2v^2}{3 - v^2}. \quad (2.113)$$

The dependence of the visibility v_I on the bias voltage $eV = 2\mu$, the temperature T and the bath spectrum is displayed in Fig. 2.10, for bath spectra of type (b) and (c). The decrease of v_I at $\mu = 0$ with increasing temperature T in case (b) is well approximated by Eq. (2.74) for $v(T, V \rightarrow 0)$ (employing the relation $v_I = v^2/(2 - v^2)$ for $\mu = 0$). (The functions $P_{(-)}(E)$ for finite temperatures have been calculated numerically using the fast Fourier transform, from the defining equation (2.51)).

Note that at any finite temperature, the bath spectrum (a) (rising as $\omega^{1.5}$) has $z = 0$, just as the Ohmic bath (d,e). Therefore, the visibility vanishes entirely (at any V) for these spectra, as has been explained in the previous sections. We have already pointed out that this picture is expected to change if one treats the tunnel-coupling to higher order. However, we have to leave this analysis for the future. A promising approach to a nonperturbative (but still approximate) treatment of both the tunnel-coupling and the system-bath coupling at the same time seems to be the numerical “real-time renormalization group” scheme [Schoeller99].

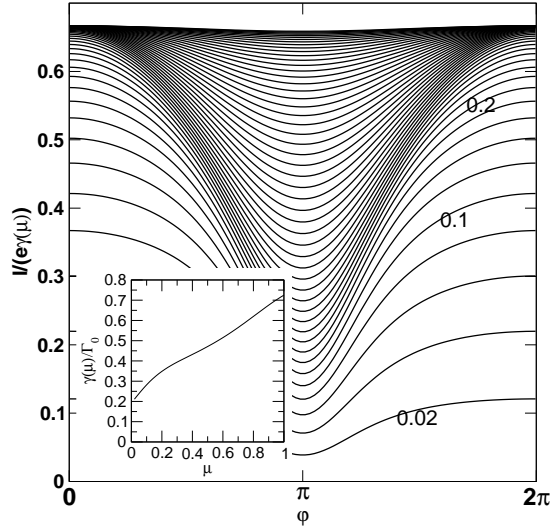


Figure 2.9: The current $I(\varphi)$ as a function of bias voltage $eV = 2\mu$, with $\mu/\omega_c = 0.02, 0.04, \dots, 1$ (from bottom to top) for the case of the acoustic-phonon type bath (b) (see above, spectrum rising like ω^3). The temperature T has been chosen as $T/\omega_c = 0.1$. For better clarity, the current has been scaled by γ , whose dependence on μ is displayed in the inset.

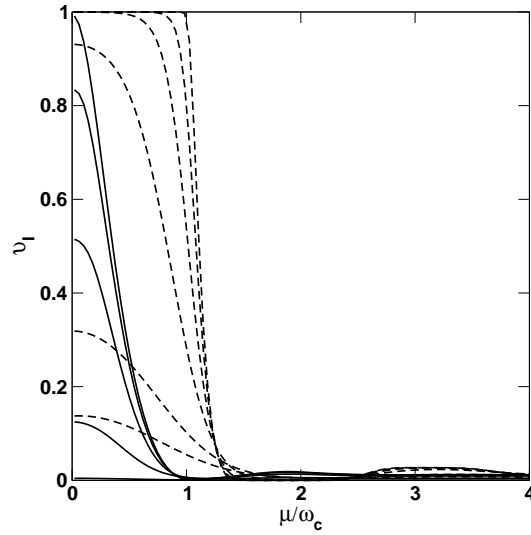


Figure 2.10: The visibility v_I of the pattern $I(\varphi)$, for the acoustic phonon bath (b) (solid line) and the optical phonons (c) (dashed line), plotted vs. $\mu = eV/2$, at different temperatures $T/\omega_c = 0.01, 0.05, 0.1, 0.2, 0.4$ (top to bottom).

2.4 Cotunneling and connection to the Feynman-Vernon influence functional

The analogy between a conventional double-slit experiment and a mesoscopic transport interference experiment becomes closer in a cotunneling setup, where the traveling electron cannot stay on the central island, because it does not have enough energy. In that situation, the electron is forced to tunnel from the left electrode to the right electrode in an uninterrupted two-step process, via a virtual intermediate state on the island. Constructive or destructive interference between cotunneling through different states is similar to the interference between different paths in the double-slit experiment, and it may be affected by the fluctuations of the environment. According to Heisenberg's uncertainty relation, the intermediate state is only occupied for a short amount of time, on the order of $1/\Delta E$, where ΔE is the typical energy barrier separating the intermediate state from the energy of an electron at the Fermi level of the reservoirs. An optical analogy consists in evanescent light waves leaking from one medium into another, across a region of space where they are subject to a fluctuating index of refraction.

We will also explain how the two-particle Green's function and the cotunneling current can be related to the Feynman-Vernon influence functional in the case of the independent boson model, affording a somewhat clearer physical picture. Usually, there is no simple generalization of the influence functional from the single-particle to the many-particle case (disregarding a purely formal treatment, where the whole many-particle system is treated as the "system" in question). Although just such a generalization has been derived recently [Golubev99], evaluating the resulting expressions in a reliable way leads to great difficulties. We treat the independent boson model, which is an exceptionally simple case, since no transitions are induced by the bath, that would lead to complicated many-particle physics. Nevertheless, the Pauli principle still becomes important for cotunneling through a set of localized levels coupled to a bath. Energy conservation and Pauli blocking of final states suppress the dephasing effects of the bath's zero-point fluctuations at low bias voltages and temperatures, as has been demonstrated for sequential tunneling in the previous section. Therefore, the treatment explained below is a particularly simple special example of a slightly modified influence functional applied to a situation where the Pauli principle matters.

2.4.1 Two-particle Green's function and influence functional

An introduction to the Feynman-Vernon influence functional [Feynman63, 65] will be given in Chapter 5. Here we merely point out that it encodes the complete influence of a dissipative bath onto a quantum system coupled to that bath. Knowledge of the influence functional suffices in principle to calculate the time-evolution of the reduced system density matrix under any circumstances. Formally, it is obtained as the overlap between two different bath states, $|\chi^>\rangle$ and $|\chi^<\rangle$, that arise out of a given initial state $|\chi_0\rangle$ under the action of the system passing along the trajectories $q^>(\cdot)$ and $q^<(\cdot)$, respectively.

In this notation, q is the system variable that couples to the bath, and $q^>(\cdot)$, $q^<(\cdot)$ are to be treated as c -number functions of time. The functional must be known for arbitrary pairs of trajectories, since, in the end, it is to be used in a path integral expression where one has to integrate over all such pairs of paths in order to obtain the time-evolution of the reduced density matrix of the system. At zero temperature, the state $|\chi_0\rangle$ is the ground state of the unperturbed bath, which is not yet coupled to the system. At finite temperatures, a thermal average over $|\chi_0\rangle$ has to be performed in order to obtain the influence functional.

We would like to interpret the two-particle Green's functions of the independent boson model, such as (2.32), in terms of the influence functional. As explained above, the electronic part becomes (nearly) trivial, and it is the remaining average over bath operators $\exp(i\hat{\phi}_j)$ (see Eq. (2.35)) which we want to rewrite as an overlap between bath states.

In order to do so, we will use that $\exp(i\hat{\phi}_j)$ is the displacement operator which produces the ground-state of the bath in presence of a particle on level j out of the ground-state in absence of the particle (all other particles being spectators). More generally, from a specialization of the canonical transformation in Eq. (2.13), we find for any bath eigenstate $|B\rangle$:

$$(\hat{F}_j + \hat{H}_B[\{n_k\}])e^{i\hat{\phi}_j}|B\rangle = (E_B + \delta E_j)e^{i\hat{\phi}_j}|B\rangle. \quad (2.114)$$

Here E_B is the energy of the state $|B\rangle$, which is assumed to be an energy eigenstate of the bath for a given configuration $\{n_k\}$ of occupation numbers (with $n_j = 0$), i.e. for the Hamiltonian $\hat{H}_B[\{n_k\}] \equiv \hat{H}_B + \sum_k n_k \hat{F}_k$. The energy shift δE_j upon introduction of particle j has been given in Eq. (2.21), and it depends on the initial configuration $\{n_k\}$.

In the time-evolution of a coherent superposition of states l and j , we expect the suppression of the off-diagonal elements of the density matrix to be governed by the overlap between bath states $|\chi_l\rangle$ and $|\chi_j\rangle$ that evolve out of the initial state $|\chi_0\rangle$ in presence of an extra particle on level l or j (compare the discussion for the diagonal spin-boson model around Eq. (2.7)). In our case, these states are given by:

$$\begin{aligned} |\chi_j(t)\rangle &\equiv e^{-i(\hat{F}_j + \hat{H}_B[\{n_k\}])t} |\chi_0\rangle = \\ &e^{-i\delta E_j t} e^{i\hat{\phi}_j} e^{-i\hat{H}_B[\{n_k\}]t} e^{-i\hat{\phi}_j} |\chi_0\rangle = \\ &e^{-i(\delta E_j + \delta E[\{n_k\}])t} e^{i\sum_k n_k \hat{\phi}_k} e^{i\hat{\phi}_j} e^{-i\hat{H}_B t} e^{-i\hat{\phi}_j} e^{-i\sum_k n_k \hat{\phi}_k} |\chi_0\rangle. \end{aligned} \quad (2.115)$$

We have employed the canonical transformation (2.114) twice and denoted by $\delta E[\{n_k\}]$ the difference in ground state energies between the Hamiltonians $\hat{H}_B[\{n_k\}]$ and \hat{H}_B . If $|\chi_0\rangle$ has been an energy eigenstate of $\hat{H}_B[\{n_k\}]$, then

$$e^{-i\sum_k n_k \hat{\phi}_k} |\chi_0\rangle \quad (2.116)$$

in the last line of (2.115) is an eigenstate of \hat{H}_B itself, according to Eq. (2.114). We denote it by $|0_B\rangle$. Therefore, the overlap is equal to

$$\langle \chi_j(t) | \chi_l(t) \rangle = e^{-i(\delta E_l - \delta E_j)t} \left\langle 0_B | e^{i\hat{\phi}_j} e^{-i\hat{\phi}_j(t)} e^{i\hat{\phi}_l(t)} e^{-i\hat{\phi}_l} | 0_B \right\rangle. \quad (2.117)$$

Here, the time-evolution of $\hat{\phi}_j(t)$ is governed by \hat{H}_B alone, and any reference to the initial configuration is only in the values of the energy shifts $\delta E_{j,l}$. At zero temperature, $|0_B\rangle$ refers to the bath ground state, while a further thermal average over $|0_B\rangle$ is necessary at finite T .

However, by comparing (2.117) to the expression for the two-particle Green's function that describes the decay of a superposition of levels l and j , Eq. (2.34), we find that they differ in the order of operators. This has a straightforward physical reason: In the Green's function, l and j do not enter on an equal footing. It describes a situation where, initially, level j has been occupied, such that the bath has adapted to the presence of a particle on j . Then a perturbation creates a small admixture of level l . After some time t , the resulting off-diagonal element of the density-matrix is read out. In contrast, what we have employed up to now amounts to a version of “factorized” initial conditions, in which the initial states of bath and system are assumed to be uncorrelated. More precisely, the initial bath state $|\chi_0\rangle$ has been assumed to be affected only by the fixed configuration of particles on levels other than l and j . Now we have to define $|\chi_0\rangle$ as the ground state of $\hat{H}_B[\{n_k\}']$, with $n_j = 1$ in $\{n_k\}'$, instead of $\hat{H}_B[\{n_k\}]$ with $n_j = 0$. In (2.117), this amounts to replacing $|0_B\rangle$ by $\exp(i\hat{\phi}_j)|0_B\rangle$. This replacement then leads to

$$\langle \chi'_j(t) | \chi'_l(t) \rangle = e^{-i(\delta E_l - \delta E_j)t} \left\langle e^{-i\hat{\phi}_j(t)} e^{i\hat{\phi}_l(t)} e^{-i\hat{\phi}_l} e^{i\hat{\phi}_j} \right\rangle, \quad (2.118)$$

where we take the angular brackets on the right hand side to denote a thermal average. Consequently, the result for the two-particle Green's function, Eq. (2.34), can be identified as:

$$\begin{aligned} & \left\langle \hat{d}_j^\dagger(t) \hat{d}_l(t) \hat{d}_l^\dagger(0) \hat{d}_j(0) \right\rangle = \\ & e^{-i(\epsilon_l - \epsilon_j)t} \left\langle (1 - n_l) n_j \langle \chi'_j(t) | \chi'_l(t) \rangle \right\rangle_{\{n_k\}}. \end{aligned} \quad (2.119)$$

The overlap of bath states (i.e. the influence functional) still has to be averaged over configurations $\{n_k\}$ (employing \hat{H}'_{el} , see Eq. (2.18)), since the energies δE_l and δE_j depend on the configuration. For the same reason, we cannot simply pull out a factor referring to the unperturbed Green's function, as the occupation numbers $n_{l,j}$ may be changed in thermal equilibrium due to coupling to the bath. If the bath expectation value of Eq. (2.118) is pulled out of the configuration average in (2.119), the remaining factor just reproduces the “electronic” part $\langle \cdot \rangle_{el}$ introduced earlier in Eq. (2.18). This formula simplifies at sufficiently low temperatures, when only the single ground-state configuration is occupied. Nevertheless, in spite of the configurational average, (2.119) is of course far simpler than usual applications of the influence functional, because the integration over pairs of system paths may be omitted, due to the diagonal coupling.

The original overlap (2.117) of bath states that evolve under the action of a particle being either in level l or in level j , comes into play in situations where initially neither l nor j are occupied. Formally, it enters Green's functions like

$$\begin{aligned} & \left\langle \hat{d}_j(0) \hat{d}_j^\dagger(t) \hat{d}_l(t) \hat{d}_l^\dagger(0) \right\rangle = \\ & \left\langle \hat{d}_j(0) \hat{d}_j^\dagger(t) \hat{d}_l(t) \hat{d}_l^\dagger(0) \right\rangle_{el} \left\langle e^{i\hat{\phi}_j} e^{-i\hat{\phi}_j(t)} e^{i\hat{\phi}_l(t)} e^{-i\hat{\phi}_l} \right\rangle = \\ & e^{-i(\epsilon_l - \epsilon_j)t} \langle (1 - n_j)(1 - n_l) \langle \chi_j(t) | \chi_l(t) \rangle \rangle_{\{n_k\}} . \end{aligned} \quad (2.120)$$

Physically, it occurs in situations that are comparable to a double-slit experiment, where an electron passes through either state l or j while traveling through the set of localized levels coupled to a bath. The appropriate mesoscopic realization is a cotunneling setup, where two-particle Green's functions and, therefore, the influence functional directly enter the cotunneling current as an observable quantity. This is the subject of the next section.

2.4.2 Cotunneling expressions for the independent boson model

For a general review on cotunneling, we refer the reader to [Averin92]. Cotunneling in the presence of dissipation, stemming from a resistor in series with the tunnel junctions, has been treated in [Odintsov92]. General formulas for cotunneling through localized levels that are coupled to a bath in the form of the independent boson model, such as those derived below, have been derived previously in [Chen93]. However, the bath-induced effective interaction was not treated properly, no discussion of interference effects was given, and the treatment was restricted to electronically inelastic cotunneling. In earlier work by Wingreen et al. [Wingreen88], an exact result for the transmission coefficient of an electron tunneling through a single level subject to a fluctuating potential was derived, for arbitrary tunnel coupling (see also [Groshev91]). Unfortunately, this does not imply an exact result for the current, due to possible correlations between subsequent tunneling events (see also the discussion of this point in [König96]). Nevertheless, in the limit of small tunnel coupling, the expression for the current in [Wingreen88] coincides with the appropriate expression given below (cf. Eq. (2.143)), when the latter is specialized to a single level.

The Hamiltonian to be considered is the sum of the independent boson Hamiltonian \hat{H}_{IB} (2.10), describing localized levels coupled to a bath, the Hamiltonian \hat{H}_{LR} describing the left (L) and right (R) reservoir electrodes, and a tunneling Hamiltonian \hat{H}_T :

$$\hat{H} = \hat{H}_{IB} + \hat{H}_{LR} + \hat{H}_T , \quad (2.121)$$

with

$$\hat{H}_{IB} = \sum_j (\varepsilon_j + \hat{F}_j) \hat{n}_j + \hat{H}_B \quad (2.122)$$

$$\hat{H}_{LR} = \sum_{r=L,R} \epsilon_{rk} \hat{a}_{rk}^\dagger \hat{a}_{rk} \quad (2.123)$$

$$\hat{H}_T = \hat{L}^+ + \hat{L}^- + \hat{R}^+ + \hat{R}^- . \quad (2.124)$$

Here $\hat{L}^{+(-)}$ describes tunneling onto (off) the localized levels through the left junction, and $\hat{R}^{+(-)}$ stands for tunneling onto (off) these levels through the right junction,

$$\begin{aligned} \hat{L}^+ &= \sum_{kj} T_{jk}^L \hat{d}_j^\dagger \hat{a}_{Lk} \\ \hat{L}^- &= (\hat{L}^+)^\dagger, \end{aligned} \quad (2.125)$$

and the same with $L \mapsto R$.

We assume a Coulomb blockade situation, where it is not possible for the number of charges on the central island to change permanently, since the resulting state would have an energy larger than the energy available to electrons in the reservoirs. The goal is to calculate the cotunneling current that flows from the left to the right electrode if a bias voltage is applied between the electrodes, i.e. when the chemical potentials differ by an amount $\mu_L - \mu_R = eV$. In the limit of small tunnel couplings, the cotunneling current can be derived either by solving for the nonlinear response of the current to the tunneling perturbation [Averin92, Odintsov92, Chen93], or by employing the Golden Rule. We will start from the Golden Rule, since it allows a clearer physical picture.

According to the standard second-order Golden Rule expression [Landau77], transitions from some initial state $|i\rangle$ to a final state $|f\rangle$ via any intermediate state $|\nu\rangle$ occur at the rate

$$\Gamma_{f \leftarrow i} = 2\pi \left| \sum_{\nu} \frac{V_{f\nu} V_{\nu i}}{E_{\nu} - E_i} \right|^2 \delta(E_f - E_i), \quad (2.126)$$

which is to be summed over the appropriate set of final states in the end. This holds as long as there are no direct transitions from $|i\rangle$ to $|f\rangle$ ($V_{fi} = 0$) and if the intermediate energies E_{ν} are different from the initial energy E_i , such that $|\nu\rangle$ represents a barrier.

In the present case, the perturbation \hat{V} is given by the tunnel Hamiltonian \hat{H}_T . The states $|i\rangle$, $|f\rangle$ and $|\nu\rangle$ refer to energy eigenstates of the complete system, comprised out of the island levels coupled to the bath, together with the electron reservoirs, but without the tunnel coupling. In particular, $|f\rangle$ differs from $|i\rangle$ by an electron having moved from the left to the right reservoir (or vice versa), in order to contribute to the current flow. In addition, $|f\rangle$ may contain an electron-hole excitation left over on the island (electronically inelastic cotunneling) and/or an excitation in the bath (inelastic cotunneling with respect

to the bath). In the intermediate state $|\nu\rangle$, the number of electrons on the central island is changed by ± 1 , relating to an extra electron (extra hole) being present. Although the tunneling by itself does not change the state of the bath, $V_{\nu i}$ and $V_{f\nu}$ nevertheless connect to bath states that differ from the initial one. This is because in the presence of an extra electron (or hole) the Hamiltonian acting on the bath is changed, such that the bath energy eigenstates occurring in $|\nu\rangle$ are different from the eigenstates in $|i\rangle$ and $|f\rangle$ (compare Fig. 2.2). Physically, we may imagine the extra electron to shift the bath oscillators, while leaving their ground state wave functions (at $T = 0$) unperturbed initially. In the displaced oscillator potentials, these wave functions start to oscillate back and forth in the form of coherent states. After the electron has left the island, the potentials are back to their initial position, but the wave function now contains a superposition of excited states. Obviously, these inelastic cotunneling processes may lead to dephasing of the interference between different tunneling paths $|\nu\rangle$, since the electron can leave a trace in the bath.

As we are to employ expressions involving averages of bath operators at different times (such as those discussed in the previous section), we go over from the sum over intermediate energies to a time-integral:

$$\begin{aligned} \sum_{\nu} \frac{V_{f\nu} V_{\nu i}}{E_{\nu} - E_i} &= i \sum_{\nu} \int_0^{\infty} d\tau V_{f\nu} e^{-i(E_{\nu} - E_i)\tau} V_{\nu i} \\ &= i \int_0^{\infty} d\tau \langle f | \hat{V} \hat{V}(-\tau) | i \rangle. \end{aligned} \quad (2.127)$$

We denote by Γ^+ the total tunneling rate where electrons move from left to right. There are exactly two possible processes that enter (2.127) in that case: Either an electron hops onto the island through the left junction, and then leaves through the right junction (extra electron in $|\nu\rangle$), or an electron first leaves through the right junction, creating an extra hole on the island, and afterwards another electron enters from the left. Therefore, we have to replace $\hat{V} \hat{V}(-\tau)$ in (2.127) by

$$\hat{L}^+ \hat{R}^-(\tau) + \hat{R}^- \hat{L}^+(\tau), \quad (2.128)$$

in order to obtain Γ^+ . Since this selects the correct final states, we are allowed to sum over all $|f\rangle$. In addition, a thermal average over initial states $|i\rangle$ has to be carried out:

$$\begin{aligned} \Gamma^+ &= \langle \Gamma_{f \leftarrow i}^+ \rangle_{fi} \\ &\equiv 2\pi \left\langle \sum_f \left| \int_0^{\infty} d\tau \langle f | \hat{L}^+ \hat{R}^-(\tau) + \hat{R}^- \hat{L}^+(\tau) | i \rangle \right|^2 \delta(E_f - E_i) \right\rangle_i \\ &\equiv \Gamma_{pp}^+ + \Gamma_{ph}^+ + \Gamma_{hp}^+ + \Gamma_{hh}^+. \end{aligned} \quad (2.129)$$

The four contributions in the last line arise from expanding the square and are classified according to whether they contain an extra particle or hole in the first or second

intermediate state. We discuss the evaluation of Γ_{pp}^+ , which relates to the simplest possibility of interference between two states through which an electron can tunnel. The energy-conserving δ function is expressed as a time-integral:

$$\Gamma_{pp}^+ = \int_{-\infty}^{+\infty} dt \int_0^{\infty} d\tau^> \int_0^{\infty} d\tau^< \left\langle \hat{L}^-(t - \tau^<) \hat{R}^+(t) \hat{R}^-(0) \hat{L}^+(-\tau^>) \right\rangle \quad (2.130)$$

We employ the explicit expressions for the tunneling operators, Eq. (2.125), and use Wick's theorem to evaluate the contribution from the reservoir fermion operators. This gives

$$\begin{aligned} \Gamma_{pp}^+ = & \sum_{k_L, k_R} f_L (1 - f_R) \sum_{j_1 j_2 j_3 j_4} T_{j_1}^{L*} T_{j_2}^R T_{j_3}^{R*} T_{j_4}^L \times \\ & \int_{-\infty}^{+\infty} dt e^{i(\epsilon_L - \epsilon_R)t} \int_0^{\infty} d\tau^> \int_0^{\infty} d\tau^< \times \\ & \left\langle \hat{d}_{j_1}(t - \tau^<) \hat{d}_{j_2}^\dagger(t) \hat{d}_{j_3}(0) \hat{d}_{j_4}^\dagger(-\tau^>) \right\rangle e^{i\epsilon_L(\tau^> - \tau^<)}. \end{aligned} \quad (2.131)$$

Here k_L is the electronic state in the left electrode that has been emptied, k_R is the state in the right electrode which the electron has gone into, and we have introduced the abbreviations $\epsilon_L \equiv \epsilon_{Lk_L}$, $f_L = f(\epsilon_L - \mu_L)$ (with f the Fermi function at the given temperature T), and $T_j^L \equiv T_{jk_L}^L$. This expression is still general and holds for cotunneling through any interacting system, whose two-particle Green's function $\langle \hat{d}\hat{d}^\dagger\hat{d}\hat{d}^\dagger \rangle$ has to be calculated in order to obtain Γ_{pp}^+ .

Now we specialize to the independent boson model. In contrast to an arbitrary interacting system, at most two different states can occur in the two-particle Green's function. There are two possibilities for pairing the indices. The first case, $j_1 = j_2$, $j_3 = j_4$, refers to an electronically elastic cotunneling process, where the final state of the island coincides with the initial state. Then, the energy of the electron going through the system can only change due to interaction with the bath. We have (with $j_1 \equiv j$ and $j_3 \equiv l$):

$$\begin{aligned} & \left\langle \hat{d}_j(t - \tau^<) \hat{d}_j^\dagger(t) \hat{d}_l(0) \hat{d}_l^\dagger(-\tau^>) \right\rangle = \\ & \left\langle \hat{d}_j(t - \tau^<) \hat{d}_j^\dagger(t) \hat{d}_l(0) \hat{d}_l^\dagger(-\tau^>) \right\rangle_{el} \times \\ & \left\langle e^{i\hat{\phi}_j(t - \tau^<)} e^{-i\hat{\phi}_j(t)} e^{i\hat{\phi}_l(0)} e^{-i\hat{\phi}_l(-\tau^>)} \right\rangle \end{aligned} \quad (2.132)$$

Again, the average of bath operators can be evaluated with the help of a generalization of Eq. (2.22) to the case of four exponents. It yields an exponential $\exp K_{lj}[\tau^>, \tau^<, t]$, with:

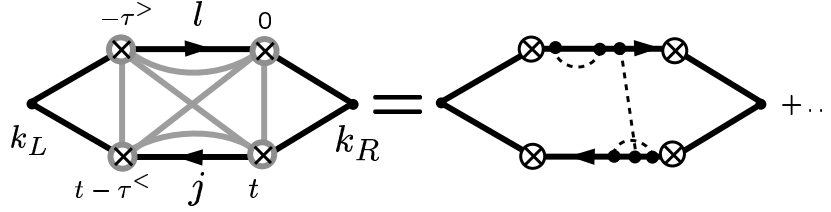


Figure 2.11: Illustration of the process described by Eq. (2.132): The crosses denote tunneling between the indicated electronic states. The left diagram shows the six phase-correlators (gray lines) that arise in Eq. (2.133) by connecting these vertices. This stands for an infinite series of diagrams such as that shown to the right, with an arbitrary number of bath correlators (dashed lines).

$$K_{lj}[\tau^>, \tau^<, t] \equiv K_{jj}(-\tau^<) - K_{jl}(t - \tau^<) + K_{jl}(t - \tau^< + \tau^>) + K_{jl}(t) - K_{jl}(t + \tau^>) + K_u(\tau^>). \quad (2.133)$$

This is shown schematically in Fig. 2.11.

In particular, if the bath fluctuations coupling to j, l are independent, this reduces to the sum of the exponents from the corresponding single-particle Green's functions, as expected (for $j \neq l$):

$$K_{jj}(-\tau^<) + K_u(\tau^>) = K_{jj}^*(\tau^<) + K_u(\tau^>) \quad (2.134)$$

In the case of $j = l$ or for $\hat{F}_j = \hat{F}_l$, no further simplification of (2.133) is possible (other than $K_{jj} = K_u = K_{jl}$).

The case of electronically inelastic cotunneling ($j_1 = j_4, j_2 = j_3$) can be evaluated in the same manner. However, it will not be described here, since we will not be interested in dephasing by electronic inelastic transitions, which become important at bias voltages and/or temperatures comparable to (or larger) than the level spacing on the island.

The other contributions to the total forward-tunneling rate Γ^+ , such as Γ_{ph}^+ , are described in Appendix A.3. The backward-tunneling rate Γ^- is obtained by interchanging L with R in all the expressions.

2.4.3 Generalized influence functional for cotunneling

We can show the relation to the Feynman-Vernon influence functional by inserting a set of bath eigenstates $|f_B\rangle$ into the bath average of Eq. (2.132)

$$\sum_{f_B} \left\langle e^{-i(E_f^B - E_i^B)t} \left\langle i_B \left| e^{i\hat{\phi}_j(-\tau^<)} e^{-i\hat{\phi}_j(0)} \right| f_B \right\rangle \left\langle f_B \left| e^{i\hat{\phi}_l(0)} e^{-i\hat{\phi}_l(-\tau^>)} \right| i_B \right\rangle \right\rangle_{i_B} =$$

$$\left\langle \sum_{f_B} e^{-i(E_f^B - E_i^B)t} e^{iE_i^B(\tau^> - \tau^<) - iJ_{ll}\tau^> + iJ_{jj}\tau^<} \langle \chi_j(\tau^<) | f_B \rangle \langle f_B | \chi_l(\tau^>) \rangle \right\rangle_{i_B} . \quad (2.135)$$

Here the bath state that evolves under the influence of an extra electron on state j is defined as (compare the more general version in (2.115)):

$$\begin{aligned} |\chi_j(\tau)\rangle &\equiv e^{-i(\hat{H}_B + \hat{F}_j)\tau} |i_B\rangle = \\ &e^{i\hat{\phi}_j} e^{-i(\hat{H}_B - J_{jj})\tau} e^{-i\hat{\phi}_j} |i_B\rangle . \end{aligned} \quad (2.136)$$

Note that in this section $|i_B\rangle$ and $|f_B\rangle$ always refer to eigenstates of \hat{H}_B alone, without any “initial electronic configuration” taken into account; this only enters the electronic part of the Green’s function.

We can define a kind of “generalized influence functional” that is equal to the spectral decomposition of the overlap between the two bath states that evolve under the presence of an extra electron on j or l , respectively:

$$F_{lj}[\tau^>, \tau^<, \omega] \equiv \sum_{f_B} \left\langle e^{iE_i^B(\tau^> - \tau^<)} \langle \chi_j(\tau^<) | f_B \rangle \delta(\omega - (E_f^B - E_i^B)) \langle f_B | \chi_l(\tau^>) \rangle \right\rangle_{i_B} . \quad (2.137)$$

The overlap between bath states is taken only between those components of these states that belong to an excitation energy of ω . This will be equal to the energy transferred from the electron to the bath, and it will determine the suppression of dephasing at low temperatures and bias voltages, due to Pauli blocking of final states in the right electrode. Note that this feature is absent in the usual single-particle influence functional, where one does not care about the energy transferred to the environment. Therefore, in applying the standard functional to situations involving the Pauli principle, it has been suggested to drop the contribution of zero-point fluctuations of the bath in order to account for Pauli blocking in a phenomenological way [Cohen99]. In our particularly simple special case, we do not need any such considerations. Furthermore, this example shows that the conclusion drawn in [Golubev99] from a generalized influence functional about the irrelevance of the Pauli principle for dephasing in weak localization cannot be a generic feature, even if it were true for that physical situation (see Chapter 5).

If *any* possible excitation energy ω is allowed, and, in addition, the two bath states are evolved for the same time, $\tau^> = \tau^<$, we recover the usual influence functional, which enters dephasing in terms of the decay of the density matrix (compare the previous section):

$$F_{lj}[\tau] \equiv \langle \chi_j(\tau) | \chi_l(\tau) \rangle = \int_{-\infty}^{+\infty} d\omega F_{lj}[\tau, \tau, \omega] . \quad (2.138)$$

Using F , we may express the electronically elastic contribution to Γ_{pp}^+ (cf. (2.131) with (2.132)) in the following form:

$$\Gamma_{pp}^+(el.el.) = 2\pi \sum_{k_L, k_R} f_L(1 - f_R) \sum_{jl} T_j^{L*} T_j^R T_l^{R*} T_l^L \times \int_0^\infty d\tau^> d\tau^< e^{i\epsilon_L(\tau^> - \tau^<) - iJ_U \tau^> + iJ_{jj} \tau^<} \left\langle \hat{d}_j(-\tau^<) \hat{d}_j^\dagger(0) \hat{d}_l(0) \hat{d}_l^\dagger(-\tau^>) \right\rangle_{el} \times F_{lj}[\tau^>, \tau^<, \epsilon_L - \epsilon_R]. \quad (2.139)$$

We have carried out the t -integral and made use of the fact that the electronic contribution in (2.132) does not depend on t . This reflects the physical fact that, in the electronically elastic process, no energy is transferred to the electronic state of the island. The electron emits the energy $\epsilon_L - \epsilon_R$ into the bath (or absorbs it, if $\epsilon_L - \epsilon_R$ is negative).

2.4.4 Dephasing in cotunneling: General discussion

Formally, quantum-mechanical interference results from the superposition of complex probability amplitudes, whose magnitude squared gives the probabilities. In the simplest description of an interference experiment, we deal with several different paths whose amplitudes are superposed:

$$\left| \sum_j A_j \right|^2 = \sum_{j,l} A_j^* A_l. \quad (2.140)$$

The terms $|A_j|^2$ describe classical probabilities, while the cross terms are responsible for interference. In the case of cotunneling, the sum over amplitudes is given by the sum over intermediate states $|\nu\rangle$ in expression (2.126). Coupling to a fluctuating environment will, in general, alter *all* the terms that contribute to the probability or the cotunneling current. However, if dephasing occurs, the cross terms will be reduced compared to the “classical” contributions. Thus, interference is destroyed.

It is important and not always straightforward to distinguish the effects of dephasing from other effects related to the bath, such as energy shifts, mass renormalization or a change in the effective potential seen by the particle. All of these can change the interference pattern, i.e., in our case, the cotunneling current as a function of some external parameter.

However, such a distinction becomes possible if, instead of constructive interference, we consider the case of *perfect destructive* interference, where cotunneling is completely blocked without coupling to a bath. This has already been pointed out in the previous section on sequential tunneling through a double-dot. Then, the appearance of a finite cotunneling current may be interpreted as a genuine sign of dephasing. This holds as long as the bath couples *symmetrically* to the different paths, in such a way that energy shifts (and effective interactions) will only change the magnitudes $|A_j|$ by the same factor, without, by themselves, lifting the destructive interference.

Let us consider these issues in more detail for the case of electronically elastic cotunneling, employing the formulas for the cotunneling rate and the “influence functional” given in the previous section. Assuming all the levels to be empty in equilibrium, we can express the rate Γ_{pp}^+ in the following form, similar to Eq. (2.140):

$$\Gamma_{pp}^+ = \sum_{l,j} A_j^* A_l \gamma_{jl}, \quad (2.141)$$

where the amplitude A_j to tunnel from the left to the right electrode via state j is given as

$$A_j = T_j^{R*} T_j^L, \quad (2.142)$$

and the factors γ_{jl} contain the influence of the bath (as well as that of the level energies). We evaluate the electronic contribution in Eq. (2.139), taking into account the energy renormalization. This yields:

$$\begin{aligned} \gamma_{jl} &\equiv 2\pi D_L D_R \int d\epsilon_L d\epsilon_R f_L(1-f_R) \int_0^\infty d\tau^> d\tau^< e^{-i(\epsilon_l - \epsilon_L)\tau^> + i(\epsilon_j - \epsilon_L)\tau^<} \times \\ &\quad F_{lj}[\tau^>, \tau^<, \epsilon_L - \epsilon_R] \\ &= D_L D_R \int d\epsilon_L d\epsilon_R f_L(1-f_R) \int_0^\infty d\tau^> d\tau^< e^{-i\Delta_l \tau^> + i\Delta_j \tau^<} \times \\ &\quad \int_{-\infty}^{+\infty} dt e^{i(\epsilon_L - \epsilon_R)t} e^{K_{lj}[\tau^>, \tau^<, t]}. \end{aligned} \quad (2.143)$$

We have assumed the transmission matrix elements to be independent of the wave vectors $k_{L,R}$ in the relevant energy region. Therefore, we can also pull out the density of states $D_{L(R)}$ of the left (right) electrode at the Fermi level in Eqs. (2.131), (2.139). The second line follows directly from (2.131)-(2.133). Furthermore, we have defined the activation energy for tunneling through level l as:

$$\Delta_l \equiv \epsilon_l - J_l - \epsilon_L. \quad (2.144)$$

If the voltage and temperature are sufficiently low (much smaller than the activation energies), we may set $\epsilon_L = \epsilon_R = \epsilon_F$ everywhere, except for the energy difference $\omega = \epsilon_L - \epsilon_R$. Then, we can rewrite the integration over Fermi functions by defining a weight for the energy transfer ω :

$$\begin{aligned} S(\omega) &\equiv \int d\epsilon_L d\epsilon_R f_L(1-f_R) \delta(\omega - (\epsilon_L - \epsilon_R)) \\ &= \frac{\omega - eV}{e^{\beta(\omega - eV)} - 1}. \end{aligned} \quad (2.145)$$

In this way, γ_{jl} can be expressed as a weighted average of the “influence functional” at different possible energy transfers ω :

$$\begin{aligned}\gamma_{jl} &= 2\pi D_L D_R \int d\omega S(\omega) \int_0^\infty d\tau^> d\tau^< e^{-i(\epsilon_l - \epsilon_F)\tau^> + i(\epsilon_j - \epsilon_F)\tau^<} F_{lj}[\tau^>, \tau^<, \omega] \\ &= D_L D_R \int d\omega S(\omega) \int_0^\infty d\tau^> d\tau^< e^{-i\Delta_l \tau^> + i\Delta_j \tau^<} \int_{-\infty}^{+\infty} dt e^{i\omega t} e^{K_{lj}[\tau^>, \tau^<, t]}\end{aligned}\quad (2.146)$$

At $T = 0$, we have $S(\omega) = 0$ for $\omega > eV$, since the electron cannot supply more energy than provided by the bias voltage. At $\omega < eV$, we get $S(\omega) = eV - \omega$, favoring smaller energy transfers. The case $\omega < 0$ is irrelevant, since the bath cannot feed energy to the electron at zero temperature, it can only be excited by the electron.

As has been explained above, the backward tunneling rate Γ_{pp}^- can be obtained by interchanging L with R in the expression for Γ_{pp}^+ . In terms of Eq. (2.141), this means that A_j is to be replaced by A_j^* (see Eq. (2.142)). Furthermore, by assuming $f_R(\epsilon, V) = f_L(\epsilon, -V)$ and renaming ϵ_L into ϵ_R in Eq. (2.143), we find that γ_{jl} is to be replaced by $\gamma_{jl}[V \mapsto -V]$. Therefore, we have for the total tunneling rate:

$$\Gamma = \Gamma_{pp}^+ - \Gamma_{pp}^- = \sum_{j,l} A_j^* A_l (\gamma_{jl} - \gamma_{lj}[V \mapsto -V]) \equiv \sum_{j,l} A_j^* A_l \gamma_{jl}^{tot}. \quad (2.147)$$

In expression (2.146) for γ_{jl} , the bias voltage only enters $S(\omega)$.

This concludes our general discussion of dephasing in cotunneling transport. In the remainder of this section, we discuss a few special cases, in which the structure of the general results may be simplified.

First of all, if $l \neq j$ and \hat{F}_l, \hat{F}_j are independent, we have $K_{lj} = K_{jl} = 0$, such that the exponent $K_{lj}[\tau^>, \tau^<, t]$ becomes $K_{ll}(\tau^>) + K_{jj}(-\tau^<)$. Therefore, Eq. (2.146) reduces to:

$$\gamma_{jl} = 2\pi D_L D_R S(0) G_{jj}^{R*}(\epsilon_F) G_{ll}^R(\epsilon_F), \quad (2.148)$$

where $G_{jj}^R(\epsilon_F)$ is the Fourier transform of the level's retarded Green's function, evaluated at the Fermi level (see Eq. (2.27)). However, for $l = j$, the expression cannot be simplified in this way. Therefore, $S(\omega)$ at $\omega \neq 0$ will enter the expression for γ_{ll} , effectively enhancing the terms $l = j$ over the interference terms $l \neq j$.

There are two cases in which definitely no dephasing occurs: Either the bath cannot distinguish between different paths ($\hat{F}_l = \hat{F}_j$), or there is not enough energy to be transferred, such that the electron cannot leave a trace in the bath. In both cases, perfect destructive interference will not be lifted, provided both the initial energies and the coupling strengths have been symmetric for the different paths. In contrast, the cotunneling current at any point away from perfect destructive interference will be altered and no conclusion about the presence or absence of dephasing could be drawn from that fact.

In the first case, $\hat{F}_l = \hat{F}_j$, one obtains $\gamma_{ll} = \gamma_{lj} = \gamma_{jl} = \gamma_{jj}$, if $\Delta_l = \Delta_j$. Therefore, the common factor γ_{ll} can be pulled out of the sum in Eq. (2.141), and the destructive interference, with $\sum_l A_l = 0$, is preserved regardless of coupling strength.

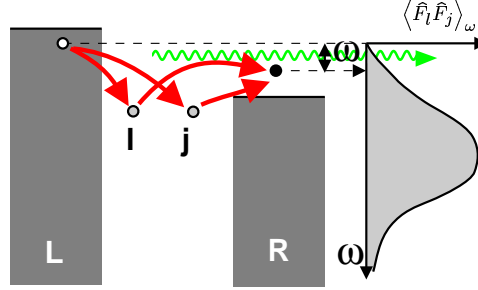


Figure 2.12: Inelastic cotunneling (with respect to coupling to the bath): Emission of a bath “phonon” of frequency ω leads to an incoherent contribution to the tunneling current, where the destructive interference between the two paths shown here is lost. The probability of emission depends on the bath spectrum $\langle \hat{F}_l \hat{F}_j \rangle_\omega$.

The other case, where the electron cannot pass any energy into the bath, may be discussed by assuming a bath with an energy gap much larger than the available energies. In this case, only $\omega = 0$ contributes, such that initial and final bath states are the same. Consequently, the influence functional (2.137) and γ_{jl} (2.143) factorize into separate contributions from the two states j and l , again leading to Eq. (2.148), now also for $l = j$.

This means that the complete rate Γ_{pp}^+ can be written in the form

$$\Gamma_{pp}^+ = 2\pi D_L D_R S(\omega = 0) \left| \sum_l A_l G_l^R(\epsilon_F) \right|^2. \quad (2.149)$$

This corresponds to the result without coupling to the bath, but with renormalized amplitudes. Again, this means that destructive interference is preserved, if both the initial energies as well as the coupling to the bath have been symmetric for all the levels, or for pairs of levels l, j with $A_l = -A_j$. In that case, from $\epsilon_l = \epsilon_j$, $J_{ll} = J_{jj}$ and $K_{ll} = K_{jj}$, we have $G_{ll}^R = G_{jj}^R$, such that the sum over amplitudes still vanishes.

2.4.5 Perturbative evaluation of the cotunneling rate

Although evaluation of the cotunneling current has been reduced to integrations via Eqs. (2.133), (2.147), and (2.143), these usually cannot be carried out analytically, even when the expression for the exponential $\exp(K_{lj}[\tau^>, \tau^<, t])$ is known explicitly (see Appendix A.4 for the Ohmic bath). Therefore, in this section, we will evaluate Γ_{pp} to first order in the coupling to the bath. We use Eq. (2.146) for γ_{jl} as a starting point and expand the exponential up to first order in K_{lj} . The 0^{th} order expression gives

$$\gamma_{jl}^{(0)} = 2\pi \frac{D_L D_R}{\Delta_l \Delta_j} S(0). \quad (2.150)$$

Note that the energy differences, as defined in Eq. (2.144), still contain the level shift $-J_{ll}$ induced by coupling to the bath, such that $\gamma_{jl}^{(0)}$ contains higher order contributions of the system-bath coupling, which have to be combined with those from $\gamma_{jl}^{(1)}$ (see below).

The first order $\gamma_{jl}^{(1)}$ (with respect to the exponential) is found with the help of Eq. (2.133) for $K_{lj}[\tau^>, \tau^<, t]$. We denote by $K_{jl}(\nu)$ the Fourier transform of $K_{jl}(t)$ (see Eq. (2.25)):

$$\begin{aligned} K_{jl}(t) &= \int d\nu e^{-i\nu t} K_{jl}(\nu) \\ K_{jl}(\nu) &= \frac{\langle \hat{F}_l \hat{F}_j \rangle_\nu}{\nu^2} - \delta(\nu) \int d\omega \frac{\langle \hat{F}_l \hat{F}_j \rangle_\omega}{\omega^2}. \end{aligned} \quad (2.151)$$

Then, the integrations over $\tau^>, \tau^<, t$ in Eq. (2.146) (or Eq. (2.143)) yield:

$$\begin{aligned} 2\pi\delta(\omega) \int d\nu \left\{ \frac{K_{jj}(\nu)}{(\Delta_j + \nu)\Delta_l} + \frac{K_{ll}(\nu)}{(\Delta_l + \nu)\Delta_j} \right\} + \\ 2\pi K_{jl}(\omega) \frac{\omega^2}{\Delta_l(\Delta_l + \omega)\Delta_j(\Delta_j + \omega)}. \end{aligned} \quad (2.152)$$

From the expression (2.151) for $K_{jl}(\nu)$, we find:

$$\int d\nu \frac{K_{ll}(\nu)}{\Delta_l + \nu} = - \int d\nu \frac{\langle \hat{F}_l \hat{F}_l \rangle_\nu}{\nu \Delta_l(\Delta_l + \nu)}. \quad (2.153)$$

Since we want to use Eq. (2.146) for γ_{jl} , where $S(\omega)$ has been introduced by approximating $\epsilon_L \approx \epsilon_R$, we have to set $\Delta_l + \omega \approx \Delta_l$ for consistency of the approximation. In that case, $\langle \hat{F}_l \hat{F}_l \rangle_\nu$ in (2.153) may be replaced by the zero-temperature correlator, since the frequency-symmetric finite temperature contribution (see Eq. (2.26)) cancels. This leads to the expression (2.14) for the energy shift J_{ll} . Furthermore, we replace $\omega^2 K_{jl}(\omega)$ in (2.152) by $\langle \hat{F}_j \hat{F}_l \rangle_\omega$ (see Eq. (2.151)), since the δ -peak at $\omega = 0$ is suppressed. Thus:

$$\gamma_{jl}^{(1)} = 2\pi \frac{D_L D_R}{\Delta_j \Delta_l} \left\{ -S(0) \left(\frac{J_{ll}}{\Delta_l} + \frac{J_{jj}}{\Delta_j} \right) + \int d\nu S(\nu) \frac{\langle \hat{F}_j \hat{F}_l \rangle_\nu}{\Delta_j \Delta_l} \right\}. \quad (2.154)$$

In combining this with (2.150), we set $\Delta_j \equiv \Delta_{j0} - J_{jj}$, where Δ_{j0} is the energy barrier without coupling to the bath. Then it is found that the terms involving J_{jj} cancel:

There is no change in the cotunneling rate due to the shift in level energies (in the order considered here). The reason for this is that the level shape is distorted in such a way that the center-of-mass of the DOS remains at the same place, in spite of coupling to the bath [Wingreen88]. Therefore, the expression for γ_{jl} , up to first order in the system-bath coupling, is given by:

$$\gamma_{jl} = 2\pi \frac{D_L D_R}{\Delta_{j0} \Delta_{l0}} \left\{ S(0) + \int d\nu S(\nu) \frac{\langle \hat{F}_j \hat{F}_l \rangle_\nu}{\Delta_{j0} \Delta_{l0}} \right\}. \quad (2.155)$$

The second term in Eq. (2.155) describes dephasing due to inelastic cotunneling. Note that it is the correlator of the fluctuations \hat{F}_j themselves which enters this expression. This is in contrast to the $P(E)$ results for sequential tunneling, where the phase-correlators appear, with $K_{jl}(\omega) = \langle \hat{F}_j \hat{F}_l \rangle_\omega / \omega^2$ (at $\omega \neq 0$). Therefore, the Ohmic bath (and any bath with a finite energy renormalization, i.e. exponent $s > 0$) yields a finite result in this order of perturbation theory for the cotunneling rate.

This conclusion is not changed if the replacement $\Delta_l + \omega \mapsto \Delta_l$ is not performed, since it is the low-frequency behaviour which matters. Note that at finite temperatures there may be a divergent contribution from a second-order pole in the integration over the term involving $K_{jl}(\omega)$ in Eq. (2.152), at $\omega = -\Delta_l$ (for $l = j$). This corresponds to the possibility of real transitions onto the level (induced by the bath), which we neglect together with sequential tunneling, assuming these contributions to be, in fact, exponentially small for sufficiently low temperatures and voltages (i.e. the pole will be cut off by a finite tunneling rate).

The cotunneling current may be evaluated by inserting the expressions for $S(\omega)$ and $\langle \hat{F}_j \hat{F}_l \rangle_\omega$ into Eq. (2.155) and using Eq. (2.147). This will be carried out below, for a situation involving two levels.

2.4.6 Interference in cotunneling through a double-dot

We take up again the model of tunneling through two single-level dots, introduced in Section 2.3 (but we will use the notation of the preceding sections on cotunneling). The energies and coupling strengths are symmetric, but there is a possible phase difference between the transmission amplitudes through the two dots (the two “arms of the interferometer”):

$$A_+ = A, \quad A_- = e^{i\varphi} A. \quad (2.156)$$

Therefore, the total cotunneling rate is (cf. Eq. (2.147)):

$$\Gamma = 2|A|^2 (\gamma_{++}^{tot} + \gamma_{+-}^{tot} \cos(\varphi)). \quad (2.157)$$

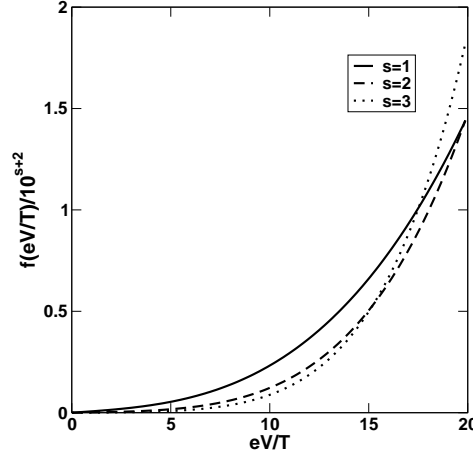


Figure 2.13: The function $f(eV/T)$, which is essentially the incoherent cotunneling rate $\Gamma_{\varphi=\pi} \propto T^{s+2}f(eV/T)$, according to Eqs. (2.158) and (2.162). At low bias voltages ($eV < T$), there is a finite incoherent contribution to the linear conductance, while at higher bias voltages the zero-temperature behaviour $\Gamma_{\varphi=\pi} \propto (eV)^{s+2}$ (2.160) applies.

Here we have already made use of the symmetry which leads to $\gamma_{++} = \gamma_{--}$ and $\gamma_{+-} = \gamma_{-+}$. No electronically inelastic processes can occur in this model, since double-occupancy is forbidden.

As the bath fluctuations couple to the two dots with opposite sign, $\hat{F}_+ = \hat{F}$ and $\hat{F}_- = -\hat{F}$, we have to insert $\langle \hat{F}_+ \hat{F}_+ \rangle_\omega = \langle \hat{F} \hat{F} \rangle_\omega = -\langle \hat{F}_+ \hat{F}_- \rangle_\omega$ into the perturbative result (2.155). Using the relation $(2\pi)^2 D_L D_R |A|^2 \equiv \Gamma_L \Gamma_R$ for the bare tunneling rates $\Gamma_{L,R}$ through the two junctions, we can express the result as

$$\Gamma = \frac{\Gamma_L \Gamma_R}{\pi \Delta_0^2} \left((1 + \cos \varphi) eV + (1 - \cos \varphi) \frac{1}{\Delta_0^2} \int d\nu (S(\nu) - S^-(\nu)) \langle \hat{F} \hat{F} \rangle_\nu \right), \quad (2.158)$$

where $S^-(\nu) \equiv S(\nu)[V \mapsto -V]$, and we have used $S(0) - S^-(0) = eV$, which holds at any temperature.

We will now evaluate the “incoherent” contribution to the cotunneling current, i.e. the integral in Eq. (2.158), for power-law bath spectra of the form given in Eq. (2.64), i.e.:

$$\langle \hat{F} \hat{F} \rangle_\omega^{T=0} = 2\alpha\omega_c \left(\frac{\omega}{\omega_c} \right)^s \theta(\omega) \theta(\omega_c - \omega). \quad (2.159)$$

At zero temperature, we obtain an incoherent contribution to the rate that rises as V^{s+2} (assuming $eV < \omega_c$):

$$\int d\nu S(\nu) \langle \hat{F} \hat{F} \rangle_\nu = \int_0^{eV} (eV - \nu) \langle \hat{F} \hat{F} \rangle_\nu^{T=0} = 2\alpha\omega_c^3 \left(\frac{eV}{\omega_c} \right)^{s+2} ((s+1)^{-1} - (s+2)^{-1}) . \quad (2.160)$$

In contrast, the current at constructive interference is linear in the bias voltage V . Therefore, the incoherent contribution is suppressed compared to the coherent one at small bias voltages, the ratio being given by:

$$\frac{\Gamma_{\varphi=\pi}}{\Gamma_{\varphi=0}} = 2\alpha \frac{\omega_c^2}{\Delta_0^2} \left(\frac{eV}{\omega_c} \right)^{s+1} ((s+1)^{-1} - (s+2)^{-1}) . \quad (2.161)$$

Thus, in the linear cotunneling conductance, no “zero-temperature dephasing” is observed in that case. The electron does not have enough energy to supply to the bath, which it would have to do in order to leave a trace with appreciable probability. In particular, this holds also for the Ohmic bath ($s = 1$), which shows anomalous behaviour for the case of sequential tunneling (see Section 2.3). Note that the dependence of the incoherent current on the bias voltage V for $s = 1$ is like that for electronically inelastic cotunneling through an island with many levels [Averin92], although physically the two situations are of course different. Roughly speaking, the bath spectrum appears two powers in frequency less strong for cotunneling than for sequential tunneling. The physical reason for the difference between sequential and co-tunneling is that in the former case the bath is permitted an infinite amount of time (more precisely, $\sim \Gamma^{-1}$) to relax in the presence of the particle, while co-tunneling is more similar to a scattering situation, where the interaction only lasts a short amount of time ($\sim \Delta^{-1}$).

At finite temperatures, we cannot evaluate the integral in Eq. (2.158) in closed form any more. However, in the limit of large bath cutoff ($\omega_c \gg T, eV$), we can express it as

$$\int d\nu (S(\nu) - S^-(\nu)) \langle \hat{F} \hat{F} \rangle_\nu = \beta^{-(s+2)} f(\beta eV) , \quad (2.162)$$

with $f(x)$ an odd function of its argument (see Eqs. (2.145) and (2.26)):

$$f(x) \equiv \int dy \left\{ \frac{y-x}{e^{y-x}-1} - \frac{y+x}{e^{y+x}-1} \right\} \frac{|y|^s}{|e^{-y}-1|} . \quad (2.163)$$

Therefore, the incoherent cotunneling rate rises as $T^{s+1}V$, for small voltages at finite temperatures ($eV \ll T$), compare Fig. 2.13.

2.5 Dephasing by correlated two-particle tunneling

Up to now, we have treated tunneling only in leading order. In this section, we will briefly discuss one example of an effect that becomes important for stronger tunnel coupling.

The gapped bath has been a particularly transparent example, since any incoherent current (that would lift perfect destructive interference) is completely suppressed below

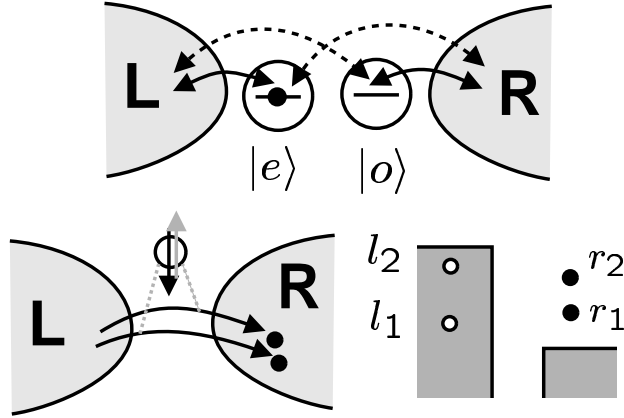


Figure 2.14: Top: At $\varphi = \pi$, tunneling from the even state $|e\rangle$ to the right lead (or from $|o\rangle$ to the left lead) is possible only via simultaneous excitation of the bath (dashed lines), such that destructive interference remains perfect for a gapped bath at low V , in leading order of the tunneling. Bottom left: Streamlined model for dephasing via correlated two-particle tunneling, where a spin is flipped in the intermediate state. Bottom right: Energy diagram (see text).

the threshold ω of the bath spectrum, both in sequential tunneling and cotunneling. The interpretation has been straightforward: For dephasing to take place, the electron has to leave a trace in the bath, which it cannot do if the bias voltage does not provide enough energy to excite a bath oscillator.

For the case of the double-dot, this result can also be understood by rewriting the tunnel Hamiltonian \hat{V}' (2.76) in terms of the operators $\hat{d}_{e(o)}$ of the even and the odd state (at destructive interference, $\varphi = \pi$). We get for the left (right) junction:

$$e^{i\hat{\phi}}\hat{d}_+ \pm e^{-i\hat{\phi}}\hat{d}_- = \frac{1}{\sqrt{2}}((e^{i\hat{\phi}} \pm e^{-i\hat{\phi}})\hat{d}_e + (e^{i\hat{\phi}} \mp e^{-i\hat{\phi}})\hat{d}_o). \quad (2.164)$$

At $T = 0$ and $eV < \omega$, tunneling processes do not lead to an excited bath state. Therefore, the matrix elements entering the tunneling rates are obtained by taking the expectation value with respect to the bath ground state $|\chi_0\rangle$ in Eq. (2.164). This leads to the renormalization of tunneling amplitudes for the terms with $e^{i\hat{\phi}} + e^{-i\hat{\phi}}$, while the expectation value of $e^{i\hat{\phi}} - e^{-i\hat{\phi}}$ vanishes completely. Therefore, no current can flow, since the even state still couples only to the left lead, while the odd state couples to the right lead (see Fig. 2.14).

It may be argued that this picture is incomplete. Imagine an electron goes through the setup, leaving behind an excited bath state. Shortly thereafter, a second electron also passes from the left to the right lead, de-exciting the bath on its way. Both electrons

have been able to overcome destructive interference, since it is no longer the expectation value with respect to the ground state of the bath which determines the tunnel matrix elements. Nevertheless, after completion of the whole process, the energy is conserved. In fact, this qualitative argument shows that a finite incoherent current will flow also for bias voltages below the bath threshold, by a process of correlated two-particle tunneling, where a “virtual trace” is left in the bath for a short time. This is a feature that is, of course, absent in discussions of dephasing based on a single-particle picture (augmented, perhaps, by the Pauli blocking constraint).

However, in the following we will show in a streamlined model that this dephasing process does not lead to finite dephasing in the linear conductance (at $T = 0$), since it corresponds to a sort of two-particle scattering process, where the phase space of final states is severely restricted for low bias voltages. In other words, the probability of a second electron passing through the setup shortly after the first one diminishes very rapidly for decreasing V .

The simple model consists of two tunnel-coupled leads (without dots in-between), where tunneling depends on excitation of a spin (playing the role of the bath), see Fig. 2.14. That is, we take the tunnel Hamiltonian to be

$$\hat{V} = g \sum_{r,l} \hat{a}_{Rr}^\dagger \hat{\sigma}_x \hat{a}_{Ll} + h.c., \quad (2.165)$$

where we have already neglected any dependence of the tunnel matrix elements on the lead states l, r in the left and right lead. The spin has the Hamiltonian

$$\hat{H}_B = \frac{\omega}{2} \hat{\sigma}_z, \quad (2.166)$$

such that it corresponds to a bath with a threshold ω . By comparing (2.165) with (2.164), it is seen that this model captures the essential feature: Tunneling is blocked in lowest order if the bath cannot be excited (since then only the expectation value of $\hat{\sigma}_x$ contributes, which is zero).

Now we calculate the tunneling rate in second-order perturbation theory, employing the Golden Rule expression (2.126). In the present case, the final state $|f\rangle$ is specified by the two states of the right lead r_1, r_2 which have become occupied, and the two states of the left lead, l_1, l_2 , which have been emptied (see Fig. 2.14). In the intermediate state $|\nu\rangle$, the spin has been flipped to its excited state. There are four possible combinations of intermediate electronic states, depending on whether l_1 or l_2 has been emptied and whether r_1 or r_2 has been occupied. Adding the four contributions in the sum over $|\nu\rangle$, and taking into account properly the fermionic signs, we get

$$2g\omega \left\{ \frac{1}{\omega^2 - (\epsilon_{r_1} - \epsilon_{l_1})^2} - \frac{1}{\omega^2 - (\epsilon_{r_1} - \epsilon_{l_2})^2} \right\} \approx \frac{2g}{\omega^3} \{ (\epsilon_{r_1} - \epsilon_{l_1})^2 - (\epsilon_{r_1} - \epsilon_{l_2})^2 \}, \quad (2.167)$$

where we have omitted a possible overall sign depending on the states. The approximation in the second line holds for bias voltages much smaller than the bath threshold, i.e. the energy differences much smaller than ω . Squaring this result and summing over all possible final states, we get for the total rate (of this two-electron tunneling process):

$$\Gamma = 2\pi \frac{|g|^2}{\omega^6} D_L D_R \int_{-\infty}^{eV} d\epsilon_{l_1} d\epsilon_{l_2} \int_0^{\infty} d\epsilon_{r_1} d\epsilon_{r_2} \left[(\epsilon_{r_1} - \epsilon_{l_1})^2 - (\epsilon_{r_1} - \epsilon_{l_2})^2 \right]^2 \delta((\epsilon_{l_1} + \epsilon_{l_2}) - (\epsilon_{r_1} + \epsilon_{r_2})). \quad (2.168)$$

After performing the substitution $\epsilon_{r_1} = eV \epsilon'_{r_1}$ etc., this is seen to rise as V^7 , i.e. with a very high power of the bias voltage, due to the restriction of final states (and the partial cancellation in the sum over intermediate states shown above).

Nevertheless, this example demonstrates that arguments based on single-particle physics are to be employed with caution, and that a nonperturbative investigation into the physics of these models at stronger tunnel coupling may be interesting.

2.6 Conclusions

We have analyzed dephasing in model situations of tunneling through localized levels coupled to a bath. The disappearance of perfect destructive interference in a symmetric setup has been taken as a criterion for “genuine” dephasing, as opposed to mere renormalization. The coupling to the bath has been taken into account exactly, via the “independent boson model” and the concepts of the “ $P(E)$ theory” of tunneling in a dissipative environment, while the tunnel coupling has been treated perturbatively.

In particular, we have considered a symmetric double-dot setup of two single-level quantum dots with a fluctuating energy difference between the dots.

For the case of sequential tunneling, we have discussed in detail the behaviour of the density matrix of a single electron that has been placed in a superposition of the two dot levels. The bath measures (to some extent) the position of the electron, such that the electron’s density matrix becomes mixed. However, this allows direct conclusions about the “incoherent current” only in the limit of high bias voltages, corresponding to a fast “projection” measurement of the electron’s state. For lower voltages, only the low-frequency part of the bath spectrum contributes to the lifting of destructive interference. Thus, for any “weak bath”, whose spectrum falls off fast towards low frequencies, the visibility of the interference effect becomes perfect in the limit of low bias voltages V and temperatures T , when the energy supplied to the electron is vanishingly small. This is the case for a fluctuation spectrum $\propto \omega^s$ with $s > 1$ ($s > 2$) for $T = 0$ ($T > 0$). The visibility may show a nonmonotonous behaviour as a function of bias voltage. For “stronger” spectra (smaller exponent s), including the Ohmic bath ($s = 1$), there is the well-known zero-bias anomaly (suppression of the tunneling current at low voltages), which affects equally both the cases of constructive and destructive interference. Therefore, the visibility vanishes

exactly at any bias voltage in our approach, where the tunnel coupling has been treated only in leading order. Although there is always a suppression of the magnitude of the tunnel current for the case of constructive interference, this may be interpreted as a mere renormalization of the effective tunnel-coupling, since the perfect destructive interference is not affected and since it occurs even for a bath with an excitation gap. The full dependence of the sequential tunneling current $I(\varphi)$ on voltage, temperature, bath spectrum and phase difference φ between the interfering paths has been derived by setting up a master equation for the state of the double-dot (which is special due to the degeneracy of dot levels).

For the case of cotunneling, the density matrix is not the appropriate quantity to look at. Rather, we have rewritten both the two-particle Green's function and the expressions for the cotunneling rates in terms of the overlap between bath states that have evolved under the action of an electron passing through either of two localized levels. This has enabled us to make contact with the Feynman-Vernon influence functional and to show how this may be modified in a situation where Pauli blocking (of final states in the tunneling process) becomes important. We have offered a general discussion of dephasing in cotunneling for the independent boson model, pointing out situations where the destructive interference remains perfect in spite of coupling to the bath and the resulting renormalization effects. The general expressions for the current (exact in the system-bath coupling) have been evaluated perturbatively, showing that the bath spectrum itself replaces the phase correlators which had entered the calculation in the case of sequential tunneling. At $T = 0$, the incoherent current rises as V^{s+2} , such that the visibility always becomes perfect at low bias voltages (for any bath that does not lead to an infinite renormalization of level energies, $s > 0$). Physically, this difference comes about because cotunneling corresponds more to a scattering situation with respect to the interaction between electron and bath, since the electron only stays on the central island for a short amount of time.

Finally, we have briefly discussed an example where the changes expected for stronger tunnel coupling show up. Dephasing (i.e. the appearance of an incoherent current at destructive interference) is possible even below the threshold of a bath. This is due to a process of correlated two-particle tunneling, where the first electron passing through the setup leaves a “virtual trace” that is erased by the second electron, such that energy conservation is fulfilled. However, this process is severely suppressed at low bias voltages.

These calculations may serve as illustrative examples of the difference between the “optics” type of interference experiments (employing *single* particles), in which the semiclassical approximation and/or the usual Feynman-Vernon influence functional may be applied to discuss dephasing, and the linear-transport interference experiments encountered in mesoscopic physics, in which special care has to be taken in the analysis of dephasing at low temperatures.

Chapter 3

Aharonov-Bohm ring with fluctuating magnetic flux

3.1 Introduction

One of the simplest mesoscopic interference effects is realized in the Aharonov-Bohm ring geometry, where a magnetic flux threading the ring induces an additional geometric phase for electrons moving around the ring [Imry97]. There are actually two distinct versions of the effect in mesoscopic physics: In a clean sample, the Aharonov-Bohm phase leads to persistent currents and to a contribution to the transmission through the ring which is periodic in the flux, with period $\Phi_0 = hc/e$. In an ensemble of diffusive samples, this contribution is lost due to the random phases introduced by the elastic scatterers. However, the interference of two paths that wind around the ring completely, instead of only halfway, is insensitive to these phases, such that a contribution at period $\Phi_0/2$ survives.

In the following, we will describe a simple theoretical toy model for dephasing in such a geometry. The ring is assumed to be clean and we will consider only one transverse

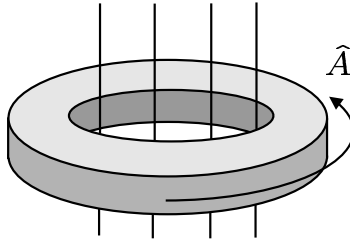


Figure 3.1: The model situation: A fluctuating flux leads, via a time-dependent vector potential, to a fluctuating force for the electrons on the Aharonov-Bohm ring. This results in dephasing of the electronic motion, among other effects.

channel, i.e. a purely one-dimensional situation. Dephasing is brought into the picture by fluctuations of the magnetic flux threading the ring (see Fig. 3.1). As in previous sections, these fluctuations are not treated as random classical noise, but rather as deriving from a linear bath. In fact, this model may be viewed as a version of the Caldeira-Leggett model of Quantum Brownian motion, generalized to a situation involving more than one particle. In addition, the force derives from a vector potential, rather than a scalar potential. That is why we start our discussion in the next section with a brief review of Quantum Brownian motion in the vector gauge.

Recent experimental investigations of dephasing in Aharonov-Bohm setups ([Hansen01, Kobayashi02]) have dealt with open geometries rather than the tunneling transport which we will treat below. In addition, it is probable that the most important dephasing mechanisms in these experiments will have been electron-electron or electron-phonon scattering, such that our results cannot be applied in their interpretation. On the theoretical side, early investigations of dephasing in a mesoscopic Aharonov-Bohm ring have dealt with coupling to completely phase-incoherent electron reservoirs [Büttiker85]. The single-particle version of the present model has been considered before, in [Park92], with coupling to an Ohmic bath (corresponding to $1/f$ fluctuations of the flux, see below). It was concluded that persistent currents in a normal metal ring would be destroyed completely under these circumstances because of the velocity-proportional friction. The possibility of *spontaneous* persistent currents due to the zero-point fluctuations of the electromagnetic field was investigated (and ruled out) in [Loss93], using a Luttinger liquid picture for the electrons and taking into account their electromagnetic self-interaction. Dephasing of a single electron going around the two arms of an Aharonov-Bohm ring has been considered both in [Loss91], using the influence functional, and in [Stern90], using a semiclassical picture. In the latter article, the connection between phase fluctuations and the trace left by the system in the environment was emphasized (compare the introduction in Chapter 1). In [Büttiker01, Cedraschi00, 01] a ring containing a single quantum dot with fluctuating gate voltage was considered and the properties of the quantum-mechanical ground state were found, with particular emphasis on the low-temperature behaviour of the persistent current. An analysis of a mesoscopic Mach-Zehnder type interference setup (albeit restricted to higher temperatures) is given in [Seelig01]. Cotunneling through a Luttinger liquid Aharonov-Bohm ring (without coupling to an external bath) has been treated in [Rollbühler00].

Note that we deviate from the notation (and, in some parts, the methods of solution) from [Marquardt02a], where the work reported in this chapter has been published already.

3.2 Caldeira-Leggett model in vector potential gauge

We start from the Hamiltonian describing a free particle whose coordinate \hat{q} is coupled in a translationally invariant way to a bath of harmonic oscillators [Caldeira83, Hakim85, Weiss00]:

$$\hat{H} = \frac{\hat{p}^2}{2m} + \sum_j \frac{M_j \Omega_j^2}{2} (\hat{q} - \hat{Q}_j)^2 + \sum_j \frac{\hat{P}_j^2}{2M_j}. \quad (3.1)$$

When the square is expanded, we obtain three terms - a coupling between \hat{q} and a fluctuating force \hat{F} , the potential energies of the bath oscillators, and a parabolic potential in \hat{q} that serves as a counter-term for the bath-induced destabilizing potential:

$$\frac{1}{2} \hat{q}^2 \left(\sum_j M_j \Omega_j^2 \right) - \hat{F} \hat{q} + \sum_j \frac{M_j \Omega_j^2}{2} \hat{Q}_j^2, \quad (3.2)$$

with

$$\hat{F} = \sum_j M_j \Omega_j^2 \hat{Q}_j. \quad (3.3)$$

Note that \hat{F} has been used to denote a fluctuating potential (dimension of energy) in previous sections, while in this section it denotes a fluctuating force. We want to describe the force as deriving from a vector potential, instead of the scalar potential in (3.2):

$$\hat{F} = -\frac{e}{c} \frac{d}{dt} \hat{A}, \quad (3.4)$$

where the time-derivative is understood with respect to the unperturbed time-evolution of the bath oscillators. This means that the power-spectrum of \hat{A} is related to that of the force via (see below for the meaning of the superscript (0))

$$\langle \hat{A} \hat{A} \rangle_\omega^{(0)} = \left(\frac{c}{e} \right)^2 \frac{1}{\omega^2} \langle \hat{F} \hat{F} \rangle_\omega, \quad (3.5)$$

and \hat{A} may be written explicitly as

$$\hat{A} = \frac{c}{e} \sum_j \hat{P}_j. \quad (3.6)$$

The transition from scalar to vector potential in the Hamiltonian is accomplished by the gauge transformation with generator

$$\hat{\chi} = -\frac{e}{c} \hat{q} \hat{A}, \quad (3.7)$$

which leads to

$$\hat{H}' = e^{-i\hat{\chi}} \hat{H} e^{i\hat{\chi}} = \frac{1}{2m} \left(\hat{p} - \frac{e}{c} \hat{A} \right)^2 + \sum_j \frac{\hat{P}_j^2}{2M_j} + \frac{M_j \Omega_j^2}{2} \hat{Q}_j^2. \quad (3.8)$$

The transformation used here has been applied to Quantum Brownian motion in [Hakim85]. Again, the detailed expression for \hat{A} in (3.6) and the explicit form of the

bath hamiltonian in (3.8) are not needed to describe the dissipative system dynamics. It is enough to know the correlator (3.5), since we are dealing with a linear bath.

In the vector-potential gauge, the dynamical momentum \hat{p} of the particle is a constant of the motion. All the effects induced by the bath, such as fluctuations, mass renormalization and, possibly, friction, are visible only in the behaviour of the kinematical momentum $\hat{p} - \frac{e}{c}\hat{A}$, i.e. the velocity.

Mass renormalization and friction can be analyzed in this picture if we imagine the particle to be given a kick at time $t = 0$, such that its momentum p jumps from zero to a finite value. Then, the subsequent time-evolution of the average velocity is governed by the response of the vector potential to the perturbation $-(pe/mc)\hat{A}$, which has been switched on at $t = 0$. According to Kubo, it is given by

$$\langle \hat{A} \rangle(t) = \frac{ipe}{mc} \int_0^t ds \langle [\hat{A}(t), \hat{A}(s)] \rangle, \quad (3.9)$$

which may be written in terms of the bath spectrum:

$$\langle \hat{A} \rangle(t) = \frac{2pe}{mc} \int_0^\infty d\omega \langle \hat{A}\hat{A} \rangle_\omega^{T=0} \frac{1 - \cos(\omega t)}{\omega}. \quad (3.10)$$

However, in this formula, it is not the spectrum $\langle \hat{A}\hat{A} \rangle_\omega^{(0)}$ which enters, but rather the spectrum of \hat{A} that derives from the combination of the bath Hamiltonian in Eq. (3.8) with the quadratic term from the kinetic energy:

$$\hat{H}'_B = \frac{e^2}{2mc^2} \hat{A}^2 + \hat{H}_B. \quad (3.11)$$

Although this Hamiltonian is still quadratic, the (classical) eigenfrequencies and eigenvectors are changed. It is shown in Appendix A.5 how the spectrum $\langle \hat{A}\hat{A} \rangle_\omega$ is obtained in terms of the original spectrum $\langle \hat{A}\hat{A} \rangle_\omega^{(0)}$:

$$\langle \hat{A}\hat{A} \rangle_\omega^{T=0} = \frac{1}{2\pi C} \text{Im} \left\{ \left[4C \int_0^\infty d\nu \frac{\langle \hat{A}\hat{A} \rangle_\nu^{(0)T=0}}{\omega^2 - \nu^2 - i0^+} \right]^{-1} - 1 \right\}^{-1}. \quad (3.12)$$

Here the constant C is the prefactor of \hat{A}^2 in Eq. (3.11), $C = e^2/(2mc^2)$. For $C \rightarrow 0$, the influence of the extra term in the bath Hamiltonian vanishes, and we recover the original spectrum by expanding Eq. (3.12). The same holds in the limit of weak fluctuations $\langle \hat{A}\hat{A} \rangle_\nu^{(0)T=0}$ (small system-bath coupling). However, these remarks only apply to original bath spectra that are comparatively “weak” at low frequencies, i.e. where $\langle \hat{A}\hat{A} \rangle_\nu^{(0)T=0}$

does not diverge. Otherwise, the spectrum under the integral does not become uniformly small when the prefactor determining the strength of the bath is sent to zero.

The last remark applies in particular to the Ohmic bath, which leads to Quantum Brownian motion. For that kind of bath, the force spectrum is

$$\left\langle \hat{F} \hat{F} \right\rangle_{\omega}^{T=0} = \frac{\eta}{\pi} \omega \theta(\omega_c - \omega) \theta(\omega), \quad (3.13)$$

which results in a divergent original spectrum of the vector potential, $\left\langle \hat{A} \hat{A} \right\rangle_{\omega}^{(0)T=0} \propto \omega^{-1}$. Nevertheless, upon insertion into (3.12), the effective spectrum is found to rise linearly in ω at low frequencies. For $\omega \ll \omega_c$, we obtain

$$\left\langle \hat{A} \hat{A} \right\rangle_{\omega} \approx \left(\frac{c}{e} \right)^2 \frac{\frac{\eta}{\pi} \omega}{\gamma^2 + \omega^2}, \quad (3.14)$$

where the damping rate γ is related to the friction coefficient by $\gamma = \eta/m$. Thus, the time-evolution of the average velocity is found from (3.10) as

$$\langle \hat{v} \rangle(t) = \frac{1}{m} \left(p - \frac{e}{c} \left\langle \hat{A} \right\rangle(t) \right) \approx \frac{p}{m} e^{-\gamma t}, \quad (3.15)$$

which is the exponential decay due to friction that is expected for the Ohmic bath.

For bath spectra that are weaker at low frequencies, the velocity does not decay to zero, but to a finite value, which is proportional to p . The constant of proportionality may serve to define an effective mass, $1/m_{eff}$. This can be found from (3.12), together with the long-time limit of (3.10). It gives

$$\frac{1}{m_{eff}} \equiv \frac{p - \frac{e}{c} \left\langle \hat{A} \right\rangle(t \rightarrow \infty)}{mp} = \frac{1}{m} (1 - \zeta), \quad (3.16)$$

with

$$\zeta \equiv \frac{2e^2}{mc^2} \int_0^\infty d\omega \frac{\left\langle \hat{A} \hat{A} \right\rangle_{\omega}^{T=0}}{\omega}. \quad (3.17)$$

However, it is hard to see the most important properties from this formula, as the relation to the original bath spectrum, Eq. (3.12), is relatively complicated. There is another way to arrive at the effective mass: We minimize the total potential energy with respect to \hat{A} , taking into account the terms from the kinetic energy of the particle (see Appendix A.5). This yields $\left\langle \hat{A} \right\rangle(t \rightarrow \infty)$ once again, from which we find the effective mass:

$$\frac{1}{m_{eff}} = \frac{1}{1 + \xi} \frac{1}{m}, \quad (3.18)$$

where

$$\xi \equiv \frac{2e^2}{mc^2} \int_0^\infty d\omega \frac{\langle \hat{A}\hat{A} \rangle_\omega^{(0)T=0}}{\omega}. \quad (3.19)$$

Note that it is the original spectrum which enters here. By comparing (3.18) and (3.16), we observe $\zeta = (1 + \xi^{-1})^{-1}$. If $\langle \hat{A}\hat{A} \rangle_\omega$ is approximated as $\langle \hat{A}\hat{A} \rangle_\omega^{(0)}$, one obtains $\zeta = \xi$ and $1/m_{eff} = (1 - \xi)/m$ in Eq. (3.18).

In the case of the Ohmic bath, ξ diverges ($\zeta = 1$) and the effective mass is infinite - the low frequency behaviour is dominated by friction, not any longer by inertia. A physically important example of a bath that does not lead to friction, but to a finite mass renormalization, is provided by the zero-point fluctuations of the vacuum electromagnetic field. In the dipole approximation, these correspond to a fluctuating spatially homogeneous force acting on the electron. The power spectrum of these fluctuations rises as $\langle \hat{F}\hat{F} \rangle_\omega \propto \omega^3$ at $T = 0$, which leads to $\langle \hat{A}\hat{A} \rangle_\omega^{(0)} \propto \omega$, making the effective mass finite. There is no friction for this bath, since a charge will not radiate away energy unless it is accelerated. A detailed discussion of the effects of different bath spectra in the Caldeira-Leggett model for a free particle has been given in [Schramm87].

3.3 The model

The system of electrons on the ring is described by

$$\hat{H} = \sum_p \hat{d}_p^\dagger \frac{(p - \frac{e}{c}(\hat{A} + A^{ext}))^2}{2m} \hat{d}_p + \hat{H}_B. \quad (3.20)$$

As usual, the Hamiltonian \hat{H}_B of the linear bath only enters via the fluctuation spectrum of the vector potential, $\langle \hat{A}\hat{A} \rangle_\omega^{(0)}$. The classical, fixed vector potential A^{ext} belongs to an external static magnetic flux. The possible values of the electron momentum p are quantized due to the finite circumference L of the ring: $p = 2\pi n/L$ with an integer n . As in previous sections, we have denoted the fermion operators on the ring as $\hat{d}_p^{(\dagger)}$.

No intrinsic interaction between the electrons has been taken into account, which would lead to Luttinger-liquid physics in this one-dimensional situation. In addition, any inductive self-interaction has been neglected. As we are interested in dephasing of the electronic motion itself, we are dealing with spinless electrons.

In the previous section, it has been shown that, for a single particle moving on an infinite line, a gauge transformation leads from the usual scalar potential coupling to the form shown here. For the present geometry, this is the natural form that is compatible with the periodic boundary conditions. It arises in a physical situation where the magnetic flux threading the ring fluctuates, possibly because of the Nyquist noise of the current in

an external coil. Note that we will not be able to deal with shot noise in our model, since it is unclear how nonequilibrium noise should be treated within such a description.

The Nyquist noise of the current in the external coil is white noise at finite temperatures, i.e. it has a constant power spectrum at low frequencies $\omega < T$. Since the current is proportional to the magnetic flux and, therefore, to the vector potential, the same can be said about $\langle \hat{A}\hat{A} \rangle_\omega^{(0)}$ at $T > 0$. This implies that $\langle \hat{A}\hat{A} \rangle_\omega^{(0)T=0}$ must rise linearly at low frequencies in order to describe Nyquist noise. The term “Nyquist noise”, in this context, refers to something different from the Ohmic bath. The latter would lead to velocity-proportional friction for the electrons on the ring. It is described by “ $1/f$ ” fluctuations of the flux, i.e. a spectrum $\langle \hat{A}\hat{A} \rangle_\omega^{(0)T=0} \propto 1/\omega$, as has been shown in the previous section.

Before we proceed, we will point out some simplifying features of this situation as well as some important aspects of the dephasing problem in degenerate fermion systems that are beyond the scope of this model.

The magnetic flux is assumed to thread the ring in such a way that the situation is axially symmetric with respect to the axis which goes through the center of the ring and is perpendicular to its plane. In this case, we can choose the gauge such that the vector potential is everywhere tangential to the ring and of constant magnitude around the whole circumference. The same holds for the fluctuating electric field, which is given by the time-derivative of the vector potential.

Since the coupling between system and bath is via the momentum, which itself is a constant of the motion for the original uncoupled electron system (“diagonal coupling”), the Hamiltonian (3.20) (for constant particle number) is an instance of the “independent boson model”, discussed at length in Section 2.2.2. This will lead to “pure dephasing”. Some features of this model are therefore very simple: In spite of the interaction with the bath, the momentum of a particle will stay constant, only its velocity and kinetic energy can fluctuate. This simplifies the many-electron problem as well: Although the fluctuating force influences the center-of-mass motion of the electrons and introduces some kind of “effective interaction” between them, the occupation of different p -states cannot be changed by the bath. Note that this simplification would be spoiled if one takes into account impurities and/or a coupling that depends on the position. For example, the latter would arise if one considered an arbitrary fluctuating electromagnetic field or the electric field between the plates of a gate capacitor, which is a constant vector field in space but is not constant with respect to its projection onto the direction of motion of the electrons on the ring. Other situations where the coupling depends on position include interaction with phonons or a localized spin on the ring. In addition, we cannot treat any transport situation involving a strong coupling to external leads, since that would destroy translational invariance as well.

Despite the effective interaction, the decay rates of Green’s functions will not show any dependence on the distance to the Fermi surface, in contrast to the usual behaviour of interacting Fermi systems. This is, again, due to the diagonal coupling between system and bath, which means that there are no energy-relaxation processes which change the

occupation numbers of the electrons and which would feel the restriction by the Pauli principle. Considerations related to Pauli blocking occur in cotunneling through the ring (compare Section 2.4). We will be able to discuss this issue further both in an exactly solvable model of fermions in a damped oscillator (Chapter 4), as well as on a more general basis (Chapter 5).

It must be emphasized that this model is a theoretical toy model, since it neglects intrinsic interactions, and since the magnitude of the effects related to a fluctuating magnetic flux is very small under realistic circumstances (see below). It is designed to be the simplest possible extension of Quantum Brownian motion to the many-particle case.

3.4 Qualitative semiclassical discussion of dephasing in this model

At higher temperatures, we may use a semiclassical picture to describe dephasing of a single electron traveling around the ring. Consider two wave packets traversing the left and right arm of the Aharonov-Bohm ring with constant velocity v and meeting again after some time $t = L/(2v)$ at the opposite end. The resulting interference pattern depends on the total phase difference between the two paths. In a semiclassical calculation, the phase difference is produced by the vA -term in the Lagrangian of the particle, and it is given by

$$\phi = 2\frac{e}{c} \int_0^t v A(t') dt'. \quad (3.21)$$

The factor 2 arises because the phases are equal up to a change in sign. $A(t')$ gives the time-dependence of the fluctuating vector potential which is assumed (in this approximation) to be a classical Gaussian random process with zero mean, as in the introduction of Chapter 1. The visibility of the interference pattern will be suppressed due to the fluctuations in the phase ϕ . Since ϕ is a Gaussian random variable, we obtain for the suppression factor

$$\langle e^{i\phi} \rangle = e^{-\langle \phi^2 \rangle / 2}. \quad (3.22)$$

The variance $\langle \phi^2 \rangle$ of the phase is:

$$\langle \phi^2 \rangle = 4 \left(\frac{ev}{c} \right)^2 \int_0^t dt_1 \int_0^t dt_2 \langle A(t_1) A(t_2) \rangle. \quad (3.23)$$

If the traversal time t is much larger than the correlation time of the fluctuations in A , we may apply the standard ‘‘Golden Rule’’ approximation introduced in Eq. (1.11), which gives:

$$\langle \phi^2 \rangle \approx t \cdot 4 \left(\frac{ev}{c} \right)^2 \cdot 2\pi \langle AA \rangle_{\omega=0}. \quad (3.24)$$

The physical interpretation of this result is clear: The fluctuating electric field $\propto \dot{A}$ leads to a fluctuating velocity $\propto A$, so that the random shift in the interference pattern is $\Delta x \propto \int A(t') dt'$. The interference pattern will be completely washed out once the spread in Δx becomes comparable to the wavelength $\lambda \propto 1/v$. This coincides with the criterion $\langle \varphi^2 \rangle \approx 1$ (see also Section 3.6).

In particular, for the case of Nyquist noise (white noise in A at finite T) we obtain a finite “dephasing rate” that grows linearly with temperature. The dephasing rate will vanish for $v \rightarrow 0$. For a bath that is weaker at low frequencies ($\langle \hat{A}\hat{A} \rangle_\omega \propto \omega^s$ with $s > 1$) we do not obtain a suppression factor that decays exponentially with time, hence the dephasing rate is always zero. For the Ohmic bath ($1/f$ fluctuations of the flux), we should insert $\langle A A \rangle_\omega \propto T/\omega^2$, which leads to a divergent integral for the phase fluctuations. This is because $\langle A(t)^2 \rangle = \infty$ in that case, which also means the fluctuations of the velocity are infinite. Therefore, we conclude that the simple semiclassical approximation employed here breaks down, and we postpone the discussion to the selfconsistent treatment of Section 3.6.

3.5 Effective mass, interaction and persistent current

The vector potential now couples to the center-of-mass momentum $\hat{P} = \sum_p p \hat{n}_p$. In addition, the prefactor of the \hat{A}^2 -term changes into $C = Ne^2/(2mc^2)$, as compared to the single-particle case (for fixed particle number N). We may ask again for the center-of-mass velocity which the system adopts in the long-time limit after the center-of-mass momentum has been switched to a finite value P at time $t = 0$. This yields

$$V = \frac{1}{Nm} (P - \frac{e}{c} N \langle \hat{A} \rangle (t \rightarrow \infty)) = \frac{P}{Nm(1 + N\xi)}, \quad (3.25)$$

where we have employed the definition of ξ in Eq. (3.19), but inserted the new value of C , which leads to the factor of N in front of ξ . Therefore, the total mass $M = Nm$ increases to the effective value of

$$M_{\text{eff}} = M(1 + N\xi). \quad (3.26)$$

The effective total mass M_{eff} also determines the factor by which the persistent current on the ring is reduced, as compared to the situation without coupling to a bath. If an external static magnetic flux penetrates the ring, it produces an extra vector potential A^{ext} , such that the center-of-mass velocity is given by

$$V = \frac{1}{Nm} (P - \frac{e}{c} N (\langle \hat{A} \rangle (t \rightarrow \infty) + A^{\text{ext}})), \quad (3.27)$$

where P can only adopt quantized values and is chosen to minimize the total energy (for the $T = 0$ situation, at fixed particle number N). In calculating $\langle \hat{A} \rangle (t \rightarrow \infty)$, the momentum P has to be replaced by $P - \frac{e}{c} N A^{\text{ext}}$. As a result, we get

$$V = \frac{1}{M_{\text{eff}}} \left(P - N \frac{e}{c} A^{\text{ext}} \right), \quad (3.28)$$

which is reduced by the factor M_{eff}/M . Therefore, the persistent current $I = NeV/L$ is also changed by the same factor. In fact, since the argument given here does not rely on the actual distribution of the particles over the individual momentum states (only on P), it holds also at finite temperatures (but fixed N), when an average over such configurations has to be carried out:

$$\langle \hat{I} \rangle = \langle \hat{I} \rangle^{(0)} \frac{M}{M_{\text{eff}}}. \quad (3.29)$$

The magnitude of the reduction of the persistent current may be understood physically in the following way: If one imagines suddenly switching on the external magnetic flux, an electric field pulse will be produced, which, at first, freely accelerates the electrons on the ring, leading to a current which is proportional to the number N of electrons. This again produces a change in the magnetic flux which prompts a reaction of the bath (e.g. the external coil producing the Nyquist noise). The back-action onto the electrons decelerates them, decreasing the velocity of each electron by an amount proportional to N and depending on the coupling strength between the ring and the external coil, which is contained in ξ . This leads to the reduction factor $1/(1 + \xi N)$ obtained above.

We conclude that, in this model, the suppression of the persistent current may be understood completely in terms of mass renormalization, where all the frequencies of the bath contribute (see the expression (3.19) for ξ). The low-frequency properties of the bath spectrum do not lead to any qualitative differences at this point, unless the effective mass diverges, which happens for the Ohmic bath with $\langle \hat{A}\hat{A} \rangle_{\omega}^{(0)T=0} \propto 1/\omega$. This qualitative independence of the bath spectrum is in contrast to the Green's functions, whose long-time behaviour depends drastically on the exponent of the bath spectrum at low frequencies (see below).

It is not possible to ascribe the change in M_{eff} to an increase of the single-particle masses. Rather, there is an effective interaction between particles via the center-of-mass momentum. We write the Hamiltonian (3.20) in the generic form (2.10) of the independent boson model:

$$\hat{H} = \sum_p \left(\epsilon_p - \frac{e\tilde{p}}{mc} \hat{A} \right) \hat{n}_p + \frac{Ne^2}{2mc^2} \hat{A}^2 + \hat{H}_B. \quad (3.30)$$

Here we have introduced the kinematic momentum $\tilde{p} \equiv p - eA^{\text{ext}}/c$ and the single-particle energies $\epsilon_p \equiv \tilde{p}^2/(2m)$. In addition, we have assumed a fixed particle number N , and the \hat{A}^2 -term should be combined with \hat{H}_B to form \hat{H}'_B , leading to an effective bath spectrum $\langle \hat{A}\hat{A} \rangle_{\omega}$ (compare Section 3.2). We will remark on the case of variable particle number N further below.

After performing the unitary transformation introduced in (2.13), with the fluctuating fields $\hat{F}_p = -e\tilde{p}\hat{A}/mc$ (in the notation of the independent boson model, see Section 2.2.2), we are led to the Hamiltonian describing the effective interaction between the particles on the ring:

$$\begin{aligned} \sum_p \epsilon_p \hat{n}_p - \frac{\zeta}{2m} \sum_{p,p'} \tilde{p}\tilde{p}' \hat{n}_p \hat{n}_{p'} + \hat{H}'_B = \\ \sum_p \epsilon_p \hat{n}_p - \frac{\zeta}{2m} \tilde{P}^2 + \hat{H}'_B, \end{aligned} \quad (3.31)$$

where the interaction constant ζ has been defined in Eq. (3.17), and $\tilde{P} = \hat{P} - eNA^{ext}/c$. The effective total mass can also be obtained from this formula, by rewriting the sum over kinetic energies ϵ_p in terms of center-of-mass and relative momenta. Combining this with the second term, we find $1/M_{\text{eff}} = (1 - N\zeta)/M$, which is equal to (3.26), since $1 - N\zeta = (1 + N\xi)^{-1}$ (using the results of Section 3.2, with C multiplied by N). Note that the total kinetic energy given here is still positive (semi-)definite in the momenta, in spite of the negative \tilde{P}^2 -term.

Damping and dephasing only affects the center-of-mass motion in this model, as the bath couples to the total momentum \hat{P} . However, this fact is not easily visible in the results for the Green's functions or cotunneling transport (to be discussed below), when properties of single particles play a role. We will analyze a similar situation in the case of fermions in a damped harmonic oscillator (Chapter 4), where the center-of-mass coordinate couples to a fluctuating force.

3.6 Two-particle Green's function and dephasing

We can take over the results given in the section on the independent boson model in order to discuss dephasing of the electronic motion on the ring, in terms of the two-particle Green's function. Essentially, of course, these are well-known results for the single-particle case [Caldeira83, Hakim85, Schramm87], that are expressed in terms of the two-particle Green's function in our many-particle situation.

We have to remember to make use of the effective bath spectrum $\langle \hat{A}\hat{A} \rangle_\omega$, instead of $\langle \hat{A}\hat{A} \rangle_\omega^{(0)}$. The dependence of $\langle \hat{A}\hat{A} \rangle_\omega$ on N does not present any difficulties in this case, since we are dealing with a process where the number of particles stays constant, only the state of a single particle is changed. Then, according to Eqs. (2.34) and (2.35), we find

$$\begin{aligned} \langle \hat{d}_p^\dagger(t) \hat{d}_{p'}(t) \hat{d}_{p'}^\dagger(0) \hat{d}_p(0) \rangle = \\ \langle \hat{d}_p^\dagger(t) \hat{d}_{p'}(t) \hat{d}_{p'}^\dagger(0) \hat{d}_p(0) \rangle_{el} \times e^{-(p-p')^2 \kappa(t)}, \end{aligned} \quad (3.32)$$

where we have used (compare Eq. (2.25)):

$$K_{pp'}(t) = \tilde{p}\tilde{p}' \left(\frac{e}{mc}\right)^2 \int d\omega \frac{\langle \hat{A}\hat{A} \rangle_\omega}{\omega^2} (e^{-i\omega t} - 1) \equiv -\tilde{p}\tilde{p}' \kappa(t). \quad (3.33)$$

The result is physically very transparent. The strength of dephasing, as measured by the decay of (3.32), is determined by the difference of momenta in the two states, $(p-p')^2$, since the bath couples to the momentum of each particle. The real part of $\kappa(t)$ can be identified as

$$\text{Re } \kappa(t) = \frac{1}{2} \left(\frac{e}{mc}\right)^2 \left\langle \left(\int_0^t ds \hat{A}(s) \right)^2 \right\rangle. \quad (3.34)$$

Therefore, the exponential suppression factor $\exp[-(p-p')^2 \kappa(t)]$ is just what one expects for the suppression of the interference term $\exp[i(p-p')x]$ in the probability density for a superposition of plane wave states p and p' . This suppression is brought about by the fluctuations $\Delta\hat{x}$ of the position, which are related to the fluctuating velocity:

$$\Delta\hat{x} \equiv \int_0^t ds \hat{v}(s) = -\frac{e}{mc} \int_0^t ds \hat{A}(s). \quad (3.35)$$

This yields

$$\langle e^{i(p-p')\Delta\hat{x}} \rangle = \exp \left[-\frac{1}{2} (p-p')^2 \langle \Delta\hat{x}^2 \rangle \right], \quad (3.36)$$

which is equal to the factor derived above, in Eq. (3.32). Note that it is only the symmetrized (fluctuation) part of the correlator of \hat{A} which enters these expressions.

The time-evolution of $\kappa(t)$ for different bath spectra has been described already in Section 2.2.5. In particular, for a spectrum that rises linearly at low frequencies (the Nyquist noise introduced above),

$$(ep_F/mc)^2 \langle \hat{A}\hat{A} \rangle_\omega^{T=0} = 2\alpha\omega^1 \theta(\omega), \quad (3.37)$$

we find exponential decay at finite temperatures, with a rate

$$\frac{1}{\tau_\phi} = 2\pi\alpha T (p-p')^2 / p_F^2, \quad (3.38)$$

and power-law decay at $T = 0$, of the form

$$(\omega_c t)^{-2\alpha(p-p')^2/p_F^2}. \quad (3.39)$$

Here the momentum p_F has been introduced for dimensional reasons (to keep α a dimensionless coupling constant); it could denote the Fermi momentum in the many-particle situation.

For the “Ohmic bath” with $1/f$ -fluctuations of the flux, the semiclassical approach of Eq. (3.23) had failed, giving a divergent result due to the infinite variance of the vector potential. However, if the “effective” spectrum of \hat{A} is used, the variance of \hat{A} and that of the velocity is finite, because it is limited by the friction (which is neglected in the semiclassical version). At $T = 0$, for $N\gamma t \gg 1$, one gets for the Ohmic bath the following result (after taking into account the replacement $C_{new} = C_{old}N$ in the transformation (3.12)):

$$\text{Re } \kappa(t) \approx \frac{1}{N^2 \eta \pi} \ln(N\gamma t). \quad (3.40)$$

This again leads to a power-law decay in time of the interference term, just as for the Nyquist bath. However, physically the situation is quite different, since the Ohmic bath leads to friction, which would (for example) slow down a moving interference pattern (where $p' \neq -p$), in contrast to the Nyquist bath.

We briefly comment on the relation of these results to the usual formulation for a fluctuating scalar potential (see Appendix A.9 for the density matrix propagator of the free particle subject to the Ohmic bath). Comparing the density matrix obtained in that approach with the time-evolution discussed here, we note, first of all, that the smearing of the velocity distribution is not visible here, since it is contained indirectly in the relation between the momentum and the velocity. However, this does not affect the correct description of the decaying interference term. In fact, in the limit $\gamma t \gg 1$, the results for the exponential suppression factor obtained here and that obtained using the density matrix propagator (A.60) from Appendix A.9 coincide for an initial superposition of plane wave states. A difference arises in the contribution from small times, since the usual factorized initial conditions have been used in the appendix (implying no initial velocity fluctuations), while the treatment given here is selfconsistent.

Further insight into the low-temperature behaviour in the case of Nyquist noise can be obtained by using the analogy to the zero-point fluctuations of the vacuum electromagnetic field. The Nyquist bath is characterized by a fluctuation spectrum of flux and vector potential which is linear in ω (at zero temperature), therefore leading to a spectrum for the electric field that behaves like ω^3 . This is exactly the spectrum of the zero-point fluctuations of the electric field in vacuum. The main distinction between those fluctuations and the Nyquist noise considered here is that the latter leads to a force which is homogeneous around the ring and therefore is compatible with the translational invariance of our one-dimensional system of electrons. Furthermore, its magnitude depends on the geometry and resistance of the external circuit producing the equilibrium current noise.

Free ballistic motion is not affected, since the radiation reaction force only acts on an accelerated charge. Therefore, the populations of the electronic momentum eigenstates do not decay, as we have already observed. Consequently, the system is not ergodic, since the memory of the initial conditions is not lost completely. In a basis other than the momentum basis, the off-diagonal elements of the density matrix show only partial decay. That there *is* some decay of the coherences is connected to the smearing of the position

of the particle in the course of time. Usually, this effect is neglected in the discussion of dissipative quantum motion of a free particle under the influence of electromagnetic vacuum fluctuations, since the ballistic expansion of an initially localized ensemble of particles dominates. In our case, it is important, since, for example, a superposition of two counterpropagating plane waves on the ring will first form a standing wave pattern, whose visibility then gradually decreases (as discussed above). The fact that, at $T = 0$, the decay of the visibility proceeds as a power-law (for Nyquist noise or vacuum fluctuations, respectively) is also related to the results of an old semiclassical analysis of the Lamb-shift due to Welton [Welton48, Milonni94]: The vacuum fluctuations of the electric field lead to fluctuations of the electron position, such that the variance $\langle \Delta x^2 \rangle$ of its coordinate is given by the logarithm containing the ratio of an upper cutoff-frequency (there taken to be the Compton frequency) and a lower cutoff (the characteristic frequency of electron motion around the nucleus). In our case, the lower cutoff frequency actually is given by the inverse of the observation time, such that $\langle \Delta x^2 \rangle \propto \ln(\omega_c t)$. As explained above, this leads to complete decay of the interference pattern even at $T = 0$.

The discussion given above applies to a single particle as well as the many-particle system considered here. However, we note that $p - p'$ is actually the difference of total momenta in the two many-particle states that have been superimposed. A superposition of many-particle states of total momentum zero would not be decohered by coupling to the bath.

Although we have shown that the coherence decays as a power-law (for Nyquist noise and the Ohmic bath) at $T = 0$, we do not label this as “zero-temperature dephasing”, in the sense used in weak localization. This is because here we have been considering a superposition of excited states of the system. In other problems of dephasing, such as those encountered in weak localization, one usually discusses the limit of zero-frequency response of the system to a small perturbation. A situation which comes closer to this kind of question is the cotunneling setup discussed in the next section.

We will now briefly discuss the expected magnitude of the effect due to Nyquist noise in an external current coil. If the equilibrium current fluctuations are produced by a single current loop of resistance R , whose circumference is similar to that of the Aharonov-Bohm ring (L) and which is placed about a distance L away, the dephasing rate at finite temperatures (see (3.37), (3.38); evaluated for $p - p' \approx p_F$) is estimated to be

$$\frac{1}{\tau_\phi} \sim \left(\frac{e^2}{\hbar c} \right)^2 \left(\frac{v_F}{c} \right)^2 \frac{k_B T}{R/R_K}. \quad (3.41)$$

Here v_F is the Fermi velocity on the ring, R is the resistance of the external coil and $R_K = h/e^2$ is the quantum of resistance. Both the square of the fine-structure constant in front of the expression and the ratio of the Fermi velocity to the speed of light render the effect very small under reasonable experimental conditions, where charge fluctuations and phonons will be more important sources of dephasing.

Turning to other possible bath spectra, we note that the fluctuations of the vacuum *magnetic* field have a weaker power-spectrum, which leads to $\langle AA \rangle_\omega \propto \omega^3$ at $T = 0$,

instead of $\langle AA \rangle_\omega \propto \omega$. The vacuum fluctuations of the *electric* field, however, do lead to a linear spectrum in the vector potential fluctuations (see discussion above). On the other hand, the electric field (at large wavelengths) is homogeneous only in free space, not with respect to its projection onto the ring, where it has a position dependence $\cos(2\pi x/L)$. Thus, the coupling is not diagonal in the momentum basis and is not included in our model. If one estimates the order of magnitude of the corresponding “dephasing rate” (inelastic transition rate), one arrives at $\tau_{\phi(em)}^{-1} \sim (e^2/\hbar c) (v_F/c)^2 (v_F/L)$. Similarly, one may estimate the strength of fluctuations due to shot-noise of the external current. In a situation where the external current loop producing a static magnetic flux on the order of $\sim \Phi_0$ is identical with that where the Nyquist noise originates, the shot noise may lead to an effective dephasing rate of $\tau_{\phi(shot)}^{-1} \sim (e^2/\hbar c) (v_F/c) v_F/L$, which may be much larger than that due to the Nyquist noise. Note that shot noise cannot be described by our model, since it (probably) cannot be represented by a bath of harmonic oscillators at low temperatures. However, the effects of shot noise would be reduced in a different geometry where the static component of the magnetic flux is produced by a larger current (with correspondingly smaller *relative* magnitude of the shot noise).

3.7 Variable particle number

Up to now we have been dealing with a fixed number N of particles on the ring. However, for tunneling transport, we have to consider a variable N . This raises the question of how the term $\propto N\hat{A}^2$ in the electrons’ kinetic energy should be treated. This term is not very important for baths such as the Nyquist noise due to an external coil, since at least in the limit of weak coupling we have $\langle \hat{A}\hat{A} \rangle_\omega \approx \langle \hat{A}\hat{A} \rangle_\omega^0$ for the bath spectra calculated with and without this term, respectively. On the other hand, as has been explained in Section 3.2, the \hat{A}^2 -term is crucial for describing correctly the friction induced by the Ohmic bath, where the effective spectrum $\langle \hat{A}\hat{A} \rangle_\omega$ does not diverge at low frequencies precisely because of this term. There are two possibilities - either to leave away the coupling to the vector potential for the electrons in the reservoirs or to keep it. If we take serious the model of a fluctuating magnetic flux, only the latter possibility is realistic, since an electron tunneling from the ring onto an electrode will still feel the fluctuating vector potential and the corresponding electric field. Unfortunately, this results in several problems: Firstly, it complicates severely the description of tunneling transport, since then the reservoirs cannot be assumed as non-interacting any longer. Therefore, we choose to treat them as free-electron reservoirs nevertheless, assuming that the most important physical effect of the fluctuations is to dephase the electronic motion around the ring, while the coupling to the reservoirs does not alter this effect in a qualitatively important way. If the electrodes are clean wires projecting perpendicularly from the ring, the fluctuating electric field will mainly affect the transverse motion of electrons inside these wires. Secondly, the spectrum $\langle \hat{A}\hat{A} \rangle_\omega$ depends on the total number of electrons that couple to the fluctuating flux. This

number will be increased effectively beyond the number of particles on the ring itself. The vector potential decays as $1/r$, such that the prefactor in front of the \hat{A}^2 term contains a contribution $\propto \sum_j 1/r_j^2$ due to the reservoir electrons, where r_j denote their distances from the center of the ring. This sum will even diverge if the electrodes are not (quasi-)one-dimensional. There is a good physical reason for that, which may be understood already in the picture of classical fluctuations of the magnetic flux: The total power transferred to the electron reservoir by the fluctuating electric field would also diverge in that case, unless the power-absorption is treated self-consistently, resulting in a screening of the transverse electric field fluctuations (skin effect). As these considerations go far beyond the purpose of the present toy model, we will not attempt a “realistic” description of these aspects. Rather, in the following discussion we will assume the interaction with the bath to be confined to the interference region, i.e. the ring itself. Even this assumption leaves us with the problem that, when an extra electron hops onto the ring, the effective bath spectrum is changed, since $N \mapsto N + 1$. However, as has been explained above, this is unimportant for the weak-coupling limit of bath spectra like that of the (physically relevant) Nyquist noise, or “weaker” spectra. Therefore, it will not affect the perturbative results concerning dephasing in the cotunneling current, to be derived below. It will play a role for the Ohmic bath ($1/f$ fluctuations of the flux), for which we cannot offer a selfconsistent description of tunneling transport, for the reasons explained in this section.

3.8 Single-particle Green’s function

Tunneling of an electron from a single electrode onto the ring is described by the single-particle Green’s function and the resulting DOS calculated in Section 2.2.3, provided the \hat{A}^2 term may be neglected. Then, we have:

$$\left\langle \hat{d}_p(t) \hat{d}_p^\dagger(0) \right\rangle = \left\langle \hat{d}_p(t) \hat{d}_p^\dagger(0) \right\rangle_{el} e^{-\tilde{p}^2 \kappa(t)}. \quad (3.42)$$

We will now discuss briefly the temperature-dependence of the linewidth that results from the average over electronic configurations contained in Eq. (3.42). The lineshape (given by $P(\omega)$, see Section 2.2.3) is smeared over a certain range due to the average over configurations with different total momenta P . The configuration-dependent energy shift δE_j has been defined in Eq. (2.21) as $\delta E_j = -2 \sum_{k \neq j} J_{kj} n_k - J_{jj}$. In our model, we have (see Eq. (3.31)) $J_{pp'} = (\zeta/2m) \tilde{p} \tilde{p}'$, such that $\delta E_p = -(\zeta/m) \tilde{p} \tilde{P} - J_{pp}$, where \tilde{P} is the total (kinetic) momentum in the respective configuration. In a first approximation (to lowest order in the system-bath coupling), we may neglect the influence of the bath on the probability distribution of \tilde{P} . Then, the resulting linewidth is given by

$$\delta\omega = \frac{\zeta}{m} \tilde{p} \delta P, \quad (3.43)$$

where $\delta P = \sqrt{\langle P^2 \rangle_0}$ is the spread in total momentum, calculated for the *original* free-electron system. We have $\langle P^2 \rangle_0 = NmT$ and therefore a linewidth which increases

with the square root of T :

$$\delta\omega \propto \zeta\sqrt{T}. \quad (3.44)$$

Note that the corresponding spread $\delta p = \delta\omega/v$ in momentum space is given by $\zeta\sqrt{NmT}$ and can very well exceed the distance $2\pi/L$ of the quantized momenta (even in the degenerate regime, where $\sqrt{mT} \ll p_F$).

If we take into account the \hat{A}^2 -term which is “switched on” by the extra electron appearing on the ring, the time-evolution between 0 and t is governed by a bath Hamiltonian different from that which determines the initial bath equilibrium state. In fact, this would lead to “squeezed states” of the bath oscillators, but we have not succeeded in simplifying the resulting expression, and will not discuss this case any further.

3.9 Cotunneling through the Aharonov-Bohm ring

In the following, we will discuss the influence of the bath on the Aharonov-Bohm (AB) effect, i.e. on the flux-dependence of the transport current through the ring. We consider tunneling into and out of the ring, taking place at two electrodes to the left and right of the ring (see Fig. 3.2). A tunneling situation is the appropriate one for our model, since attaching current leads would severely alter the system. We will consider a Coulomb blockade situation, in which any electron tunneling into (or out of) the ring will enhance the total energy by the charging energy which is assumed to be much larger than eV and the temperature T . In such a case, transport through the ring is possible only via cotunneling, i.e. a two-step process involving a virtual intermediate state belonging to a different number of electrons on the ring. A strong dependence of the tunneling current on the external magnetic flux, with a complete suppression at $\Phi_0/2$ due to destructive interference, is visible only in the “electronically elastic” cotunneling contribution, where the electronic state of the ring is left unaltered in the process. It is linear in the bias voltage and will dominate the inelastic contribution at low temperatures and for small bias voltages (see the discussion at the end of this section and [Averin92]).

The basic idea has been stated in Section 2.4: We may arrange for destructive interference and observe how this is affected by the bath. Perfect destructive interference occurs in a situation where the electrodes couple to exactly opposite points on the ring, the static magnetic flux threading the ring is equal to half a flux quantum, and the number of electrons on the ring is even. Then, the amplitudes for an electron to go through the ring add up to zero, due to pairwise cancellation between the contributions from states with opposite kinetic momenta, $\pm\tilde{p}$ (compare Fig. 3.3). These states have the same energies, such that the energy denominators appearing in the sum over intermediate states (2.126) are equal. On the other hand, at half a flux quantum, the corresponding momenta are p and $-p + 2\pi/L$ (since $\tilde{p} = p - \pi/L$ in that case). Therefore, the wave functions of these states, evaluated at the point $x = L/2$ that is halfway around the ring, enter with opposite signs: $\exp(ipx) + \exp(i(-p + 2\pi/L)x) = 0$.

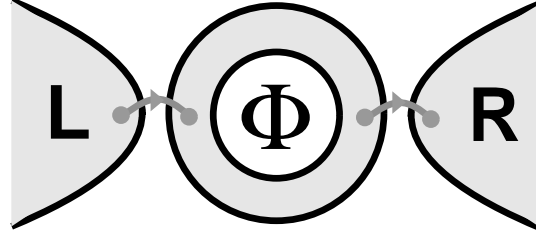


Figure 3.2: The tunneling setup discussed in the text.

A semiclassical single-particle analysis of dephasing brought about by fluctuations in the flux has been given in Section 3.4. However, at low bias voltages and temperatures, such a picture is misleading even on a qualitative level, since it effectively assumes the electron can emit or absorb an arbitrary amount of energy. It is even more inappropriate in the cotunneling situation, where the electron stays on the ring only for a short time. In the quantum-mechanical calculation, suppression of interference is due to the electron leaving a trace in the bath that permits, at least in principle, to decide through which of the two counterpropagating momenta the electron has traveled. This involves a transfer of energy between electron and bath. The bath spectrum determines the amount of bath oscillators able to absorb the small energy $\leq eV$ which can be emitted by the electron. Therefore, dephasing at zero temperature is suppressed for $V \rightarrow 0$ due to the energy conservation constraint and Pauli blocking, as has been emphasized already in Section 2.4.2. This will be confirmed by the calculation described in the following. Away from the point of perfect destructive interference, $\Phi = \Phi_0/2$, there will be renormalization effects that change the strength of the tunneling current, which are not to be mistaken for dephasing.

We will build on the general results for cotunneling through a set of localized levels coupled to a bath, derived in Section 2.4.2. However, since the levels on the ring are not empty initially, we have to go beyond the discussion in Section 2.4.4: First of all, the energy shifts now depend on the configuration of electrons on the ring. We will consider the simplest case, where the temperature is small compared to the single-particle level spacing, such that only the ground-state configuration contributes significantly to the average contained in the electronic part of the two-particle Green's function (cf. Eq. (2.139)). Furthermore, we need to keep the contributions to the total cotunneling rate that are due to intermediate states with an extra hole on the ring (Γ_{ph}^+ , Γ_{hp}^+ , Γ_{hh}^+). If the voltage is sufficiently small, we are entitled to neglect electronically inelastic transitions. The effects of a change in the bath spectrum $\langle \hat{A}\hat{A} \rangle_\omega$ due to an extra electron tunneling onto the ring will be neglected (compare the previous section), and we will therefore not deal with spectra that are stronger than the Nyquist noise at low frequencies.

The electronic part of the two-particle Green's function now reads (compare Eq.

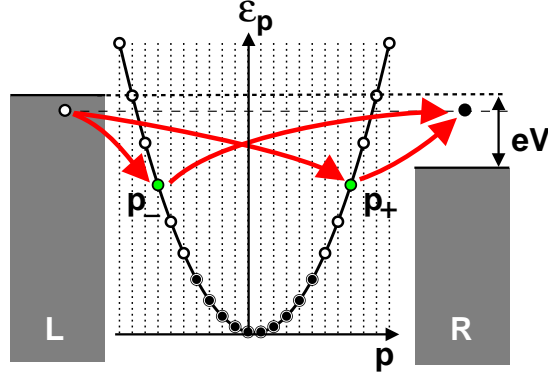


Figure 3.3: Energy diagram for cotunneling through the AB-ring, at $\Phi = \Phi_0/2$. The initial, final and two destructively interfering intermediate states are indicated (see main text).

(2.20)):

$$\begin{aligned} & \left\langle \hat{d}_j(-\tau^<) \hat{d}_j^\dagger(0) \hat{d}_l(0) \hat{d}_l^\dagger(-\tau^>) \right\rangle_{el} = \\ & (1 - n_l)(1 - n_j) e^{-i\delta E_l \tau^> + i\delta E_j \tau^<} . \end{aligned} \quad (3.45)$$

Here $n_{l,j}$ are the occupation numbers in the ground state, and the energy shifts $\delta E_{l,j}$ in our model are given by $\delta E_p = -(\zeta/m)\tilde{p}\tilde{P} - J_{pp}$, where \tilde{P} is the total (kinetic) momentum in the ground state. Therefore, the activation energy Δ_p (cf. Eq. (2.144)) has to be increased by $-(\zeta/m)\tilde{p}\tilde{P}$. In addition, we take into account a charging energy E_C^e that arises due to Coulomb interaction between the electrons on the ring:

$$\Delta_p = \epsilon_p - \epsilon_L - J_{pp} - (\zeta/m)\tilde{p}\tilde{P} + E_C^e . \quad (3.46)$$

This replacement, together with the occupation factors $(1 - n_l)(1 - n_j)$, is the only change in Eq. (2.143) for γ_{jl} .

We will now list the changes required in Eq. (2.143) for the other three cotunneling rate contributions, using the rules of Appendix A.3. The amplitudes A_j themselves are not changed, since they are not affected by the order of electron tunneling in the two junctions. For Γ_{ph}^+ and Γ_{hp}^+ , there is a negative sign in front of the expression for γ_{jl} . In addition, in the exponential $K_{lj}[\tau^>, \tau^<, t]$, given in Eq. (2.133), the signs of the cross-correlators K_{jl} are inverted. There is a simple physical reason for this: In the intermediate state, with an extra hole in state p , the total momentum is changed by $-\tilde{p}$, instead of \tilde{p} for the electron state. Furthermore, the corresponding activation energy (i.e. Δ_l for Γ_{ph}^+ , Δ_j for Γ_{hp}^+ , $\Delta_{j,l}$ for Γ_{pp}^+) is to be replaced by that of the hole state. This follows from the change in exponentials in Appendix A.3, together with the evaluation of the electronic part of the Green's function:

$$\Delta_p^h = \epsilon_R - \epsilon_p - J_{pp} + (\zeta/m)\tilde{p}\tilde{P} + E_C^h. \quad (3.47)$$

We have used $\delta E_l^h = J_{ll} + 2\sum_{k \neq l} J_{kl}n_k = -J_{ll} + 2\sum_k J_{kl}n_k$ for the energy change resulting from taking away a particle on level l (where $n_l = 1$).

In addition, occupation factors of n_l or $(1 - n_l)$ have to be inserted for electron or hole states, respectively.

We will evaluate the resulting cotunneling rate in perturbation theory, see Section 2.4.5. Equation (2.155) is changed in the way discussed above, i.e. there are appropriate occupation factors, and the activation energies turn into $\Delta_{j0}^{(h)} \equiv \Delta_j^{(h)} + J_{jj}$, with $\Delta_j^{(h)}$ given in Eqs. (3.46), (3.47). In addition, for the cases Γ_{ph}^+ and Γ_{hp}^+ , there is an overall negative sign, as well as an additional negative sign in front of the correlator $\langle \hat{F}_j \hat{F}_l \rangle$, due to the afore-mentioned change in the exponential $K_{lj}[\tau^>, \tau^<, t]$.

For our specific model the correlator factorizes:

$$\langle \hat{F}_p \hat{F}_{p'} \rangle_\omega = (e/mc)^2 \langle \hat{A} \hat{A} \rangle_\omega \tilde{p} \tilde{p}'. \quad (3.48)$$

This enables us to write the forward cotunneling rate, resulting from all these considerations, in a very compact way. The elastic contribution (with respect to electronic transitions *and* the bath) is, at $T = 0$:

$$\Gamma_{elastic}^+ = 2\pi D_L D_R eV \left| \sum_p T_p^{R*} T_p^L \left(\frac{1 - n_p}{\Delta_{p0}} - \frac{n_p}{\Delta_{p0}^h} \right) \right|^2. \quad (3.49)$$

In this formula, the bath-induced energy shift contained in $\Delta_{p0}^{(h)}$ (see above) should be retained up to first order in the result, for consistency.

The inelastic contribution, leading to an “incoherent” cotunneling current, is found to be:

$$\Gamma_{incoh}^+ = 2\pi D_L D_R W \left| \sum_p T_p^{R*} T_p^L \tilde{p} \left(\frac{1 - n_p}{\Delta_{p0}^2} + \frac{n_p}{\Delta_{p0}^{h2}} \right) \right|^2, \quad (3.50)$$

with the prefactor W giving the strength of dephasing (compare Eq. (2.155), with $\hat{F}_p = -e\tilde{p}\hat{A}/mc$):

$$W \equiv \int d\omega S(\omega) \left(\frac{e}{mc} \right)^2 \langle \hat{A} \hat{A} \rangle_\omega, \quad (3.51)$$

where $S(\omega)$ has been defined in Eq. (2.145) (at $T = 0$, $S(\omega) = (eV - \omega)\theta(eV - \omega)$). In (3.50), $\Delta_{p0}^{(h)}$ should be taken without the contribution $\propto \zeta\tilde{p}\tilde{P}$, since W is already of first order in the bath correlator.

For the geometry considered here, we use $T_p^L = t^L$ and $T_p^R = t^R e^{ipx}$, where $x = L/2$ is the point on the ring which couples to the right electrode, and $t^{L/R}$ are constant tunnel amplitudes.

For an even number of electrons, at a static magnetic flux of $\Phi_0/2$, we obtain $\tilde{P} = 0$. Therefore, $\Delta_{p0}^{(h)}$ does not contain any bath-induced energy shift. The pairwise cancellation of terms from the states with kinetic momenta $\pm\tilde{p}$ makes $\Gamma_{elastic}^+$ vanish, i.e. the perfect destructive interference can only be lifted when $\Gamma_{incoh}^+ \neq 0$. In Eq. (3.50) for Γ_{incoh}^+ , the terms from $\pm\tilde{p}$ do not cancel, due to the prefactor of \tilde{p} inside the sum over states: The bath, coupling to the momentum, can distinguish between electrons moving around the ring clockwise or counterclockwise, respectively.

In contrast, away from $\Phi_0/2$, there is no perfect pairwise cancellation anyway, due to the difference in energies for the states at $\pm\tilde{p}$.

To compare the magnitude of the elastic cotunneling current $\Gamma_{elastic}^+$ (away from $\Phi_0/2$) and that of the incoherent current at $\Phi_0/2$, it is necessary to evaluate the sums over states, taking into account the energy denominators that involve the “charging energies” $E_C^{e/h}$ introduced above. In the limit of large particle numbers, this can be done by employing the Euler-MacLaurin formula [Abramowitz84] in order to convert sums to integrals. We find approximately, for the sum in the elastic cotunneling current (3.49) (without bath-induced shifts):

$$t^{R*}t^L \frac{\delta\epsilon}{2} \left\{ \frac{1}{E_C^{e2}} - \frac{1}{E_C^{h2}} + \frac{1}{(E_C^h + \epsilon_F)^2} \right\},$$

with $\delta\epsilon$ the single-particle level spacing on the ring (around the Fermi energy of ϵ_F , which is measured with respect to the lowest states on the ring).

On the other hand, the corresponding sum in the incoherent current turns out to be given by a similar expression, where $\delta\epsilon/2$ is replaced by p_F , the Fermi momentum on the ring. Therefore, the ratio of the incoherent cotunneling current to the magnitude of the elastic current is (at $T = 0$):

$$\begin{aligned} & \frac{\Gamma_{incoh}^+[\Phi_0/2]}{\Gamma_{elastic}^+[\Phi \approx 0]} \sim \frac{W p_F^2}{eV \delta\epsilon^2} \\ &= \left[\int_0^{eV} d\omega \left(1 - \frac{\omega}{eV}\right) \left(\frac{ep_F}{mc}\right)^2 \left\langle \hat{A}\hat{A} \right\rangle_\omega \right] \frac{1}{\delta\epsilon^2}. \end{aligned} \quad (3.52)$$

This can be interpreted as the magnitude of the energy fluctuations of a single particle level on the ring (measured by the variance), divided by the square of the single-particle level spacing. However, it is not the energy fluctuations at arbitrary frequencies which enter here, but rather their low-frequency part, up to the bias voltage eV . This is qualitatively similar to the behaviour of the Green’s functions, but different from that of the persistent current or the effective mass. Therefore, the ratio rises as V^{s+1} at small bias voltages (for $s \geq 0$). This means in particular that, for the Nyquist bath, there is no incoherent current contribution in the *linear* conductance at $T = 0$. Only a finite supply of energy due to the bias may lead to dephasing at zero temperature. The zero-point fluctuations of bath oscillators at frequencies larger than eV lead to renormalization effects, but not to any dephasing.

For bias voltages eV smaller than the single-particle energy spacing $\delta\epsilon$ on the ring, dephasing is merely due to the coupling to the fluctuating flux. At higher voltages, the electronically inelastic cotunneling processes become important. In these, one electron tunnels into the ring, while *another* electron goes out at the opposite electrode, thus leaving behind a particle-hole excitation on the ring [Averin92]. Since all the corresponding final states are different, their contributions to the cotunneling current sum up incoherently. Therefore, like dephasing produced by the bath, they also lead to a nonvanishing contribution to the tunneling current at $\Phi_0/2$, where, ideally, one should have perfect destructive interference. The number of possibilities to create a particle-hole excitation with an energy of at most eV is $\propto (eV/\delta\epsilon)^2$, if we assume $eV \gg \delta\epsilon$. This leads to a bias dependence $\propto V^3$ of the incoherent current [Averin92]. In that regime, the ratio of the incoherent current contribution due to the external bath to the electronic inelastic contribution is estimated to be given by the integral in (3.52), multiplied by $(\delta\epsilon/(E_C eV))^2$ (where we have assumed the charging energies $E_C^{e/h}$ to be of the same order of magnitude E_C). The electronic inelastic contribution will be the dominant one.

At small but finite temperatures, the formula for $\Gamma_{elastic}$ is still given by Eq. (3.49), while in Γ_{incoh} we have to subtract the backward tunneling rate, i.e. the result obtained for $V \mapsto -V$, which effectively changes W (compare Eq. (2.162)). The probability of inelastic scattering processes increases, both because of a larger energy supply of the electrons, as well as the possibility of induced emission and absorption of thermal bath excitations. Consequently, there is a finite incoherent contribution to the linear conductance, rising as T^{s+1} (see Section 2.4.6). However, as soon as the temperature becomes comparable to the single-particle level spacing on the ring, two further effects deteriorate the visibility of the interference pattern. Firstly, at $T \geq \delta\epsilon$, one would have to take into account the thermal averaging over different electronic configurations on the ring (still at a fixed particle number determined by the gate voltage). The perfect destructive interference at $\Phi_0/2$ depends on the presence of an electronic configuration which is symmetric in the occupancy of equal-energy states $\pm\tilde{p}$. The thermal average includes other configurations as well and therefore leads to a suppression of the destructive interference in the *elastic* tunneling current, even without the bath. Furthermore, the electronic *inelastic* contribution is also enhanced at finite temperatures and becomes linear in the voltage [Averin92]. For still larger temperatures, comparable to the charging energy, sequential tunneling will contribute as well.

We have not treated sequential tunneling through the Aharonov-Bohm ring. Obviously, if the gate voltage and charging energies are adjusted such that only two states $\pm\tilde{p}$ contribute, then the results of the previous chapter hold, provided the \hat{A}^2 term may be neglected. However, if more states are accessible, then the perfect destructive interference may be destroyed even for a gapped bath, due to the effective interaction induced between the electrons. The degeneracy of many-particle states that differ only in the distribution of right-movers and left-movers will be lifted, since there is an extra dependence of the energy on the total momentum. This may ruin the perfect destructive interference between an electron tunneling via state $+\tilde{p}$ or $-\tilde{p}$, respectively.

3.10 Comparison with other models

Concerning the effects of a fluctuating environment on the persistent current in an Aharonov-Bohm ring, there have been several investigations in the past: In [Park92] the persistent current was found to vanish for the Ohmic bath (in the single-particle case), in agreement with our results. In contrast, the thorough investigation of Guinea [Guinea02] for different bath spectra led to a dependence of the persistent current on the circumference of the ring, with an exponential decrease for growing circumference L in the case of the Ohmic bath. The difference in the results is due to a difference in coupling. The coupling was taken to be translationally invariant in our case (and in [Park92]), while it contained terms of the form $\cos(2\pi x/L)$ and $\sin(2\pi x/L)$ in [Guinea02]. Physically, this means that the force is not directed along the ring, but rather across the ring (as the electrical field of a capacitor, for example). For our model, there is only a trivial dependence of the results on the circumference L , if the bath spectrum $\langle \hat{A}\hat{A} \rangle_\omega$ is (reasonably) assumed to remain constant as L is increased (corresponding to constant strength of the force fluctuations). Another recent investigation into this issue was performed in [Büttiker01, Cedraschi00, 01], where the effects of a fluctuating gate voltage, coupled to a quantum dot inside the ring, have been analyzed. The problem was mapped onto a spin-boson model, by considering only the two electron states corresponding to an electron on the dot and outside the dot. It was found that the magnitude of the current is reduced and it starts to fluctuate with increasing coupling strength. However, although the analysis was performed for the Ohmic bath, these general features of the result would have been obtained for any type of bath spectrum. It is also what we find in our model, for the case of baths that are weaker than the Ohmic bath (see above). In this sense, we believe these general features to represent the effects of renormalization, as they are observed for any bath spectrum. If the frequency-spectrum of the persistent current fluctuations were analyzed in the model of [Cedraschi00], it would simply reflect the bath spectrum at low frequencies. However, it is not possible to compare this model with ours in more detail, since it features a non-diagonal coupling between system and bath, whereas we have treated the opposite situation of a diagonal coupling.

Concerning the dephasing of transport interference effects, an analysis of a mesoscopic Mach-Zehnder interferometer has been given in [Seelig01]. Fluctuations of the electrochemical potential in the arms of the interferometer have been assumed to be due to the Nyquist noise of the electrons themselves, whose spectrum was calculated selfconsistently. A dephasing rate rising linearly with temperature was found. However, the analysis has not yet been extended to low temperatures, where a single-particle description, as employed in [Seelig01], will be inadequate. This situation cannot be compared directly with our model, since the leads are coupled strongly to the ring (in fact, the electrons never backscatter at the junctions).

3.11 Conclusions

We have analyzed a model of a fluctuating magnetic flux threading an Aharonov-Bohm ring and discussed its effects on various properties, such as the persistent current, the two-particle Green's function and the cotunneling current through the ring. The fluctuating vector potential only couples to the total momentum of the electrons on the ring, which leads to the physics of Quantum Brownian motion (described in the vector gauge). The suppression of the persistent current is entirely due to the enhancement of the effective total mass. In particular, for the case of Nyquist noise (white flux noise at finite temperatures) and similar “weak baths”, this leads to a finite renormalization factor, while the persistent current vanishes in the case of the “Ohmic bath” ($1/f$ flux noise at $T = 0$), since it leads to velocity-proportional friction.

Concerning dephasing of an arbitrary initial superposition of momentum states, the differences between the various bath spectra are much more pronounced than for the persistent current, as is known from the theory of Quantum Brownian motion of a single free particle. In the long-time limit, both the Nyquist noise and the Ohmic bath result in power-law decay of the interference pattern at $T = 0$, and in an exponential decay with a rate rising linearly with T for $T > 0$.

For the “weak” baths we have also treated cotunneling through the ring, where the Aharonov-Bohm effect may lead to perfect destructive interference at a static magnetic flux of $\Phi_0/2$. Employing the results of the previous chapter, we have shown that there is no dephasing in the linear cotunneling conductance at zero temperature.

Chapter 4

Fermi sea in a damped harmonic oscillator

4.1 Introduction

In the previous chapters, we have analyzed dephasing in models with diagonal coupling between system and bath, in particular the independent boson model and a system of free fermions in one dimension, subject to a fluctuating force. These are many-particle generalizations of the diagonally coupled spin-boson model and the Caldeira-Leggett model of a free particle coupled to a bath, respectively. The only other well-known exactly solvable model of a dissipative quantum system is the damped harmonic oscillator. There, the coupling of the particle coordinate to a fluctuating force is non-diagonal, as it can lead to transitions between different energy levels. We will now analyze the many-particle version of this situation, where the levels of the oscillator are filled with fermions. The Pauli principle will play an important role in the dynamics of the system, because of the non-diagonal coupling. This model might be of some relevance for clouds of fermions in (one-dimensional) harmonic traps, when they are subject to a homogeneous equilibrium noise force at low temperatures.

The research reported here has been performed in collaboration with D. S. Golubev.

4.2 The model

We consider a system of N identical fermions (non-interacting and spinless) confined in a one-dimensional harmonic oscillator potential. They are subject to a fluctuating force \hat{F} that acts on each fermion, i.e. it couples to the center-of-mass coordinate of the system of fermions (see Fig. 4.1). This force derives from a bath of oscillators:

$$\hat{H} = \omega_0 \sum_{n=0}^{\infty} n \hat{c}_n^\dagger \hat{c}_n + \hat{H}_B +$$

$$\frac{\hat{F}}{\sqrt{2m\omega_0}} \sum_{n=0}^{\infty} \sqrt{n+1} (\hat{c}_{n+1}^\dagger \hat{c}_n + h.c.) \quad (4.1)$$

The \hat{c}_n are fermion annihilation operators, and the oscillation frequency of a fermion of mass m in the parabolic potential is ω_0 (we have set $\hbar = 1$). Note that ω_0 already contains a counterterm that depends on the coupling to the bath, see Eq. (4.8) below. The bath Hamiltonian is given by:

$$\hat{H}_B = \sum_{j=1}^{N_B} \frac{\hat{P}_j^2}{2} + \frac{m\Omega_j^2}{2} \hat{Q}_j^2. \quad (4.2)$$

Here the bath oscillator masses have been chosen to be equal to that of the fermions, without any loss of generality, in order to streamline a few expressions derived in the next section. In this chapter, \hat{F} denotes a fluctuating force (instead of a potential), which is given as a sum over the bath normal coordinates \hat{Q}_j (with a prefactor g of dimensions energy over length squared):

$$\hat{F} = \frac{g}{\sqrt{N_B}} \sum_{j=1}^{N_B} \hat{Q}_j. \quad (4.3)$$

Its spectrum

$$\langle \hat{F} \hat{F} \rangle_\omega = \frac{1}{2\pi} \int_{-\infty}^{+\infty} \langle \hat{F}(t) \hat{F} \rangle e^{+i\omega t} dt \quad (4.4)$$

is still arbitrary and depends on the distribution of bath oscillator frequencies. At $T = 0$, it is given by:

$$\langle \hat{F} \hat{F} \rangle_\omega^{T=0} = \frac{g^2}{N_B} \sum_j \frac{1}{2m\Omega_j} \delta(\omega - \Omega_j). \quad (4.5)$$

The special case of an Ohmic bath, as it is used in the theory of Quantum Brownian motion [Caldeira83], is defined by

$$\langle \hat{F} \hat{F} \rangle_\omega^{T=0} = \frac{\eta}{\pi} \omega \theta(\omega_c - \omega) \theta(\omega), \quad (4.6)$$

where $\eta = m\gamma$ is the coefficient entering the friction force $-\eta v$ acting on a single particle of mass m , with γ the corresponding damping rate.

The Hamiltonian (4.1) can be derived from the following form, where the fermions are treated without second quantization and the translational invariance of the coupling between fermions and bath particles is apparent:

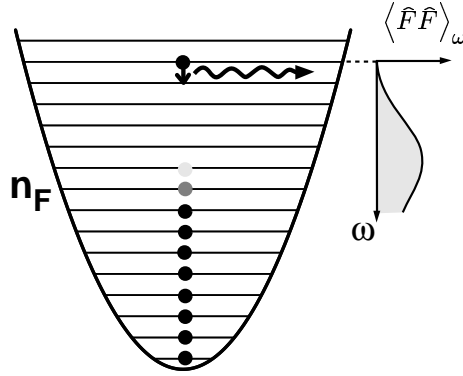


Figure 4.1: The coupling of the fermions to the irreversible bath leads both to relaxation of excited fermions as well as some smearing of the level occupation in equilibrium.

$$\sum_{l=1}^N \frac{\hat{p}_l^2}{2m} + \frac{m\omega_{00}^2}{2} \hat{x}_l^2 + \frac{1}{N} \sum_{l=1}^N \sum_{j=1}^{N_B} g_j (x_l - \hat{Q}_j)^2 + \sum_{j=1}^{N_B} \frac{\hat{P}_j^2}{2m} \quad (4.7)$$

Here the couplings g_j are given in terms of the parameter g as $g_j = g^2 N^2 / (2m\Omega_j^2 N_B)$, and the rescaled bath coordinates are $\hat{Q}_j = \hat{Q}_j(m\Omega_j^2 \sqrt{N_B} / (gN))$. Note that the frequency ω_0 introduced above already contains the counterterm that arises from the x_l^2 -terms in (4.7) and which is essential to prevent the effective oscillator potential from becoming unstable for larger coupling strengths g . In terms of the bare oscillator frequency ω_{00} , it is given by:

$$\omega_0^2 = \omega_{00}^2 + 2 \frac{N}{m} \int_0^\infty d\omega \frac{\langle \hat{F} \hat{F} \rangle_\omega^{T=0}}{\omega}. \quad (4.8)$$

4.3 Solution by bosonization and diagonalisation

Since the fluctuating force acts only on the center-of-mass (c.m.) coordinate of the particles and, in the case of the harmonic oscillator potential, the c.m. motion is independent of the relative motion, the model defined above is in principle exactly solvable in a straightforward manner. The solution can be carried out by finding the classical eigenfrequencies

and eigenvectors of the total system of $N + N_B$ coupled oscillators, setting up the quantum-mechanical wave functions in the total Hilbert space and performing the antisymmetrization with respect to the fermion coordinates. Afterwards, any desired observable (reduced density matrix, occupation numbers, fermion Green's functions etc.) may be calculated in principle. However, due to the antisymmetrization and the appearance of the oscillator eigenfunctions in the intermediate steps of the calculation, this procedure gets extremely cumbersome, so we prefer a different route which is approximately valid for large fermion numbers N .

We assume the number N of fermions in the oscillator potential to be so large that the lowest-lying oscillator states are always occupied, for any given many-particle state that becomes relevant in the calculation (at the given interaction strength and temperatures). In other words, the excitations in the fermion system, induced by the bath (and temperature), are confined to the region near the Fermi surface. Then we may employ the method of bosonization where the energy of the fermions is rewritten as a sum over boson modes (i.e. sound waves in the fermion system). This is possible since the energies of the oscillator levels increase linearly with quantum number, just as the kinetic energy of electrons in the Luttinger model of interacting electrons in one dimension. For recent pedagogical reviews on Luttinger liquids and bosonization, see [Grabert01, Delft98].

To this end, we introduce the (approximate) boson operators, for any integer $q \geq 1$:

$$\hat{b}_q = \frac{1}{\sqrt{q}} \sum_{n=0}^{\infty} \hat{c}_n^\dagger \hat{c}_{n+q}. \quad (4.9)$$

One may check that they fulfill the usual boson commutation relations, up to terms involving levels near $n = 0$ that vanish when acting on the many-particle states occurring under our assumptions. Alternatively, one may make these relations hold exactly by redefining the original model to incorporate an infinite number of artificial single-particle levels of negative energy, as is done in the Luttinger model.

Then the central result of bosonization may be applied, i.e. the fermion energy (bilinear in $\hat{c}_n^{(\dagger)}$) may be written as a bilinear expression in $\hat{b}_q^{(\dagger)}$. This is possible only due to the linear dependence of energies on the quantum number n :

$$\omega_0 \sum_{n=0}^{\infty} n \hat{c}_n^\dagger \hat{c}_n = \omega_0 \sum_{q=1}^{\infty} q \hat{b}_q^\dagger \hat{b}_q + E_{\hat{N}}. \quad (4.10)$$

Here $E_{\hat{N}} = \omega_0 \hat{N}(\hat{N} - 1)/2$ is the total energy of the N -fermion noninteracting ground state. We keep \hat{N} as an operator at this point since we will be interested in calculating Green's functions where the particle number changes.

Under the same assumption of large $N \gg 1$ we get

$$\sum_{n=0}^{\infty} \sqrt{n+1} (\hat{c}_{n+1}^\dagger \hat{c}_n + h.c.) \approx \sqrt{N} (\hat{b}_1 + \hat{b}_1^\dagger). \quad (4.11)$$

Again, this has to be understood as an approximate operator identity which is valid when applied to the many-particle states we are interested in, where $n \approx N$. We approximate N to be a number instead of an operator in this formula. This expression shows that the fluctuating force only couples to the lowest boson mode (with $q = 1$), corresponding to the c.m. motion. Therefore, the Hamiltonian now has become (within the approximations described above):

$$\hat{H} \approx \omega_0 \sum_{q=1}^{\infty} q \hat{b}_q^\dagger \hat{b}_q + \sqrt{\frac{N}{2m\omega_0}} \hat{F}(\hat{b}_1 + \hat{b}_1^\dagger) + \hat{H}_B + E_{\hat{N}}. \quad (4.12)$$

This can be solved by diagonalization of the (classical) problem of the boson oscillator $q = 1$ coupled to the bath oscillators (see Appendix A.6 and below). Note that coupling of a Luttinger liquid to a linear bath has been considered in [Neto97], although the physics discussed there (as well as the calculation) is quite distinct from our model, where we have only employed bosonization as a tool.

However, at the end we are interested in quantities relating to the fermions themselves, e.g. the occupation numbers $\langle \hat{c}_n^\dagger \hat{c}_n \rangle$ or the Green's functions, like $\langle \hat{c}_n(t) \hat{c}_n^\dagger(0) \rangle$. This means we have to go back from the boson operators \hat{b}_q to the fermion operators, by employing the relations which are also used in the Luttinger liquid. In order to do that, we have to introduce auxiliary fermion operators $\hat{\psi}(x)$:

$$\hat{\psi}(x) = \frac{1}{\sqrt{2\pi}} \sum_n e^{inx} \hat{c}_n \quad (4.13)$$

$$\hat{c}_n = \frac{1}{\sqrt{2\pi}} \int_0^{2\pi} e^{-inx} \hat{\psi}(x) dx \quad (4.14)$$

Note that the $\hat{\psi}(x)$ are *not* directly related to the fermion operators of the particles in the oscillator (which would involve the oscillator eigenfunctions). They are useful because they fulfill

$$[\hat{b}_q, \hat{\psi}(x)] = -\frac{1}{\sqrt{q}} e^{-iqx} \hat{\psi}(x). \quad (4.15)$$

This means the application of $\hat{\psi}(x)$ on the noninteracting N -particle ground state creates an $N - 1$ -particle state that is a coherent state with respect to the boson modes, i.e. an eigenstate of \hat{b}_q for every q . As a consequence, the fermion operators $\hat{\psi}(x)$ may be expressed as [Delft98]:

$$\hat{\psi}(x) = \hat{K} \lambda(x) e^{i\hat{\varphi}^\dagger(x)} e^{i\hat{\varphi}(x)} = \hat{K} \lambda e^{i\hat{\phi}r}, \quad (4.16)$$

with

$$\hat{\varphi}(x) = -i \sum_{q=1}^{\infty} \frac{1}{\sqrt{q}} e^{iqx} \hat{b}_q \quad (4.17)$$

$$\hat{\phi} = \hat{\varphi} + \hat{\varphi}^\dagger \quad (4.18)$$

$$r \equiv e^{-[\hat{\varphi}^\dagger, \hat{\varphi}]/2}. \quad (4.19)$$

The exponential $\exp(i\hat{\varphi}^\dagger(x))$ in (4.16) may be recognized as creating a coherent state with the eigenvalues of \hat{b}_q prescribed by Eq. (4.15). The other terms are necessary to give the correct normalization and phase-factor, and to deal with states other than the N -particle ground state.

The second equality in (4.16) follows from the Baker-Hausdorff identity. The “Klein factor” \hat{K} is defined to commute with the boson operators $\hat{b}_q^{(\dagger)}$ and to produce the noninteracting $(N-1)$ -particle ground state out of the noninteracting N -particle ground state. Its time-evolution follows from $[\hat{K}, \hat{H}] = [\hat{K}, E_{\hat{N}}] = \hat{K}\omega_0(\hat{N}-1)$ as $\hat{K}(t) = \hat{K} \exp(-i\omega_0(\hat{N}-1)t)$. The factor $\lambda(x)$ is given by $\exp(i(\hat{N}-1)x)/\sqrt{2\pi}$. Actually, $[\hat{\varphi}^\dagger, \hat{\varphi}] = -\sum_{q=1}^{\infty} 1/q$ diverges, so we would have to introduce an artificial cutoff e^{-aq} ($a \rightarrow 0$) into the sum. However, this drops out in the end result, because r from Eq. (4.16) is canceled by the contributions from the equal-time $\hat{\phi}$ -correlators in the exponent of Eq. (4.21). The phase $\hat{\phi}$ enters subsequent formulas in a way similar to previous chapters, as it is, again, linear in boson variables. However, the bosonic excitations initially are those of the fermion system itself, not those of the bath. They will become mixed via the coupling.

Using the relation (4.14), we have, for example:

$$\langle \hat{c}_n^\dagger(t) \hat{c}_n \rangle = \frac{1}{2\pi} \int_0^{2\pi} e^{in(x'-x)} \langle \hat{\psi}^\dagger(x', t) \hat{\psi}(x, 0) \rangle dx dx'. \quad (4.20)$$

The Green’s function involving $\hat{\psi}$ may be expressed directly in terms of the correlator of the boson operator $\hat{\phi}$, using Eq. (4.16):

$$\langle \hat{\psi}^\dagger(x', t) \hat{\psi}(x, 0) \rangle = \frac{1}{2\pi} e^{in_F((x-x')+\omega_0 t)} \langle e^{-i\hat{\phi}(x', t)} e^{i\hat{\phi}(x, 0)} \rangle r^2. \quad (4.21)$$

We have used the abbreviation $n_F = N-1$ for the quantum number of the highest occupied state (in the noninteracting system). The expectation value on the right-hand side is evaluated using the (by now well-known) Eq. (2.23). This yields:

$$\exp \left[-\frac{1}{2} \left(\langle \hat{\phi}(x', t)^2 \rangle + \langle \hat{\phi}(x, 0)^2 \rangle \right) + \langle \hat{\phi}(x', t) \hat{\phi}(x, 0) \rangle \right] \quad (4.22)$$

These results permit us to calculate the hole propagator $\langle \hat{c}_n^\dagger(t) \hat{c}_n \rangle$, from which we obtain the equilibrium density matrix by setting $t = 0$. Note that we have particle-hole symmetry in our problem, such that the particle propagator gives no additional

information. Writing down the expressions analogous to (4.20) and (4.21), and using the properties of $\lambda(x)$ and $\hat{K}(t)$ defined above, we find:

$$\begin{aligned} \left\langle \hat{c}_{n_F+\delta n}(t) \hat{c}_{n_F+\delta n}^\dagger \right\rangle = \\ \left\langle \hat{c}_{n_F+1-\delta n}^\dagger(t) \hat{c}_{n_F+1-\delta n} \right\rangle e^{-i\omega_0(2n_F+1)t}. \end{aligned} \quad (4.23)$$

It remains to calculate the correlator of $\hat{\phi}$ in the interacting equilibrium: This is where the coupling to the bath enters, since the original $q = 1$ mode will get mixed with the bath modes. All the other boson modes are unaffected. The different boson modes remain independent. Therefore, we obtain (using Eqs. (4.17) and (4.18)):

$$\left\langle \hat{\phi}(x', t) \hat{\phi}(x, 0) \right\rangle = - \sum_{q=1}^{\infty} \frac{1}{q} \left\langle (e^{iqx'} \hat{b}_q(t) - h.c.) (e^{iqx} \hat{b}_q - h.c.) \right\rangle. \quad (4.24)$$

The expectation values for $q > 1$ are simply the original ones, for example

$$\left\langle \hat{b}_q(t) \hat{b}_q^\dagger \right\rangle = e^{-i\omega_0 q t} (n(\omega_0 q) + 1), \quad (4.25)$$

with $n(\epsilon) = (e^{\beta\epsilon} - 1)^{-1}$ the Bose distribution function.

In order to obtain the time-evolution and equilibrium expectation values relating to the $q = 1$ mode (c.m. mode), we have to diagonalize a quadratic Hamiltonian describing the coupling between this mode and the bath oscillators. We define the annihilation operators of the bath modes (for $j \geq 1$) as

$$\hat{d}_j = \sqrt{\frac{m\Omega_j}{2}} (\hat{Q}_j + i \frac{\hat{P}_j}{m\Omega_j}) \Rightarrow \hat{Q}_j = (\hat{d}_j + \hat{d}_j^\dagger) / \sqrt{2m\Omega_j}, \quad (4.26)$$

and $\hat{d}_0 \equiv \hat{b}_1$, which makes \hat{Q}_0 and \hat{P}_0 the canonical variables of the c.m. mode and the coupling in Eq. (4.12) equal to $\sqrt{N}\hat{F}\hat{Q}_0$. Therefore, we have to diagonalize the following quadratic Hamiltonian, according to Eqs. (4.12) and (4.5):

$$\hat{H}' = \frac{1}{2m} P^t P + \frac{m}{2} Q^t (\Omega^2 + V) Q. \quad (4.27)$$

Here P and Q are (column) vectors, with operator entries \hat{P}_j, \hat{Q}_j ($j = 0 \dots N_B$), where $j > 0$ refers to the bath oscillators, and $j = 0$ refers to the $q = 1$ mode. The diagonal matrix Ω^2 contains the eigenvalues Ω_j^2 of the original problem (with $\Omega_0 \equiv \omega_0$) and V is the coupling matrix, with the nonvanishing entries $V_{j0} = V_{0j} = (g/m) \sqrt{N/N_B}$ ($j > 0$).

We denote by C the orthogonal matrix that diagonalizes the problem of coupled oscillators defined in (4.27), such that

$$C^t C = 1, \quad C^t (\Omega^2 + V) C = \tilde{\Omega}^2, \quad (4.28)$$

with a diagonal matrix $\tilde{\Omega}^2$ containing the new eigenfrequencies. Then we can express the old coordinates, momenta and boson operators in terms of the new normal modes:

$$Q = C\tilde{Q} \quad (4.29)$$

$$P = C\tilde{P} \quad (4.30)$$

$$\tilde{d} = \sqrt{\frac{m\tilde{\Omega}}{2}}(\tilde{Q} + i\frac{\tilde{P}}{m\tilde{\Omega}}), \quad (4.31)$$

where \tilde{d} denotes a column vector whose entries are the operators \tilde{d}_j . In order to evaluate the correlator of the c.m. mode, we have to relate the old annihilation operators \hat{d}_j to the new ones. This is accomplished by inserting the relations (4.29), (4.30) into (4.26) and expressing \tilde{Q} , \tilde{P} by \tilde{d} according to (4.31). In matrix notation, the result reads:

$$\begin{aligned} d &= \sqrt{\frac{m\Omega}{2}}(Q + i\frac{P}{m\Omega}) = \\ &= \frac{1}{2} \left(\sqrt{\Omega}C\frac{1}{\sqrt{\tilde{\Omega}}} - \frac{1}{\sqrt{\Omega}}C\sqrt{\tilde{\Omega}} \right) \tilde{d}^\dagger + \\ &+ \frac{1}{2} \left(\sqrt{\Omega}C\frac{1}{\sqrt{\tilde{\Omega}}} + \frac{1}{\sqrt{\Omega}}C\sqrt{\tilde{\Omega}} \right) \tilde{d}. \end{aligned} \quad (4.32)$$

Here \tilde{d}^\dagger is to be understood as the column-vector containing the hermitian conjugate operators as entries. Correlators of the form $\langle \hat{b}_1(t)\hat{b}_1^\dagger \rangle$ are then obtained by inserting the result for $\hat{d}_0 = \hat{b}_1$ and using the time-evolution of the “good” boson operators

$$\tilde{d}(t) = e^{-i\tilde{\Omega}t}\tilde{d}, \quad (4.33)$$

as well as their thermal equilibrium expectation values.

4.4 Evaluation of the Green’s function for $T = 0$

At $T = 0$, some simplifications apply to the evaluation of the $\hat{\phi}$ -correlator and, consequently, the fermion Green’s function $\langle \hat{c}_n^\dagger(t)\hat{c}_n \rangle$ (that will also yield the occupation numbers for $t = 0$).

We have, for example:

$$\langle \hat{b}_1(t)\hat{b}_1 \rangle = \langle \hat{d}_0(t)\hat{d}_0 \rangle =$$

$$\begin{aligned}
\frac{1}{4} \left\langle \left[\left(\sqrt{\Omega} C \frac{1}{\sqrt{\tilde{\Omega}}} + \frac{1}{\sqrt{\Omega}} C \sqrt{\tilde{\Omega}} \right) \tilde{d}(t) \right]_0 \times \right. \\
\left. \left[\left(\sqrt{\Omega} C \frac{1}{\sqrt{\tilde{\Omega}}} - \frac{1}{\sqrt{\Omega}} C \sqrt{\tilde{\Omega}} \right) \tilde{d}^\dagger \right]_0 \right\rangle = \\
\frac{1}{4} \sum_{j=0}^{N_B} C_{0j}^2 \left(\frac{\omega_0}{\tilde{\Omega}_j} - \frac{\tilde{\Omega}_j}{\omega_0} \right) e^{-i\tilde{\Omega}_j t}.
\end{aligned} \tag{4.34}$$

At $T > 0$ we would have to consider $\langle \tilde{d}_j^\dagger(t) \tilde{d}_j \rangle \neq 0$ as well.

By defining the spectral weight of the c.m. mode in the new eigenbasis,

$$W(\omega) = \sum_{j=0}^{N_B} C_{0j}^2 \delta(\omega - \tilde{\Omega}_j), \tag{4.35}$$

which is normalized to 1, we can rewrite (4.34) as

$$\langle \hat{b}_1(t) \hat{b}_1 \rangle = \frac{1}{4} \int_0^\infty W(\omega) \left(\frac{\omega_0}{\omega} - \frac{\omega}{\omega_0} \right) e^{-i\omega t} d\omega \equiv \alpha(t). \tag{4.36}$$

In a completely analogous fashion, we find

$$\langle \hat{b}_1(t) \hat{b}_1^\dagger \rangle = \frac{1}{4} \int_0^\infty W(\omega) \left(\sqrt{\frac{\omega_0}{\omega}} + \sqrt{\frac{\omega}{\omega_0}} \right)^2 e^{-i\omega t} d\omega \equiv \beta_+(t) \tag{4.37}$$

$$\langle \hat{b}_1^\dagger(t) \hat{b}_1 \rangle = \frac{1}{4} \int_0^\infty W(\omega) \left(\sqrt{\frac{\omega_0}{\omega}} - \sqrt{\frac{\omega}{\omega_0}} \right)^2 e^{-i\omega t} d\omega \equiv \beta_-(t), \tag{4.38}$$

and $\langle \hat{b}_1^\dagger(t) \hat{b}_1^\dagger \rangle = \langle \hat{b}_1(t) \hat{b}_1 \rangle = \alpha(t)$.

The calculation of $W(\omega)$ by diagonalization of the classical problem of coupled oscillators is described in Appendix A.6. The resulting Eq. (A.29) relates $W(\omega)$ to the bath spectrum $\langle \hat{F} \hat{F} \rangle_\omega^{T=0}$. For weak coupling, $W(\omega)$ is a Lorentz peak centered around ω_0 . That is why $\alpha(t)$ and $\beta_-(t)$ are small, since the spectrum $W(\omega)$ is multiplied by a function that vanishes at the resonance near ω_0 . Both α and β_- vanish exactly at zero coupling. In contrast, $\beta_+(t)$ describes damped oscillations around ω_0 (see below for a discussion of the damping rate), starting from $\beta_+(0) \approx 1$.

Evaluation of the c.m. mode contribution to the correlator of $\hat{\phi}$ (given in Eq. (4.24)) then leads to the following expression:

$$\begin{aligned}
& \left\langle (e^{ix'} \hat{b}_1(t) - h.c.) (e^{ix} \hat{b}_1 - h.c.) \right\rangle = \\
& (e^{i(x'+x)} + c.c.) \alpha(t) - e^{i(x'-x)} \beta_+(t) - e^{i(x-x')} \beta_-(t).
\end{aligned} \tag{4.39}$$

Now we are prepared to evaluate the Green's functions of the fermions in the damped oscillator.

It is convenient to introduce the abbreviations

$$X \equiv e^{ix}, X' \equiv e^{ix'}. \quad (4.40)$$

Then Eq. (4.39) leads to

$$\begin{aligned} \langle \hat{\phi}(x', t) \hat{\phi}(x, 0) \rangle &= \langle \hat{\phi}(x', t) \hat{\phi}(x, 0) \rangle_{(0)} + \\ &\quad \frac{X'}{X} (\beta_+(t) - e^{-i\omega_0 t}) + \frac{X}{X'} \beta_-(t) - \\ &\quad \alpha(t) (XX' + (XX')^{-1}), \end{aligned} \quad (4.41)$$

where the subscript (0) refers to the case without coupling to a bath:

$$\langle \hat{\phi}(x', t) \hat{\phi}(x, 0) \rangle_{(0)} = \sum_{q=1}^{\infty} \frac{(e^{-i\omega_0 t} X'/X)^q}{q}. \quad (4.42)$$

We insert this expression for the $\hat{\phi}$ -correlator into the exponent (4.22) that appears in the $\hat{\psi}$ Green's function, Eq. (4.21), and perform the Fourier transform (4.20) with respect to x, x' to go back to the original oscillator fermion operators \hat{c}_n . Then we find that the Green's function (hole propagator) $\langle \hat{c}_{n_F - \delta n}^\dagger(t) \hat{c}_{n_F - \delta n} \rangle$ is given by the prefactor of $(X'/X)^{\delta n}$ in the power series generated from

$$G_{(0)} e^E. \quad (4.43)$$

Here the factor $G_{(0)}$ stems from the terms $\langle \hat{\phi}(x', t) \hat{\phi}(x, 0) \rangle_{(0)}$ and reproduces the correct result for the non-interacting case, namely

$$\langle \hat{c}_{n_F - \delta n}^\dagger(t) \hat{c}_{n_F - \delta n} \rangle = e^{i(n_F - \delta n)\omega_0 t} \quad (\delta n \geq 0). \quad (4.44)$$

It is equal to

$$G_{(0)} = e^{in_F \omega_0 t} \sum_{k=0}^{\infty} (X'/X)^k e^{-i\omega_0 k t}. \quad (4.45)$$

The exponent E describes the influence of the bath on the Green's function. It follows from (4.41), which also has to be evaluated for $t = 0$ and $x \mapsto x'$ (or $x' \mapsto x$), due to terms like $\langle \hat{\phi}(x, 0)^2 \rangle$ from Eq. (4.22). It is constructed out of the c.m. mode correlators α, β_{\pm} , as well as binomials in X and X' :

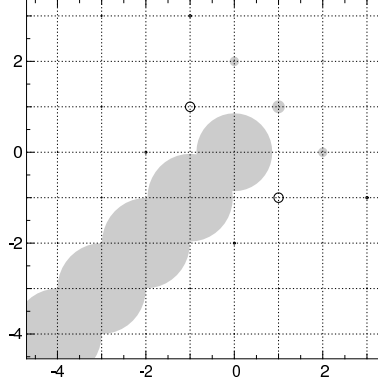


Figure 4.2: Equilibrium density matrix $\rho_{\delta n' \delta n} \equiv \langle \hat{c}_{n_F + \delta n'}^\dagger \hat{c}_{n_F + \delta n} \rangle$ for fermions in the damped oscillator, coupled to an Ohmic bath with $N\gamma/\omega_{00} = 1.6$ at $T = 0$; plotted vs. $\delta n, \delta n'$. The radius of each circle is equal to $|\rho_{\delta n' \delta n}|$, and empty circles indicate negative values.

$$\begin{aligned}
 E \equiv & 1 - \beta_+(0) - \beta_-(0) + \\
 & \frac{\alpha(0)}{2} (X'^2 + X^2 + X'^{-2} + X^{-2}) - \\
 & (X'X + 1/(X'X))\alpha(t) + \\
 & (X'/X)(\beta_+(t) - e^{-i\omega_0 t}) + (X/X')\beta_-(t).
 \end{aligned} \tag{4.46}$$

The series expansion of Eq. (4.43) has been carried out using a symbolic computer algebra system. In order to obtain the Green's function in frequency space, the resulting terms of the form $\alpha(t)^{n_\alpha} \beta_+(t)^{n_+} \beta_-(t)^{n_-}$ have then been Fourier-transformed (which leads to repeated convolutions of their Fourier spectra, i.e. essentially $W(\omega)$, see Eqs. (4.36), (4.37), (4.38)). This is done numerically (using a fast Fourier transform).

4.5 Discussion of the Green's function

The numerical results obtained for the equilibrium density matrix and the Green's function in the case of coupling to an Ohmic bath are depicted in Figs. 4.2, 4.3 and 4.4.

The *general* long-time behaviour of the Green's function (independently of the bath spectrum) can be read off directly from the exponent (4.46) given above: Since the coupling to the bath damps away the c.m. motion, the functions $\alpha(t)$, $\beta_+(t)$ and $\beta_-(t)$ all decay to zero at $t \rightarrow \infty$ (excluding cases such as a gapped bath). The temporal evolution of the exponent in Eq. (4.46) is then determined by the undamped oscillations at the frequencies $\omega_0 q$ belonging to the unaffected modes $q > 1$ of the relative motion. This leads to the conclusion that the Green's function $\langle \hat{c}_{n_F - \delta n}^\dagger(t) \hat{c}_{n_F - \delta n} \rangle$ does not decay to

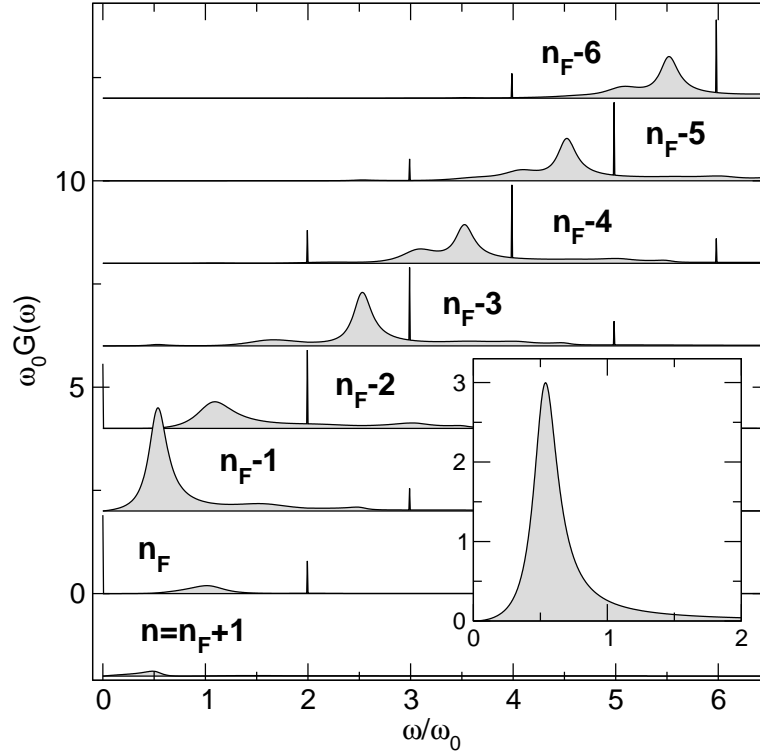


Figure 4.3: Green's function of fermions in a harmonic oscillator, coupled to an Ohmic bath: Fourier transform of $\langle \hat{c}_n^\dagger(t) \hat{c}_n \rangle$ vs. ω/ω_0 , for different values of n (curves displaced vertically for clarity). Note that ω is measured with respect to $-n_F \omega_0$. The strength of the coupling is given by $N\gamma/\omega_{00} = 0.4$ in this plot. Inset: $\omega_0 W(\omega)$ vs. ω/ω_0 . The height of the smaller δ peaks is an indication of their weight. (In the expansion of the exponential, starting from Eq. (4.46), a maximum combined power of α, β_\pm of 6 was kept.)

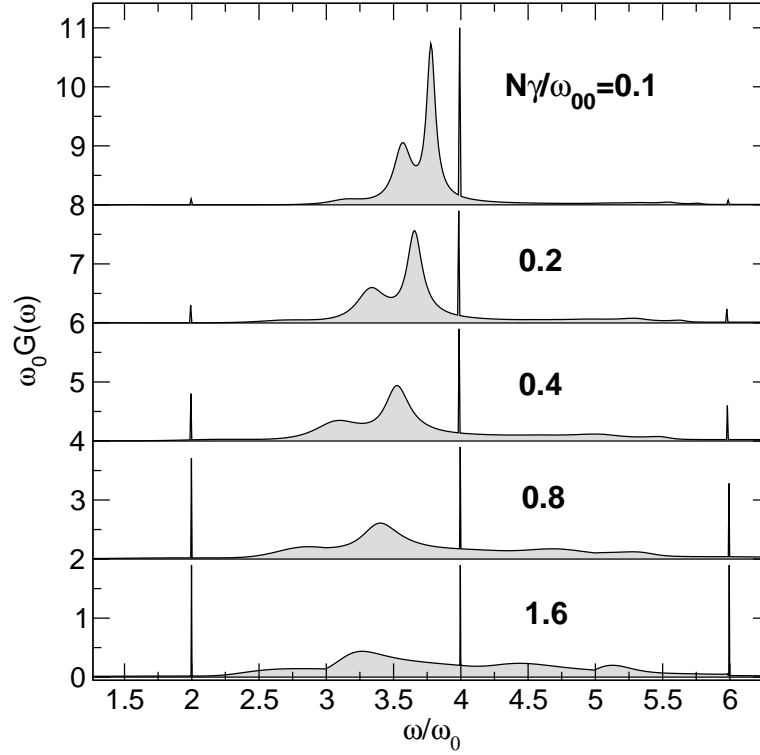


Figure 4.4: Green's function of fermions in a harmonic oscillator, coupled to an Ohmic bath: Fourier transform of $\langle \hat{c}_n^\dagger(t) \hat{c}_n \rangle$ vs. ω/ω_0 , for different values of the coupling strength, indicated in the plot (curves displaced vertically for clarity). Note that ω is measured with respect to $-n_F \omega_0$, and that ω_0 changes with γ , for fixed ω_{00} , see Eq. (4.54). This plot is produced for a fixed excitation number, $n = n_F - 4$. (In the expansion a maximum combined power of α, β_\pm of 10 was kept.)

zero in the limit $t \rightarrow \infty$, for any $\delta n > 1$, since contributions from $(X'/X)^{\delta n}$ with $\delta n > 1$ remain. In frequency space, it consists of a number of delta peaks superimposed onto an incoherent background related to the damped c.m. mode (see plots).

This result may be unexpected, since according to a *naive* application of the Golden Rule to the Hamiltonian (4.1), any electron inserted into the system at $n > n_F + 1$ (and any hole inserted at $n < n_F$) should decay towards lower (higher) single-particle energy levels by spontaneous emission of energy into the bath (for $T = 0$). The rate is expected to be:

$$\Gamma_{GR} = 2\pi \left\langle \hat{F} \hat{F} \right\rangle_{\omega_0} \frac{n_F}{2m\omega_0}. \quad (4.47)$$

Here we have used the approximation $n \approx n_F (\approx N)$ that was also introduced above. For an electron inserted just above the Fermi surface ($n = n_F + 1$), or a hole inserted at $n = n_F$, the Pauli principle blocks relaxation and the corresponding Golden Rule rate vanishes. The decay rate of the wave function (i.e. of Green's functions) is expected to be $\Gamma_{GR}/2$. In the following, we discuss the deviations from this naive expectation.

For weak coupling, the decay of the Green's function $\langle \hat{c}_n^\dagger(t) \hat{c}_n \rangle$ calculated above is determined by the decay of $\beta_+(t)$, while α and β_- are approximately zero. For example, at $n = n_F - 1$ the hole-propagator is directly proportional to $\beta_+(t)$:

$$\left\langle \hat{c}_{n_F-1}^\dagger(t) \hat{c}_{n_F-1} \right\rangle \approx \beta_+(t) e^{in_F \omega_0 t}. \quad (4.48)$$

The decay of this function is determined by the width of the Lorentz peak appearing at $\omega \approx \omega_0$ in the “spectral weight” $W(\omega)$ defined above (see Eqs. (4.35) and (4.37)) and calculated in Appendix A.6. According to Eq. (A.29), at weak coupling this width is given by

$$2\omega_0 \Delta\omega = \frac{\Gamma(\omega_0^2)}{2}. \quad (4.49)$$

By inserting the definition of $\Gamma(\omega_0^2)$, see Eq. (A.27), this yields $\Delta\omega = \Gamma_{GR}/2$ for the decay rate of $\beta_+(t)$, as expected. Therefore, there is quantitative agreement between the exact calculation and the Golden Rule result at $n = n_F - 1$. This is true also at $n = n_F$, where the Green's function evaluated in the preceding section only has a delta peak, related to Pauli blocking (apart from corrections that vanish in the limit of weak coupling), see Fig. 4.3. However, at $n < n_F - 1$, there is always an additional δ peak that is incompatible with the Golden Rule expectation, as explained above. Essentially, this discrepancy stems from the fact that the many-particle states in the harmonic oscillator are in general strongly degenerate, and that they may be split up into contributions from the c.m. and the relative motion. Therefore, the preconditions for the usual derivation of a master equation [Blum96] are violated. The relative motion is unaffected by the coupling to the bath and leads to the δ peak, as will be explained in more detail in the following paragraphs.

The excited many-particle state $|\Psi\rangle$, which is created by adding an extra hole (or extra particle) and whose time-evolution determines the Green's function, can be written as a superposition of states, each of which distributes the given number of excitation quanta δn differently onto center-of-mass ("cm") and relative ("r") motion. Therefore, in the weak-coupling limit, where one starts out of the factorized ground state $|0\rangle_{cm} |0\rangle_r |0\rangle_B$, it is of the form:

$$|\Psi\rangle = |0\rangle_B (a_0 |0\rangle_{cm} |\delta n\rangle_r + a_1 |1\rangle_{cm} |\delta n - 1\rangle_r + \dots). \quad (4.50)$$

The first state does not contain any extra excitation of the c.m. mode. Therefore, it is unaffected by the c.m.-bath coupling and does not decay. This leads to the main δ -peak contribution at a frequency $\delta n \omega_0$, which is determined by the number of excitation quanta δn .

The other states will decay. Furthermore, the resulting broadened peaks in the Green's function are shifted towards lower frequencies, due to the renormalization of the c.m. mode frequency to the value ω_{00} . Thus these peaks occur at frequencies of the form $(\delta n - n_{cm})\omega_0 + n_{cm}\omega_{00}$, where n_{cm} counts the number of quanta in the c.m. mode. This is visible in Figs. 4.3 and 4.4, where the Fourier transform of the Green's function is displayed. In the limit of weak coupling, the weights of the different peaks are given by

$$|a_{n_{cm}}|^2 = \frac{1}{n_{cm}!} \sum_{j=0}^{\delta n - n_{cm}} \frac{(-1)^j}{j!}, \quad (4.51)$$

for $0 \leq n_{cm} \leq \delta n$. These weights are normalized ($\sum_{n_{cm}=0}^{\delta n} |a_{n_{cm}}|^2 = 1$), since the application of a particle annihilation operator onto the non-interacting ground state creates a normalized state $|\Psi\rangle$ (for $\delta n \geq 0$).

The weights can be obtained by expanding the exponential that is derived from Eq. (4.46) when setting $\alpha = \beta_- = 0$ and $\beta_+(0) = 1$ (weak coupling):

$$\exp \left[\sum_{q=2}^{\infty} \frac{(e^{-i\omega_0 t} X'/X)^q}{q} + (X'/X) \beta_+(t) \right] \quad (4.52)$$

The prefactor of $(X'/X)^{\delta n} \beta_+^{n_{cm}}$ in this expansion will yield the weight (4.51) of the state that contains exactly n_{cm} excitations of the c.m. mode. In particular, the weight of the $n_{cm} = 0$ -component, which leads to the δ peak, goes to the constant value of $1/e$ in the limit $\delta n \rightarrow \infty$. Thus, there is a non-decaying contribution even at arbitrarily high excitation energies. However, this fact is connected to the assumption of large N under which the present results have been obtained, see the discussion in the following section. The weight of the contribution from $n_{cm} = \delta n - 1$ always vanishes, as may be observed in the plots as well.

For stronger coupling, other δ peaks start to grow both above and below the frequency of the main peak. They are a consequence of the more complicated self-consistent ground state that forms due to the coupling between the c.m. mode and the bath oscillators.

This ground state contains contributions from excited c.m. states and bath states. We can write it down in the following schematic form, where $|j\rangle_B$ denotes a bath state for which the sum of all harmonic oscillator excitations is equal to j :

$$|GS\rangle_{cm+B} = c_{00} |0\rangle_{cm} |0\rangle_B + c_{11} |1\rangle_{cm} |1\rangle_B + c_{20} |2\rangle_{cm} |0\rangle_B + \dots \quad (4.53)$$

Any of the excited states discussed above, containing n_{cm} c.m. excitations (see Eq. (4.50)), may therefore have a finite overlap with this ground state of the coupled system c.m.-bath. Thus, a non-decaying contribution at the frequency $(\delta n - n_{cm})\omega_0$ of the remaining excitation in the *relative* motion survives. This explains the δ peaks at frequencies equal to integer multiples of ω_0 , situated *below* the unperturbed excitation energy of $\delta n\omega_0$. In order to understand the peaks at still *larger* frequencies, we have to take into account that the additional particle (or hole) is introduced into the many-particle ground state that already contains excitations of the c.m. mode, see Eq. (4.53). Therefore, the resulting excited many-particle state $|\Psi\rangle$ will also contain contributions with more than δn excitations of c.m. and relative motion combined, in contrast to the weak-coupling form, Eq. (4.50). Since adding δn excitations to one of the states $|j\rangle_{cm} |0\rangle_r$ that appear in the many-particle ground state may lead to states containing up to $\delta n + j$ excitations in the *relative* motion alone, this explains the appearance of δ peaks at $(\delta n + j)\omega_0$ in the Green's function. For the same reason, the “incoherent background” due to the c.m. mode extends beyond the main frequency of $\delta n\omega_0$.

Finally, it may be noted from the figures that the additional δ peaks appear only at frequencies of the form $(\delta n + 2j)\omega_0$, i.e. they are removed by an *even* multiple of ω_0 from the main peak. Formally, this may be derived from the long-time limit of the exponent (4.46), when $\alpha(t), \beta_{\pm}(t)$ have decayed to zero: Frequencies different from $\omega_0\delta n$ may contribute only because the sum over modes $q \geq 2$ is multiplied by the terms associated with $\alpha(0)$, and these contain *even* powers of X' and X . Physically, the reason is the following: The coupled ground state of c.m. and bath remains symmetric under inversion of the c.m. and oscillator coordinates. Therefore, the sum of c.m. and bath excitations is always even, as indicated in (4.53). When adding δn extra excitations to the many-particle ground state (which is (4.53), multiplied by the ground state of the relative motion), a part of those excitations may go into the c.m. motion, leading to peaks below and above the main frequency. Only if the number of added or subtracted c.m. excitations is even, a nonvanishing overlap with the many-particle ground state may develop, leading to a non-decaying component in the Green's function.

The shape of the broadened peaks in the incoherent background reflects the Fourier-transforms of $\alpha(t), \beta_{\pm}(t)$. All of them are related to the spectral function $W(\omega)$ which is associated to the damped c.m. motion (see Eqs. 4.36, 4.37 and 4.38). In particular, at weak coupling, the Fourier transform of the dominant contribution $\beta_+(t)$ is essentially given by $W(\omega)$, see Eq. (4.37).

For the Ohmic bath, whose power spectrum is given in Eq. (4.6), we have (see (4.8)):

$$\omega_0^2 = \omega_{00}^2 + \frac{2}{\pi} N \gamma \omega_c. \quad (4.54)$$

The resulting spectral function $W(\omega)$ associated to the damped c.m. motion, see Eqs. (4.35) and (A.29), is found to be

$$W(\omega) = \frac{2\gamma N}{\pi} \omega^2 \left[(\omega^2 - \omega_{00}^2 - \frac{\gamma N}{\pi} \omega \ln \frac{\omega_c + \omega}{|\omega_c - \omega|})^2 + (\gamma N \omega)^2 \right]^{-1}. \quad (4.55)$$

This expression holds for $0 \leq \omega < \omega_c$. The denominator becomes 0 at some $\omega > \omega_c$, which yields a δ peak whose weight vanishes for $\gamma N \rightarrow 0$. In order to obtain this peak, one has to replace $2\gamma N \omega$ by an infinitesimal $+0$ for $\omega > \omega_c$ (this would be different for smooth cutoffs, and it does not affect any of our results). The function $W(\omega)$ is displayed in the inset of Fig. 4.3 (where $\omega_c/\omega_{00} = 10$). At low frequencies $\omega \ll \omega_c$ and damping rate $\gamma N \ll \omega_c$, $W(\omega)$ is proportional to the magnitude squared of the susceptibility derived for the linear response of the velocity of the damped c.m. oscillator, with renormalized frequency ω_{00} and damping rate γN :

$$|\chi_{xx}(\omega)|^2 \propto \omega^2 [(\omega^2 - \omega_{00}^2)^2 + (\gamma N \omega)^2]^{-1}. \quad (4.56)$$

In the overdamped case, $\gamma N > 2\omega_{00}$, the zeroes of the denominator occur at purely imaginary frequencies. However, the shape of the function (4.56) shows a qualitative change already at $\gamma N = \sqrt{2}\omega_{00}$, when the curvature at $\omega = 0$ changes sign (in the susceptibility $|\chi_{xx}(\omega)|^2$, the maximum vanishes). This may be observed by comparing the lowest curve in Fig. 4.4, corresponding to $\gamma N/\omega_{00} = 1.6$, to the other curves.

The considerations of the current section apply to the approximate Hamiltonian (4.12) that is good in the limit $N \rightarrow \infty$ of large particle number, and which has been amenable to bosonization. However, the qualitative arguments concerning the contributions of c.m. and relative motion remain valid for finite N as well. This is the topic of the next section.

4.6 Finite particle number: Center-of-mass motion in excited Fock states

In this section we want to analyze in more detail the splitting into c.m. and relative motion for arbitrary *finite* N . We will also point out that the weight of the “coherent” component in the Green’s function (with no c.m. excitation) decays when moving towards higher excitation energies, on a scale set by the number N of particles. This explains why this weight even saturates at a constant value for excited states arbitrarily far above the Fermi surface in the limit $N \rightarrow \infty$. It is this limit that has been solved by bosonization in the preceding sections, and the results of this section constitute a kind of check on that procedure. However, we will not actually evaluate Green’s functions for the finite N case, which is still much more difficult.

For simplicity, we will set $m = \omega_0 = 1$ throughout this section, without loss of generality. Then the coordinates and momenta of the individual particles are related to the harmonic oscillator raising and lowering operators by

$$\hat{x}_j = \frac{1}{\sqrt{2}}(\hat{a}_j + \hat{a}_j^\dagger), \quad \hat{p}_j = \frac{-i}{\sqrt{2}}(\hat{a}_j - \hat{a}_j^\dagger), \quad (4.57)$$

where it is understood that \hat{a}_j acts only on the coordinate of particle j . The center-of-mass motion is described by

$$\hat{X} = \frac{1}{N} \sum_{j=1}^N \hat{x}_j, \quad \hat{P} = \sum_{j=1}^N \hat{p}_j, \quad (4.58)$$

such that we obtain for the operator that lowers the excitation of the c.m. harmonic oscillator by one:

$$\hat{A} = \sqrt{\frac{N}{2}}(\hat{X} + i\frac{\hat{P}}{N}) = \frac{1}{\sqrt{N}} \sum_{j=1}^N \hat{a}_j. \quad (4.59)$$

Here we have used that the total mass is $M = Nm = N$.

Let us consider an N -particle Fock state $|\Psi_{N,\delta n}\rangle$ consisting of the Fermi sea filled up to (and including) level $n_F - 1 = N - 2$ and an additional single particle that has been placed into the excited level at $n_F + \delta n$. It is our goal to find the probability P_n of having n excitations in the c.m. mode, given this many-particle state. In particular, the probability of having 0 excitations will be the weight of the “coherent component” that does not decay in spite of coupling to the bath. This holds quantitatively in the weak-coupling limit, where we may neglect the change in the eigenstates of the c.m. mode, see the previous discussion. For arbitrary coupling, it is still the correct qualitative picture (compare the results above).

First, we rewrite \hat{A} in second quantization:

$$\hat{A} = \frac{1}{\sqrt{N}} \sum_{k=0}^{\infty} \sqrt{k+1} \hat{c}_k^\dagger \hat{c}_{k+1}. \quad (4.60)$$

Using this, it is straightforward to check that

$$\langle \Psi_{N,\delta n} | \hat{A}^{\dagger j} \hat{A}^j | \Psi_{N,\delta n} \rangle = \frac{\delta n + n_F}{N} \cdots \frac{\delta n + n_F - j + 1}{N}, \quad (4.61)$$

for $j \leq \delta n$, otherwise this is 0. On the other hand, if we think of $|\Psi_{N,\delta n}\rangle$ as being written in a basis that splits relative and c.m. motion (compare Eq. (4.50)) and take into account the usual matrix elements of a harmonic oscillator lowering operator, we obtain for the same expectation value (with P_n the occupation probabilities for the different c.m. states):

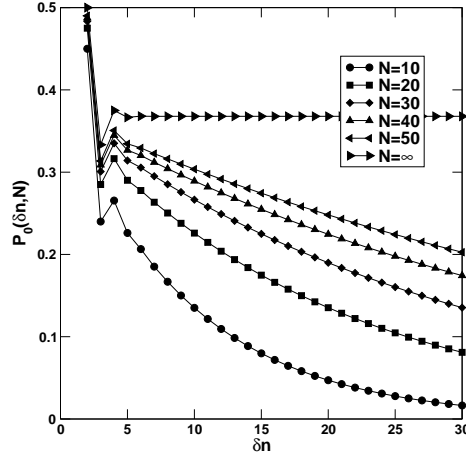


Figure 4.5: Weight of the center-of-mass ground state as a function of excitation δn , for different particle numbers N , including the bosonization result from Eq. (4.51) (“ $N = \infty$ ”).

$$\sum_{n=j}^{\infty} P_n n(n-1) \cdot \dots \cdot (n-j+1). \quad (4.62)$$

Now we make use of the fact that the total number of excitations in the c.m. mode is limited by δn , i.e. $P_n = 0$ for $n > \delta n$. Therefore, it is possible to start at $j = \delta n$, equate (4.61) to (4.62), solve for $P_{\delta n}$, and then proceed iteratively all the way down to P_0 . In each step, only the probabilities that have been calculated before appear in addition to the unknown P_j . We can write down the set of equations very transparently by introducing the abbreviation

$$p_l = (\delta n - l)! \frac{(N-1)!}{(\delta n + N - 1)!} N^{\delta n} P_{\delta n - l}. \quad (4.63)$$

Then we have (from equating (4.61) to (4.62)) the recursive relation:

$$p_l = \frac{N^{l-1}}{(N+l-1) \cdot \dots \cdot (N+1)} - \sum_{k=1}^l \frac{p_{l-k}}{k!}. \quad (4.64)$$

The solution starts with $p_0 = 1$. Note that we always get $p_1 = 0$ (for any N), corresponding to $P_{\delta n-1} = 0$: This has been observed already in the context of the bosonization solution (see previous section). It is also remarkable that the equation for p_l does not depend on δn . Therefore, we can solve the problem at once for arbitrary δn (which then only enters in P_n via Eq. (4.63)).

After solving these equations, it is found that the weight of the c.m. ground state, $P_0 = \frac{(\delta n + N - 1)!}{(N-1)!} N^{-\delta n} p_{\delta n}$, decays as a function of excitation energy δn (for large δn), on a scale set by N , see Fig. 4.5.

Finally, we remark that the general structure of the exact eigenfunctions of our problem (defined by the original Hamiltonian, Eq. (4.1)) remains identical to that found in the limit $N \rightarrow \infty$, using bosonization. For arbitrary system-bath coupling, the eigenstates of the full system will be of the form

$$|\Psi^{SB}\rangle = |\Phi^{CM-B}\rangle \otimes |\psi^{rel}\rangle, \quad (4.65)$$

where “SB” refers to the full Hilbert space of fermions coupled to a bath, while $|\Phi^{CM-B}\rangle$ is a new eigenstate of the coupled system c.m./bath and $|\psi^{rel}\rangle$ is an *unaltered*, antisymmetric eigenstate of the relative motion. However, the evaluation of quantities like Green’s functions or the reduced density matrix, starting from this expression, becomes very cumbersome, which is the reason why we have restricted most of the discussion to the bosonization solution.

4.7 Two-particle Green’s function: decay of populations and dephasing

While the single-particle Green’s function reveals how fast an electron is scattered out of an initial state, we have to turn to the two-particle Green’s function in order to learn about the time-evolution of the reduced single particle density matrix. For our purposes, we will be interested in the following two-particle Green’s function of fermions in the damped oscillator:

$$\langle \hat{c}_n(0) \hat{c}_{l'}^\dagger(t) \hat{c}_l(t) \hat{c}_{n'}^\dagger(0) \rangle. \quad (4.66)$$

Without coupling to the bath, we could apply Wick’s theorem to obtain:

$$\begin{aligned} \langle \hat{c}_n(0) \hat{c}_{l'}^\dagger(t) \hat{c}_l(t) \hat{c}_{n'}^\dagger(0) \rangle = \\ \delta_{nl'} \delta_{ln'} (1 - \langle \hat{n}_n \rangle) (1 - \langle \hat{n}_{n'} \rangle) e^{i\omega_0(n-n')t} + \\ \delta_{nn'} \delta_{ll'} (1 - \langle \hat{n}_n \rangle) \langle \hat{n}_l \rangle, \end{aligned} \quad (4.67)$$

If the bath damps the motion of the fermions, we may rewrite (4.66) in terms of the auxiliary fermion operators $\hat{\psi}(x)$ defined in (4.14):

$$\begin{aligned} \langle \hat{c}_n(0) \hat{c}_{l'}^\dagger(t) \hat{c}_l(t) \hat{c}_{n'}^\dagger(0) \rangle = \\ \frac{1}{(2\pi)^2} \int_0^{2\pi} dx dx' dy dy' e^{i(l'x' + n'y' - lx - ny)} \times \\ \langle \hat{\psi}(y, 0) \hat{\psi}^\dagger(x', t) \hat{\psi}(x, t) \hat{\psi}^\dagger(y', 0) \rangle \end{aligned} \quad (4.68)$$

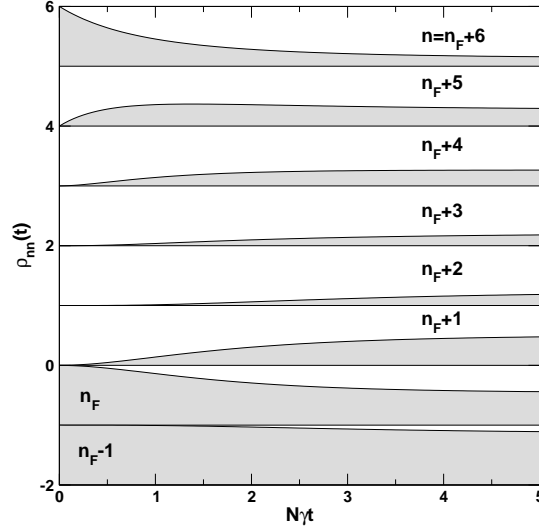


Figure 4.6: Time-evolution of the populations $\rho_{nn}(t)$ (see Eq. (4.69)) for an electron placed in an initial state $\tilde{n} = n_F + 6$ above the Fermi sea (weak-coupling result, see text). Different curves have been displaced vertically for clarity.

Starting from the representation of $\hat{\psi}$ in terms of boson operators $\hat{\phi}$, Eq. (4.16), this may be evaluated using the same methods as in Sections 4.3 and 4.4. In Appendix A.7, it is shown how the two-particle Green's function is obtained via a series expansion, similar to the single-particle Green's function.

Using the result for the two-particle Green's function given in Appendix A.7 (Eqs. (A.38), (A.39), and (A.40)), we may answer questions like the following: If we introduce an extra single particle in some level \tilde{n} above the Fermi sea, how does it decay towards lower-lying levels, by emitting some of its energy into the bath? Of course, we expect the Pauli principle to play an important role, which makes this model particularly interesting.

More precisely, we look at the time-evolution of the populations

$$\rho_{nn}(t) = \left\langle \hat{c}_{\tilde{n}} \hat{c}_n^\dagger(t) \hat{c}_n(t) \hat{c}_{\tilde{n}}^\dagger \right\rangle, \quad (4.69)$$

where the two outermost operators create the desired state at time 0, while the two operators in the middle test for the population. We note that, in principle, the newly created state may have norm less than 1, if the level \tilde{n} happens to be partially occupied already in the ground state on which the creation operator $\hat{c}_{\tilde{n}}^\dagger$ acts. In that case, it would be necessary to divide (4.69) by the norm, $\left\langle \hat{c}_{\tilde{n}} \hat{c}_{\tilde{n}}^\dagger \right\rangle$.

However, we will restrict the evaluation to the weak-coupling case, where the states above n_F are empty at $T = 0$ and where we set $\alpha(t) = \beta_-(t) = 0$, $\beta_+(0) = 1$ and keep only the (slowly decaying) $\beta_+(t)$, which is approximated by $\beta_+(t) \approx e^{-i\omega'_0 t - N\gamma t/2}$. Here ω'_0 is shifted with respect to the frequency ω_0 , being equal to ω_{00} in the limit $\omega_c \gg \omega_0$ (see

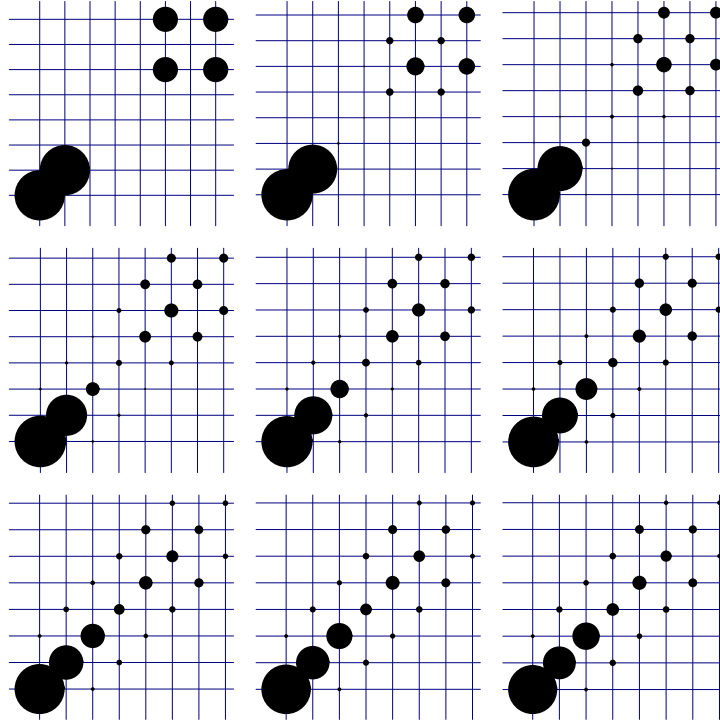


Figure 4.7: Time-evolution of the single-particle density matrix $\rho_{nn'}(t)$ (see Eq. (4.70)) for fermions in a damped oscillator, after a single particle has been placed in a superposition of states above the Fermi sea. Time points $N\gamma t = 0, 0.5, 1, \dots, 4$ from top left to bottom right (increasing along the rows). Levels $n, n' = n_F - 1, n_F, \dots, n_F + 6$ are indicated by grid lines. The radius of each dot gives $|\rho_{nn'}(t)|$ (which starts at 1 for the two occupied states in the lower left corner). The final panels essentially show the long-time limit, indicating incomplete decay.

Eq. (4.54) and (4.55) for the special case of the Ohmic bath). In general the difference between ω_0 and ω'_0 can be of any sign, depending on the details of the bath spectrum. This frequency shift between the c.m. mode and all the other boson modes may lead to beating oscillations that are visible in the time-evolution of the populations or the density matrix. In Figs. 4.6 and 4.7, however, we have assumed $\omega'_0 = \omega_0$ (e.g. the bath spectrum is taken to be symmetric around the transition frequency but the decay rate is set to be the same as that obtained for the Ohmic bath).

Although in principle the expression (A.38) permits evaluation of the two-particle Green's function at arbitrary coupling strength, this task has proven to be computationally much more difficult than the analogous calculation for the single-particle Green's function, due to the larger number of terms generated in the power series. The weak-coupling results for $\rho_{nn}(t)$ are shown in Fig. 4.6.

We note that, contrary to naive expectation, the particle does not decay all the way down to the lowest unoccupied state $n_F + 1$. Rather, in the long-time limit (which is already reached at $N\gamma t \approx 5$ to a good approximation), the extra particle is distributed over the range of excited levels above the Fermi surface, up to the initial level \tilde{n} . Again, this is because only the c.m. mode couples to the bath, such that, even at $T = 0$, a fraction of the initial excitation energy remains in the system. Moreover, we see that the population of the highest occupied states in the Fermi sea decreases. The fermions in these states become partly excited at the expense of the extra particle, due to the effective interaction mediated by the bath.

Another application of the two-particle Green's function (A.30) consists in looking at the decay of a superposition of states. We imagine that, at time 0, a particle is placed in an equally-weighted superposition of two levels n_1 and n_2 above the Fermi surface. This will introduce off-diagonal contributions in the single-particle density matrix of the fermions. The subsequent relaxation will suppress the coherence (i.e. the off-diagonal elements) and transfer population to the lower levels. In Fig. 4.7, we have plotted the time-evolution of the density matrix defined by

$$\rho_{nn'}(t) = \frac{1}{2} \left\langle (\hat{c}_{n_1} + \hat{c}_{n_2}) \hat{c}_{n'}^\dagger(t) \hat{c}_n(t) (\hat{c}_{n_1}^\dagger + \hat{c}_{n_2}^\dagger) \right\rangle. \quad (4.70)$$

Again, we have evaluated only the weak-coupling case, such that no additional normalization factor is necessary (for $n_1, n_2 > n_F$).

Apart from the features already mentioned above, we observe the decay of the off-diagonal elements (i.e. dephasing) to be incomplete. A part of the coherence survives in the relative motion which is unaffected by the bath. If a slight anharmonicity were introduced in the potential, such that c.m. and relative motion are no longer independent, we would expect to see the same behaviour at short to intermediate times. Only in the long-time limit, the fermion system would relax fully to the $N + 1$ -particle Fermi sea ground state.

4.8 Conclusions

We have analyzed a model system of fermions in a harmonic oscillator, that are subject to a fluctuating force deriving from a linear bath of oscillators. The force couples to the center-of-mass motion of the fermions. This is a generalization of a single particle in a damped harmonic oscillator, and it is, in principle, exactly solvable. However, here we have analyzed the limit of large particle numbers, using the method of bosonization, i.e. we have considered particle-hole excitations around the Fermi surface. One of the boson modes corresponds to the center-of-mass motion, experiencing dephasing and damping, while the others belong to the relative motion which forms a kind of “decoherence-free subspace”. We have derived exact (for $N \rightarrow \infty$) analytic expressions for Green’s functions, that can be obtained from the coefficients of a power series expansion. These have been evaluated with the help of a symbolic computer algebra program. The single-particle Green’s function has been discussed in detail, showing the smearing of the Fermi surface, the effect of Pauli blocking, the dependence of level shapes on the bath spectrum and the coupling strength, as well as the appearance of coherent peaks, due to the relative motion. Based on the expression for the two-particle Green’s function, we have analyzed the decay of an excited state created by adding one particle above the Fermi surface, where one can observe the “heating” around the Fermi surface (due to the effective interaction between particles), as well as the incomplete decay of the excited particle. In addition, we have discussed the time-evolution of the single-particle density matrix for an extra particle that has been added in a coherent superposition of excited states.

Chapter 5

The role of friction in the description of low-temperature dephasing

5.1 Introduction

The Feynman-Vernon influence functional [Feynman63, 65] plays a prominent role in discussions of dephasing that aim to go beyond a simple master equation approach. In principle, the influence functional takes into account every effect of the environment (the “bath”) on the system under consideration. This includes heating, dephasing, friction and renormalization effects (changing the external potential or the effective mass of a particle). Its popularity arises not only from the fact that it constitutes an exact approach, but also from the direct physical meaning which it acquires in some situations. In particular, this holds for typical interference experiments, where two wave packets describing a single particle follow two different trajectories in order to be recombined later on. For such a case, the influence functional is equal to the overlap between the two different bath states which result due to the particle moving along either one of the semiclassical trajectories. If the bath can distinguish between the two paths, it acts as a which-way detector, and the diminished magnitude of the overlap directly gives the ensuing decrease of the visibility of the interference pattern. Writing the overlap in the form of an exponential, $\exp(iS_R - S_I)$, one can obviously conclude that only the imaginary part S_I of the “influence action” is responsible for this decrease and, therefore, S_I alone describes dephasing *in such a situation*. Furthermore, if the system is subject to a fluctuating external *classical* field, only S_I remains, while S_R vanishes identically. This is because S_I is due to the fluctuations of the bath, while S_R stems from the back-action of the bath onto the system (including friction effects), which is absent for an external noise field. The approach of evaluating S_I along semiclassical trajectories has been successfully applied to the calculation of dephasing rates in many situations [Chakravarty86, Stern90, Cohen97].

However, near the ground state of a system, an analysis along these lines is likely to fail. Qualitatively, this may already be deduced from the fact that dropping S_R means replacing the environment by an artificial fluctuating classical field whose correlation

function includes the zero-point fluctuations of the original quantum bath. Therefore, even at zero temperature, this fluctuating field will, in general, heat the system, which directly leads to dephasing. The role of S_R is to counteract this effect. In this chapter, it is our aim to display explicitly, in a detailed manner, the necessity of keeping the real part S_R of the influence action in discussions of dephasing and decay near the ground state of a system.

This issue derives its importance partly from the fact that the evaluation of S_I along semiclassical trajectories has proven to be an efficient way of extracting dephasing rates in the problem of weak localization in the limit of high temperatures [Chakravarty86, Stern90], when zero-point fluctuations of the bath may be omitted. In contrast, at low temperatures, a single-particle semiclassical calculation may become invalid, since it neglects the Pauli principle which is known to play an important role for the inelastic scattering of electrons and is not included in the Feynman-Vernon influence functional. However, recently an extension of the influence functional to the case of a many-fermion system has been derived, using an exact procedure [Golubev99, Golubev00, Zaikin00] and including the Pauli principle. This permitted a discussion of dephasing in a disordered metal even for the case of low temperatures. Following the general strategy of earlier works [Chakravarty86] dealing with the high-temperature case, the dephasing rate was deduced from S_I in a semiclassical calculation and found to be finite even at zero temperature. Since the “orthodox” theory [Altshuler82] had predicted a vanishing rate in the limit $T \rightarrow 0$, the new results prompted considerable criticism [Aleiner99, Vavilov99, Cohen99, Kirkpatrick02], which mostly emphasized technical aspects of impurity averaging or used perturbation theory to arrive at different conclusions. We will try to clarify some essential aspects of the roles of S_R and S_I , using physically much more transparent exactly solvable models.

We have already emphasized in the introduction (Chapter 1) that “zero-temperature dephasing” as such is perfectly possible: If one prepares a system in any superposition of excited states and couples it to a bath, it will, in general, decay towards its ground state by spontaneous emission of energy into the bath (at $T = 0$). This will destroy any coherent superposition, thus leading to dephasing. Considerations of this kind are relevant (for example) in quantum-information processing, where one necessarily deals with nonequilibrium situations involving excited qubit states of finite energy [Shnirman02]. The situation is different for the weak-localization problem (and similar transport interference effects): There, one is interested in the zero-frequency limit of the system’s linear response, which depends on the coherence properties of arbitrarily low-lying excited states. It is the subtleties associated with a path-integral description of these situations which we want to address here.

After a brief review of the influence functional and its meaning in semiclassical situations (Sec. 5.2), we will rewrite the expressions for S_I and the Golden Rule decay rate, in order to compare the two (Sec. 5.3). In doing so, we will closely follow the analysis of Cohen and Imry [Cohen97, 99]. Then, we will show how and why the effects of S_R and S_I may compensate each other in the derivation of a decay rate starting from the path

integral expression for the time-evolution of the density matrix (Sec. 5.4), even though they cannot cancel each other in the influence action. There, it may be observed that drawing conclusions about decay directly from the exponent $iS_R - S_I$ of the influence functional is usually not possible. The crucial cancellation takes place at a later stage of the calculation, after proper integration over the fluctuations around the classical paths and after averaging over the initial state. In order to prove that this compensation takes place not only in lowest order perturbation theory, we will then specialize to exactly solvable linear dissipative systems, i.e. the damped harmonic oscillator (Sec. 5.5) and the free particle (Sec. 5.6). We will also point out that there is an important difference between the oscillator and the free particle: Dropping S_R has a much more drastic effect on the former, leading to an artificial finite decay rate of the ground state at zero temperature. However, in order to discuss the importance of S_R for the calculation of dephasing rates (involving decay of excited states), we have to extend our analysis to nonlinear models (Sec. 5.7). We will explain in a more qualitative fashion why the essential insights gained from the exactly solvable models should remain valid both for the nonlinear models as well as for systems of degenerate fermions.

5.2 The influence functional and dephasing in simple situations

We are interested in the time-evolution of the reduced density matrix of a system with coordinate q which is coupled to some environment (the bath). If system and bath had been uncoupled prior to $t = 0$ (factorized initial conditions), then the density matrix at a later time t is linearly related to that at time 0:

$$\rho(q_t^>, q_t^<, t) = \int dq_0^> dq_0^< J(q_t^>, q_t^< | q_0^>, q_0^<; t) \rho(q_0^>, q_0^<, 0). \quad (5.1)$$

The propagator J on the right-hand-side of this equation is given by

$$J = \iint Dq^> Dq^< \exp[i(S_0^> - S_0^<)] \exp[iS_R - S_I]. \quad (5.2)$$

Here we have introduced an abbreviated notation: The path integral extends over all “forward” paths $q^>(\cdot)$ running from the given value of $q_0^>$ to $q_t^>$, likewise for the “backward” paths $q^<(\cdot)$. The value of the action of the uncoupled system, evaluated along $q^{>(<)}(\cdot)$, is denoted by $S_0^{>(<)}$. The second exponential in Eq. (5.2) is the Feynman-Vernon influence functional [Feynman63, Feynman65]. Both S_R and S_I are real-valued functionals that depend on both paths simultaneously. The influence functional is the overlap of bath states which have time-evolved out of the initial bath state χ_0 under the action of either $q^>(\cdot)$ or $q^<(\cdot)$:

$$e^{iS_R - S_I} \equiv \langle \chi[q^<(\cdot)] | \chi[q^>(\cdot)] \rangle. \quad (5.3)$$

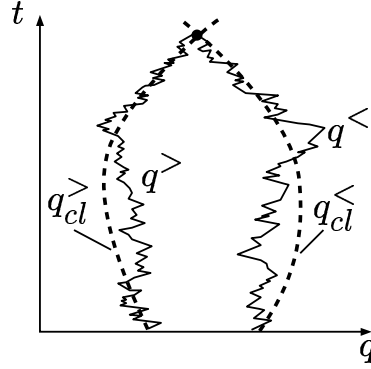


Figure 5.1: A sketch of the paths involved in the path-integral description of a simple interference situation (see text).

At zero temperature, the state χ_0 is the ground state of the unperturbed bath, while at finite temperatures an additional thermal average over χ_0 has to be performed. From this representation, it follows [Feynman63, Feynman65] that S_R changes sign on interchanging $q^>$ and $q^<$ while S_I always remains nonnegative - the magnitude of the overlap can only be decreased compared with its initial value of one.

A brief remark on the use of factorized initial conditions is in order: Although they lead to certain artificial transient effects after switching on the interaction (compare [Hakim85, Schramm87]), they are not at all related to the kind of long-time “heating” behaviour which is observed in the examples to be discussed below when S_R is neglected.

The meaning of S_R and S_I becomes particularly transparent for an interference setup, where two wave packets $\Psi_>$ and $\Psi_<$ travel along two different paths $q_{cl}^>(\cdot)$ and $q_{cl}^<(\cdot)$. We want to assume a situation which can be described semiclassically, i.e. the wave-length is supposed to be much smaller than the size of a wave packet and this again is much smaller than the typical separation between the paths and the typical dimensions over which the external potential changes. Then, it suffices to evaluate S_R and S_I just for the combination of these two paths, since the fluctuations around them are comparatively unimportant (see Fig. 5.1). The environment will affect the interference pattern on the screen mainly by changing the interference term [Stern90] (compare the introduction 1.2):

$$\rho(q, q, t) \approx |\Psi_>(q, t)|^2 + |\Psi_<(q, t)|^2 + 2 \operatorname{Re} [\Psi_>(q, t) \Psi_<^*(q, t) e^{iS_R - S_I}] . \quad (5.4)$$

In this equation, $\Psi_{>(<)}(q, t)$ are assumed to represent the unperturbed time-evolution of the wave packets. To a first approximation, $S_{R,I}$ do not enter the “classical” terms in the first line of Eq. (5.4), since $S_{R,I}[q_{cl}^>, q_{cl}^>] = 0$. Deviations from this first approximation stem from the integration over fluctuations away from $q_{cl}^{>(<)}$ and describe, for example, mass- and potential renormalization as well as slowing-down of the wave packet due

to friction. Obviously, $S_I \equiv S_I[q_{cl}^>, q_{cl}^<]$ determines directly the decrease in visibility of the interference pattern while $S_R \equiv S_R[q_{cl}^>, q_{cl}^<]$ only gives a phase-shift. Averaging the interference pattern over different configurations of the external potential (appropriate for impurity averaging in mesoscopic samples) may further decrease the visibility. However, if the two paths are time-reversed copies of each other (as is the case in discussions of weak-localization [Altshuler82, Chakravarty86, Stern90]), the phase difference between $\Psi_>$ and $\Psi_<$ vanishes in a time-reversal invariant situation, so that the impurity-average over the corresponding phase factor does not lead to a suppression in the situation without the bath. If S_R is kept (which was not done in [Altshuler82, Chakravarty86, Stern90], since they considered classical noise), then the average over $\exp(iS_R)$ will, in general, decrease further the magnitude of the interference term. Note that the impurity average of S_R itself (which corresponds to a properly weighted average over all possible pairs of trajectories) vanishes *in general*, simply because $S_R[q^>, q^<] = -S_R[q^<, q^>]$. In any case, given the simple physical picture presented here, one would not expect S_I and S_R to be able to cancel each other's effects, since they represent, respectively, the real and imaginary part of an exponent.

For the special case of a force \hat{F} deriving from a bath of harmonic oscillators (linear bath), with vanishing average $\langle \hat{F} \rangle = 0$ and a linear interaction $\hat{V} = -\hat{q}\hat{F}$, we have:

$$S_I = \int_0^t dt_1 \int_0^{t_1} dt_2 (q_1^> - q_1^<) \text{Re} \langle \hat{F}_1 \hat{F}_2 \rangle (q_2^> - q_2^<) \quad (5.5)$$

$$S_R = - \int_0^t dt_1 \int_0^{t_1} dt_2 (q_1^> - q_1^<) \text{Im} \langle \hat{F}_1 \hat{F}_2 \rangle (q_2^> + q_2^<) \quad (5.6)$$

Here we have used the notation $q_1^> \equiv q^>(t_1)$. The angular brackets denote averaging over the equilibrium state of the unperturbed bath. S_I only depends on the symmetrized part of the bath correlator $\text{Re} \langle \hat{F}(\tau) \hat{F}(0) \rangle = \langle \{ \hat{F}(\tau), \hat{F}(0) \} \rangle / 2$, which becomes the classical correlator $\langle F(\tau) F(0) \rangle$ for the case of a classical Gaussian random process. In the latter case, S_R vanishes and the influence functional $\exp(-S_I)$ is simply the classical average of the phase factor

$$\exp \left[i \int_0^t (q^<(\tau) - q^>(\tau)) F(\tau) d\tau \right]. \quad (5.7)$$

If one drops S_R in a dephasing calculation (noting that it does not enter dephasing in semiclassical situations such as those that can be described by Eq. (5.4)), one effectively replaces the quantum bath by a classical fluctuating force whose correlator is determined by the symmetrized part of the quantum correlator. This contains the zero-point fluctuations, since

$$\begin{aligned} \langle \{ \hat{Q}(\tau), \hat{Q}(0) \} \rangle &\propto \\ (2n(\omega) + 1) \cos(\omega\tau) &= \coth(\omega/2T) \cos(\omega\tau) \end{aligned} \quad (5.8)$$

for the coordinate \hat{Q} of a single bath oscillator of frequency ω , with $n(\omega)$ being the Bose distribution function that vanishes at $T = 0$.

Although replacing the quantum bath by a classical noise force seems to be a drastic step, it can lead to correct predictions for the dephasing rate in semiclassical situations such as the one discussed above, even at zero temperature. It is instructive to observe how this comes about in an exactly solvable model. A particularly simple situation is the one analyzed by Caldeira and Leggett [Caldeira85] (see also [Loss91]). They considered a damped quantum harmonic oscillator, where the initial state consisted of a superposition of Gaussian wavepackets, one centered at the origin, the other at a distance z . In the course of time, the displaced wavepacket oscillates back and forth in the oscillator potential well. Whenever the packets overlap, an interference pattern results (due to the difference in the respective momenta). The environment leads both to damping and dephasing, where the latter typically proceeds at a much faster rate. For our purposes, we are interested in the limit of small damping, where, to a first approximation, the center-of-mass motion of the wave packets is not appreciably altered by friction in the period of the oscillation. In this case, it turns out that, indeed, the result predicted by the approximation Eq. (5.4) for the attenuation of the interference pattern is correct, including the effect of the zero-point fluctuations. This can be seen in [Caldeira85] by taking the limit of weak damping ($\gamma \rightarrow 0$, $\omega \rightarrow \omega_R$) in their exact result for the exponent of the attenuation factor (see Eq. (2.13) of [Caldeira85]) and comparing this to S_I (see Eq. (5.5)), which is to be evaluated for the pair of classical paths followed by the two wave packets, $q_{cl}^>(t) = z \cos(\omega t)$ and $q_{cl}^<(t) \equiv 0$. In terms of the quantity C_{00} listed in Appendix A.8, both results may be obtained by multiplying C_{00} by $\sin(\tilde{\omega}t)^2$ and setting $\gamma = 0$, $\tilde{\omega} = \omega$. In addition, in order to obtain $S_I[q_{cl}^>, q_{cl}^<]$, the factors $\sin(\omega(t-t_1))$ and $\sin(\omega(t-t_2))$ must be replaced by $\cos(\omega t_1)$ and $\cos(\omega t_2)$. The results obviously coincide for the points in time when the wave-packets meet ($\omega t = \pi/2 + n\pi$). We emphasize that the correspondence to the semiclassical result holds only for a situation far away from the ground state of the system, where at least one of the wave packets is in a superposition of highly excited oscillator states (which is the case considered by [Caldeira85]).

At zero bath temperature, the dephasing is purely due to spontaneous emission, as pointed out in the discussion of [Caldeira85]. Energy is transferred from the oscillating wave-packet into the bath and the system relaxes towards lower-energy states. The dephasing rate is proportional to the total rate Γ_{out} at which the system leaves a given energy level [Caldeira85]. Of course, this rate may be obtained using the Golden Rule (i.e. a master equation description) only for weak coupling, but the qualitative picture seems to be general [Caldeira85]. In the correct description of the physical situation considered here, the rate Γ_{out} is given entirely by the rate of spontaneous emission, Γ_{sp}^{em} . However, if S_R is neglected, then S_I describes a classical noise force (equivalent to the zero-point fluctuations of the bath at $T = 0$) and there will be both induced emission and absorption, proceeding at equal rates $\Gamma_{ind}^{em} = \Gamma_{ind}^{abs}$. Therefore, the system is also excited by the bath in that approximation. Nevertheless, we have pointed out above that the total dephasing rate comes out right. The reason is the following: The rate Γ_{out} is the same in both cases,

because the rate of spontaneous emission in the correct description is exactly twice that of induced emission in the approximation:

$$\Gamma_{out} = \Gamma_{sp}^{em} \equiv \Gamma_{ind}^{em} + \Gamma_{ind}^{abs}. \quad (5.9)$$

At this point, it is easy to see the physical reason why such an approximation may fail near the ground state of the system. Then, the transitions downwards in energy may be blocked, which completely suppresses Γ_{sp}^{em} , but not Γ_{ind}^{abs} . We will make this argument more precise in the following sections.

5.3 Decay rates from S_I and Golden Rule: Dependence on the spectra of bath and system motion

The growth of S_I with time depends on the spectral density of the bath fluctuations at frequencies which appear in the system's motion. Formally, this can be seen by introducing the spectrum of the system motion related to the given pair of paths $q^{>(<)}$ (following the ideas of [Cohen97, 99]):

$$\begin{aligned} P(\omega, s) \equiv & \frac{1}{2\pi} \int_{-\infty}^{+\infty} d\tau e^{i\omega\tau} (q^>(s + \frac{\tau}{2}) - q^<(s + \frac{\tau}{2})) \\ & \times (q^>(s - \frac{\tau}{2}) - q^<(s - \frac{\tau}{2})) \end{aligned} \quad (5.10)$$

Here, $s \equiv (t_1 + t_2)/2$ and $\tau \equiv t_1 - t_2$ are sum and difference times. Therefore, P is the Fourier transform with respect to τ of the q -dependent terms in S_I (Eq. (5.5)). We take $q^{>(<)}(t')$ to be zero whenever t' falls outside the range $[0, t]$.

Furthermore, we define $\langle FF \rangle_\omega$ to be the Fourier-transform of the symmetrized correlator of \hat{F} ,

$$\langle FF \rangle_\omega \equiv \frac{1}{4\pi} \int_{-\infty}^{+\infty} d\tau e^{i\omega\tau} \left\langle \left\{ \hat{F}(\tau), \hat{F}(0) \right\} \right\rangle, \quad (5.11)$$

so it is real and symmetric in frequency. The same holds for the system spectrum $P(\omega, s)$.

Using this, S_I can be expressed in the following way:

$$S_I = \pi \int_0^t ds \int_{-\infty}^{+\infty} d\omega \langle FF \rangle_\omega P(-\omega, s). \quad (5.12)$$

If the dependence of P on s is not essential, then S_I grows linearly with time t , at a rate given by the “overlap of bath and system spectra”. Similar expressions can be derived for a spatially inhomogeneous fluctuating force [Cohen97, 99], leading to an additional k -dependence.

Applying this kind of reasoning to a *single* electron moving in a dirty metal [Cohen97], the system motion is found to contain frequencies up to (at least) $1/\tau_{el}$, such that the growth of S_I with time depends on the bath-spectrum up to this cutoff, including the zero-point fluctuations of the corresponding high-frequency bath modes (which become important at low temperatures).

As explained above (Sec. 5.2), the description of dephasing in terms of S_I alone may be trusted in a semiclassical situation, where the electron is in a highly excited state. This holds even at zero temperature, when the qualitative physical picture is essentially the same as in the model of oscillating wave packets due to Caldeira and Leggett, discussed above: Dephasing is due to spontaneous emission of energy into the bath. The contribution of frequencies up to $1/\tau_{el}$ in this situation then implies that the spontaneous emission (and the resulting dephasing) is facilitated by the impurity scattering. The physics behind this is well-known in another context: In quantum electrodynamics, the emitted radiation would be called “bremsstrahlung”, since it is the scattering off an external potential that induces the electron to emit radiation.

On the other hand, one can express in a similar manner decay rates from a simple Golden Rule calculation [Cohen99]. For the decay of an initial state $|i\rangle$, we have

$$\Gamma_i = 2\pi \int d\omega \left\langle \hat{F}\hat{F} \right\rangle_\omega \langle \hat{q}\hat{q} \rangle_{-\omega}^{(i)}. \quad (5.13)$$

Here $\left\langle \hat{F}\hat{F} \right\rangle_\omega$ and $\langle \hat{q}\hat{q} \rangle_{-\omega}^{(i)}$ are the Fourier transforms of the *unsymmetrized* correlators of \hat{F} and \hat{q} , taken in the equilibrium state of the bath or the initial state of the system, respectively:

$$\begin{aligned} \left\langle \hat{F}\hat{F} \right\rangle_\omega &\equiv \frac{1}{2\pi} \int d\tau e^{i\omega\tau} \left\langle \hat{F}(\tau)\hat{F}(0) \right\rangle \\ \langle \hat{q}\hat{q} \rangle_\omega^{(i)} &\equiv \frac{1}{2\pi} \int d\tau e^{i\omega\tau} \langle i | \hat{q}(\tau)\hat{q}(0) | i \rangle \end{aligned} \quad (5.14)$$

The important point to notice is that, near the ground state of the system, the quantum correlator $\langle \hat{q}\hat{q} \rangle_\omega^{(i)}$ is very asymmetric in frequency space, as the system can mostly be excited only ($\omega > 0$). At low temperatures, the same holds for the bath. Thus, the decay rate (5.13), containing the product of correlators evaluated at ω and $-\omega$, is very much suppressed below the value that it would acquire if either the bath-correlator or the system-correlator were symmetrized (becoming symmetric both in time and frequency). Since dropping S_R is equivalent to symmetrizing the bath correlator and, furthermore, semiclassical calculations give a symmetric spectrum $P(\omega, s)$ of the system motion as well, it becomes clear why there are situations when the decay rate, as deduced from S_I , is finite at low temperatures, while the Golden-rule decay rate vanishes. The question then arises whether any procedure that amounts to symmetrization of the correlators, thus leading to drastically wrong results for Golden Rule decay rates at zero temperature, may

be justified to discuss dephasing using a path-integral approach. Observations such as this have led Cohen and Imry to conclude that, in their semiclassical analysis of electron dephasing inside a metal [Cohen99], the contribution of the bath's zero-point fluctuations to the dephasing rate should be dropped. Their argument was not a mathematical proof, but rather drawn from physical intuition and analogies, and similar to what had been done in earlier calculations [Altshuler82, Chakravarty86]. In the following sections, we try to elucidate the importance of S_R in descriptions of dephasing and decay near the ground state of a system, demonstrating exactly how a cancellation between S_R and S_I may arise.

5.4 Cancellation of S_R and S_I in lowest-order perturbation theory

We consider a system which is in its ground state at $t = 0$ before being coupled to a linear bath. From the Golden Rule, we expect there to be no finite decay-rate for the ground state at zero-temperature. It is well-known [Feynman65] how to derive a master equation from the influence functional, by expanding it to lowest order in the exponent, $iS_R - S_I$. We display that calculation here in order to point out where and how S_R and S_I do cancel. The time-evolution of the probability to find the system in its unperturbed ground state is:

$$\begin{aligned}
P_0(t) &\equiv \langle \Psi_0 | \hat{\rho}(t) | \Psi_0 \rangle = \text{tr} [\hat{\rho}(0) \hat{\rho}(t)] \\
&= \int dq_t^> dq_t^< \rho_0(q_t^<, q_t^>) \rho(q_t^>, q_t^<, t) \\
&= \int Dq^> Dq^< \rho_0(q_t^<, q_t^>) e^{i(S_0^> - S_0^<) + iS_R - S_I} \rho_0(q_0^>, q_0^<) \\
&\approx 1 + \int Dq^> Dq^< e^{i(S_0^> - S_0^<)} \rho_0(q_t^<, q_t^>) \\
&\quad \times (iS_R - S_I) \rho_0(q_0^>, q_0^<) .
\end{aligned} \tag{5.15}$$

Here $\hat{\rho}_0$ is the density matrix of the unperturbed ground state, and the path integration also includes integrals over the initial and final coordinates. Now one can insert the expressions for S_R and S_I from Eq. (5.6). The integration over the trajectories and the endpoints produces the *unsymmetrized* correlators of the system coordinate, such as (for $t_1 > t_2$):

$$\begin{aligned}
\int Dq^> e^{iS_0^>} \Psi_0^*(q_t^>) q^>(t_1) q^>(t_2) \Psi_0(q_0^>) = \\
\langle \Psi_0 | \hat{q}(t_1) \hat{q}(t_2) | \Psi_0 \rangle e^{-iE_0 t} .
\end{aligned} \tag{5.16}$$

Evidently, both the unperturbed action S_0 and the integrations involving the state Ψ_0 are essential for obtaining the correct correlator. In the long-time limit, we obtain the decay rate which also follows from the Golden Rule (5.13):

$$P_0(t) \approx 1 - \int_0^t dt_1 \int_0^{t_1} dt_2 2 \operatorname{Re} \left[\left\langle \hat{F}(t_1) \hat{F}(t_2) \right\rangle \langle \Psi_0 | \hat{q}(t_1) \hat{q}(t_2) | \Psi_0 \rangle \right] \approx 1 - \Gamma_0 t. \quad (5.17)$$

Only the term growing linearly in time has been retained at the end of this equation.

We emphasize that the decay of $P_0(t)$ is not governed by S_I alone. Both the real (fluctuation) part of the correlator $\left\langle \hat{F}(t_1) \hat{F}(t_2) \right\rangle$ from S_I , as well as the imaginary (dissipative) part from S_R enter Γ_0 , since the “system correlator” $\langle \Psi_0 | \hat{q}(t_1) \hat{q}(t_2) | \Psi_0 \rangle$ is complex-valued. In particular, these two contributions to the rate cancel when one starts out of the ground state, at $T = 0$. If S_R were dropped, then only the (real-valued) symmetrized version of the bath correlator would appear in Eq. (5.17). In that case, the decay rate would only depend on the (real-valued) symmetric part of the system correlator as well. Therefore, a finite decay rate of the ground state would result even at zero temperature, where really there would have been none. The physical reason is the heating introduced by the classical noise field, whose correlator contains the zero-point fluctuations of the original quantum bath, as we have discussed before.

Note that, of course, there will always be a small reduction in the probability of finding the unperturbed ground state after switching on the interaction, since the ground state of the coupled system contains contributions from other system states as well. This point has been discussed in more detail recently for the case of the damped harmonic oscillator [Nagaev02]. It does not contribute to Γ_0 which describes the decay linear in time.

On a formal level, we may argue that the decay of the density matrix is not governed by S_I alone since the “weighting factor” that is used when “averaging” over many paths contains the *phase* factor $\exp(i(S_0^> - S_0^<))$. Therefore, such an average is not the same as a classical average, for which the decay could not be overestimated by dropping S_R , since then we could use $|\langle \exp(iS_R - S_I) \rangle| \leq \langle \exp(-S_I) \rangle$. Furthermore, the integration over the density matrix of the initial state is obviously essential, as it is needed to produce the correct form of the system correlator. Both facts mean that it would be premature to draw any conclusions about dephasing and decay at an early stage of the calculation, by merely looking at the influence action.

5.5 Exactly solvable linear systems: “Cancellation to all orders” for the damped oscillator

In order to show how S_R and S_I can cancel also beyond lowest-order perturbation theory, we will now turn to linear quantum dissipative systems. Although the exact solutions for the damped harmonic oscillator and the free particle have been well-known for a long

time [Caldeira83], we will review the essential steps in the derivation, pointing out where S_R and S_I do enter. We will first turn to the oscillator, for which the Golden Rule result suggests that one would obtain an artificial decay of the ground state at zero temperature if S_R were neglected. For simplicity, our discussion is restricted to $T = 0$, since that is the limit where these effects show up most clearly.

For any linear system which is linearly coupled to a bath of oscillators, the propagator J for the density matrix (Eq. (5.2)) can be evaluated exactly, since the integration over system paths is Gaussian. In fact, J is found to be given by the “semiclassical” result, i.e. an exponential containing the action along stationary paths, multiplied by a prefactor which does not contain the endpoints of the paths (a specialty of linear systems):

$$J(q_t^>, q_t^< | q_0^>, q_0^<; t) = \frac{1}{N(t)} e^{iS[q_{cl}^>, q_{cl}^<]}, \quad (5.18)$$

with $S = S_0^> + S_0^< + S_R + iS_I$. The paths $q_{cl}^{>(<)}$ make the full action stationary,

$$\frac{\delta S}{\delta q_{cl}^>} = \frac{\delta S}{\delta q_{cl}^<} = 0, \quad (5.19)$$

and fulfill boundary conditions of the form $q_{cl}^>(0) = q_0^>$. The prefactor $N(t)$ can be obtained most easily from the condition for normalization of the density matrix,

$$\int dq_t J(q_t, q_t | q_0, q_0; t) = 1. \quad (5.20)$$

$N(t)$ is found to be independent of S_I , but it does depend on S_R (see, for example, the general proof in Appendix E of [Golubev00]).

In the following, we will turn to the special case of the *Ohmic* bath, which leads to a velocity-proportional friction force and has a power spectrum rising linearly at low frequencies (for $T = 0$):

$$\langle \hat{F} \hat{F} \rangle_\omega = \frac{\eta \omega}{\pi} \theta(\omega). \quad (5.21)$$

We will argue below that, in the case of the damped harmonic oscillator, no essential qualitative result will be changed by using other bath spectra, unless these have an excitation gap exceeding the oscillator frequency.

As usual, we introduce the center-of-mass coordinate $R(\tau) \equiv (q^>(\tau) + q^<(\tau))/2$ and the difference coordinate $r(\tau) \equiv q^>(\tau) - q^<(\tau)$ in order to write down the equations for the semiclassical paths, obtained from (5.19), for the case of the Ohmic bath:

$$\frac{d^2 r}{d\tau^2} - \gamma \frac{dr}{d\tau} + \omega_0^2 r = 0 \quad (5.22)$$

$$\frac{d^2 R}{d\tau^2} + \gamma \frac{dR}{d\tau} + \omega_0^2 R = -i \int_0^t d\tau' \operatorname{Re} \langle \hat{F}(\tau) \hat{F}(\tau') \rangle r(\tau') \quad (5.23)$$

Here $\gamma \equiv \eta/m$ is the damping rate and ω_0 is the unperturbed frequency of the oscillator. Note that the second equation leads to a complex-valued solution $R(\cdot)$. It is also possible to formulate the calculation slightly differently [Caldeira83, Hakim85], by using stationary solutions with respect to the real part of S only. In any case, inserting the solutions $R (\equiv R_{cl})$ and $r (\equiv r_{cl})$ into the action S shows that the imaginary part of the action $S_{cl} \equiv S[q_{cl}^>, q_{cl}^<]$ is determined directly only by S_I (in spite of the complex-valued $R(\cdot)$). As expected, S_{cl} turns out to be a bilinear expression in the endpoints R_t, R_0, r_t, r_0 :

$$\begin{aligned} \text{Re } S_{cl} &= S_0^> + S_0^< + S_R = \\ &\quad R_t r_t L_{tt} + R_t r_0 L_{t0} + R_0 r_t L_{0t} + R_0 r_0 L_{00} \end{aligned} \quad (5.24)$$

$$\text{Im } S_{cl} = S_I = r_0^2 C_{00} + 2r_0 r_t C_{0t} + r_t^2 C_{tt}. \quad (5.25)$$

All the coefficients are real-valued functions of time. For our purposes, it is sufficient to know that the entries of the matrix L are independent of S_I (while they do depend on the damping γ from S_R). In contrast, the entries of C depend both on S_I and S_R . The dependence on S_R arises only because the path r , which is inserted into Eq. (5.5), is affected by the friction described by S_R , see Eq. (5.22). The entries of C are proportional to the strength of the bath fluctuations (i.e. the magnitude of $\langle FF \rangle_\omega$). Explicit expressions for all of these coefficients can be found in [Caldeira83] (cf. their Section 6; note that the damping constant γ used here corresponds to 2γ in [Caldeira83], starting from their Eq. (6.8)). For reference, the quantities used in the following discussion have been listed in Appendix A.8.

At this point, evaluation of the coefficients for $\text{Im } S_{cl}$ shows that they will grow in time beyond all bounds, regardless of whether the path r is calculated by taking into account S_R or neglecting it (setting $\gamma = 0$ in Eq. (5.22)). However, no conclusion about dephasing and decay can be drawn from this, since the foregoing discussions lead us to expect that any potential cancellation between S_R and S_I will take place only *after* proper integration over the initial density matrix. This can be deduced from the derivation of the Golden Rule decay rate given in the preceding section. It is also very reasonable that S_I grows without bounds for any semiclassical path $r(\cdot)$, since all paths contribute more or less to the time-evolution of all eigenstates, and decay of excited states is perfectly correct in the model of the damped harmonic oscillator.

The initial ground state density matrix has the form

$$\begin{aligned} \rho_0(q_0^>, q_0^<) &\propto \exp \left(-(q_0^{>2} + q_0^{<2}) / (4 \langle \hat{q}^2 \rangle_0) \right) \\ &= \exp \left(-(R_0^2 + r_0^2/4) / (2 \langle \hat{q}^2 \rangle_0) \right), \end{aligned} \quad (5.26)$$

with $\langle \hat{q}^2 \rangle_0 = 1/(2m\omega_0)$ as the square of the ground state width. After performing the Gaussian integrals over R_0 and r_0 , which are needed to evaluate Eq. (5.1), we obtain the final result for the density matrix $\rho(q_t^>, q_t^<, t)$ at a time t after switching on the interaction with the bath. It has the general form

$$\frac{1}{\tilde{N}(t)} \exp \left(-(aR_t^2 + bR_t r_t + cr_t^2) \right) . \quad (5.27)$$

In particular, the prefactor of R_t^2 gives the width of the probability distribution at time t ,

$$\langle \hat{q}^2(t) \rangle = (2a)^{-1} . \quad (5.28)$$

Let us now look at the behaviour of the width in order to analyze the effect of dropping S_R in the calculation. The expression for $\langle \hat{q}^2(t) \rangle$ has been derived already by Caldeira and Leggett [Caldeira83] (cf. their Eq. 6.34):

$$\langle \hat{q}^2(t) \rangle = (2C_{00} + m\omega_0/2 + L_{00}^2/(2m\omega_0)) / L_{t0}^2 . \quad (5.29)$$

This expression clearly contains quantities both from the imaginary part (C_{00}) and from the real part (L_{00} , L_{t0}) of the action. Formally speaking, real and imaginary parts have become intermixed when integrating over R_0 , due to quadratic completion of the expression $iR_0(r_t L_{0t} + r_0 L_{00}) - m\omega_0 R_0^2$ in the exponent (the former term is from Eq. (5.24), while the latter term is from the initial density matrix, Eq. (5.26)). Physically, this result is to be expected, since the growth of the width of the probability distribution will be governed by the balance between the bath fluctuations (S_I) and the friction (S_R).

The complete time-evolution of $\langle \hat{q}^2(t) \rangle$ after switching on the interaction at $t = 0$ is displayed in Fig. 5.2. This includes cases where the value of the damping constant γ has been artificially set to zero or to other values different from that prescribed by the fluctuation-dissipation theorem (FDT), which connects γ to the strength of the bath fluctuations described by $\langle FF \rangle_\omega$ (see Eq. (5.21) for the case of $T = 0$). If S_R is neglected completely (no friction, $\gamma = 0$), heating takes place, causing the variance to grow linearly in time, at a rate given by the Golden Rule expression involving the *symmetrized* bath correlator. Formally, the growth of C_{00} with time cannot be compensated in that case, since L_{00} and L_{t0} acquire their original unperturbed values. For small $\gamma > 0$, the width saturates at a value much larger than that of the ground state. On the other hand, if the friction is too strong, the width saturates at a value below that of the ground state, and the Heisenberg uncertainty relation is violated (since $\langle \hat{p}^2 \rangle$ also shrinks). This point is discussed in the book of Milonni in the context of an atom interacting with the vacuum electromagnetic field [Milonni94]. If, however, γ has the correct value prescribed by the FDT, $\langle \hat{q}^2 \rangle$ changes only slightly from its unperturbed value.

In fact, for a linear system like the quantum harmonic oscillator, its behaviour under the action of the linear bath can be described and understood entirely using a classical picture [Weiss00]. The reason for this is as follows: one starts out with an initial state for system and bath that has a positive definite Gaussian Wigner-density, which can be interpreted directly as a classical phase space density whose time-evolution then corresponds one-to-one to the evolution of the Wigner-density (see Appendix A.9). Thus, the quan-

tum dissipative dynamics may be described by a *classical* Langevin equation including friction and a fluctuating driving force:

$$\frac{d^2q}{dt^2} + \gamma \frac{dq}{dt} + \omega_0^2 q = \frac{1}{m} F(t). \quad (5.30)$$

In this equation, the damping term incorporates the effects of S_R . It counteracts the fluctuations of $F(\cdot)$ that are described by S_I in the path-integral picture and whose correlation function is, therefore, given by the *symmetrized* part of the bath correlator.

The behaviour of the width has been discussed above using the influence functional, but it can be understood more easily in this picture. We can use the susceptibility of the damped oscillator to find its response to the force fluctuations F , which, at zero temperature, are entirely due to the zero-point fluctuations. In particular, for the limit $t \rightarrow \infty$, we obtain

$$\langle \hat{q}^2(t) \rangle \rightarrow \int_{-\infty}^{+\infty} d\omega |\chi(\omega)|^2 \langle FF \rangle_\omega, \quad (5.31)$$

where

$$\chi(\omega) = \frac{1/m}{\omega_0^2 - \omega^2 - i\omega\gamma} \quad (5.32)$$

is the susceptibility of the damped oscillator, and $\langle FF \rangle_\omega$ is the symmetrized power spectrum (see Eq. (5.21)). For the correct equilibrium state (obtained by fully keeping S_R and S_I), the width at $t \rightarrow \infty$ can also be found by applying the FDT to the oscillator coordinate (cf. Eq. 6.37 of [Caldeira83]). In contrast, the effect of dropping S_R is obtained by letting $\gamma \rightarrow 0$ in Eq. (5.30), while $\langle FF \rangle_\omega$ is kept fixed.

The example of the damped harmonic oscillator demonstrates that the proper behaviour near the ground state of the system cannot be observed at the early stages of the calculation, by looking at the action evaluated along classical paths (Eqs. (5.24), (5.25)), regardless of whether these paths properly include the damping or not. Only after correct integration over the initial state density matrix the contributions from S_R and S_I can compensate each other (in Eq. (5.29)), such that no artificial finite decay rate of the ground state results, if S_R is kept.

5.6 Power-law behaviour in quantum Brownian motion

We now turn to a discussion of the free particle, i.e. the Caldeira-Leggett model of quantum Brownian motion. There, the reasoning is the same as before in principle: Neglecting S_R means that the zero-point fluctuations of the bath contained in S_I may heat up the particle. However, there is an important difference: The spectrum of the free motion does not contain any resonance peak, unlike that of the harmonic oscillator.

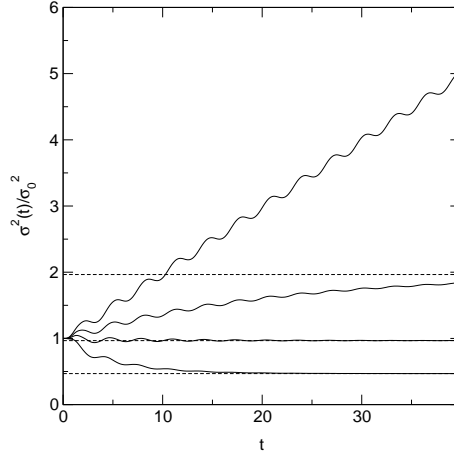


Figure 5.2: The variance $\sigma^2(t) \equiv \langle \hat{q}^2(t) \rangle$ of the probability density $\rho(q, q, t)$ for the damped harmonic oscillator, plotted in units of the unperturbed ground state variance σ_0^2 , as a function of time t for the following friction strengths (top to bottom): $\gamma/(2\pi \langle FF \rangle_{\omega=1}) = 0, 0.5, 1, 2$ (other parameters are $m = \omega_0 = 1$). A ratio of 1 corresponds to the correct value prescribed by the FDT, while $\gamma = 0$ means S_R has been neglected completely, such that $\sigma^2(t)$ grows without bound. The dashed lines give the limit for $t \rightarrow \infty$ (see Eq. (5.31)).

Therefore, only the low-frequency components ($\omega \rightarrow 0$, in the limit $t \rightarrow \infty$) of the bath spectrum will contribute to heating and decay (compare Eq. (5.12)), which results in a peculiar long-time behaviour [Caldeira83, Hakim85, Schramm87] that cannot be captured using the Golden Rule, as has been emphasized in [Golubev00].

One can observe the distinction between oscillator and free particle most easily in the picture of the classical Langevin equation (5.30) introduced above. In Appendix A.9, it is shown how the density matrix propagator J may be obtained in general via the time-evolution of the Wigner density. This approach is physically more transparent than the path-integral calculation. For the purposes of our present discussion, however, it will suffice to consider the time-evolution of the diagonal elements of the density matrix in momentum space. These have also been analyzed in [Golubev00], in order to demonstrate the failure of the Golden Rule calculation to describe the decay of the original ground state ($p = 0$) at zero temperature. We will confirm and explain the outcome of this analysis using a simple argument based on the Langevin equation (5.30). Then we will point out the role of S_R and describe the important difference to the damped oscillator.

If the particle has momentum p_0 at time 0, its momentum p at time t will be determined by the fluctuating force $F(\cdot)$ in the following way (by solving Eq. (5.30) for $\omega_0 = 0$):

$$p = p_0 e^{-\gamma t} + \int_0^t ds e^{-\gamma(t-s)} F(s). \quad (5.33)$$

Since $F(\cdot)$ is a Gaussian random process, the probability density of finding a momen-

tum p at time t is a Gaussian, of variance

$$\langle \delta p^2 \rangle \equiv \int_0^t ds_1 \int_0^t ds_2 e^{-\gamma(2t-s_1-s_2)} \langle F(s_1)F(s_2) \rangle. \quad (5.34)$$

The behaviour of $\langle \delta p^2 \rangle$ as a function of time is as follows (at $T = 0$): As long as $t \ll 1/\gamma$, friction is unimportant and it is the double time-integral over the correlator of F which is to be evaluated. For the Ohmic bath considered here, the power spectrum is relatively strong at low frequencies (rising linearly with ω , see Eq. (5.21)). This leads to a slow decay in time, $\langle F(t)F(0) \rangle \propto 1/t^2$, which results in a logarithmic growth of $\langle \delta p^2 \rangle$,

$$\langle \delta p^2 \rangle \approx 2 \frac{\eta}{\pi} \ln(\omega_c t). \quad (5.35)$$

Here ω_c is the cutoff frequency of the bath spectrum and we have assumed $\omega_c t \gg 1$. It is this logarithmic behaviour which cannot be obtained using the Golden Rule approximation, to be discussed below. At later times, $t \gg 1/\gamma$, the growth saturates at a constant value,

$$\langle \delta p^2 \rangle \rightarrow \frac{\eta}{\pi} \ln(\omega_c/\gamma). \quad (5.36)$$

The perturbation expansion in the coupling between system and bath can be carried out by expanding the influence action in the propagator J (Eq. (5.2)) in powers of $iS_R - S_I$ (see Eq. (5.15) in the present article or Eq. (E13) of [Golubev00]). We want to discuss the time-evolution of the diagonal elements $\rho_{pp}(t)$ of the density matrix in momentum space. The evolution starts from the equilibrium density matrix, which is a Gaussian momentum distribution of variance $\langle p_0^2 \rangle = mT$ (the following formulas will be analyzed for arbitrary T). After a time t , the density matrix is still a Gaussian, but of variance (compare Eq. (5.33)):

$$\langle p^2 \rangle = \langle p_0^2 \rangle e^{-2\gamma t} + \langle \delta p^2 \rangle. \quad (5.37)$$

From this we can easily derive the result for $\delta\rho_{pp}^{(1)}(t)$ which could alternatively be obtained by first expanding J to first order in $iS_R - S_I$, going over to the momentum representation and finally integrating over the initial density matrix (as was done in [Golubev00]; see Eq. (E18), which is, however, still written in terms of matrix elements of the coordinate operator):

$$\begin{aligned} \rho_{pp}(t) &= \frac{1}{\sqrt{2\pi \langle p^2 \rangle}} \exp \left[-\frac{p^2}{2 \langle p^2 \rangle} \right] \\ &\approx \rho_{pp}(0) \cdot \left(1 + \frac{\langle p^2 \rangle - \langle p_0^2 \rangle}{2 \langle p_0^2 \rangle} \left(\frac{p^2}{\langle p_0^2 \rangle} - 1 \right) + \dots \right). \end{aligned} \quad (5.38)$$

In evaluating $\langle p^2 \rangle$, only the terms up to first order in γ and $\langle FF \rangle_\omega$ must be kept for the purposes of this expansion. At finite temperature T , the behaviour of $\langle p^2 \rangle$ at long times

$t \gg 1/T$ is governed by the linear decrease stemming from $\langle p_0^2 \rangle e^{-2\gamma t} \approx \langle p_0^2 \rangle (1 - 2\gamma t)$ and the linear increase from $\langle \delta p^2 \rangle \approx 2\eta T t$. If the initial density matrix really describes the equilibrium distribution, then detailed balance holds and these terms cancel. For times $t \ll 1/\gamma$, the time-evolution of $\langle p^2 \rangle$ is governed by $\langle \delta p^2 \rangle$, evaluated for the correlator $\langle FF \rangle_\omega$ taken at $T = 0$ (which only contains the zero-point fluctuations of the bath). For consistency of the expansion, $\langle \delta p^2 \rangle$ in Eq. (5.34) has to be evaluated by setting $\gamma = 0$. Therefore, only the discussion given above for times $t \ll 1/\gamma$ is relevant. The logarithmic growth of $\langle \delta p^2 \rangle$ given in Eq. (5.35) corresponds to a power-law behaviour of the (exact) time-evolution of $\rho_{pp}(t)$ for $t \ll 1/\gamma$. This logarithm, that appears in the perturbation expansion (5.38), is “overlooked” in the Golden Rule approximation, where only terms growing linearly with time are kept. Therefore, the Golden Rule rate turns out to vanish [Golubev00]. These power-laws are characteristic of the density matrix propagator J of quantum Brownian motion at zero temperature (see Appendix A.9).

On the other hand, the effect of neglecting S_R may be analyzed by setting the friction constant γ to zero in Eq. (5.34). Then, the spread $\langle \delta p^2 \rangle$ of the momentum distribution grows without bounds for all times, which is obviously not the correct physical behaviour. It is qualitatively similar to the heating produced in the damped oscillator model. However, since the growth proceeds only logarithmically in time, the artefacts of this approximation, when applied to the free particle, are not nearly as drastic as the finite decay rate of the ground state observed for the oscillator. In particular, within perturbation theory, no qualitative change is obtained by dropping S_R for the free particle (no finite decay rate is produced).

Furthermore, if we had considered a super-Ohmic bath (e.g. due to phonons), whose spectrum decays faster than ω^1 for $\omega \rightarrow 0$, the growth of $\langle p^2 \rangle$ would saturate even without friction (as it should, since there is no velocity-dependent friction for such a bath). In contrast, the behaviour of the harmonic oscillator discussed above would remain qualitatively the same as for the Ohmic bath, since its decay depends on the bath spectrum at the resonance frequency of the oscillator and is not affected in any essential way by the details of the spectrum at low frequencies. This is consistent with the fact that in the oscillator case already the Golden Rule is sufficient to obtain an essentially correct picture of the artificial decay produced by dropping S_R , while, for quantum Brownian motion, it fails to describe the subtle power-laws associated with the low-frequency (long-time) properties of the Ohmic bath at zero temperature.

The difference between oscillator and free particle also shows up clearly in the behaviour of the imaginary part of the influence action: For the free particle, S_I *always* grows only logarithmically with time t (at $T = 0$), independent of whether one keeps S_R or sets it to zero (i.e. $\gamma \equiv 0$ in the equations of motion). This can be derived from the formulas given in Appendix A.9 or those of [Golubev00], Appendix E (or [Caldeira83], Section 6, with the proper limit $\omega_R \rightarrow 0$ for the free particle).

Hence, we conclude that for the oscillator (or any motion containing an extended spectrum) the effects of dropping S_R are much more pronounced than for the free motion, since they lead to an artificial finite decay rate. We have also observed that this effect can

already be understood within the framework of the Golden Rule approximation, whereas that approximation is incapable of describing the more subtle “power-law decay” found for the free particle.

5.7 Qualitative discussion of other models: Nonlinear coupling and Pauli principle

It could be argued that our discussion of the damped oscillator has only demonstrated the importance of S_R in preventing an artificial decay of the *ground state* and has little to do with dephasing. Indeed, if one wants to discuss dephasing, one should rather consider the decay of a coherent superposition of the ground state and some excited state (see, for example, the previous chapter). This is relevant both for arbitrary nonequilibrium situations as well as for the calculation of the system’s linear response, where the perturbation creates a superposition of excited states and the ground state. In the example of the damped harmonic oscillator, full relaxation into the ground state will *always* take place (at $T = 0$), for any such excited state. This holds regardless of the bath spectrum, provided the latter does not vanish around the resonance frequency of the oscillator. For weak coupling, the decay of the density matrix (and, therefore, the linear response) may be described conveniently using a simple master equation approach (taking into account the special regular energy spectrum). What is more, even if one neglects S_R in a path-integral calculation, the predicted decay rates will be correct, excepting only that for the ground state, which we have discussed above. The reason for this, however, is a specialty of the linearly damped harmonic oscillator. Since the bath couples to the coordinate operator, whose matrix elements only connect adjacent oscillator levels, the relevant “system correlator” (in Eq. (5.10)) turns out to be symmetric for any state but the lowest one. Therefore, the decay rate will depend only on the symmetric part of the bath correlator as well, see Eq. (5.17). Hence, for all the excited states, the evaluation of the total decay rate is not affected by dropping S_R . This point has already been discussed in connection with the model of two oscillating wave packets, at the end of Section 5.2.

Since we are interested in demonstrating the (generic) importance of S_R for the dephasing of a superposition of low-lying levels, the natural choice is to consider a bath with an excitation gap larger than the resonance frequency of the oscillator (see Fig. 5.3). In that case, we expect the lowest levels to remain coherent in the correct description. Unfortunately, in the model of the linearly damped oscillator discussed above, we would not obtain any finite decay rate, *regardless* of whether S_R is kept or not. This is because the corresponding classical noise force is out of resonance and cannot heat the oscillator.

Therefore, in order to analyze a situation where the importance of retaining S_R is displayed even for excited states, we have to go beyond exactly solvable linear models. As a consequence, the following discussion is necessarily incomplete insofar as we cannot give exact proofs of the statements to be made below. These statements will be based on the experience acquired in the simpler models discussed above. We will also make use

of some Golden Rule type arguments, noting that the Golden Rule has been sufficient to understand the behaviour of the damped oscillator in a qualitatively correct way. In any case, we believe it is useful to contrast the results obtained by dropping S_R with the “commonly accepted” picture.

Let us, therefore, consider the following model: We retain the harmonic oscillator, but change the coupling between system and bath from $\hat{V} = -\hat{q}\hat{F}$ to $\hat{V} = -f(\hat{q})\hat{F}$, with a *nonlinear* function f . This is called state-dependent friction [Weiss00]. In that case, the transition matrix elements of the system operator $f(\hat{q})$ will, in general, be nonzero between any two states, which is the important difference to the linear case. If we introduce a bath spectrum with a gap larger than $n\omega_0$, then, for sufficiently weak coupling and according to a simple Golden Rule calculation, the first n excited states will not decay at zero temperature. Any coherent superposition of these states will therefore remain coherent. The full, non-perturbative picture will be slightly more complicated, but the essential point should remain the same: The first excited states will acquire an admixture of other levels and become entangled with the states of the bath. They will experience some frequency shifts and the transition matrix elements will be renormalized. Of course, the new eigenstates of the coupled system will remain in a coherent superposition forever (by definition). The $n + 1$ lowest ones still have a discrete spectrum and are in direct correspondence to the initial unperturbed states. When switching on the interaction at $t = 0$, a partial decay will result. Physically, this corresponds to the relaxation of the initial state into the selfconsistent coupled state of system and bath (see [Hakim85] for a discussion of these issues in the case of the free particle). However, the initial decay will saturate in time on a short time-scale. During this transient adjustment, the reduced system density matrix becomes mixed to a small extent (if the coupling is weak), but no non-saturated long-term decay (indicated by a finite decay rate) results. In any case, the transient decay is an artefact of the procedure of suddenly switching on the interaction. A full calculation of, for example, the linear response properties of the dissipative system would start out with the selfconsistent ground state of the fully interacting system (as was done in [Schramm87] for the free particle).

In contrast, dropping S_R would lead to a completely different picture, since then S_I would correspond to a classical noise force. Starting from any of the first n excited states, the fluctuating field would always be able to induce transitions *up* in energy, thus leading to a finite decay rate. The role of S_R in the correct description of a quantum noise force is precisely to cancel these upward transitions, as has been demonstrated in the case of the linearly damped oscillator. Due to this finite decay rate, any initially coherent superposition would get destroyed, leading to complete dephasing. No saturation of the decay could be observed, in spite of the gap in the bath spectrum.

It is *this* behaviour that is described qualitatively correctly by evaluating S_I along semiclassical paths of the oscillator. The expression for S_I , Eq. (5.5), is now to be changed simply by replacing q by $f(q)$. While an (unperturbed) oscillator path of the form $q(\tau) \propto \cos(\omega_0 t)$ only contains frequencies $\pm\omega_0$ which cannot couple to the gapped bath, the function $f(q(\tau))$ will, in general, contain all higher harmonics as well. This di-

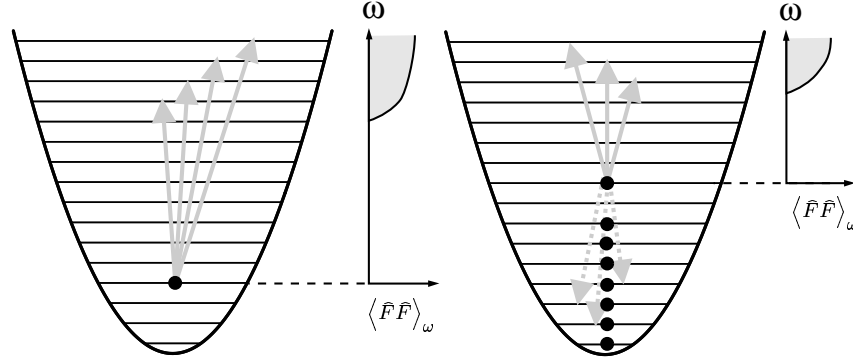


Figure 5.3: The models described in the text. *Left*: A bath with a gap would lead to the upward transitions indicated by grey arrows if (and only if) S_R were neglected. *Right*: A sea of fermions may block downward transitions (dashed) even though they are possible in the single-particle picture.

rectly corresponds to the character of the *symmetrized* system spectrum, i.e. the Fourier transform of $\langle \{f(\hat{q}(\tau)), f(\hat{q}(0))\} \rangle$. These frequencies contained in the system motion then will couple to the bath spectrum, leading to an unbounded growth of S_I with time.

Similarly, if we were to use a bath without a gap, but where the spectrum falls off fast towards low frequencies, then the correct description would also yield decay rates that quickly become smaller when going towards the ground state, while they would saturate at a finite, comparatively large level if S_R were dropped.

As pointed out in Chapter 1, the present work has been motivated in part by the ongoing controversial debate on low-temperature dephasing in an interacting disordered fermion system [Mohanty97a, Golubev99, Cohen99, Vavilov99, Aleiner99, Kirkpatrick02, Imry02]. Since the usual Feynman-Vernon influence functional deals only with a single-particle situation, it cannot be applied directly to this problem. However, the authors of [Zaikin00, Golubev99, 00] have succeeded in deriving an extension of the usual influence functional to the many-fermion situation, using an exact time-evolution equation for the reduced density matrix of a fermion system under the action of a quantum bath (which has also been rederived using different approaches, e.g. in [Marquardt00]). In their result, the Fermi distribution (and, therefore, the Pauli principle) only enters S_R , while S_I is unaffected (Eqs. (54) and (55) of [Golubev99]). Therefore, the dephasing rate, as read off from S_I , is found to equal the rate which would also be obtained in a purely single-particle calculation. Although we do not analyze the problem of weak-localization here, we will use the insights gained above in order to explain why, in our opinion, the *assumption* that the dephasing rate can be derived from S_I alone must be proven instead of being taken for granted. This holds even when S_R vanishes or is negligible on the relevant pairs of classical time-reversed trajectories (which is the case in [Golubev99]), since, in general, the integration over the fluctuations away from these trajectories will be essential

for obtaining a cancellation between the effects of S_R and S_I (see Sec. 5.4), in addition to properly taking into account the initial density matrix. Furthermore, we note that in these calculations the detailed form of the bath spectrum at low frequencies turns out to be unimportant for the essential result of a finite zero-temperature dephasing rate. This is in marked contrast to the case of the free particle (where the Ohmic bath plays a special role [Schramm87]; see also [Guinea02, Golubev02b]), but similar to what is observed for the damped harmonic oscillator when S_R is neglected. It is for this reason that we have chosen a bath with an excitation gap in order to demonstrate the importance of S_R , since there the effects come out most clearly, although they are also present for other bath spectra (compare the discussion above).

The model situation of the damped oscillator described above already contains one key ingredient related to the description of dephasing for an electron moving inside a disordered metal, namely an extended system spectrum: Due to the impurity scattering, the system spectrum (e.g., of the velocity operator) contains frequencies up to (at least) the elastic scattering rate, which may couple to the zero-point fluctuations contained in the bath spectrum. This is in contrast to the free particle, which can only couple to the low-frequency bath modes (see the discussion at the end of Section 5.6). As before, the importance of S_R will be visible most easily for a bath containing an excitation gap. For such a bath, the *free* motion (without impurity scattering) will not show any nontransient decay, *regardless* of whether S_R is taken into account or not. In contrast, the model to be discussed below, which is more similar to the situation in the disordered metal, will show a finite decay rate of low-lying levels if and only if S_R is neglected.

Apart from the extended system spectrum, we have to take into account another important feature of many calculations [Chakravarty86, Golubev99, Cohen99] dealing with electrons in a disordered metal: the use of the semiclassical analysis. For linear systems the semiclassical result for the path-integral is exact, such that it can even be used near the ground state of the system, as we have done it here. However, in such a case, the size of the fluctuations around the path is comparable to the amplitude of the path itself, which is not the situation in which semiclassics is usually applicable. In order to gain intuition for a typical semiclassical situation, we could reconsider the example with the nonlinear coupling to a gapped bath given above: Imagine an initial superposition of fast wavepackets, whose wavelength is much smaller than the packet size but whose excitation energies are still below the bath threshold. They would show a finite decay or dephasing rate (for the reasons given above), if only S_I were used for the analysis, but not in the full calculation. Still, for this scenario one might argue that it has been clear from the outset that the semiclassical analysis cannot be trusted, since those high-frequency components in the system spectrum that are responsible for the decay are necessarily larger than the energetic distance to the ground state.

It is only in a system of degenerate fermions that the following two conditions can be fulfilled all at once: On the one hand, the semiclassical analysis of a single (non-interacting) electron moving at the Fermi level is valid for an external potential which is sufficiently slowly varying, such that the system spectrum (concerning the motion of the

single electron) only contains frequencies much smaller than the Fermi energy. On the other hand, the whole many-particle system may be near (or in) its ground state.

While the first feature would lead one to believe that S_R may be omitted, we have learned from the examples discussed before that this is likely to be incorrect whenever the second condition holds as well. We stress once again that the two conditions are mutually exclusive in a single-particle problem, which is the reason why such considerations have not played any role in influence-functional calculations up to now.

In order to render the discussion concrete, we can once again make use of the example with a nonlinear coupling $f(\hat{q})$ given above, provided we suppose the N lowest oscillator states to be filled up with fermions initially (see Fig. 5.3). Apart from the nonlinear coupling, this is the model discussed in the previous chapter. For a relatively smooth function f , the matrix elements of $f(\hat{q})$ only connect states within a range much smaller than $\epsilon_F = N\omega_0$. In our example, this range should still be larger than the gap $n\omega_0$ of the bath. Dephasing of a *single* particle near ϵ_F can then certainly be described fully within the semiclassical analysis, and, to a good approximation, using S_I alone, as has been discussed above. The same holds for the many-particle system, if one explicitly considers a *classical* noise force, where S_R is absent. In that case, the many-particle problem can really be treated as a collection of independent single-particle problems, as is the case for any external time-dependent potential. Only in the end an average of the full Slater determinant over all possible realizations of the external noise has to be carried out.

If the dephasing rate is calculated solely from S_I , it turns out to be finite [Zaikin00, Golubev99, 00] and not to depend at all on the distance to the Fermi surface. This is consistent with the fact that the value of ϵ_F does not even appear in the single-particle calculation. On the other hand, for a quantum bath S_R does not vanish and should be included in the influence action. It is true that for the case of a highly excited *single* particle the dephasing rate comes out correct, regardless of whether S_R is kept or not, as we have discussed before. However, we have also pointed out that there is an important physical difference between the two calculations. Since in the correct approach (including S_R), the transitions induced by the bath are purely downwards in energy (accompanied by spontaneous emission into the bath), it is reasonable to expect that, in the *many-particle* problem, they will be blocked by the Pauli principle. In any case, this is what is found using the Golden Rule. Judging from these arguments, the growth of S_I due to the nonzero overlap of the (symmetrized) system spectrum with the high frequencies of the bath spectrum does not imply dephasing and decay. Rather, when performing the full analysis including S_R , these high frequencies most probably only lead to a renormalization, similar to that obtained for an electron interacting with optical phonon modes (a gapped bath), leading to the formation of a polaron. The formation of the polaron will be visible as an initial transient decay of the single-electron density matrix (for the artificial case of factorized initial conditions), which saturates on a short time-scale. Therefore, to lowest order, for a bath with a gap no finite relaxation rate of the lowest-lying single-particle excitations above the Fermi sea is expected, just as for the lower levels of the harmonic oscillator in the single-particle model with nonlinear coupling to a gapped bath.

We have to qualify this statement by taking into account the fact that the coupling between electrons and bath always also induces an effective interaction between the electrons (compare the previous chapters for examples). In this way, a given electron becomes coupled indirectly to the bath of other electrons, such that scattering processes will, indeed, lead to a finite decay rate even for those low-lying excited levels. This precludes any rigorous proof demonstrating the complete absence of decay and dephasing for low-lying levels even in such a rather simple situation, in spite of the assumption of an excitation gap in the bath spectrum. However, the consequences of the effective interaction can be distinguished easily from the finite dephasing rate that would be predicted by looking at S_I alone. If the coupling to the bath is of strength g , then the latter rate would go as g^2 . In contrast, the effective interaction (obtained after integrating out the bath) will itself be of strength g^2 , such that the resulting relaxation rate (due to coupling of an electron to the density fluctuations of other electrons) will be of fourth order in g . In addition, of course, the rate will depend strongly on the distance to the Fermi surface, vanishing when the Fermi energy is approached.

5.8 Conclusions

We have tried to demonstrate that the real part S_R of the Feynman-Vernon influence action cannot be neglected in an analysis of dephasing and decay *near the ground state of a system*, in spite of the fact that, in the simplest situations (involving highly excited states and the semiclassical analysis), it is only the imaginary part S_I which enters the dephasing rate. To this end, we have discussed how S_R and S_I may cancel each other's effects not only in lowest-order perturbation theory but also to all orders, by examining exactly solvable linear quantum dissipative systems. In general, the cancellation is only found after proper integration over the fluctuations away from semiclassical trajectories, taking into account the action of the unperturbed system and its initial density matrix. Furthermore, we have pointed out an essential difference between the damped oscillator and the free particle with respect to this issue. We have argued that the insight obtained in the case of the damped oscillator is also applicable to nonlinear systems and important for discussions of dephasing in systems of disordered degenerate fermions.

In summary, it may be possible to discuss dephasing and decay without considering S_R either if the noise is nearly classical (external nonequilibrium radiation or bath in the high-temperature limit) or if the system itself is in a highly excited state. Otherwise, dephasing rates obtained solely from S_I are bound to come out finite at zero temperature in most cases, even when a simpler Golden Rule calculation gives vanishing results. Judging from the examples discussed above, this is probably not because such a nonperturbative influence functional calculation goes beyond the Golden Rule approximation, but because it neglects some physics already contained even within this approximation.

Still, it has to be emphasized at the same time that there is no *general* proof showing the impossibility of zero-temperature dephasing near the ground state. There cannot

be such a proof, since there is evidently at least one counter-example (the Caldeira-Leggett model of quantum Brownian motion and similar models [Caldeira83, Guinea02, Golubev02b]; see the discussion of section 5.6 on why this is quite different from models such as the damped oscillator). Besides, of course, there is no generally applicable definition of “dephasing” that is useful under all conceivable circumstances.

It should be noted that the conclusions which have been drawn here concerning dephasing in weak-localization (made public in [Marquardt02b]) have not been accepted by the authors of [Golubev99] (see footnote in [Golubev02c], where the theory has been refined), although (in our opinion) the points raised in this chapter remain valid.

Chapter 6

Summary and open questions

In this thesis we have analyzed dephasing, i.e. the destruction of quantum-mechanical interference effects by a fluctuating environment. Particular emphasis has been put on the behaviour at low temperatures and the influence of zero-point fluctuations and the Pauli principle. These issues have been at the focus of the recent controversial discussion concerning a possible saturation of the dephasing rate in mesoscopic systems at low temperatures.

In Chapter 2, we have studied dephasing in tunneling transport through localized levels coupled to a bath, based on the “independent boson model” and the concepts of the “ $P(E)$ theory” of tunneling in a dissipative environment. In particular, we have analyzed how the fluctuations of the environment may lift perfect destructive interference in a symmetric setup, where this effect cannot be brought about by “mere renormalization”. For the case of sequential tunneling through a double-dot, we have derived a master equation whose solution yields the dependence of the current on the phase-difference, temperature, voltage and bath spectrum, treating the tunnel coupling perturbatively and the system-bath coupling exactly. In the limit of small voltages and temperatures, the “visibility” of the interference effect becomes perfect for “weak” bath spectra, while it vanishes for spectra that are comparatively strong at low frequencies, including the “Ohmic bath”. For the case of cotunneling, which is more similar to a scattering situation, there is no such anomalous behaviour. We have interpreted the expressions for the cotunneling rates in terms of a generalization of the Feynman-Vernon influence functional, demonstrating (for the special case treated here) how the influence functional may be modified in situations where energy conservation and the Pauli principle play a role.

The model of Chapter 3, a clean Aharonov-Bohm ring with a fluctuating magnetic flux, can be considered a straightforward generalization of Quantum Brownian motion of a single particle. We have shown how the magnitude of the persistent current decreases, due to the increase in the effective total mass of the electrons on the ring. For the Nyquist noise of an external coil (white noise of the flux at finite temperatures), this is merely a finite renormalization effect, while the persistent current vanishes for the “Ohmic bath” ($1/f$ fluctuations of the flux at $T = 0$), which leads to velocity-proportional friction. We

have also discussed dephasing of superpositions of momentum states on the ring, in terms of the two-particle Green's function of electrons. Both for the Nyquist noise and the Ohmic bath, “power law dephasing” is observed at $T = 0$. Finally, we have analyzed the influence of the bath on the perfect destructive interference observed in cotunneling through the ring, for a static magnetic flux of half a flux quantum. This analysis has been carried out only for the Nyquist noise (and weaker bath spectra), for reasons explained in the text. Building on the results of Chapter 2, we have shown that the incoherent current vanishes as V^3 (for Nyquist noise, at $T = 0$), such that there is no dephasing in the *linear* conductance.

In Chapter 4, we have introduced another many-particle generalization of a well-known dissipative quantum system. We have treated a model of fermions in a damped harmonic oscillator, where a fluctuating force couples to the center-of-mass motion of the electrons. In contrast to the models of previous chapters, this one shows a strong effect of the Pauli principle, due to the fact that the coupling to the bath induces transitions between the different energy eigenstates (“non-diagonal coupling”). Using the method of bosonization as a tool, we have analyzed the case of large particle numbers and derived analytic expressions for the Green's functions of the fermions. These have been discussed in detail, showing the influence both of the Pauli blocking and of the “decoherence-free subspace”, i.e. the relative motion of the fermions in the oscillator. In particular, we have shown the decay of the reduced single-particle density matrix for a particle which has been placed initially into a superposition of excited states above the Fermi sea.

From the results obtained for the various model systems, one can conclude at least that there is no hint of a “generic” zero-temperature dephasing mechanism that would be independent of the details of the bath spectrum and of the Pauli principle, and which would be active even when the energy supplied to the system (e.g. the bias voltage) is very small. This is consistent with various other models and simple Golden Rule arguments. However, it is in contrast to what had been suggested theoretically by some authors after the surprising experimental findings on a possible saturation of the weak-localization dephasing rate at low temperatures. In these calculations, the Feynman-Vernon influence functional is used to analyze dephasing at low temperatures, near the ground state of a system, and the dephasing rate is deduced from the imaginary part of the functional. Therefore, in Chapter 5 we have presented a detailed discussion of how the imaginary part of the influence functional (describing fluctuations) and the real part (describing friction) may cancel each other's effects under such circumstances. Physically, this is because the ground state of a quantum-mechanical system is stable due to the balance between zero-point fluctuations of the environment and the dissipation induced by coupling to the same environment. We have treated exactly solvable model systems, such as the harmonic oscillator and the free particle, coupled to a linear bath. Thus, we have shown how this cancellation enters the calculation beyond lowest-order perturbation theory. We have also given a qualitative discussion of systems where the Pauli principle becomes important.

There are several interesting open questions connected to the models discussed in this thesis. First of all, in the treatment of tunneling under the influence of a fluctuating

environment, we have kept the system-bath interaction exactly, but confined ourselves to a perturbative treatment of the tunnel coupling. Going beyond this approximation would be particularly important for sequential tunneling, where the crossover between finite and exactly zero visibility should become smooth. If the passage of the electron happens faster, the bath cannot adapt fully to the electron, which may diminish the difference between the various bath spectra. On the other hand, this will also introduce correlations between subsequent tunneling events. This leads to the possibility of “correlated many-particle tunneling”, where the first electron overcomes destructive interference by leaving a “virtual” trace in the bath, which is later erased by a second electron, such that energy conservation is not violated even for a gapped bath. The so-called “real-time renormalization group” [Schoeller99] seems to be a sufficiently strong (numerical) tool to address these questions.

Concerning the model of the “damped Fermi sea”, one could consider a spatially inhomogeneous fluctuating force, i.e. a nonlinear coupling to the individual electron coordinates, or a potential different from the harmonic oscillator. Although the original model cannot be solved exactly any more in that case, it may be feasible within the approximation of bosonization employed here. The details will depend on the behaviour of matrix elements of the force between different energy levels, but qualitatively one expects there to be relaxation of (and possibly coupling between) all boson modes. Such an analysis would also be important for the qualitative discussion of Chapter 5.

Appendix A

Appendices

A.1 Proof of $\langle \exp \hat{A} \rangle = \exp \left(\langle \hat{A}^2 \rangle / 2 \right)$

Here we give a proof of the relation $\langle \exp \hat{A} \rangle = \exp \left(\langle \hat{A}^2 \rangle / 2 \right)$ for the thermal average of the exponential of an operator \hat{A} that is linear in harmonic oscillator variables (and where $\langle \hat{A} \rangle = 0$). It is perhaps more transparent than the usual more abstract proofs (see e.g. [Mermin66] or [Delft98]), since it shows the connection to the corresponding classical identity, where A is a Gaussian random variable of zero mean. We have to consider only a single oscillator, since \hat{A} can always be written as a sum over normal coordinates (and -momenta), such that the average factorizes. First, \hat{A} is expressed as a linear combination of position and momentum:

$$\hat{A} = \alpha x + \beta \partial_x. \quad (\text{A.1})$$

If \hat{A} were proportional to x ($\beta = 0$), the classical relation could be applied directly, since the probability density with respect to x is Gaussian. By the Baker-Hausdorff identity, we have

$$\langle e^{\hat{A}} \rangle = \langle e^{\alpha x} e^{\beta \partial_x} \rangle e^{\alpha \beta / 2}, \quad (\text{A.2})$$

where the last exponent follows from $[x, \partial_x] = -1$. The average on the right hand side is given in terms of the density matrix:

$$\langle e^{\alpha x} e^{\beta \partial_x} \rangle = \int dx e^{\alpha x} (e^{\beta \partial_x} \rho(x, \tilde{x}))|_{\tilde{x}=x} = \int dx e^{\alpha x} \rho(x + \beta, x). \quad (\text{A.3})$$

The thermal equilibrium density matrix of a harmonic oscillator is Gaussian:

$$\rho(x', x) = \exp \left(-\frac{((x' + x)/2)^2}{2 \langle \hat{x}^2 \rangle} - \frac{\langle \hat{p}^2 \rangle}{2} (x' - x)^2 \right) / Z. \quad (\text{A.4})$$

Upon inserting $x' - x = \beta$ and $(x' + x)/2 = x + \beta/2$, we see that (A.3) corresponds to the classical average of $\exp(\alpha x)$ with a Gaussian probability distribution that has $\langle x \rangle = -\beta/2$ and $\text{Var } x = \langle \hat{x}^2 \rangle$. This yields $\exp(\alpha \langle x \rangle + \frac{\alpha^2}{2} \text{Var } x)$. Therefore, we obtain:

$$\langle e^{\alpha x} e^{\beta \partial_x} \rangle = e^{-\alpha\beta/2 + \alpha^2 \langle \hat{x}^2 \rangle / 2 - \beta^2 \langle \hat{p}^2 \rangle / 2}, \quad (\text{A.5})$$

where we have pulled out the factor $\exp(-\beta^2 \langle \hat{p}^2 \rangle / 2)$ from Eq. (A.4) that is not part of the probability density. Inserting this result into (A.2), we see that $\alpha\beta/2$ cancels in the exponent. On the other hand, we have

$$\langle \hat{A}^2 \rangle = \langle (\alpha \hat{x} + \beta i \hat{p})^2 \rangle = \alpha^2 \langle \hat{x}^2 \rangle - \beta^2 \langle \hat{p}^2 \rangle,$$

which completes the proof.

A.2 Current expression for sequential tunneling through the double-dot

At $T = 0$, for the symmetric situation, the current I is given by $I = e\gamma I_0[v, \delta_L, \delta_R]$, with:

$$\begin{aligned} I_0[v, \delta_L, \delta_R] = & 2 \cdot [-\delta_L^2 + (v^2 - 1)(1 + \delta_R^2) + \\ & 2\delta_L\delta_R(v^2 - 1)\cos\varphi + \delta_L^2 v^2 \cos^2\varphi] \cdot \\ & [-3\delta_L^2 + 2\delta_L\delta_R v^2 + (1 + \delta_R^2)(v^2 - 3) + \\ & 2(v^2(1 + \delta_L^2 + \delta_R^2) + \delta_L\delta_R(v^2 - 3))\cos\varphi + \\ & \delta_L(\delta_L + 2\delta_R)v^2 \cos^2\varphi]^{-1} \end{aligned} \quad (\text{A.6})$$

A.3 Cotunneling rate contributions

Here we describe the remaining contributions to the forward-tunneling rate Γ^+ . They differ from Γ_{pp}^+ only in the order of tunneling operators entering Eq. (2.130):

$$\begin{aligned} \Gamma_{pp}^+ : & \quad \hat{L}^- \hat{R}^+ \hat{R}^- \hat{L}^+ \\ \Gamma_{ph}^+ : & \quad \hat{L}^- \hat{R}^+ \hat{L}^+ \hat{R}^- \\ \Gamma_{hp}^+ : & \quad \hat{R}^+ \hat{L}^- \hat{R}^- \hat{L}^+ \\ \Gamma_{hh}^+ : & \quad \hat{R}^+ \hat{L}^- \hat{L}^+ \hat{R}^- \end{aligned} \quad (\text{A.7})$$

The resulting expression, Eq. (2.131), is changed in the following respects. First of all, the tunnel matrix elements $T_j^{L(R)}$ and the operators $\hat{d}_j^{(\dagger)}$ are re-ordered according to (A.7), while the indices j_1, \dots, j_4 and the time-points stay in the same order as before.

Furthermore, accounting for the electron operators of the reservoirs leads to different oscillating factors. We display only those parts of Eq. (2.131) that have to be changed:

$$\Gamma_{pp}^+ : e^{i\epsilon_L(\tau^> - \tau^<)} T_{j_1}^{L*} T_{j_2}^R T_{j_3}^{R*} T_{j_4}^L \hat{d}_{j_1}(t - \tau^<) \hat{d}_{j_2}^\dagger(t) \hat{d}_{j_3}(0) \hat{d}_{j_4}^\dagger(-\tau^>) \quad (\text{A.8})$$

$$\Gamma_{ph}^+ : -e^{-i\epsilon_R\tau^> - i\epsilon_L\tau^<} T_{j_1}^{L*} T_{j_2}^R T_{j_3}^L T_{j_4}^{R*} \hat{d}_{j_1}(t - \tau^<) \hat{d}_{j_2}^\dagger(t) \hat{d}_{j_3}^\dagger(0) \hat{d}_{j_4}(-\tau^>) \quad (\text{A.9})$$

$$\Gamma_{hp}^+ : -e^{+i\epsilon_R\tau^< + i\epsilon_L\tau^>} T_{j_1}^R T_{j_2}^{L*} T_{j_3}^{R*} T_{j_4}^L \hat{d}_{j_1}^\dagger(t - \tau^<) \hat{d}_{j_2}(t) \hat{d}_{j_3}(0) \hat{d}_{j_4}^\dagger(-\tau^>) \quad (\text{A.10})$$

$$\Gamma_{hh}^+ : e^{+i\epsilon_R(\tau^< - \tau^>)} T_{j_1}^R T_{j_2}^{L*} T_{j_3}^L T_{j_4}^{R*} \hat{d}_{j_1}^\dagger(t - \tau^<) \hat{d}_{j_2}(t) \hat{d}_{j_3}^\dagger(0) \hat{d}_{j_4}(-\tau^>) \quad (\text{A.11})$$

The energies in the exponentials stem from the difference in energies between intermediate and initial state, where the initial state gives the contribution $-\epsilon_L$ to this difference in the case of a particle state and $+\epsilon_R$ in the case of a hole state. The sign in front of the expression is a consequence of fermion operator reordering in the application of Wick's theorem.

When evaluating the two-particle Green's functions in the case of the independent boson model, we still always have $j_1 = j_2 = j$, $j_3 = j_4 = l$ for the electronically elastic contributions. However, the signs in front of the exponents in the bath average change in (2.132), since \hat{d} is connected to $e^{i\hat{\phi}}$, while \hat{d}^\dagger belongs to $e^{-i\hat{\phi}}$. In Eq. (2.133), the signs in front of K_{jl} must be reversed for Γ_{ph}^+ and Γ_{hp}^+ , while they remain the same for Γ_{hh}^+ . The signs of K_{jj} and K_{ll} are never changed.

A.4 Exact integral expressions for the cotunneling rate for the Ohmic bath at $T = 0$

For an Ohmic bath spectrum of the form $\langle \hat{F} \hat{F} \rangle_\omega^{T=0} = 2\alpha\omega e^{-\omega/\omega_c} \theta(\omega)$, the integration in Eq. (2.25) can be carried out, yielding

$$K(t) = -2\alpha \ln(1 + i\omega_c t), \quad (\text{A.12})$$

and therefore

$$e^{K(t)} = (1 + i\omega_c t)^{-2\alpha}. \quad (\text{A.13})$$

In the model of two dots, which couple like $\hat{F}_+ = \hat{F} = -\hat{F}_-$, this leaves the following integral to be performed in Eq. (2.146) for the cotunneling rate contribution γ_{++} :

$$\int_0^\infty d\tau^> d\tau^< \frac{e^{i\Delta(\tau^< - \tau^>)}}{[(1 + i\omega_c \tau^>)(1 - i\omega_c \tau^<)]^{2\alpha}} \times \int_{-\infty}^{+\infty} dt e^{i\omega t} \left[\frac{(1 + i\omega_c(t - \tau^<))(1 + i\omega_c(t + \tau^>))}{(1 + i\omega_c t)(1 + i\omega_c(t - \tau^< + \tau^>))} \right]^{2\alpha}. \quad (\text{A.14})$$

In the expression for γ_{+-} , the sign of the exponent of the second bracket has to be inverted (due to $K_{+-}(t) = -K_{++}(t)$). Note that for $t \rightarrow \infty$, the second bracket goes to 1, which yields a $2\pi\delta(\omega)$ contribution to the t -integral, regardless of the value of the exponent α . This gives a coherent term $\propto S(\omega = 0)$ in the end-result, such that there is no zero-bias anomaly in contrast to the case of sequential tunneling in presence of an Ohmic bath. We emphasize that the expressions derived in [Odintsov92] for cotunneling across two junctions in series with a resistor are similar but yet different in an important respect: There, no such finite limiting value for $t \rightarrow \infty$ is obtained, since the phase-correlation functions entering the exponent are different. The physical reason for the difference is the presence of potential fluctuations between the left and right reservoir electrodes in their model, leading to a ZBA, while we always assume the fluctuations to be limited to the interference region. Those “global” fluctuations would not lead to dephasing anyway, as they do not distinguish between different paths.

For the special case of $\alpha = 1/2$, the t -integral may be evaluated using the residue theorem. The remaining integrals over $\tau^{>(<)}$ can be carried out after expanding the integrand in the limit $\omega \rightarrow 0$, in which case they give a result that rises as ω^1 (i.e. like the bath spectrum) at low frequencies, as predicted by perturbation theory.

A.5 Derivation of the transformed spectrum for the Caldeira-Leggett model in vector gauge

The spectrum of the vector potential is changed due to the quadratic term $e^2\hat{A}^2/(2mc^2) \equiv C\hat{A}^2$ from the kinetic energy of the particle. This leads to a change in classical eigenfrequencies and -vectors of the bath oscillators. As the spectrum is independent of the explicit expression for \hat{A} in terms of the oscillator variables, we deviate from the main text and take $\hat{A} = \sum_j g_j \hat{Q}_j$, as well as

$$\hat{H}_B^{tot} = C\hat{A}^2 + \sum_j \frac{\hat{P}_j^2}{2M} + \frac{M\Omega_j^2}{2}\hat{Q}_j^2, \quad (\text{A.15})$$

which is diagonalized by going over to new coordinates: $\hat{Q}_l = S_{ln}\tilde{\hat{Q}}_n$ and $\hat{P}_l = S_{ln}\tilde{\hat{P}}_n$, with a real orthogonal matrix S . Therefore, the new “effective” spectrum is

$$\begin{aligned} \langle \hat{A}\hat{A} \rangle_\omega^{T=0} &= \sum_{l,j} g_l g_j \langle \hat{Q}_l \hat{Q}_j \rangle_\omega = \sum_{l,j,n} g_l g_j S_{ln} S_{jn} \langle \tilde{\hat{Q}}_n \tilde{\hat{Q}}_n \rangle_\omega \\ &= \sum_{l,j,n} g_l g_j \frac{S_{ln} S_{jn}}{2M\tilde{\Omega}_n} \delta(\omega - \tilde{\Omega}_n), \end{aligned} \quad (\text{A.16})$$

where $\tilde{\Omega}_n$ are the new eigenfrequencies. This is evaluated using the resolvent $R_{lj}(\omega^2) =$

$\langle l | (\omega^2 - \tilde{\Omega}^2)^{-1} | j \rangle$, where l, j refer to the old (classical) basis vectors, and $\tilde{\Omega}_{lj}^2 \equiv \delta_{lj} \Omega_l^2 + (2C/M) g_l g_j$ is the matrix to be diagonalized. We obtain:

$$\langle \hat{A} \hat{A} \rangle_{\omega}^{T=0} = \sum_{l,j} \frac{g_l g_j}{M\pi} \text{Im} R_{lj}(\omega^2 - i0^+) \theta(\omega). \quad (\text{A.17})$$

The resolvent can be calculated exactly (compare the next appendix), and the sum over the resolvent turns out to be

$$\sum_{l,j} g_l g_j R_{lj}(\omega^2) = (M/2C) \left[\left((2C/M) \sum_n g_n^2 / (\omega^2 - \Omega_n^2) \right)^{-1} - 1 \right]^{-1}, \quad (\text{A.18})$$

which leads to Eq. (3.12) of the main text, after inserting $\langle \hat{A} \hat{A} \rangle_{\omega}^{(0)T=0} = \sum_n \delta(\omega - \Omega_n) g_n^2 / (2M\Omega_n)$.

Now we add a linear term $-\lambda \hat{A}$ to \hat{H}_B^{tot} and minimize the potential energy with respect to A . This leads to

$$A_j^{(\text{min})} = \sum_j g_j Q_j^{(\text{min})} = \frac{\lambda}{M} \sum_{l,j} g_l \left(\tilde{\Omega}^2 \right)_{lj}^{-1} g_j,$$

which is evaluated using a formal Taylor expansion in the “perturbation” $(2C/M) g_l g_j$ to $\tilde{\Omega}_{lj}^2$:

$$\sum_{l,j} g_l (D + G)_{lj}^{-1} g_j = - \sum_{n=1}^{\infty} \left(- \sum_l \frac{g_l^2}{D_l} \right)^n = \left(1 + \sum_l \frac{g_l^2}{D_l} \right)^{-1} \left(\sum_l \frac{g_l^2}{D_l} \right), \quad (\text{A.19})$$

where $G_{lj} \equiv g_l g_j$ and $D_{lj} \equiv \delta_{lj} \Omega_j^2 (M/2C) = \delta_{lj} D_l$. After inserting the bath spectrum, this results in Eq. (3.18) for the effective mass of the particle.

A.6 Coupled oscillator problem for the damped Fermi sea

We want to solve the problem of coupled oscillators defined in Eq. (4.27), i.e. we have to diagonalize

$$\Omega^2 + V \quad (\text{A.20})$$

with $V_{0j} = V_{j0} = (g/m) \sqrt{N/N_B}$ for $j > 0$ and all other entries of V equal to zero. In fact, for our purposes we only need the spectral weight of the mode $j = 0$ of the original problem in terms of the new eigenmodes and eigenfrequencies:

$$W(\omega) = \sum_{j=0}^{N_B} C_{0j}^2 \delta(\omega - \tilde{\Omega}_j). \quad (\text{A.21})$$

This is related directly to the resolvent

$$R(\epsilon) = \left[\frac{1}{\epsilon - (\Omega^2 + V)} \right]_{00}, \quad (\text{A.22})$$

since

$$R(\epsilon - i0) - R(\epsilon + i0) = 2\pi i \sum_{j=0}^{N_B} C_{0j}^2 \delta(\epsilon - \tilde{\Omega}_j^2), \quad (\text{A.23})$$

where $\tilde{\Omega}_j^2$ is the j -th eigenvalue of the matrix $\Omega^2 + V$. Therefore, we have

$$W(\omega) = \frac{\omega}{\pi i} (R(\omega^2 - i0) - R(\omega^2 + i0)) \theta(\omega), \quad (\text{A.24})$$

where we used $\delta(\omega - \tilde{\Omega}_j) = 2\omega \theta(\omega) \delta(\omega^2 - \tilde{\Omega}_j^2)$.

The evaluation of the resolvent $R(\epsilon)$ is straightforward, because the “perturbation” V only connects 0 and $j > 0$. Using $G^{-1} = \epsilon - \Omega^2$, we get

$$\begin{aligned} R(\epsilon) &= [G + GVG + GVGVG + \dots]_{00} \\ &= G_{00} \sum_{n=0}^{\infty} \left(\sum_{j=1}^{N_B} V_{j0}^2 G_{jj} G_{00} \right)^n \\ &= \left[\epsilon - \Omega_0^2 - \sum_{j>0} \frac{V_{j0}^2}{\epsilon - \Omega_j^2} \right]^{-1}. \end{aligned} \quad (\text{A.25})$$

In the continuum limit, we may use Eq. (4.5) to evaluate

$$\begin{aligned} \sum_{j>0} \frac{V_{j0}^2}{\epsilon + i\delta - \Omega_j^2} &= 2 \frac{N}{m} \int_0^\infty \frac{\langle \hat{F} \hat{F} \rangle_\omega^{T=0}}{\epsilon + i\delta - \omega^2} \omega d\omega \\ &\equiv \Delta(\epsilon) - \frac{i}{2} \Gamma(\epsilon) \operatorname{sgn}(\delta). \end{aligned} \quad (\text{A.26})$$

Here the definitions

$$\Gamma(\epsilon) = 2\pi \frac{N}{m} \left\langle \hat{F} \hat{F} \right\rangle_{\sqrt{\epsilon}}^{T=0} \theta(\epsilon) \quad (\text{A.27})$$

$$\Delta(\epsilon) = \frac{1}{2\pi} \int \frac{\Gamma(\nu)}{\epsilon - \nu} d\nu. \quad (\text{A.28})$$

have been introduced. (where a principal value integral is implied in the last line). Using this, we finally obtain (with (A.24)-(A.26)):

$$W(\omega) = \frac{\omega}{\pi} \theta(\omega) \frac{\Gamma(\omega^2)}{(\omega^2 - \omega_0^2 - \Delta(\omega^2))^2 + (\Gamma(\omega^2)/2)^2} . \quad (\text{A.29})$$

A.7 Two-particle Green's function of damped Fermi sea

The fermion operators \hat{c}_n in the oscillator are related to the auxiliary fermion operators $\hat{\psi}(x)$ via Eq. (4.14). Therefore, the special two-particle Green's function we need is given by:

$$\begin{aligned} & \left\langle \hat{c}_n(0) \hat{c}_{l'}^\dagger(t) \hat{c}_l(t) \hat{c}_{n'}^\dagger(0) \right\rangle = \\ & \frac{1}{(2\pi)^2} \int dx dx' dy dy' e^{i(l'x' + n'y' - lx - ny)} \times \\ & \left\langle \hat{\psi}(y, 0) \hat{\psi}^\dagger(x', t) \hat{\psi}(x, t) \hat{\psi}^\dagger(y', 0) \right\rangle \end{aligned} \quad (\text{A.30})$$

We use the expression of $\hat{\psi}$ in terms of the boson field $\hat{\phi}$, Eq. (4.16), to obtain (compare the single-particle expressions Eqs. (4.21), (4.22)):

$$\begin{aligned} & \left\langle \hat{\psi}(y, 0) \hat{\psi}^\dagger(x', t) \hat{\psi}(x, t) \hat{\psi}^\dagger(y', 0) \right\rangle = \\ & \frac{1}{(2\pi)^2} e^{i(n_F+1)(x+y-x'-y')} e^{E_{(2)}} , \end{aligned} \quad (\text{A.31})$$

with the exponent

$$\begin{aligned} E_{(2)} \equiv & \left\langle \hat{\phi}(y, 0) \hat{\phi}(x', t) \right\rangle - \left\langle \hat{\phi}(y, 0) \hat{\phi}(x, t) \right\rangle + \\ & \left\langle \hat{\phi}(y, 0) \hat{\phi}(y', 0) \right\rangle + \left\langle \hat{\phi}(x', t) \hat{\phi}(x, t) \right\rangle - \\ & \left\langle \hat{\phi}(x', t) \hat{\phi}(y', 0) \right\rangle + \left\langle \hat{\phi}(x, t) \hat{\phi}(y', 0) \right\rangle - \\ & \frac{1}{2} (C_x + C_y + C_{x'} + C_{y'}) . \end{aligned} \quad (\text{A.32})$$

Here we have introduced

$$C_x \equiv \left\langle \hat{\phi}(x, 0)^2 \right\rangle - \left\langle \hat{\phi}(x, 0) \right\rangle^2_{(0)} , \quad (\text{A.33})$$

where the second correlator refers to the non-interacting case (without bath) and stems from the factor r (see Eq. (4.16)).

Once again, we restrict the further evaluation to the special case of $T = 0$, where some of the expressions become slightly simpler. We express the nontrivial c.m. mode contribution to the correlator of $\hat{\phi}$ in terms of the $\hat{b}_1^{(\dagger)}$ -correlators $\alpha(t)$, $\beta_{\pm}(t)$ introduced above (see Eqs. (4.37), (4.38) and (4.39)). Since the two-particle Green's function involving the oscillator fermion operators \hat{c}_n is related to that of the auxiliary fermion operators $\hat{\psi}$ by means of a Fourier integral over the coordinates x, y, x', y' (cf. Eq. (A.30)), we find it convenient to introduce the following abbreviations (similar to our approach for the single-particle Green's function):

$$X^{(\prime)} \equiv e^{ix^{(\prime)}}, Y^{(\prime)} \equiv e^{iy^{(\prime)}} \quad (\text{A.34})$$

Then we obtain

$$C_x = \beta_+(0) + \beta_-(0) - 1 - \alpha(0)(X^2 + X^{-2}), \quad (\text{A.35})$$

as well as the form of the $\hat{\phi}$ -correlator given already in Eq. (4.41).

Therefore, the exponent $E_{(2)}$ (A.32) is given as a sum of terms containing α, β_{\pm} and binomials constructed out of X, X', Y and Y' , as well as non-interacting contributions $\langle \hat{\phi}(x', t) \hat{\phi}(x, 0) \rangle_{(0)}$, that also contain higher powers of these variables (see Eq. (4.42)). According to Eq. (A.30), the two-particle Green's function

$$\langle \hat{c}_n(0) \hat{c}_l^\dagger(t) \hat{c}_l(t) \hat{c}_{n'}^\dagger(0) \rangle \quad (\text{A.36})$$

is obtained by expanding $\exp(E_{(2)})$ in a power series with respect to X, X', Y and Y' , and reading off the coefficient in front of the component

$$X^{\delta l} X'^{-\delta l'} Y^{\delta n} Y'^{-\delta n'}, \quad (\text{A.37})$$

where $\delta l \equiv l - (n_F + 1)$ etc. Using (A.30), (A.31) and (A.32), as well as splitting off non-interacting terms, we find that the expression to be expanded can be written in the following form:

$$A_0 e^{\tilde{E}}. \quad (\text{A.38})$$

Here A_0 yields the correct result for the non-interacting case (cf. the application of Wick's theorem, Eq. (4.67)),

$$\begin{aligned} A_0 = & \sum_{\tilde{l} < 0} \left(\frac{X}{X'} \right)^{\tilde{l}} \sum_{\tilde{n} \geq 0} \left(\frac{Y}{Y'} \right)^{\tilde{n}} + \\ & \sum_{\tilde{n}' \geq 0} \left(\frac{X}{Y'} \right)^{\tilde{n}'} \sum_{\tilde{n} \geq 0} \left(\frac{Y}{X'} \right)^{\tilde{n}} e^{i\omega_0(\tilde{n} - \tilde{n}')t}, \end{aligned} \quad (\text{A.39})$$

and the exponent \tilde{E} is a rather lengthy expression involving $\alpha(t)$, $\alpha(-t) = \alpha^*(t)$, $\beta_{\pm}(t)$, $\beta_{\pm}(-t) = \beta_{\pm}^*(t)$ and binomials made out of X, X', Y and Y' :

$$\begin{aligned}
\tilde{E} \equiv & \alpha(t) \left(X'Y' + \frac{1}{X'Y'} - XY' - \frac{1}{XY'} \right) + \\
& \alpha^*(t) \left(XY + \frac{1}{XY} - X'Y - \frac{1}{X'Y} \right) - \\
& \alpha(0) \left(XX' + \frac{1}{XX'} + YY' + \frac{1}{YY'} \right) + \\
& \tilde{\beta}_+(t) \left(\frac{X}{Y'} - \frac{X'}{Y'} \right) + \tilde{\beta}_+^*(t) \left(\frac{Y}{X'} - \frac{Y}{X} \right) + \\
& \tilde{\beta}_+(0) \left(\frac{Y}{Y'} + \frac{X'}{X} \right) + \\
& \beta_-(t) \left(\frac{Y'}{X} - \frac{Y'}{X'} \right) + \beta_-^*(t) \left(\frac{X'}{Y} - \frac{X}{Y} \right) + \\
& \beta_-(0) \left(\frac{Y'}{Y} + \frac{X}{X'} \right) - \\
& \frac{1}{2} (C_x + C_y + C_{x'} + C_{y'}).
\end{aligned} \tag{A.40}$$

In this equation, we have employed the abbreviation $\tilde{\beta}_+(t) \equiv \beta_+(t) - e^{-i\omega_0 t}$. Note that \tilde{E} vanishes if the coupling to the bath is switched off.

The approximate weak-coupling result is obtained by setting $\alpha(t) = \beta_-(t) = 0$, $\beta_+(0) = 1$ and keeping only the (slowly decaying) $\beta_+(t)$ (compare the main text, Sec. 4.7, and the corresponding discussion for the single-particle case in Sec. 4.4).

A.8 Some quantities for the damped oscillator

In this appendix, we list, for purposes of reference, the quantities relevant to our discussion of the time-evolution of the quantum damped harmonic oscillator. These can also be found in [Caldeira83] (in a slightly different notation).

The quantity C_{00} arises in evaluating S_I along a pair of semiclassical paths, by inserting the solution $r(\cdot)$ of Eq. (5.22) for the boundary conditions given by r_t, r_0 and determining the coefficient of r_0^2 in the result (see Eq. (5.25)). Necessarily, C_{00} contains only the symmetric part of the bath correlator, since S_I depends only on that:

$$\begin{aligned}
C_{00} = & \frac{1}{4} (\sin(\tilde{\omega}t))^{-2} \int_0^t dt_1 \int_0^t dt_2 \exp \left(\frac{\gamma}{2} (t_1 + t_2) \right) \\
& \times \sin(\tilde{\omega}(t - t_1)) \left\langle \{ \hat{F}(t_1), \hat{F}(t_2) \} \right\rangle \sin(\tilde{\omega}(t - t_2)).
\end{aligned} \tag{A.41}$$

Here $\tilde{\omega} \equiv \sqrt{\omega_0^2 - (\gamma/2)^2}$ is the renormalized frequency of the (underdamped, $\gamma < 2\omega_0$) oscillator.

The other quantities needed for calculating $\langle \hat{q}^2(t) \rangle$ arise from the evaluation of $Re S_{cl}$ (Eq. (5.24)). In contrast to C_{00} , which has to be evaluated numerically, they can be given in closed form:

$$L_{00} = m(\gamma/2 + \tilde{\omega} \cot(\tilde{\omega}t)) \quad (\text{A.42})$$

$$L_{t0} = -\frac{m\tilde{\omega}e^{\gamma t/2}}{\sin(\tilde{\omega}t)} \quad (\text{A.43})$$

The exponential increase of L_{t0} cancels that of C_{00} when calculating the width in Eq. (5.29). However, if the damping rate γ is set to zero, C_{00} still grows beyond all bounds while L_{t0} remains bounded.

A.9 Density matrix propagator from the Wigner density evolution

Using the classical Langevin equation (5.30), the kernel J which relates the reduced density matrix of a linear dissipative system at time t to that at time 0 can be found in a way which is physically more transparent than the corresponding derivation using path-integrals (see Eqs. (5.1), (5.2), (5.18), (5.24) and (5.25)). One first solves for the time-evolution of the classical phase space density (i.e. the Wigner density) under the action of friction and the classical Gaussian random force $F(\cdot)$. Starting from a δ peak located in phase space, the phase space density evolves into a two-dimensional Gaussian distribution, whose covariances are related to the correlator of the force. This gives the propagator J^W of the Wigner density, which only needs to be Fourier transformed with respect to the momenta in order to obtain the density matrix propagator J , expressed via center-of-mass and difference coordinates R and r :

$$J(R_t, r_t | R_0, r_0; t) = \int dp_t dp_0 e^{i(p_t r_t - p_0 r_0)} J^W(R_t, p_t | R_0, p_0; t). \quad (\text{A.44})$$

Here we show how the propagator J for the density matrix of a free damped particle subject to the Ohmic bath may be obtained in this way. Everything works the same for the damped oscillator, only the resulting expressions are slightly more lengthy.

The propagator $J^W(R_t, p_t | R_0, p_0; t)$ of the Wigner density is found by solving the classical equations of motion for R and p for a given initial condition (R_0, p_0) , taking into account friction and the action of the force F :

$$\frac{dp}{dt} = -\gamma p + F(t) \quad (\text{A.45})$$

$$\frac{dR}{dt} = \frac{p}{m} \quad (\text{A.46})$$

This yields the solutions

$$p_t = p_0 e^{-\gamma t} + \xi_p \quad (\text{A.47})$$

$$R_t = R_0 + \frac{p_0}{\eta} (1 - e^{-\gamma t}) + \xi_R, \quad (\text{A.48})$$

where ξ_p and ξ_R are given as integrals over the force $F(\cdot)$:

$$\xi_p = \int_0^t ds e^{-\gamma(t-s)} F(s) \quad (\text{A.49})$$

$$\xi_R = \frac{1}{\eta} \int_0^t ds (1 - e^{-\gamma(t-s)}) F(s). \quad (\text{A.50})$$

Since $F(\cdot)$ is a Gaussian random process, ξ_p and ξ_R are Gaussian random variables as well. Therefore, the phase space density evolving out of $\delta(R - R_0)\delta(p - p_0)$ is a two-dimensional Gaussian distribution in phase space (R, p) :

$$J^W(R_t, p_t | R_0, p_0; t) = \langle \delta(R_t - \bar{R}_t - \xi_R) \delta(p_t - \bar{p}_t - \xi_p) \rangle. \quad (\text{A.51})$$

The average values \bar{p}_t and \bar{R}_t may be read off from eqs. (A.47) and (A.48). J^W has to be Fourier transformed with respect to p_t and p_0 in order to arrive at the density matrix propagator $J(R_t, r_t | R_0, r_0; t)$ (see Eq. (A.44)). In order to do this, we express J^W as a Gaussian density in terms of p_t, p_0 , for fixed R_t, R_0 :

$$J^W \propto \exp \left[-\frac{1}{2} \delta P^t K^{-1} \delta P \right], \quad (\text{A.52})$$

with

$$\delta P = \begin{bmatrix} p_t - \bar{p}_t \\ p_0 - \bar{p}_0 \end{bmatrix} \quad (\text{A.53})$$

and the covariance matrix

$$K = \begin{bmatrix} \langle \delta p_t^2 \rangle & \langle \delta p_t \delta p_0 \rangle \\ \langle \delta p_t \delta p_0 \rangle & \langle \delta p_0^2 \rangle \end{bmatrix}. \quad (\text{A.54})$$

We can solve (A.47) and (A.48) for p_t, p_0 , in order to find the average values and the deviations of p_t and p_0 :

$$\bar{p}_t = \lambda(R_t - R_0) \quad (\text{A.55})$$

$$\bar{p}_0 = e^{\gamma t} \lambda(R_t - R_0) \quad (\text{A.56})$$

$$\delta p_t = \xi_p - \lambda \xi_R \quad (\text{A.57})$$

$$\delta p_0 = -e^{\gamma t} \lambda \xi_R \quad (\text{A.58})$$

$$\lambda \equiv \frac{\eta}{e^{\gamma t} - 1} \quad (\text{A.59})$$

\bar{p}_0 and \bar{p}_t are the momenta at time t and 0 which the particle must have if it is to go from R_0 to R_t in time t , provided no fluctuating force acts. δp_t and δp_0 are the deviations from these values needed to compensate the effects of $F(\cdot)$.

Quadratic completion in the exponent of (A.52) immediately yields the result of the Fourier integration (A.44) over p_t and p_0 , which is the desired density matrix propagator J :

$$J(R_t, r_t | R_0, r_0; t) \propto \exp \left[i(R_t - R_0)\lambda(r_t - e^{\gamma t} r_0) - \frac{1}{2} \langle (r_t \delta p_t - r_0 \delta p_0)^2 \rangle \right]. \quad (\text{A.60})$$

This reproduces the result given in [Caldeira83] (or [Golubev00], App. E). The prefactor can be determined from the normalization condition, Eq. (5.20), and only depends on the time t . The term in angular brackets still has to be averaged over the force $F(\cdot)$. The resulting real part of the exponent equals $-S_I$ evaluated along the semiclassical paths (compare the general structure given in Eq. (5.25)). In terms of $F(\cdot)$, δp_t and δp_0 read explicitly:

$$\delta p_t = \int_0^t ds \frac{e^{\gamma s} - 1}{e^{\gamma t} - 1} F(s) \quad (\text{A.61})$$

$$\delta p_0 = \int_0^t ds \frac{e^{\gamma s} - e^{\gamma t}}{e^{\gamma t} - 1} F(s). \quad (\text{A.62})$$

Note that

$$\delta p_t - \delta p_0 = \int_0^t ds F(s). \quad (\text{A.63})$$

The averages $\langle \delta p_t^2 \rangle$, $\langle \delta p_0^2 \rangle$ and $\langle \delta p_t \delta p_0 \rangle$ to be evaluated in Eq. (A.60) contain time-integrals over the force correlator $\langle F(s_1) F(s_2) \rangle$. At zero temperature, these integrals lead to terms growing logarithmically in time, which are characteristic for the free particle coupled to an Ohmic bath (compare the discussion in the main text, Sec. 5.6, also Section 3.6).

Bibliography

- [Abramowitz84] M. Abramowitz and I. Stegun (eds.), *Pocketbook of Mathematical Functions (abridged edition)*, Verlag Harri Deutsch, Thun (1984).
- [Aleiner97] I. L. Aleiner, N. S. Wingreen, and Y. Meir: “Dephasing and the Orthogonality Catastrophe in Tunneling through a Quantum Dot: the ‘Which Path?’ Interferometer”, *Phys. Rev. Lett.* **79**, 3740 (1997).
- [Aleiner99] I. L. Aleiner, B. L. Altshuler, and M. E. Gershenson: “Interaction effects and phase relaxation in disordered systems”, *Waves in Random Media* **9**, 201 (1999).
- [Altshuler82] B. L. Altshuler, A. G. Aronov, and D. E. Khmelnitsky: “Effects of electron-electron collisions with small energy transfer on quantum localization”, *J. Phys. C Solid State* **15**, 7367 (1982).
- [Averin92] D. V. Averin and Yu. V. Nazarov, in: “Single charge tunneling”, ed. H. Grabert and M. H. Devoret, Plenum Press, New York (1992).
- [Blum96] K. Blum, *Density Matrix Theory and Applications*, Plenum, New York (1996).
- [Boese02] D. Boese, W. Hofstetter, and H. Schoeller: “Interference in interacting quantum dots with spin”, *cond-mat/0201461* (2002).
- [Brandes99] T. Brandes and B. Kramer: “Spontaneous emission of phonons by coupled quantum dots”, *Phys. Rev. Lett.* **83**, 3021 (1999).
- [Buks98] E. Buks, R. Schuster, M. Heiblum, D. Mahalu, and V. Umansky: “Dephasing in electron interference by a ‘which-path’ detector”, *Nature* **391**, 871 (1998).
- [Büttiker85] M. Büttiker: “Small normal-metal loop coupled to an electron reservoir”, *Phys. Rev. B* **32**, 1846 (1985); “Flux-Sensitive Effects in Normal Metal Loops”, *Ann. N. Y. Acad. of Sciences*, **480**, 194 (1986).

- [Büttiker01] M. Büttiker: “Irreversibility and dephasing from vacuum fluctuations”, in NATO ASI Lecture Notes Norway 2001, eds. A. T. Skjeltorp and T. Vicsek, Kluwer, Dordrecht (2001). (cond-mat/0106149)
- [Caldeira83] A. O. Caldeira and A. J. Leggett: “Path integral approach to Quantum Brownian Motion”, *Physica* **121A**, 587 (1983).
- [Caldeira85] A. O. Caldeira and A. J. Leggett: “Influence of damping on quantum interference: An exactly soluble model”, *Phys. Rev. A* **31**, 1059 (1985).
- [Cedraschi00] P. Cedraschi, V. V. Ponomarenko, and M. Büttiker: “Zero-Point Fluctuations and the Quenching of the Persistent Current in Normal Metal Rings”, *Phys. Rev. Lett.* **84**, 346 (2000).
- [Cedraschi01] P. Cedraschi and M. Büttiker: “Zero-point fluctuations in the ground state of a mesoscopic normal ring”, *Phys. Rev. B* **63**, 165312 (2001); “Quantum Coherence of the Ground State of a Mesoscopic Ring”, *Annals of Physics*, **289**, 1 (2001).
- [Chakravarty86] S. Chakravarty and A. Schmid: “Weak localization - the quasi-classical theory of electrons in a random potential”, *Phys. Rep.* **140**, 195 (1986).
- [Chen93] H. Chen and X.-Q. Li: “Influence of the electron-boson interaction on co-tunneling through two small junctions in the Coulomb-blockade regime”, *Phys. Rev. B* **48**, 8790 (1993).
- [Cohen97] D. Cohen: “Unified model for the study of diffusion, localization and dissipation”, *Phys. Rev. E* **55**, 1422 (1997); “Quantal Brownian Motion - Dephasing and Dissipation”, *J. Phys. A* **31**, 8199 (1998).
- [Cohen99] D. Cohen and Y. Imry: “Dephasing at low temperatures”, *Phys. Rev. B* **59**, 11143 (1999).
- [Delft98] J. v. Delft and H. Schoeller: “Bosonization for Beginners - Reformation for Experts”, *Annalen der Physik*, Vol. **4**, 225 (1998).
- [Devoret90] M. H. Devoret, D. Esteve, H. Grabert, G.-L. Ingold, H. Pothier, and C. Urbina: “Effect of the Electromagnetic Environment on the Coulomb Blockade in Ultrasmall Tunnel Junctions”, *Phys. Rev. Lett.* **64**, 1824 (1990).
- [Feynman63] R.P. Feynman and F.L. Vernon: “The Theory of a General Quantum System Interacting with a Linear Dissipative System”, *Ann. Phys. (N.Y.)* **24**, 118 (1963).

- [Feynman65] R. P. Feynman and A. R. Hibbs, *Quantum Mechanics and Path Integrals*, McGraw-Hill, New York (1965).
- [Fujisawa98] T. Fujisawa, T. H. Oosterkamp, W. G. van der Wiel, B. W. Broer, R. Aguado, S. Tarucha, L. P. Kouwenhoven: “Spontaneous emission spectrum in double quantum dot devices”, *Science* **282**, 932 (1998).
- [Giulini96] D. Giulini, E. Joos, C. Kiefer, J. Kupsch, I.-O. Stamatescu, and H. D. Zeh: *Decoherence and the Appearance of a Classical World in Quantum Theory*, Springer, Berlin (1996).
- [Golubev98] D. S. Golubev and A. D. Zaikin: “Quantum decoherence in disordered mesoscopic systems”, *Phys. Rev. Lett.* **81**, 1074 (1998).
- [Golubev99] D. S. Golubev and A. D. Zaikin: “Quantum decoherence and weak localization at low temperatures”, *Phys. Rev. B* **59**, 9195 (1999).
- [Golubev00] D. S. Golubev and A. D. Zaikin: “Interactions and weak localization: Perturbation theory and beyond”, *Phys. Rev. B* **62**, 14061 (2000).
- [Golubev01] D. S. Golubev and A. D. Zaikin: “Comparison between Theory and Some Recent Experiments on Quantum Dephasing”, cond-mat/0103166 (2001).
- [Golubev02a] D. S. Golubev, A. D. Zaikin, and G. Schön: “On low-temperature dephasing by electron-electron interaction”, *J. Low Temp. Phys.* **126**, 1355 (2002).
- [Golubev02b] D. S. Golubev, C. P. Herrero, and A. D. Zaikin: “Interaction-Induced Quantum Dephasing in Mesoscopic Rings”, cond-mat/0205549(2002).
- [Golubev02c] D. S. Golubev and A. D. Zaikin: “Low temperature decoherence by electron-electron interactions: Role of quantum fluctuations (reply to cond-mat/0110545)”, cond-mat/0208140 (2002).
- [Golubev02d] D. S. Golubev, G. Schön, and A. D. Zaikin: “Low-temperature Dephasing and Renormalization in Model Systems”, cond-mat/0208548 (2002).
- [Gougam00] A. B. Gougam, F. Pierre, H. Pothier, D. Esteve, N.O. Birge: “Comparison of energy and phase relaxation in metallic wires”, *J. Low Temp. Phys.* **118**, 447 (2000).
- [Grabert01] H. Grabert: “Transport in Single Channel Quantum Wires”, to appear in “Exotic States in Quantum Nanostructures” ed. by S. Sarkar, Kluwer, cond-mat/0107175 (2001).

- [Groshev91] A. Groshev: “Resonance-level broadening by environmental fluctuations”, Phys. Rev. B **44**, 11502 (1991); X.-Q. Li, S.-J. Qin, and Z.-B. Su: “Influence of electromagnetic environmental fluctuations on resonant tunneling through double-barrier systems”, Phys. Rev. B **51**, 5214 (1995).
- [Guinea02] F. Guinea: “Aharonov-Bohm oscillations of a particle coupled to dissipative environments”, Phys. Rev. B **65**, 205317 (2002).
- [Hakim85] V. Hakim and V. Ambegaokar: “Quantum theory of a free particle interacting with a linearly dissipative environment”, Phys. Rev. A **32**, 423 (1985).
- [Hansen01] A. E. Hansen, A. Kristensen, S. Pedersen, C. B. Sørensen, and P. E. Lindelof: “Mesoscopic decoherence in Aharonov-Bohm rings”, Phys. Rev. B **64**, 045327 (2001).
- [Haule99] K. Haule and J. Bonca: “Inelastic tunneling through mesoscopic structures”, Phys. Rev. B **59**, 13087 (1999).
- [Holleitner02] A. W. Holleitner, R. H. Blick, A. K. Huttel, K. Eberl, J. P. Kotthaus: “Probing and controlling the bonds of an artificial molecule”, Science **297**, 70 (2002).
- [Imry97] Y. Imry, *Introduction to Mesoscopic Physics*, Oxford University Press, Oxford (1997).
- [Imry99] Y. Imry, H. Yukuyama, P. Schwab: “Low-temperature dephasing in disordered conductors: The effect of $1/f$ fluctuations”, Europhys. Lett. **47**, 608 (1999).
- [Imry02] Y. Imry: “Elementary explanation of the inexistence of decoherence at zero temperature for systems with purely elastic scattering”, cond-mat/0202044 (2002).
- [Ingold92] G.-L. Ingold and Y. V. Nazarov: “Charge Tunneling Rates in Ultrasmall Junctions”, in: *Single Charge Tunneling*, ed. by H. Grabert and M. Devoret, NATO ASI Series B, vol. 294, Plenum, New York (1992).
- [Keil02] M. Keil and H. Schoeller: “Nonperturbative analysis of coupled quantum dots in a phonon bath”, cond-mat/0205308 (2002).
- [Kirkpatrick02] T. R. Kirkpatrick and D. Belitz: “Absence of electron dephasing at zero temperature”, Phys. Rev. B **65**, 195123 (2002); Comment by D. S. Golubev, A. Zaikin and G. Schön in cond-mat/0111527, and reply in cond-mat/0112063. See also R. Ramazashvili, cond-mat/0208030 for a critical discussion.

- [Kobayashi02] K. Kobayashi, H. Aikawa, S. Katsumoto, and Y. Iye: “Probe-Configuration-Dependent Decoherence in an Aharonov-Bohm Ring”, cond-mat/0204186 (2002).
- [König96] J. König, J. Schmid, H. Schoeller, and G. Schön: “Resonant tunneling through ultrasmall quantum dots: Zero-bias anomalies, magnetic-field dependence, and boson-assisted transport”, Phys. Rev. B **54**, 16820 (1996).
- [König02] J. König and Y. Gefen: “Aharonov-Bohm Interferometry with Interacting Quantum Dots: Spin Configurations, Asymmetric Interference Patterns, Bias-Voltage-Induced Aharonov-Bohm Oscillations, and Symmetries of Transport Coefficients”, Phys. Rev. B **65**, 045316 (2002).
- [Kramer93] B. Kramer and A. MacKinnon: “Localization: theory and experiment”, Rep. Prog. Phys. **56**, 1469 (1993).
- [Landau77] L. D. Landau and E. M. Lifshitz: *Quantum Mechanics*, Pergamon, New York (1977).
- [Leggett87] A. J. Leggett, S. Chakravarty, A.T. Dorsey, M. P. A. Fisher, A. Garg, and W. Zwerger: “Dynamics of the dissipative 2-state system”, Rev. Mod. Phys. **59**, 1 (1987).
- [Loss91] D. Loss and K. Mullen: “Dephasing by a dynamic asymmetric environment”, Phys. Rev. B **43**, 13252 (1991).
- [Loss93] D. Loss and T. Martin: “Absence of spontaneous persistent current for interacting fermions in a one-dimensional mesoscopic ring”, Phys. Rev. B **47**, 4619 (1993).
- [Loss98] D. Loss and D.P. DiVincenzo: “Quantum computation with quantum dots”, Phys. Rev. A **57**, 120 (1998).
- [Loss00] D. Loss and E. V. Sukhorukov: “Probing Entanglement and Non-locality of Electrons in a Double-Dot via Transport and Noise”, Phys. Rev. Lett. **84**, 1035 (2000).
- [Mahan81] G. D. Mahan: *Many-Particle Physics*, Plenum, New York (1981), pp. 269-310.
- [Marquardt00] F. Marquardt: “Time-evolution of reduced density matrix for fermions under the action of a quantum bath” (2000). (unpublished)
- [Marquardt01] F. Marquardt: “An introduction to the basics of dephasing”, at <http://iff.physik.unibas.ch/~florian/dephasing/dephasing.html>. (2001) (unpublished)

- [Marquardt02a] F. Marquardt and C. Bruder: “Aharonov-Bohm ring with fluctuating flux”, Phys. Rev. B **65**, 125315 (2002).
- [Marquardt02b] F. Marquardt: “The importance of friction in the description of low-temperature dephasing”, cond-mat/0207692 (2002).
- [Mello00] P. A. Mello, Y. Imry, and B. Shapiro: “Model for phase breaking in the electronic conduction in mesoscopic systems”, Phys. Rev. B **61**, 16570 (2000).
- [Mermin66] N. D. Mermin: “A Short Simple Evaluation of Expressions of the Debye-Waller Form”, Journ. of Math. Phys. **7**, 1038 (1966).
- [Milonni94] P. W. Milonni: *The Quantum Vacuum*, Academic Press, San Diego (1994).
- [Minnhagen76] P. Minnhagen: “Exact numerical solutions of a Nozieres-deDominicis-type model problem”, Phys. Lett. A **56**, 327 (1976).
- [Mohanty97a] P. Mohanty, E. M. Q. Jariwala, and R. A. Webb: “Intrinsic Decoherence in Mesoscopic Systems”, Phys. Rev. Lett. **78**, 3366 (1997).
- [Mohanty97b] P. Mohanty and R. A. Webb: “Decoherence and quantum fluctuations”, Phys. Rev. B **55**, R13452 (1997).
- [Mohanty01] P. Mohanty: “Of Decoherent Electrons and Disordered Conductors”, in NATO ASI Lecture Notes Norway 2001, eds. A. T. Skjeltorp and T. Vicsek, Kluwer, Dordrecht, (2001). (cond-mat/0205274)
- [Nagaev02] K. E. Nagaev and M. Büttiker: “Ground State Energy Fluctuations of a System Coupled to a Bath”, Europhys. Lett. **58**, 475 (2002).
- [Natelson01] D. Natelson, R. L. Willett, K. W. West, and L. N. Pfeiffer: “Geometry-dependent dephasing in small metallic wires”, Phys. Rev. Lett. **86**, 1821 (2001).
- [Neto97] A. H. C. Neto, C. D. Chamon, and C. Nayak: “Open Luttinger liquids”, Phys. Rev. Lett. **79**, 4629 (1997).
- [Odintsov92] A. A. Odintsov, V. Bujanja, and G. Schön: “Influence of electromagnetic fluctuations on electron cotunneling”, Phys. Rev. B **46**, 6875 (1992).
- [Park92] C. Park and Y. Fu: “Dephasing, dissipation, and the persistent current in a mesoscopic normal metal ring”, Physics Letters A **161**, 381 (1992).

- [Pivin99] D. P. Pivin, A. Andresen, J. P. Bird, and D. K. Ferry: “Saturation of phase breaking in an open ballistic quantum dot”, *Phys. Rev. Lett.* **82**, 4687 (1999).
- [Rollbühler00] J. Rollbühler and A. A. Odintsov: “Aharonov-Bohm effect in circular carbon nanotubes”, *Physica B* **280**, 386 (2000).
- [Schoeller99] H. Schoeller: “An introduction to real-time renormalization group”, *Lect. Notes Phys.* **544**, 137 (2000). (cond-mat/9909400)
- [Schön98] G. Schön: “Single-Electron Tunneling”, in: T. Dittrich et al., *Quantum transport and dissipation*, Wiley-VCH, Weinheim (1998).
- [Schramm87] P. Schramm and H. Grabert: “Low-Temperature and Long-Time Anomalies of a Damped Quantum Particle”, *Journal of Stat. Phys.* **49**, 811 (1987).
- [Seelig01] G. Seelig and M. Büttiker: “Charge-fluctuation-induced dephasing in a gated mesoscopic interferometer”, *Phys. Rev. B* **64**, 245313 (2001).
- [Shnirman02] A. Shnirman, Y. Makhlin, and G. Schön: “Noise and Decoherence in Quantum Two-Level Systems”, cond-mat/0202518 (2002).
- [Stern90] A. Stern, Y. Aharonov, and Y. Imry: “Phase uncertainty and loss of interference: A general picture”, *Phys. Rev. A* **41**, 3436 (1990).
- [Stoof96] T. H. Stoof and Y. V. Nazarov: “Time-dependent resonant tunneling via two discrete states”, *Phys. Rev. B* **53**, 1050 (1996).
- [Vavilov99] M. Vavilov and V. Ambegaokar: “Influence of Interaction on Weak Localization”, cond-mat/9902127 (1999).
- [Weiss00] U. Weiss: *Quantum Dissipative Systems*, World Scientific, Singapore (2000).
- [Welton48] T. A. Welton: “Some Observable Effects of the Quantum-Mechanical Fluctuations of the Electromagnetic Field”, *Phys. Rev.* **74**, 1157 (1948).
- [Wilhelm01] F. K. Wilhelm, G. Schön, and G. Zimanyi: “Superconducting single-charge transistor in a tunable dissipative environment”, *Phys. Rev. Lett.* **87**, 136802 (2001).
- [Wingreen88] N. S. Wingreen, K. W. Jacobsen, and J. W. Wilkins: “Resonant Tunneling with Electron-Phonon Interaction: An Exactly Solvable Model”, *Phys. Rev. Lett.* **61**, 1396 (1988); “Inelastic scattering in resonant tunneling”, *Phys. Rev. B* **40**, 11834 (1989).

- [Zaikin00] A. D. Zaikin and D. S. Golubev: “Interaction and quantum decoherence in disordered conductors”, *Physica B* **280**, 453 (2000).
- [Zawadowski99] A. Zawadowski, J. v. Delft, and D. C. Ralph: “Dephasing in Metals by Two-Level Systems in the 2-Channel Kondo Regime”, *Phys. Rev. Lett.* **83**, 2632 (1999).

Publications

- F. Marquardt and C. Bruder: "Superposition of two mesoscopically distinct quantum states: Coupling a Cooper-pair box to a large superconducting island", Phys. Rev. B **63**, 054514 (2001).
- F. Marquardt and C. Bruder: "Aharonov-Bohm ring with fluctuating flux", Phys. Rev. B **65**, 125315 (2002); "Visibility of the Aharonov-Bohm effect in a ring coupled to a fluctuating magnetic flux", J. Low Temp. Phys. **126**, 1325 (2002); erratum in J. Low Temp. Phys. **128**, 163 (2002).
- C. Keller, F. Marquardt, and C. Bruder: "Separation quality of a geometric ratchet", Phys. Rev. E **65**, 041927 (2002).
- H. Gassmann, F. Marquardt, and C. Bruder: "Non-Markoffian effects of a simple nonlinear bath", cond-mat/0204372 (2002) (accepted for publication in Phys. Rev. E).
- F. Marquardt: "The importance of friction in the description of low-temperature dephasing", cond-mat/0207692 (2002).

Acknowledgments

First of all, I would like to thank Christoph Bruder for accepting me as a Ph. D. student, and for numerous discussions. I would also like to thank the co-referees, Hermann Grabert and Daniel Loss, for investing their time. I thank Christian Schönenberger for agreeing to chair the defense, as well as for organizing the great monday morning topic talks.

Furthermore, I am grateful to Dmitri Golubev, Andrei Zaikin, and Jan von Delft for very stimulating discussions on the problem of low-temperature dephasing in weak localization. In addition, I thank D. Golubev for the fruitful collaboration on the “damped Fermi sea”.

I have also had the pleasure to collaborate with Christoph Keller and Hanno Gassmann on classical ratchets and nonlinear baths (respectively), for which I want to thank them very much.

Wolfgang Belzig and Hanno Gassmann have helped me with a critical reading of the manuscript. Thanks to Patrik Recher for asking for the proof which is now given in the first appendix and for supplying the reference to Mermin’s article.

I would also like to thank Florian Meier and Hanno for our trips to Graubünden and many discussions. Hansres Engel gets a big “thank you” for crucial last-minute L^AT_EX help.

Finally, there have been a number of other people with whom I discussed and from whose comments, advice or questions I benefited during the three years of this thesis. Thanks go to all of them, including particularly E. Sukhorukov, Yu. Nazarov, A. J. Leggett, J. König, V. Cerletti, M. Büttiker, K. Le Hur, G. Seelig, P. Talkner, G. Schön, A. Shnirman, and H. Schoeller.

Lebenslauf

von Florian Kai Marquardt
Staatsangehörigkeit: deutsch

- 16.7.1974 Geburt in Berlin, als erster Sohn von Dr. Dr. K.-H. Marquardt
 und G. Marquardt (geb. Pfeiffer), zwei Geschwister
- 1980-84 Besuch der Grundschule in Oettingen i. Bay.
- 1984-89 Besuch des Gymnasiums in Dinkelsbühl
- 1989-92 Besuch des Gymnasiums in Nördlingen,
 Abschluss mit dem Abitur im Juli 1992
- 1992-93 Beginn des Physikstudiums in Bayreuth
- 1993-94 Wehrdienst in Neuburg a. d. Donau
- 1994-98 Fortsetzung des Studiums in Bayreuth
- 1997-98 Diplomarbeit "Tieffrequente lineare Antwort von Supraleitern mit
 Störstellen" (zur Theorie der Wirbelbewegung) unter Prof. D. Rainer;
 Diplom "mit Auszeichnung" im Okt. 1998
- 1998-99 Softwareentwicklung im "Institut für Wirtschaftsökologie" in Dornstadt
- 1999-2002 Dissertation am Institut für Physik der Universität Basel
 unter Prof. C. Bruder, seit Okt. 1999

An der Ausbildung beteiligte Dozenten: (Bayreuth:) Profs. B. Wrackmeyer, H. Goldmann, M. Krämer, W. von Wahl, M. Wiegner, P. J. Huber, F. Lempio, M. Schwoerer, H. Pascher, A. Seilmeier, D. Haarer, F. Pobell, J. Küppers, E. Rössler, L. Oberauer, H. R. Brand, F. H. Busse, L. Kramer, W. Brenig, F. G. Mertens, H. Büttner, A. Kampf, C. Bruder, J. Voit, M. Oppen, H. Feshke, W. Pesch, D. Rainer,
(Basel:) G. Baur, P. Talkner